1997

Effect of trimodal particle size distribution on sintering of Al_2O_3 ceramics

Dale L. Anderson
San Jose State University

EFFECT OF TRIMODAL PARTICLE SIZE DISTRIBUTION ON SINTERING OF Al_2O_3 CERAMICS

A Thesis

Presented to

the Faculty of the

Department of Materials Engineering

San Jose State University

In Partial Fulfillment

of the Requirements for the Degree

Master of Science.

By

Dale L. Anderson

August, 1997

UMI Number: 1386191

APPROVED FOR THE DEPARTMENT OF MATERIALS ENGINEERING

Guna Selvaduray

Dr. Guna Selvaduray, Thesis Advisor

Melanie McNeil

Dr. Melanie McNeil
Professor of Chemical Engineering

Manfred J. H. Cantow

Dr. Manfred Cantow
Professor of Materials Engineering

APPROVED FOR THE UNIVERSITY

M. Lou Lewandowski

ABSTRACT

EFFECT OF TRIMODAL PARTICLE SIZE DISTRIBUTION
ON SINTERING OF Al_2O_3 CERAMICS

by Dale L. Anderson

The object of this study was to investigate the possibility of obtaining higher sintered densities and reducing shrinkage by maximizing the green density through the use of a trimodal mixture of particle sizes. Sintering characteristics, including green density, sintered density, porosity, and shrinkage were measured for specimens produced using unimodal, bimodal and trimodal mixtures of fine, medium and coarse alumina particles. The results show that the sintered density increases with an increase in the percent fines found in the mixture; however, so does the shrinkage. The green density was maximized and shrinkage was minimized with the use of a trimodal mixture. Shrinkage was found to be a minimum when the green density was at a maximum. The highest green density was obtained with the sample that contained 10% fines, 20% medium and 70% coarse material. This composition of particle size is similar to the composition that produced optimized trimodal packings of spheres obtained, as reported in other studies.

ACKNOWLEDGEMENTS

Sincere gratitude is expressed to Dr. Guna Selvaduray for his valuable assistance and advice on this investigation. Thanks are also extended to my thesis committee, Dr. Manfred Cantow and Dr. Melanie McNeil.

I would also like to thank Mr. Mark Chamberlain at Ceralox Corporation for supplying the alumina powders.

I would also like to thank Roy M. Wheeler Jr. for his support through the years. And a very special thanks to my family, Leo Q. and Mildred A. Anderson, and to James M. Aguilar for their support and encouragement without which this project may never have been completed.

<u>Table of Contents</u>

Table of Contents - continued

List of Figures

List of Figures - continued

List of Figures - continued

List of Tables

List of Appendices

CHAPTER 1

INTRODUCTION TO SINTERING CHARACTERISTICS

Sintering is a process used in industry to fuse fine particulate materials into a solid unit. This introductory chapter will describe the stages of sintering, the driving force for sintering, the residual porosity and the shrinkage resulting from the sintering process.

1.1 SINTERING

Sintering can be defined as the consolidation, densification, recrystallization and bonding obtained by heating compacted powders at temperatures below the melting point of the principal component [1]. Three stages of sintering are described as:

(1) The initial stage of neck growth between adjacent particles.

(2) A stage of material transport/densification.

(3) Final stage of grain growth and pore elimination.

These three stages actually overlap and are not distinctly separate. A two dimensional representation of the stages of sintering is shown in Figure 1. As described by Kingery [2], in order to effectively control sintering processes it is essential to maintain close control of the initial particle size and particle size distribution of the material, the sintering temperature and the composition.

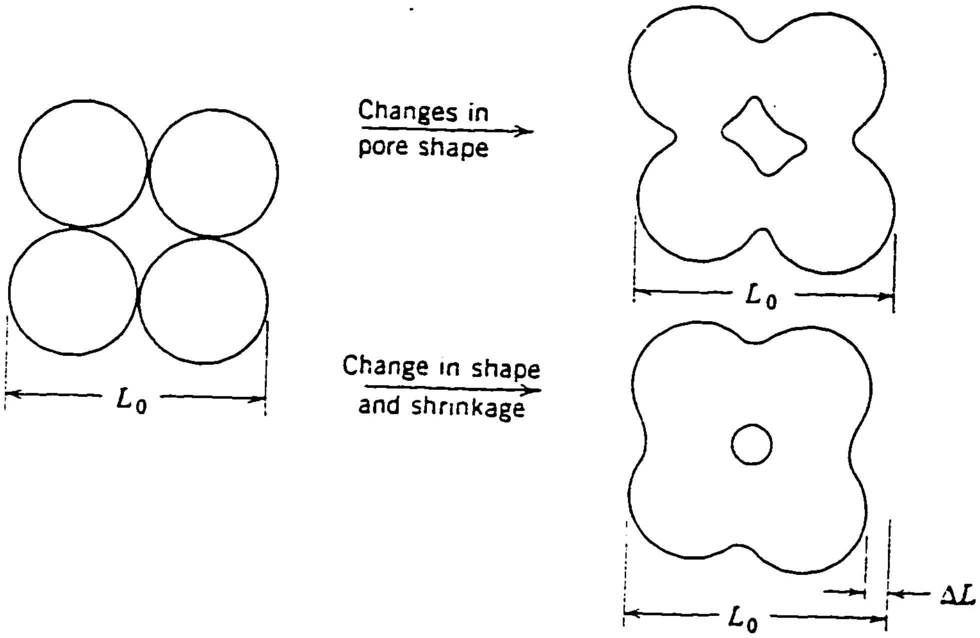

Figure 1. Stages of Sintering

(Reprinted from Kingery, p. 469)

1.2 DRIVING FORCE FOR SINTERING

The driving force for densification results from a decrease in surface-free energy, by the elimination of solid-vapor interfaces, in the absence of chemical reactions. Although lower energy solid-solid interfaces may be formed, the net decrease in free-energy drives the sintering process. If the particle size is small the surface area must be very large. This gives rise to a potentially large driving force for sintering to occur [2]. Models of sintering and practical experience in ceramic processing show that smaller particle sizes sinter more rapidly at a given temperature and can be sintered at lower temperatures than larger particles [3]. This is one of the main reasons why ceramic technology depends on the use of very fine particulate materials.

1.3 RESIDUAL POROSITY

Processing of ceramic materials is usually done by heating compacted powders to a temperature sufficient to produce useful properties. Residual porosity is a phase which is almost always present in ceramics prepared in this manner. Porosity is characterized by the volume fraction of pores present and their shape and size distribution throughout the solid matrix. The amount of porosity can vary from zero to more than 90% of the total volume. Many properties of ceramic materials, including thermal and electrical conductivity are highly dependent on the spacial distribution of residual porosity [2].

As described by Kingery [2], the major changes that occur during the firing process are related to changes in grain size and shape and to changes in pore size and shape. Before firing, a powder compact has typically between 25 and 60 volume % porosity. This depends primarily on the material used and the methods used to process it. In high density products, residual porosity after sintering may be a very small fraction of the void space found in the green compact. The optimum level of residual porosity would depend on the specific service conditions. For maximizing strength, translucency and thermal conductivity it would be desirable to eliminate as much porosity as possible [2]. Kingery has derived a relationship, for pore stability, which relates the dihedral angle and the ratio of pore size to grain size. Kingery also notes that a large difference between grain size and pore size is not required for pore stability. This will be discussed further in Section 3.2.

1.4 SHRINKAGE AND DENSIFICATION

The elimination of porosity is directly related to the volume shrinkage of the product being formed. Dense ceramic components made with a minimum of shrinkage are an important objective of the ceramic industry. One way to minimize shrinkage is to reduce the void space found in the green product. This can be done by customizing the particle size distribution. Several important effects of particle size distribution in powder processing have been widely recognized and related to the stages in the sintering process. The use of mixtures of particle sizes increases the bulk density of powder compacts [4], since small particles can fit in between the larger particles. A two dimensional rendition of a three dimensional mixed particle arrangement is shown in Figure 2. Studies of particle packing efficiency to achieve high density, reviewed by Coble [3], have led to widespread use of mixed particle sizes in practical ceramics systems. A smaller density difference between the green product and the sintered product will result in less shrinkage. This approach has been utilized in a patented process [5], developed by Toshiba of Japan, for the manufacture of injection molded sintered bodies. Toshiba finds that by using a precise proprietary distribution of particle sizes, particle packing is improved and shrinkage is minimized. In a study by Denevi [6], the standard deviations obtained for green and sintered densities were significantly lower for mixed particle size powder systems than for uniform powders. He suggests that in a mass production process, the use of mixed particle systems may enhance reproducibility.

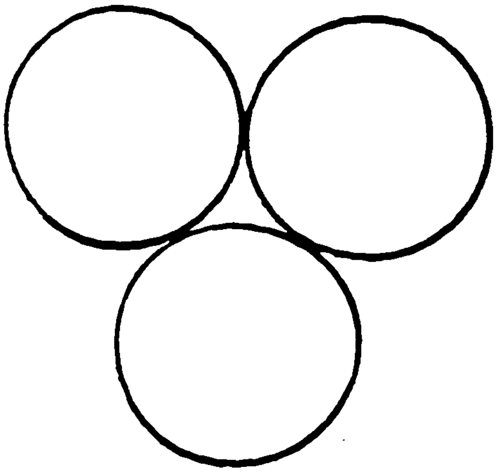

A) Uniform

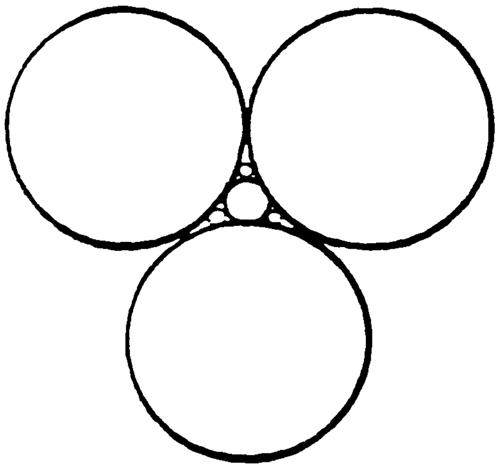

B) Mixed

Figure 2. Uniform and Mixed Particle Arrangements.

(Reprinted from Denevi, p. 25)

CHAPTER 2

THEORETICAL PARTICLE PACKING ARRANGEMENTS

Particle packing arrangements are important to consider in a process where interparticle contact provides sites for particle bonding. The packing density of monosized spheres has an upper limit that can be increased through the use of a bimodal or trimodal mixture of particle sizes.

2.1 PACKING OF MONOSIZED SPHERES

Westman and Hugill [7] showed by packing spherical particles of uniform shape and size that the packing density is independent of the size of the particles. The packing density they obtained for spherical particles averaged about 60%. This was found to be true for particles ranging in diameter from 0.0035 to 0.312 inches. Calculations based on a simple cubic arrangement of identical spheres give a packing density of 52% whereas a hexagonal close packing or face centered cubic arrangement gives a packing density of 74%. When spheres were piled so that the packing in any horizontal layer was hexagonal but in any vertical layer the packing was cubic, the calculated packing density became 60.5%. This packing arrangement was observed in numerous samples and was actually found to be the "prevailing tendency".

There are three main types of packing involving monosized spheres, ordered, random loose and random dense. The random dense packing corresponds to the maximum density without ordering or deformation. A comparison of an ordered array of spheres and a random dense array of spheres is shown in Figure 3. The accepted fractional packing density for the random dense case is 0.637, as reported by German [8]. It is based on careful measurements made by various researchers.

Based on a maximum packing density of 0.637, for monosized spheres, the maximum packing densities involving two or more size spheres were calculated, as shown below, and the values are shown in Table I.

TABLE I. Calculated Maximum Packing Density

Number of sizes	Maximum Fractional Packing Density
1	0.637
2	0.868
3	0.952
4	0.983
5	0.994

These values were calculated assuming that 63.7% of the unoccupied space between particles will be occupied by the addition of the next particle size. The maximum fractional packing density of monosized spheres is approximately 0.64, that of a bimodal mixture is about 0.87 whereas a trimodal distribution can increase the density to about 0.95, as shown

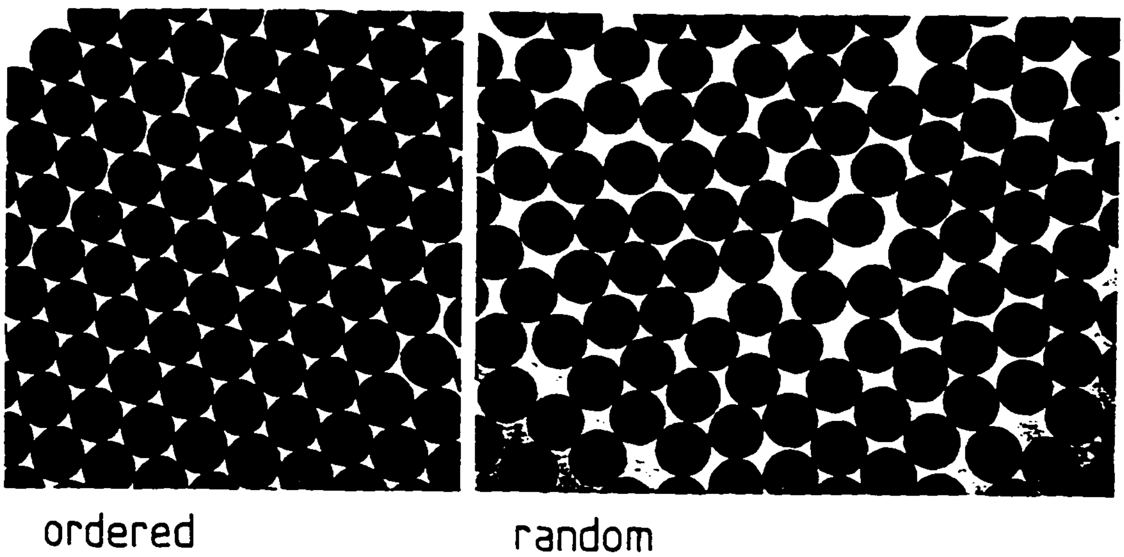

Figure 3. Comparison of monosized disks packed in a close-packed ordered array and a random dense array.

in equations (1) and (2).

$$0.64 + 0.64 * (1 - 0.64) = 0.87 \quad (1)$$

$$0.87 + 0.64 * (1 - 0.87) = 0.95 \quad (2)$$

This assumes an infinite particle size ratio between each particle size.

2.2 TRIMODAL MIXTURES

As described by German [8], evaluation of a trimodal mixture begins by considering the three binary mixtures possible from various combinations of the constituents. The density for each binary system is plotted along the sides of an equilateral triangle. This is analogous to a ternary phase diagram with isodensity contours projected onto the triangle, as shown in Figure 4. Depending on the ratio of sizes, the highest density may occur in the large-small binary. For a small ratio of large particle size to small particle size, i.e., less than 100, a trimodal mixture may not improve the packing density beyond that of a bimodal mixture of small and large components. The effect of particle size ratio on the optimal packing density is illustrated in Figure 5. With greater particle size differences ternary mixtures can yield greater packing densities [8]. Furnas [9] developed a model to predict whether optimal packing would occur in a binary, ternary or higher order system based on the ratio of the particle sizes. Bimodal mixtures give higher packing

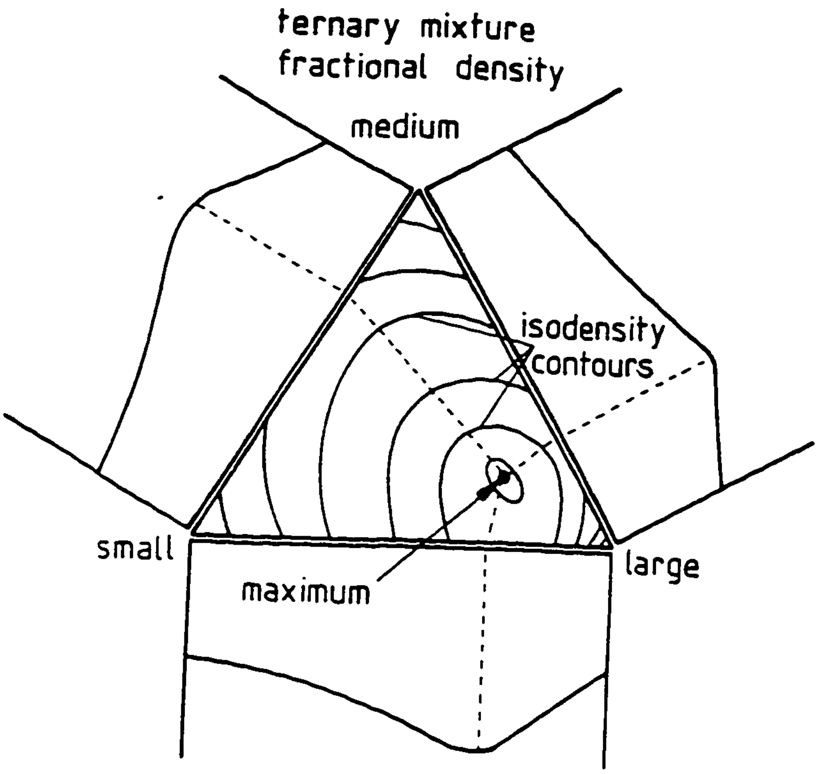

Figure 4. Isodensity contour projections on a ternary composition diagram for a trimodal mixture.

Reprinted with permission from Particle Packing Characteristics, 1989, Metal Powder Industries Federation, Princeton, New Jersey, USA, 1997.

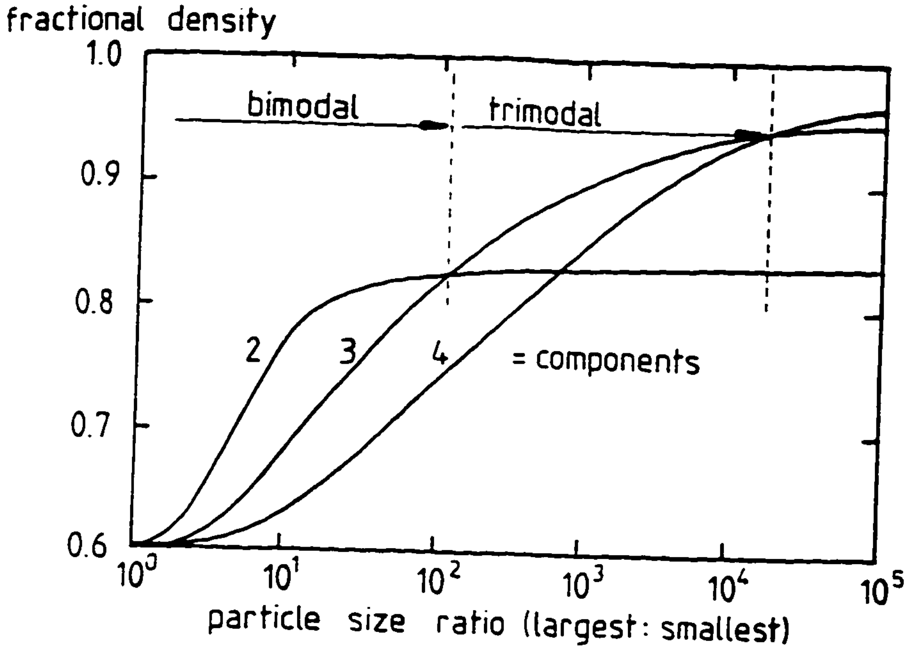

Figure 5. The effect of particle size ratio on the optimal packing density of a material with inherent packing density of 0.6

Reprinted with permission from Particle Packing Characteristics, 1989, Metal Powder Industries Federation, Princeton, New Jersey, USA, 1997.

densities than trimodal mixtures when particle size ratios are less than about 100:1. In order to significantly improve packing characteristics through the use of a trimodal particle size distribution a particle size ratio, of largest to smallest, greater than 100:1 is necessary, as shown in Figure 5. According to German [8], the optimized trimodal packing of spheres in the size ratio of 1:10:100 would consist of 11.2% small, 22.5% medium and 66.3% large, resulting in a fractional density of 0.892. Optimized trimodal packing data gathered by German are shown in Table II.

Table II. Optimized Trimodal Packings of Spheres

size ratio	% fine	% medium	% coarse	fractional density
1:5:25	21.6	9.2	69.2	0.850
1:7:49	13.2	20.7	66.1	0.878
1:7:49	11.0	14.0	75.0	0.950
1:7:77	10.0	23.0	67.0	0.900
1:10:100	11.2	22.5	66.3	0.892
1:100:10000	10.0	23.4	66.6	0.916

CHAPTER 3

LITERATURE REVIEW - PREVIOUS WORK

Particle packing arrangement has a direct effect on the sinterability of powder compacts. The effects of the state of aggregation of ceramic powders, pore shrinkage, particle rearrangement and differences in particle size are examined in this chapter.

3.1 EFFECT OF PARTICLE ARRANGEMENTS

Numerous studies have been conducted on the role the green compact microstructure has on the sintering characteristics of alumina. The lack of homogeneous packing characteristics is known to be detrimental to the sintering behavior of ceramic powders. In a study by Dynys and Halloran [10], the influence of aggregates[1] on the sintering of alumina was examined. They showed that sintering rates decrease with an increase in aggregate content and that sintered density decreased linearly with aggregate content, as shown in Figure 6. They also showed that porosity within the aggregates was eliminated more readily than the large interaggregate voids, resulting in locally dense regions within the aggregates. They suggest that voids from powder aggregates are often the strength limiting flaws in ceramics, and that, in many cases,

---

[1] An aggregate is a mass of particles strongly bound together.

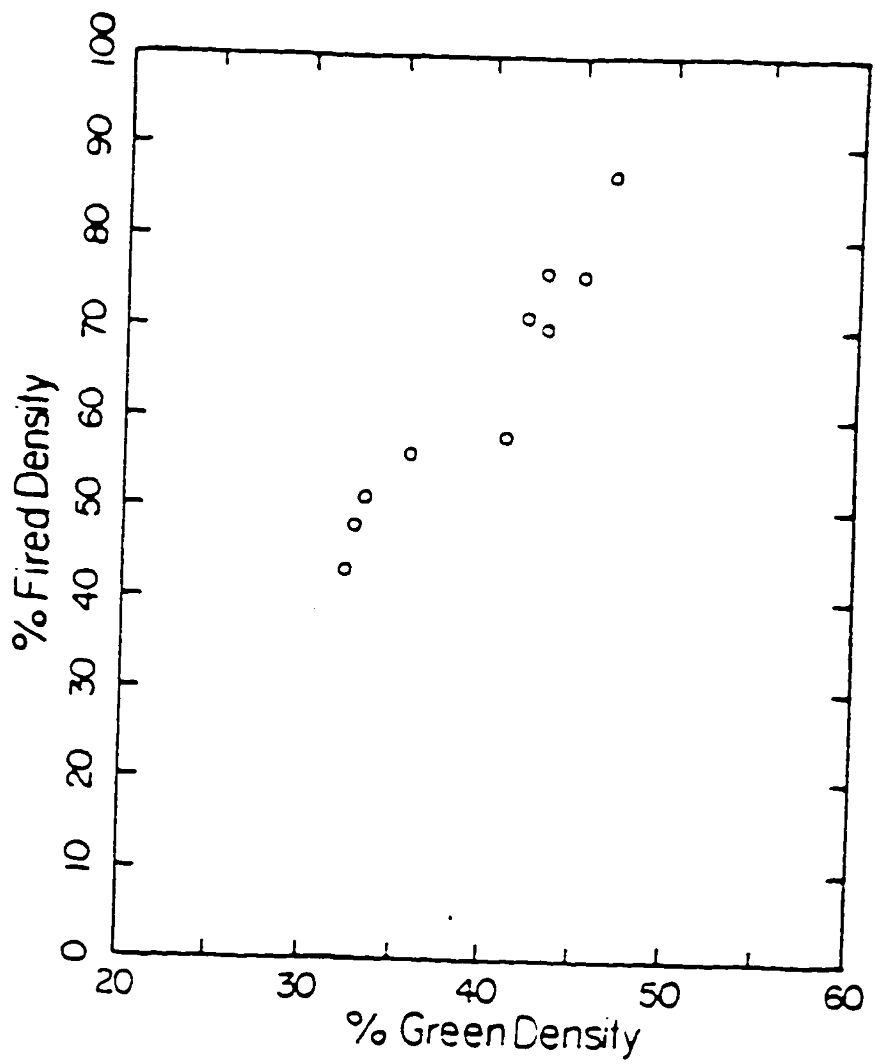

Figure 6. Sintered density as a function of green density for aggregated powders.

(Reprinted from Dynys and Halloran, p. 600) the quality of the ceramic powder depends primarily upon its state of aggregation.

Roosen, Sumita and Bowen [11], investigated the effects of interfacial chemistry on green microstructure development of two alumina powders differing only in their particle size distribution. Each powder was processed by both a colloidal forming technique and by dry pressing. The colloidal forming technique enhanced densification of the green compacts. The compacts with smaller pores exhibited maximum shrinkage rates at lower temperatures. It was therefore concluded that smaller pores can be eliminated at lower temperatures and the compacts with coarser pores densify at higher temperatures. Roosen et al. concluded that, in addition to particle size, particle arrangement is an important factor in the sinterability of green compacts. The sintered densities they measured depended strongly on the microstructure of the green compacts, as can be seen in Figure 7.

3.2 PORE SHRINKAGE

Lange [12] reiterates the importance of particle arrangement in the sinterability of powder compacts. He relates the particle arrangement to the distribution of pore coordination numbers[2], as illustrated in Figure 8. Lange

---

[2] A pore coordination number is the number of neighboring particles forming contacts with a given pore.

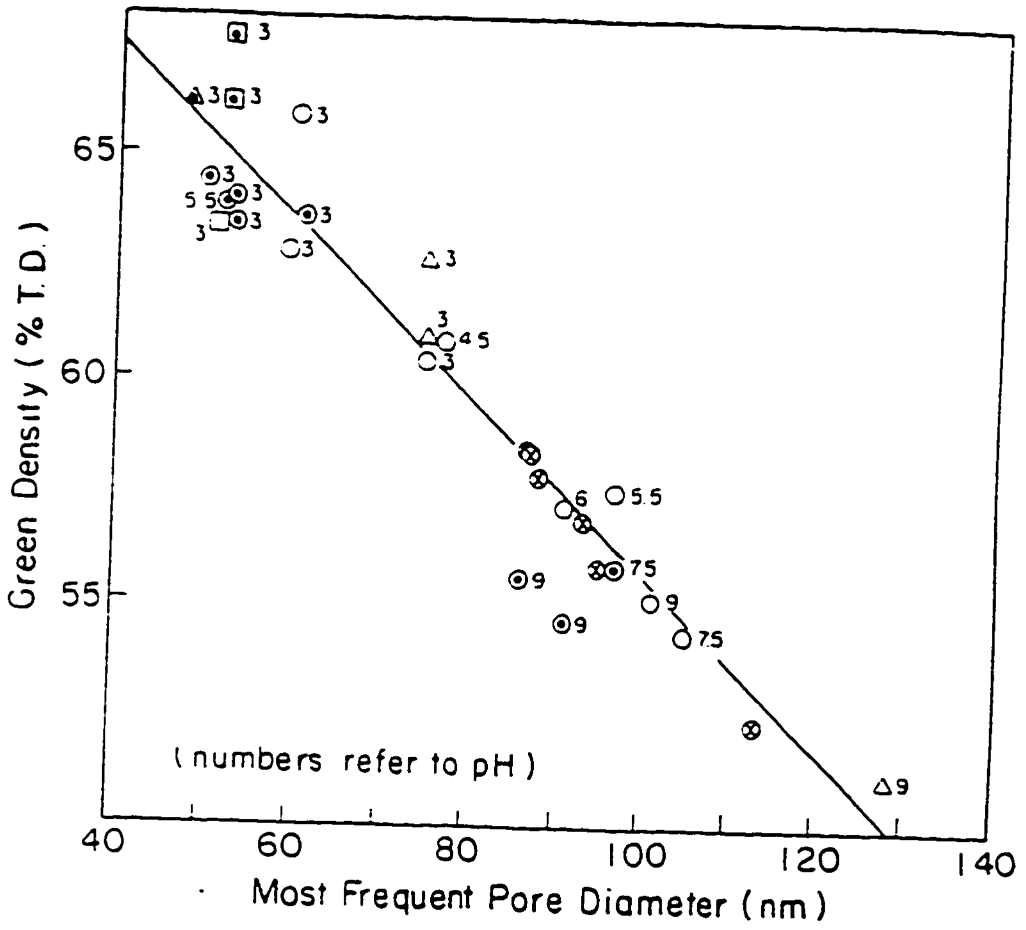

Figure 7. Green density versus most frequent pore diameter. Correlation coefficient = 0.96

(Reprinted from Roosen, Sumiya and Bowen, p. 437)

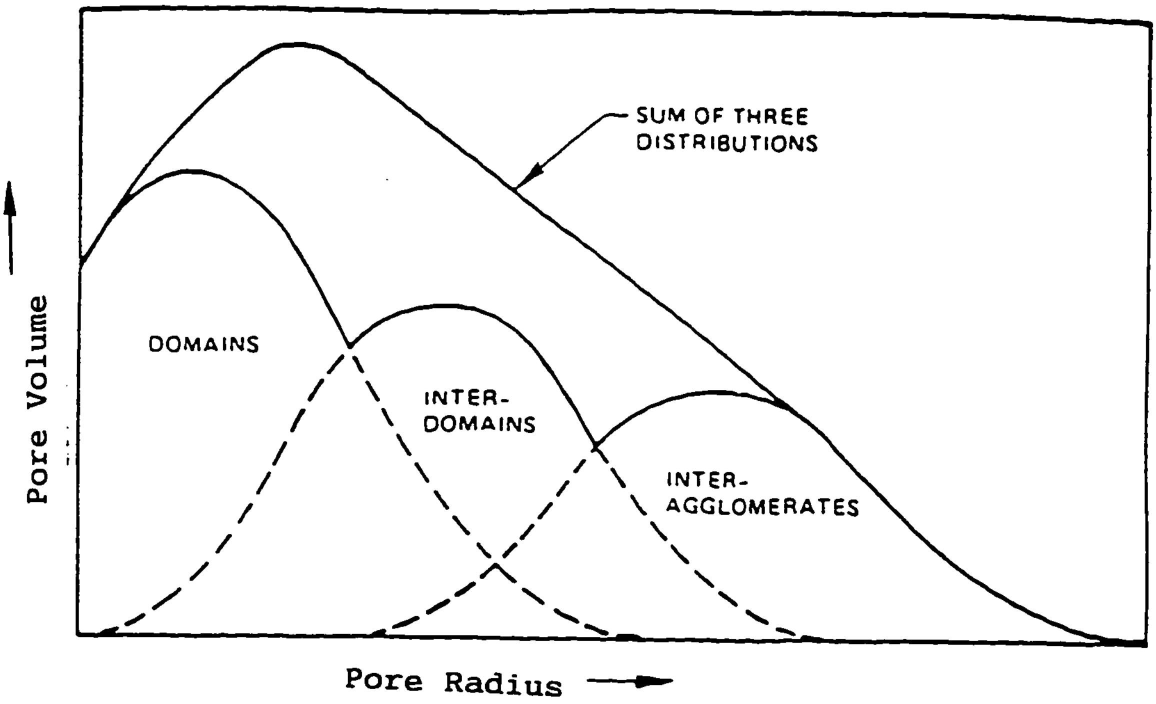

Figure 8. Pore coordination number distribution in agglomerated powders.

(Reprinted from Lange, p.84)

denotes that Kingery and Francois [13] were the first to recognize that only pores with a radius less than a critical size are able to disappear during the sintering process. The theory requires material to diffuse from grain boundaries to the pore surface. Since the direction of the diffusion depends on the curvature of the pore surface, because of the difference in activity, pores with a coordination number smaller than a critical value will shrink whereas those of a larger value will grow. The critical coordination number is the number of neighboring particles producing a change in the surface curvature of the pore from concave to convex. Pore structures with coordination numbers above and below a critical value are shown in Figure 9. Lange states that, from a thermodynamic point of view, the most important property of a pore is its coordination number.

Kellett and Lange [14] show that the free energy and the driving force for sintering increase with an increase in the dihedral angle. The critical coordination number also increases with an increase in the dihedral angle. It is noted that sintering aids that increase the dihedral angle will increase the driving force for sintering to occur. This would in turn increase the number of unstable pores within the compact, thus promoting sintering.

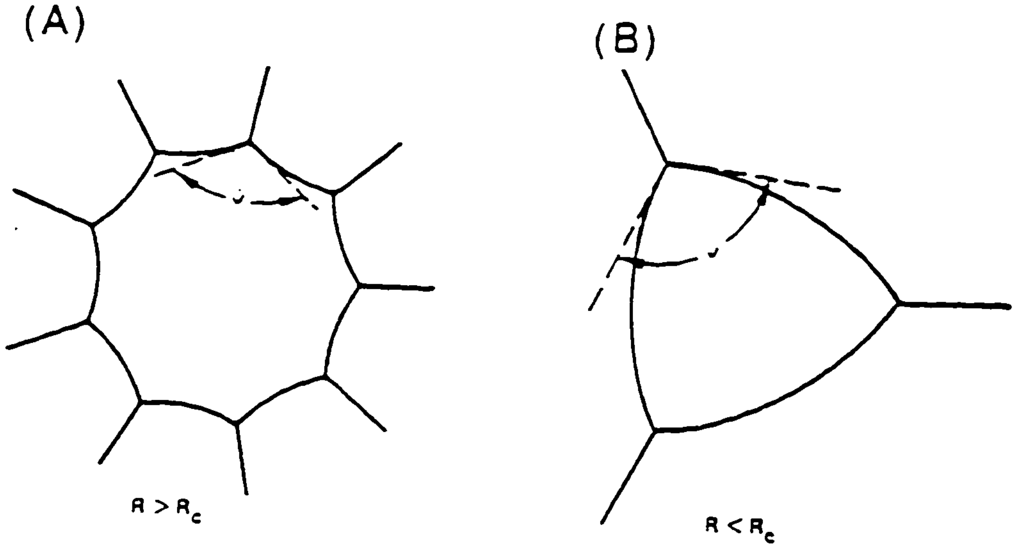

Figure 9. Surface curvature for two pores with same volume and dihedral angle, but with coordinating grain numbers (A) larger and (B) smaller than R_c

(Reprinted from Lange, p. 84)

3.3 EFFECT OF PARTICLE REARRANGEMENT

Flaws appear when high density regions of the powder compact sinter, shrink and pull away from lower density areas. Cracklike voids form which have even higher coordination numbers than before. According to Kellett and Lange, rearrangement processes due to nonuniform packing are potentially the most detrimental phenomenon that occurs during sintering [14]. Grain growth, however, will also reduce a pore's coordination number. This can also enhance densification provided the pore does not become trapped within the grain. Grain growth can occur only in previously densified areas. As the dense region grows the coordination number of the voids between them decreases, thereby improving the chances that further densification will occur. However, if grains become too large mechanical and other desired properties may be compromised.

In an analysis of the effects of particle packing characteristics on solid-state sintering, Zheng and Reed [15], differentiate porosity into two different classes. The first class contains pores all of which are smaller than a critical ratio of pore size to mean particle size. In the second class all pores are larger than the critical ratio. Figure 10 illustrates a coarse micropore in a matrix of fine microporosity. Their results show that porosity of the first class can be eliminated during sintering but the porosity of

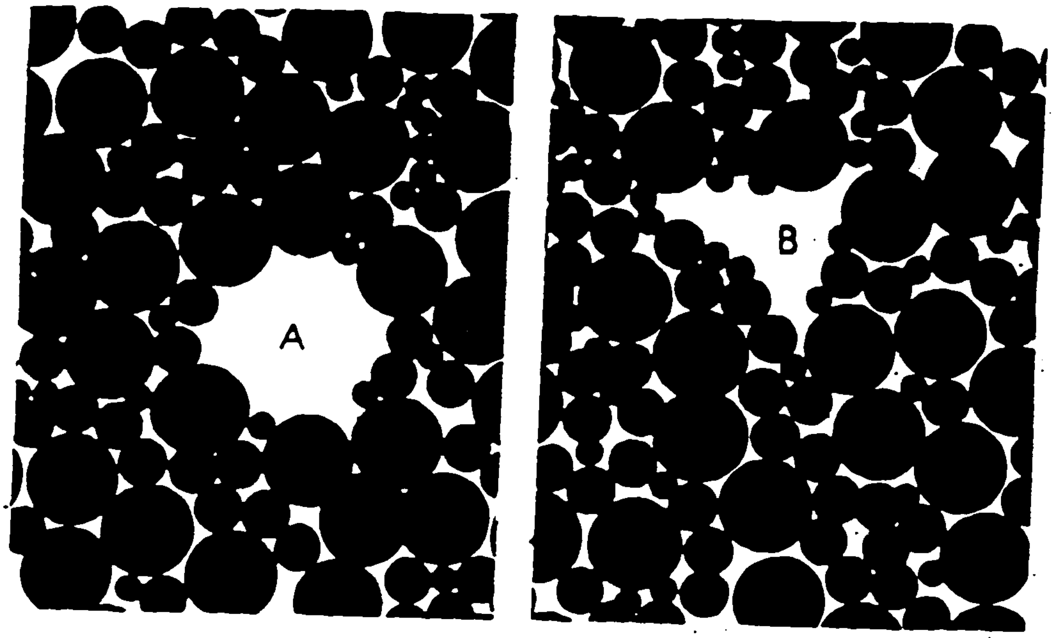

Figure 10: Coarse micropore in matrix of fine microporosity

(A) Pore inclusion; (B) Intergranular pore

(Reprinted from Zheng and Reed, p. 1414) the second class cannot. This leads to the conclusions that final shrinkage is proportional to the porosity of the first class whereas the final sintered density is inversely proportional to the porosity of the second class. This means that when the green density difference between samples is caused by porosity of the second class, i.e., agglomeration, the final sintered density would be proportional to the green density. The sintered density, as a function of green density, for pressed granules with different granular density is shown in Figure 11. It is concluded that to get the highest final sintered density it would be necessary to eliminate pores larger than the critical size when processing the green body. After further research, Zheng and Reed [16] find it necessary to expand their classification of porosity to include an intermediate pore configuration. Pores in this category, coarse micropores, are larger than half the average particle size and smaller than ten times the average particle size, the smaller being termed fine micropores and the larger called macropores. In this analysis they find the micropores are eliminated during sintering whereas the macropores are not. The elimination of coarse micropores is characterized as dependent on granular density. In their explanation of Figure 11, Zheng and Reed say that when the green density becomes larger than the granular density, only fine micropores exist in the compact. But if all macropores can be eliminated, the

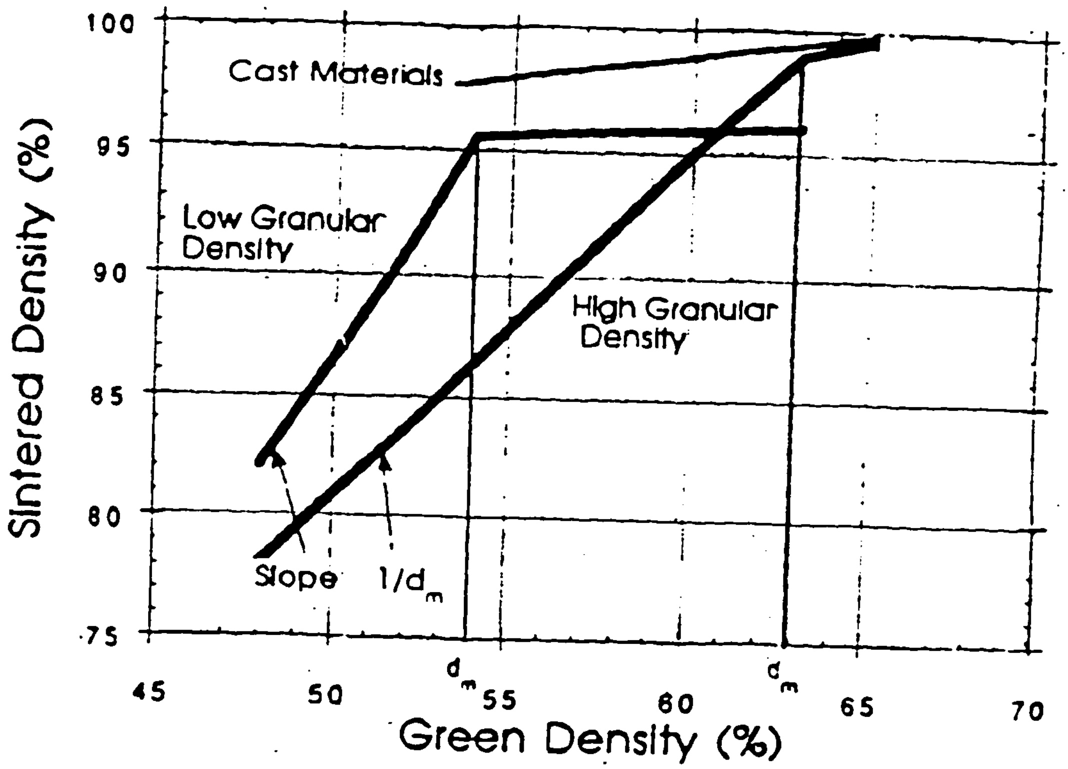

Figure 11. Sintered density versus green density for pressed granules with different granular densities, d_m.

(Reprinted from Zheng and Reed, p. 1414) reason for the difference in the final sintered density between cast and pressed or high and low granular density materials is not clear because the sintered density no longer depends on the green density. It is also not clear if this is due to localized inhomogeneities which vary with the forming process.

3.4 EFFECT OF AGGREGATE SIZE

Lange also agrees that when different size particles are packed at random, fractional bulk densities up to 0.95 are achievable. Such a multimodal system of spheres not only reduces the void volume, but would also reduce the average coordination number. For agglomerated particle arrangements, it is expected that consolidation forces, i.e., hydraulic pressing, will increase bulk density by continuously eliminating the most highly coordinated pores. Lange reasons that some voids within a powder compact have a coordination number greater than R_c and that the volume fraction of these voids will be inversely proportional to the initial bulk density of the compacted powder. This statement would tend to support the idea that higher initial green densities would improve the likelihood of obtaining higher sintered densities, which is one goal of ceramic technology.

Lange points out that it is generally believed that agglomerates limit the bulk density and that, all dry, fine particle size ceramic powders, i.e., less than ten microns, can be expected to contain soft agglomerates. Consolidation forces would tend to eliminate the most highly coordinated pores first. This also coincides with the theory that the coordination number of interagglomerate pores decreases with agglomerate size. The distribution of particle coordination of an agglomerated powder depends on the bulk density and the size distribution of the multiple-particle packing units. Pores of a higher coordination number can be eliminated by increasing bulk density and/or decreasing the packing unit size, i.e., size of the aggregates.

3.5 EXPERIMENTAL STUDIES OF BIMODAL MIXTURES

Smith and Messing [17] showed that binary powder mixtures can be used to enhance the densification of a low-reactivity, coarse powder. The degree of the densification enhancement of the low-reactivity coarse powder was directly related to the volume fraction of the finer powder added, above the calculated composition of the optimal packing density. There was, however, no enhancement of sintering due to fine/coarse particle contacts. The amount of densification for a bimodal mixture can be predicted to a first approximation by knowing the degree of densification of the unimodal fine and coarse powders alone. In their study, the experimental optimal packing occurred where predicted, i.e., at 30% fines. The average density was determined to be 63.5% of theoretical. This was much less than, 79.6% of theoretical, which was the value predicted for a uniformly packed bimodal mixture. A similar trend for experimental density values obtained by Taruta et al. is shown in Figure 12. Smith and Messing [17], postulate that the discrepancy between the experimental specific volumes and the calculated result, similar to that shown in Figure 12, was due to the inhomogeneous mixing of the bimodal mixtures and because the mixtures may not compact as well as the individual components by themselves. The discontinuity in the calculated results in Figure 12 is a result of assuming the ratio of particle size is infinite. This also may add to the discrepancy. They studied bimodal mixtures containing various fractions of fine particles ranging from 0 to 1.0 in steps of 0.1. For compositions of fine particles below 30% by weight, the fine particles should occupy the space between the larger particles. In these materials sintering of the coarse particles should and did appear to control the shrinkage, as can be seen in Figure 13. For compositions where the fines become a continuous matrix, i.e. $w_f > 0.3$, densification is controlled by the sintering of fine particles until the coarse particles come into contact, at which point further densification is controlled by the coarse component. All samples containing a large fraction of fine particles, i.e., $w_f > 0.9$, sintered to the same bulk

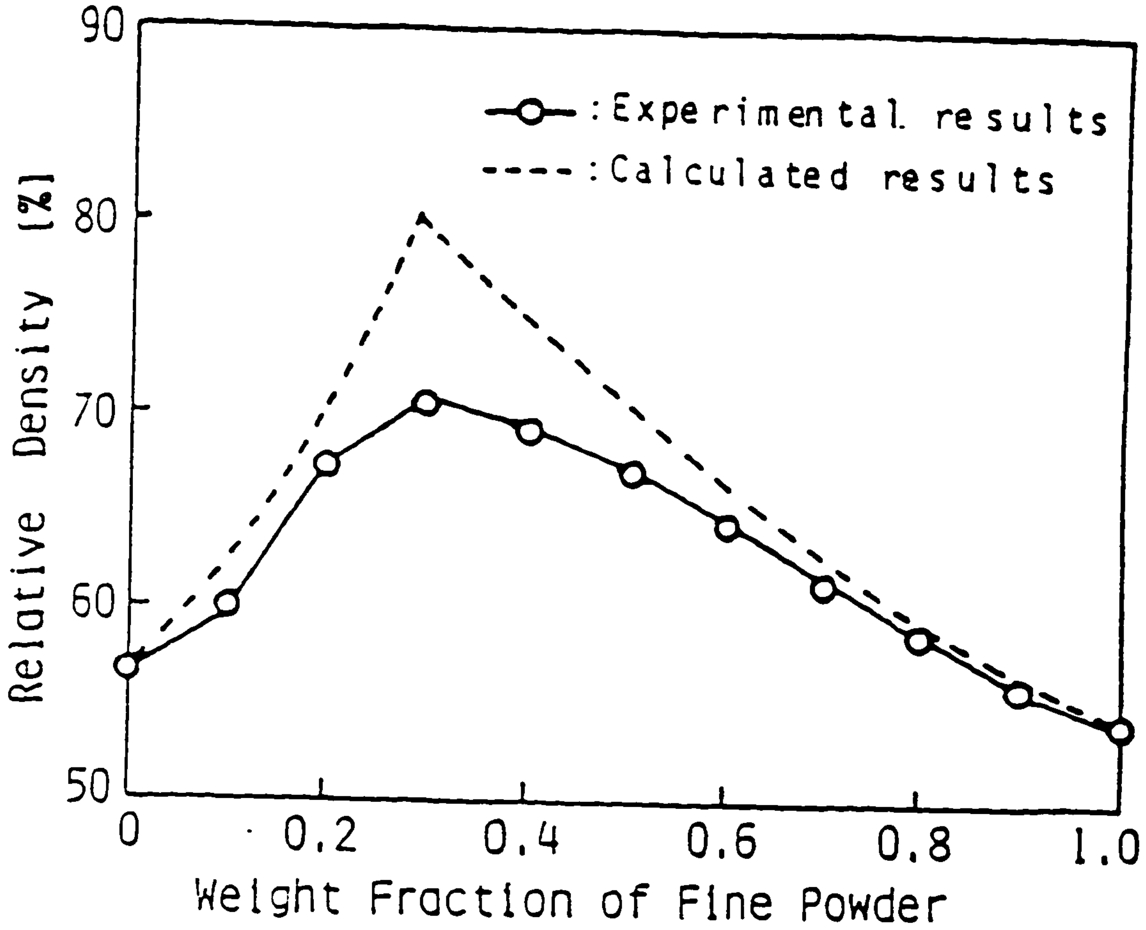

Figure 12. Calculated and experimental packing densities for binary alumina mixtures.

(Reprinted from Taruta, Okada and Otsuka, p. 33)

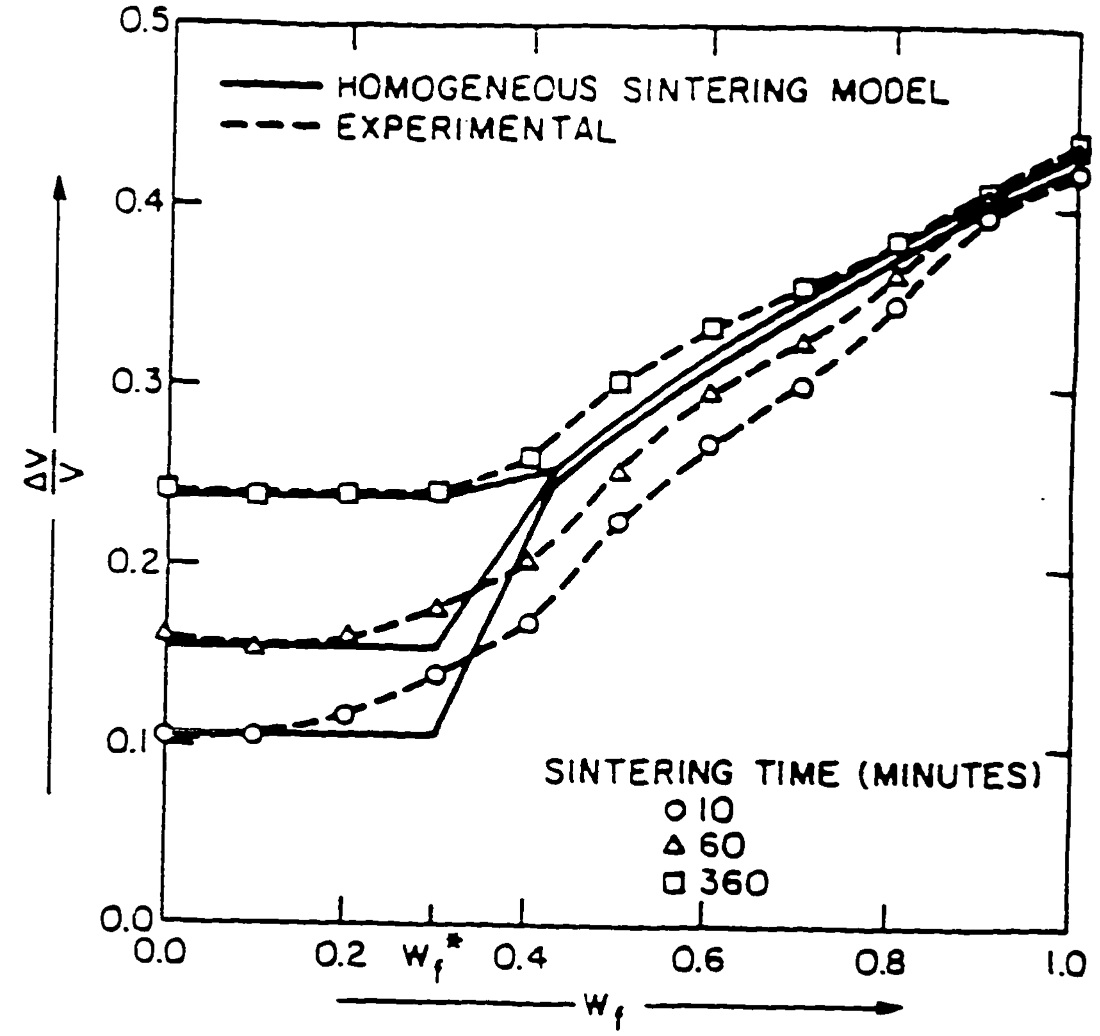

Figure 13. Comparison of Experimental Results to Homogeneous Sintering Model predictions

(Reprinted from Smith and Messing, p. 239) density, thus showing that the fine fraction controls the shrinkage of these mixtures. No enhancement of densification could be attributed to the addition of the coarse materials.

Smith and Messing [17] found it very difficult to distinguish microstructural features as a function of the original powder in the later stages of densification. However, the bimodal mixture contributed to a more uniform grain structure. Binary mixtures would however experience exaggerated grain growth under extended sintering times. Smith and Messing are convinced that bimodal mixtures may be "a feasible approach for ceramic fabrication on the basis of reduced shrinkage and the use of lower-cost coarse powder."

Taruta et al. [18] investigated the sintering behavior of bimodally distributed alumina powders with regards to the open pore size distribution. They examined the pore size distribution of the compacts both before and after firing for mixtures of course(c) and fine(f) particles ranging from c:f=10:0 to c:f=0:10. They found that for the specimen having c:f=7:3, the voids formed by coarse particles were not fully packed with fine particles. Two different pore sizes suggest a tightly packed region and a loosely packed region exist within the compact. As the fine component was increased the loosely packed regions began to decrease. For the compacts containing a large fraction of coarse particles broader pore size distributions were observed. After firing, the pore size for specimens having c:f=10:0 did not change. Firing increased the pore size in specimens having c:f=9:1 to 4:6. In those mixtures between c:f=3:7 to 1:9 there again was no change in pore size. In the compact composed only of fine particles the pore size decreased. The coarse particles appear to inhibit pore elimination. It is thought that firing decreases the pore size in the tightly packed regions where sintering proceeds faster but the pores grow in the loosely packed region due to the shrinkage of the tightly packed region. Theory suggests that pore growth is due to the difference in sintering speed between various sized particles. From the microscopic examination of the sintered bodies made from various powder mixtures sintering between fine particles is hindered by the presence of coarse particles. However the sintering between coarse particles is accelerated by the presence of fine particles. This is attributed to the development of stresses produced in part by particle rearrangement.

CHAPTER 4

RESEARCH HYPOTHESIS AND OBJECTIVES

Although some problems may arise from a broad range of particle sizes, it is expected that higher sintered densities, with lower shrinkage during sintering, can be obtained by maximizing the pre-sintered density and by optimizing particle rearrangement through the use of a trimodal mixture of particle sizes.

The objective of this study was to examine the effects of a trimodal particle size distribution on the sintering characteristics of alumina. This was done by measuring the initial green density, the final sintered density and porosity, and the shrinkage for a series of specimens. This investigation evaluated the relationships between the presintered density, i.e., green density, shrinkage after sintering, and the sintered density. By subjecting a series of particle mixtures to identical processing conditions and comparing the resulting characteristics, the effects of particle size distribution were determined.

CHAPTER 5

EXPERIMENTAL METHODOLOGY

Before processing, the raw materials must be characterized. After sintering, the products must also be evaluated. This chapter describes the characteristics of the raw materials and the equipment, used in this evaluation.

5.1 MATERIALS

High purity alumina powders were obtained in the form of three distinct products that were donated by Ceralox Corporation, namely, HPA-1.0, HPA-0.5 and DISPERAL. The HPA-1.0 is a 99.99% pure alumina powder with a nominal mean particle size of 1 micron. The HPA-0.5 is a 99.99% pure alumina powder with a nominal mean particle size of 0.5 micron. The DISPERAL, used as the fine component, is a sol-material, monohydrate of alumina which has particle sizes ranging to as low as 25 angstroms. The particle size distribution of the fine component shifted downward with time in solution. The data reported in this study was the minimum observed, however the absolute minimum was not determined. A very large difference in size ratio is theoretically desirable, however in reality it would be difficult to process and would be impractical. These materials were chosen for this examination to investigate the supposition that by sintering materials composed of mixed particle sizes, product shrinkage may be minimized and sintered density may be maximized. Chemical analysis, as provided by Ceralox Corporation, is contained in Appendix A.

Particle size data was obtained by dispersing the sample in a solution of one percent acetic acid in water using an ultrasonic wand. The solution was then analyzed using a Shimadzu SA-CP4 Centrifugal Particle Size Analyzer. Particle size data obtained for all mixtures are found in the Appendix B. Ideally each product particle size should differ from the next by a factor of ten. An analysis of the optimal particle size distribution and weight distribution for trimodal packing of spheres are presented in Appendix C and D, respectively.

It was decided to include a binder into the final product to reduce the friability of the pressed pellets. The binder chosen was PEG Compound 20M, provided by Union Carbide. In the Union Carbide product literature, Walker, Reed and Verma [19] describe that compacts pressed from granules containing PEG binders resulted in higher green density with fewer distinct granules persisting in the pressed matrix. The sintered density was also quite high and the sintered shrinkage was also minimized over other conventional binders. A preliminary evaluation, along with their recommendation led to the use of a level of 3% PEG 20M in each particle mixture that was prepared. A technical data sheet for Union Carbide Polyethylene Glycol 20M is included in Appendix A.

5.2 EQUIPMENT

The equipment used in this evaluation are listed in Table III. The ultrasonic bath and wand and the magnetic stirrer were used to disperse the fine powders in solution during mixing operations. The drying oven was used to evaporate the aqueous solution used to disperse the powder mixtures. A mortar and pestle were used to grind the dried powders and a 100 mesh sieve was used to obtain the final form of the powders used for pressing pellets. The mold and die unit is shown in Figure 14. It consists of a 1 inch diameter steel cylinder with a 0.5 inch diameter hole through the center. Two 0.5 inch cylindrical steel bolts inserted in either end of the hole in the steel sleeve provided the compression surfaces to form the alumina compacts. A pressure of 11.5 ksi (46 MPa) was applied to the ends of the die with a hydraulic press to form each 0.5 inch diameter pellet. A photograph of the pellet press and mold in the compression position are shown in Figure 15. Powdered stearic acid was applied to the mold and die surfaces to provide lubrication during pellet pressing. A CM furnace was used to sinter the alumina pellets. The STAMPFVOLUMETER model STAV2003 was used to measure tap density and the pycnometer and balance were used to determine the sintered density. Particle size measurements were made using a Shimadzu SA-CP4 Centrifugal Particle Size Analyzer.

TABLE III. EQUIPMENT USED IN THIS STUDY

Ultrasonic Bath and Ultrasonic wand
Magnetic Stirrer w/magnets
Beakers and storage containers
Drying Oven (100°C)
Pellet Press w/mold and die, i.e. compression machine
Calipers (metric)
CM Furnace
Pycnometer
Balance accurate to 0.0002 grams
tweezers
Computer for compiling and graphing data
Mortar and Pestle
100 Mesh Sieve
STAMPFVOLUMETER model STAV2003
Powdered stearic acid (lubricant)
Shimadzu SA-CP4 Centrifugal Particle Size Analyzer

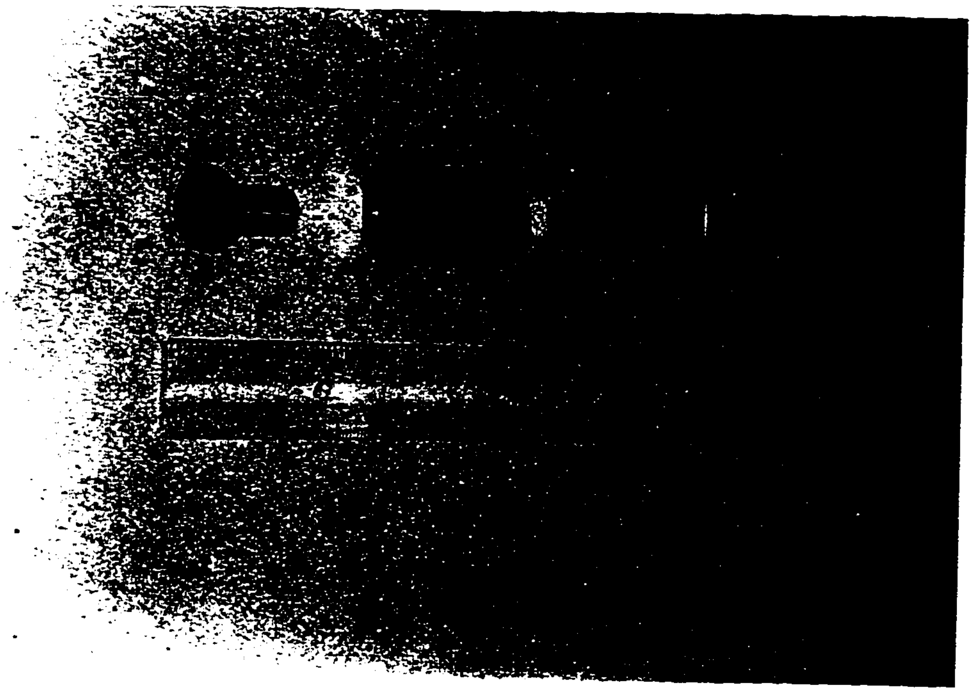

Figure 14. Mold and Die Unit

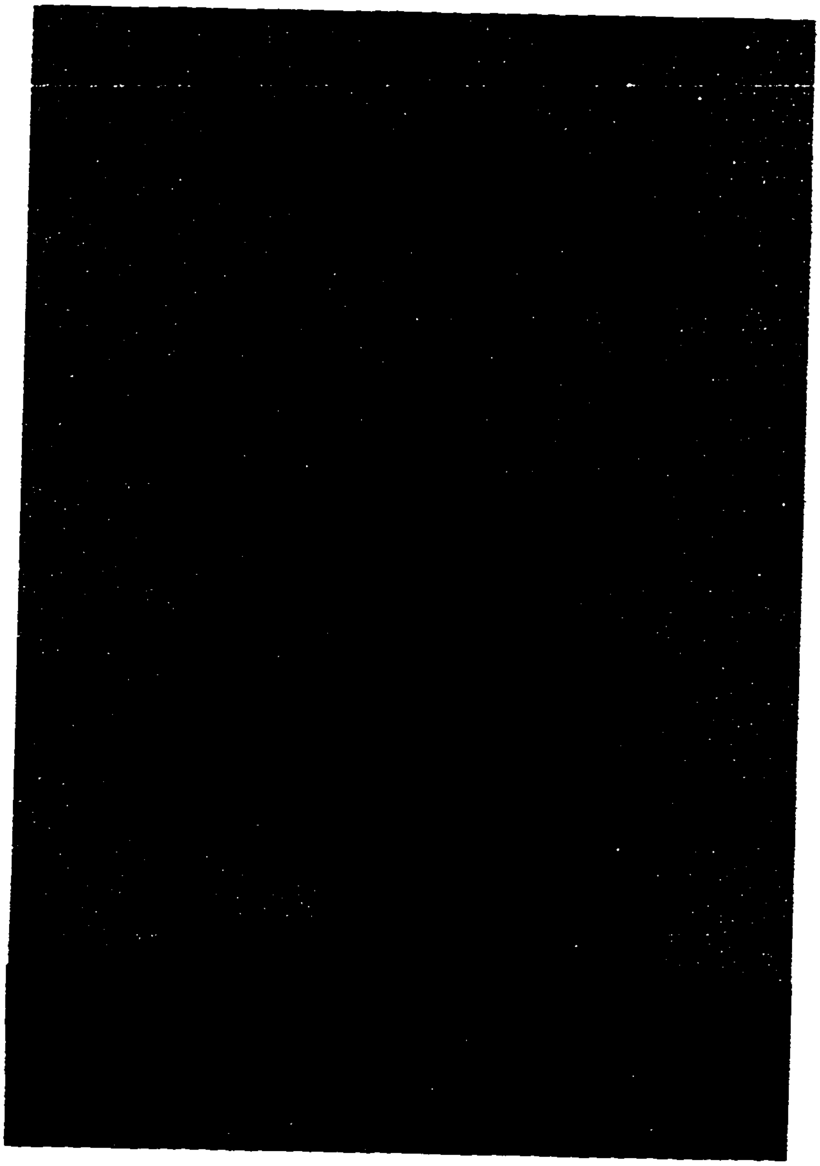

Figure 15. Pellet Press/Compression Machine

CHAPTER 6

PROCEDURE

The objective of this study was to examine the effects of a trimodal particle size distribution on the sintering characteristics of alumina. This was done by measuring the initial green density, the final sintered density and porosity, and the shrinkage for a series of specimens. Initially these sintering characteristics were determined for specimens of each of the three different particle sized raw materials. These sintering characteristics were then measured for bimodal and trimodal mixtures obtained from these raw materials. As shown in Table IV, these mixtures contained between 60 to 90 weight% coarse material, with the remainder being made up of varying fractions of medium and fine powder. Figure 16 shows the experimental compositions on a ternary diagram. Five replicates of each material were sintered. Average values and standard deviations were also determined.

6.1 POWDER PROCESSING

A flow diagram of powder processing steps and property determination methods is shown in Figure 17. To enhance mixing of the powders, the appropriate fraction of each powder was dispersed in 1% acetic acid in deionized water to form a slurry containing 50% solids by weight. The slurry also contained the appropriate amount of the binder, i.e., 3% based

TABLE IV. Composition of Specimens to be Analyzed (wt%)*.

Sample Number	Coarse Powder	Medium Powder	Fine Powder
	HPA-1.0	HPA-0.5	DISPERAL
100	100	0	0
010	0	100	0
001	0	0	100
640	60	40	0
631	60	30	10
622	60	20	20
613	60	10	30
604	60	0	40
730	70	30	0
721	70	20	10
712	70	10	20
703	70	0	30
820	80	20	0
811	80	10	10
802	80	0	20
955	90	5	5

* All samples contain 3% binder.

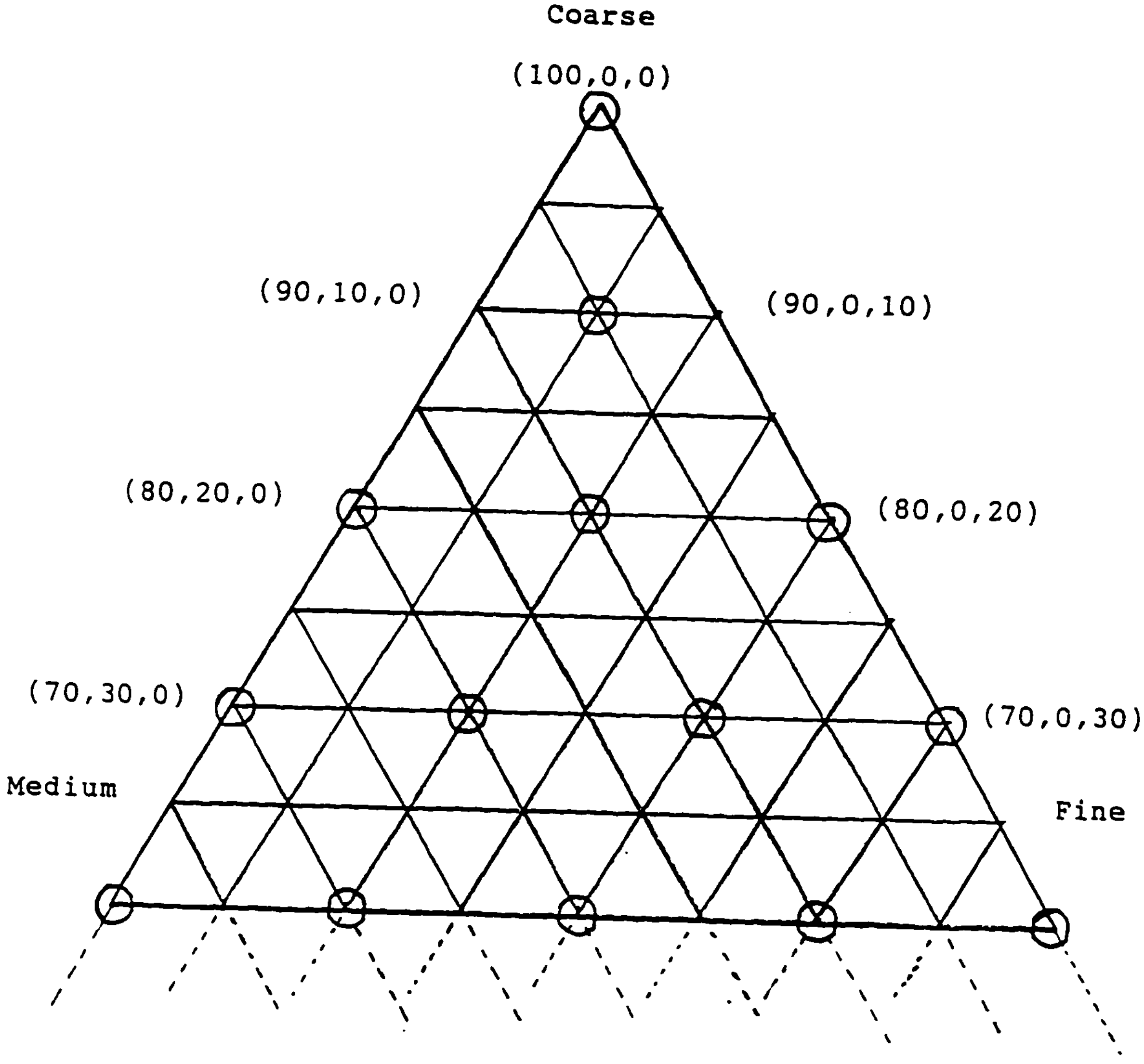

Figure 16. Ternary Diagram Showing Composition of Experimental Specimens

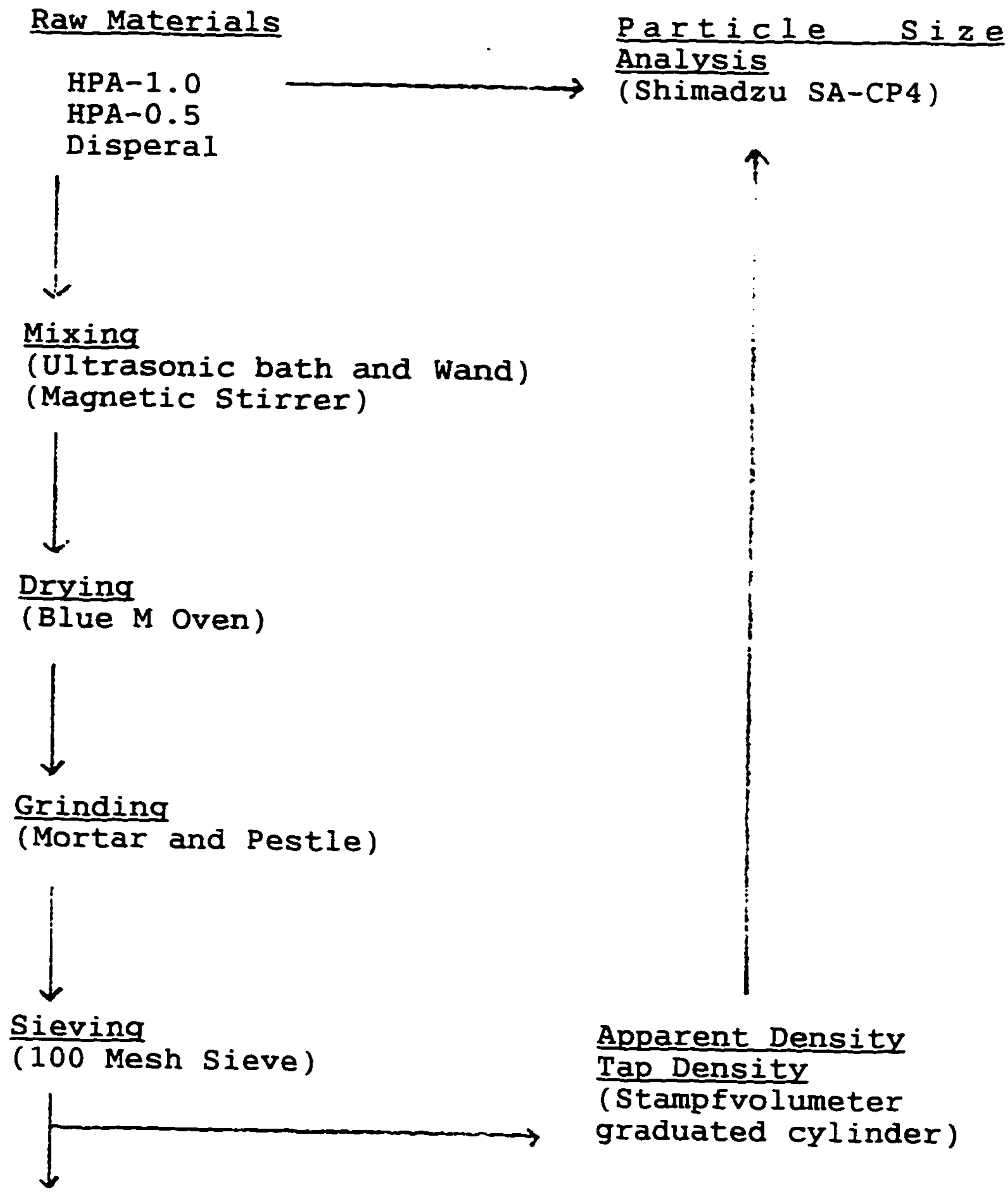

Figure 17. Flow Diagram of Ceramic Powder Processing and Property Determination Methods

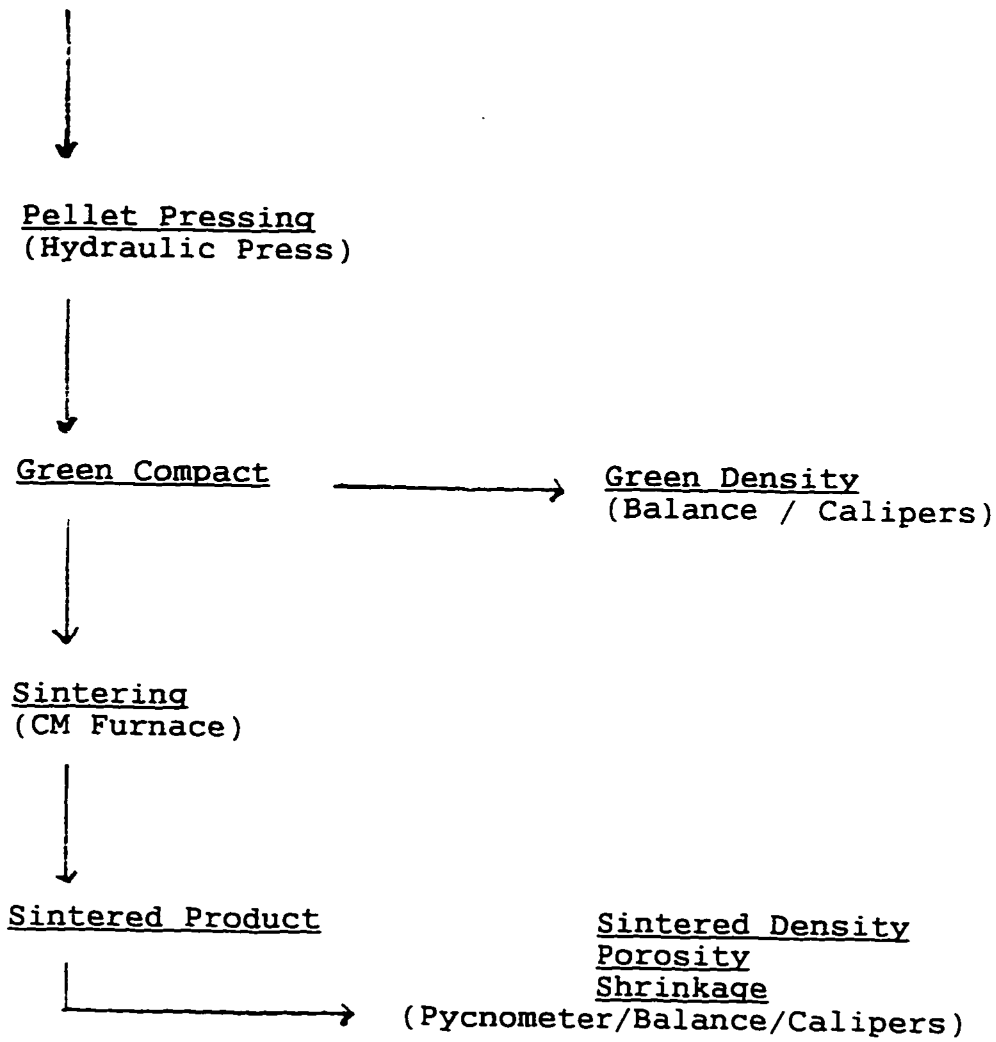

Figure 17. Flow Diagram of Ceramic Powder Processing and Property Determination Methods (continued)

on the dry weight of powder. Dispersion of the finest particles was done by adding the powder, at a level of 30% by weight, to the liquid containing the binder while the liquid was placed in an ultrasonic bath. The aqueous alumina suspension was then stirred with a magnetic stirrer while the slurries were combined to make a single slurry containing all three powders. The water was evaporated in an oven at 95°C until a constant weight had been obtained. The "monosized" materials were also dispersed in the same manner and dried to incorporate the binder into the final powder. When dry these materials were ground with a mortar and pestle and sieved through a 100 mesh screen. They were then placed in polyethylene bags and kept in a desiccator until needed for making pellets.

6.2 POWDER DENSITY MEASUREMENTS

After mixing, drying, grinding and sieving, the apparent density and the tap density were measured for each powder. Apparent density was measured using a modified version of test method A of ASTM D1895-69. The cylindrical measuring cup specified in this method was replaced with a 10 ml graduated cylinder. The tap density was measured according to ASTM B527-85 using a Stampfvolumeter model STAV2003. Tap density measurements are tabulated in Appendix E.

6.3 PELLET PRESSING

Five pellets were produced from each batch of mixed powders using the pellet press/compression machine shown in Figure 15. Approximately 0.8 grams of material was weighed and put into the mold which was prelubricated with stearic acid. The piston was inserted into the mold and the powder was compacted until the pressure gauge read 11.5 ksi, approximately 47 MPa. The pressure was maintained for approximately two minutes before being released slowly. The pellet was then removed from the mold. The green density was determined from the mass and dimensional measurements using a balance and a pair of vernier calipers.

6.4 PELLET SINTERING

Sintering was carried out using a high temperature furnace. Five pellets were placed approximately 1 inch apart on a platform consisting of two triangular rods of a refractory material. The samples were placed such that contact was minimized and uniform heating could be maintained. The pellets were also elevated to near the center of the furnace, by means of several layers of insulating material. All specimens were sintered in the same manner. A photograph of this set-up is shown in Figure 18. The furnace was programmed to go from ambient temperature to 1550°C in a period of 12 hours. It remained at 1550°C for two minutes

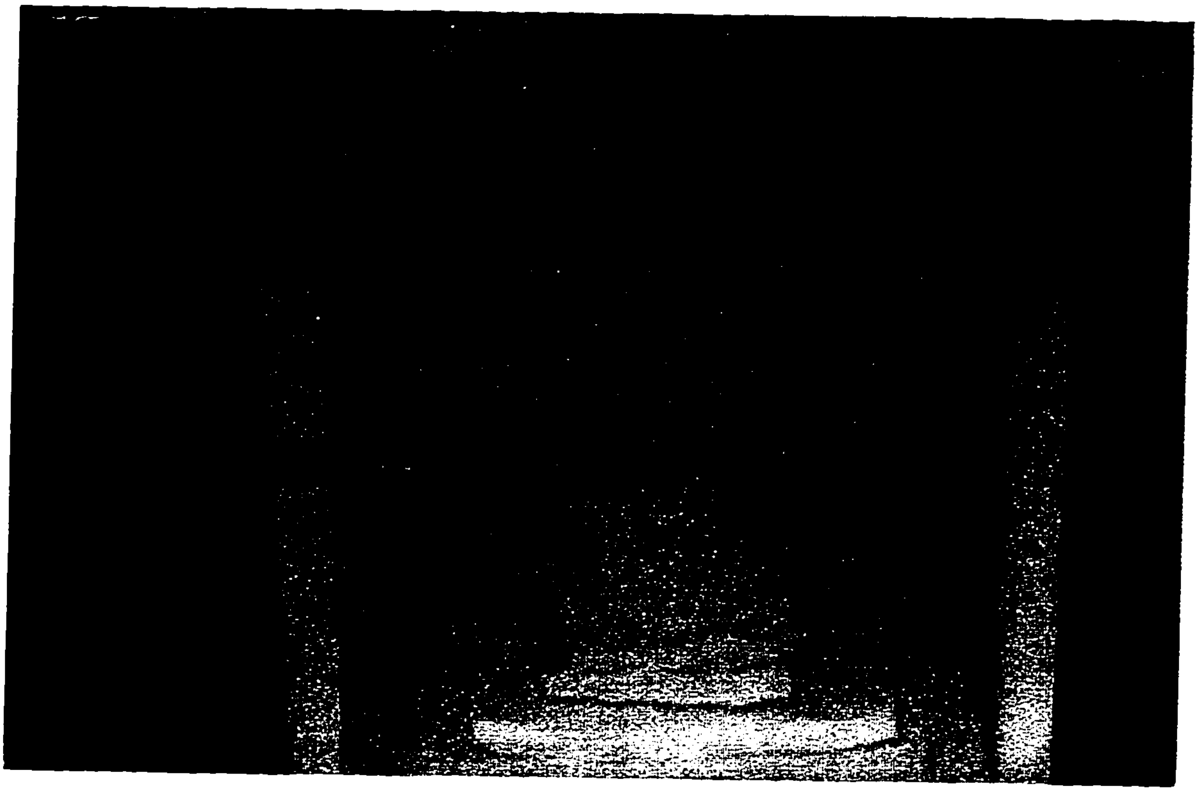

Figure 18. Furnace and Sintering Platform

then returned to ambient over the next two hours. After sintering, the density and porosity were measured again in a manner similar to that described in Section 6.3. The fired, sintered density was also measured using a pycnometer. Sintered density measurements are tabulated in Appendix F.

CHAPTER 7

EXPERIMENTAL RESULTS

Sixteen different alumina powder mixtures were prepared for this study. The powder mixtures included three bimodal mixtures of coarse and medium and three bimodal mixtures of coarse and fine powders. In these mixtures the coarse component ranged from 60% to 80% of the composition, the remainder consisted of either the medium or the fine component. Seven trimodal mixtures were also among those prepared. In these mixtures, the coarse component ranged from 60% to 90% with the remainder consisting of the medium and fine materials. A preparation of each of the raw materials was also evaluated. A particle size distribution comparison for all three raw materials is shown in Figure 19. Particle size data and SEM photographs obtained for each of the three raw materials are shown in Figures 20 through 25. In this chapter density comparisons will be made for each of these mixtures. The density measurements evaluated include: the apparent density or loose packed powder density, the tap density also referred to as the maximum density attainable without compression, the Hausner ratio, the green density and the sintered density.

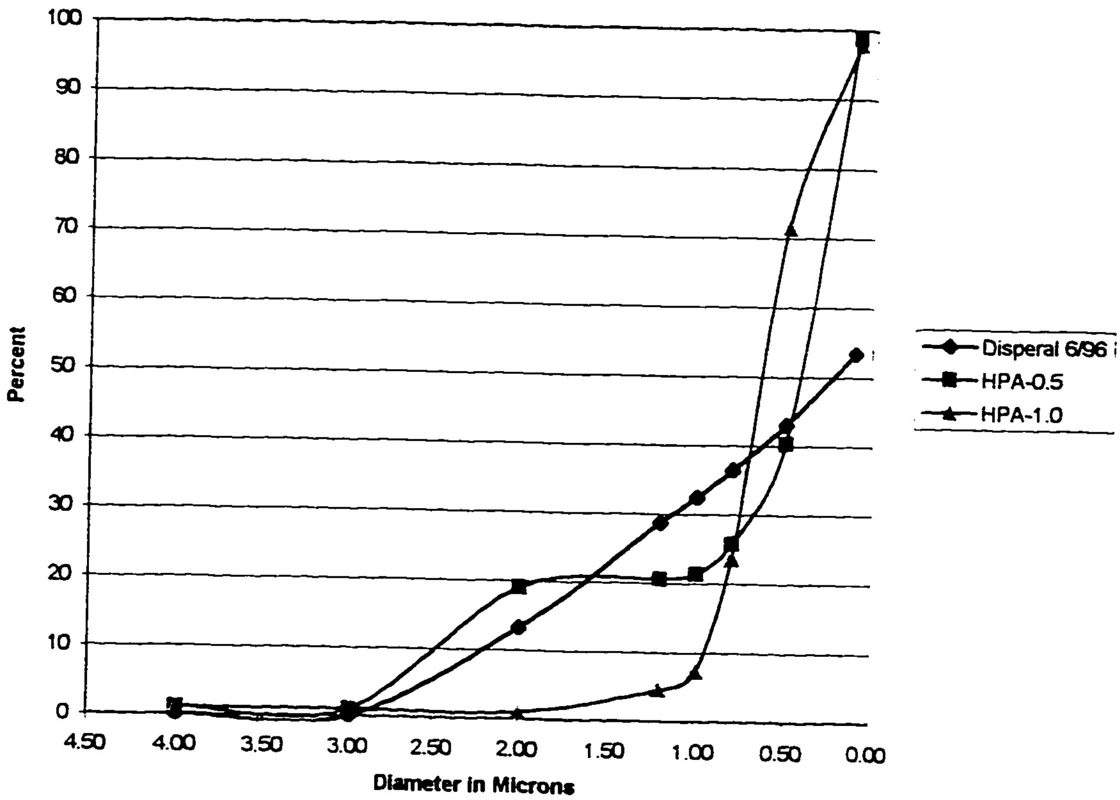

Figure 19. Cumulative Particle Size Distribution Comparison

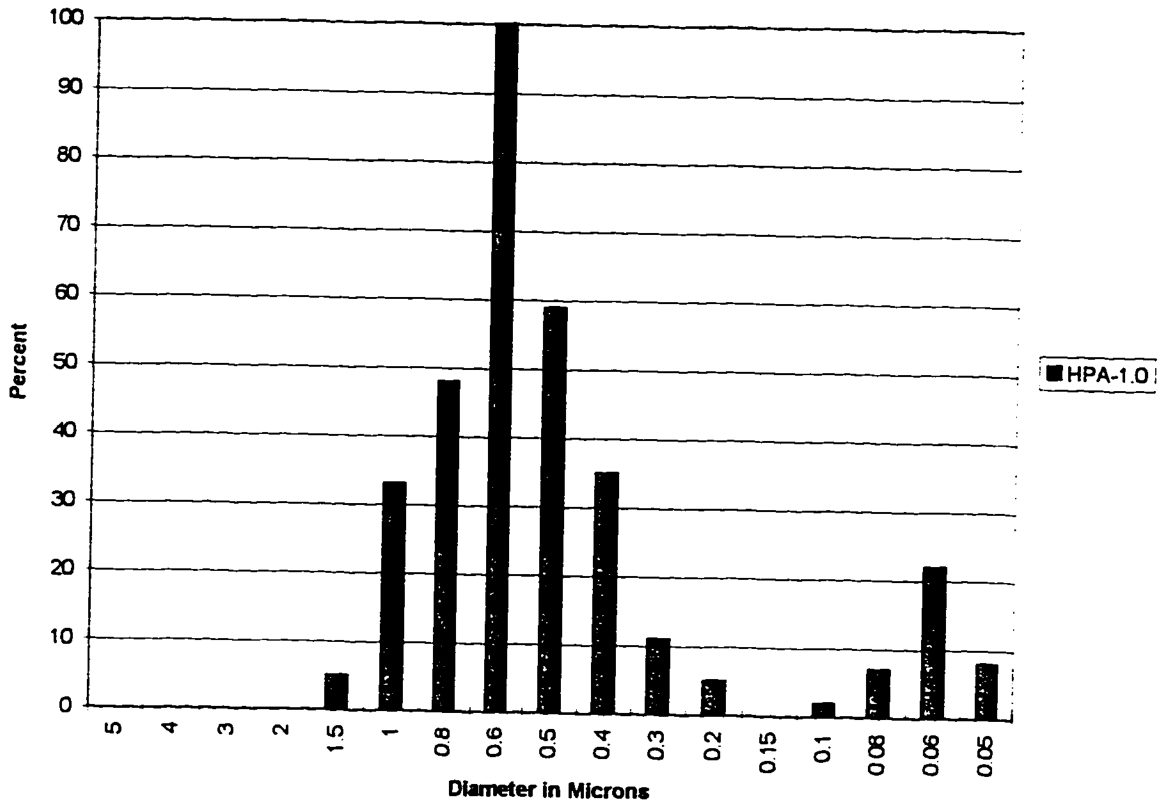

Figure 20. Particle Size Analysis for Coarse Component

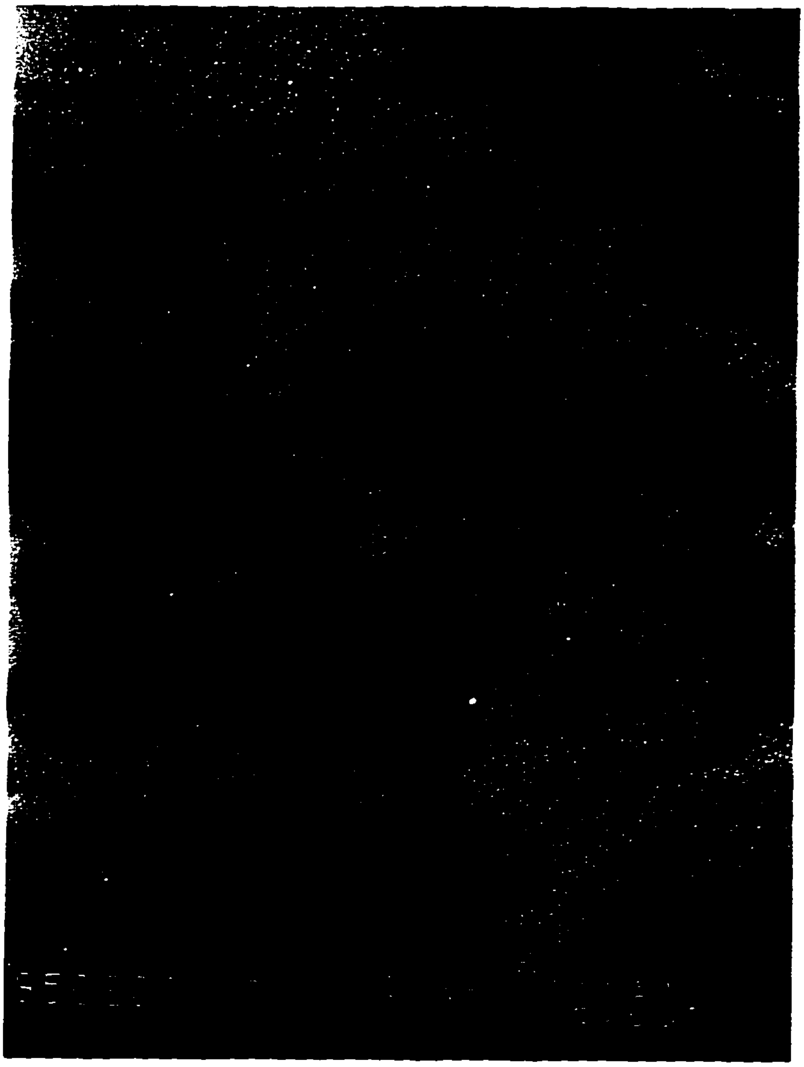

Figure 21. SEM micrograph of Coarse Component

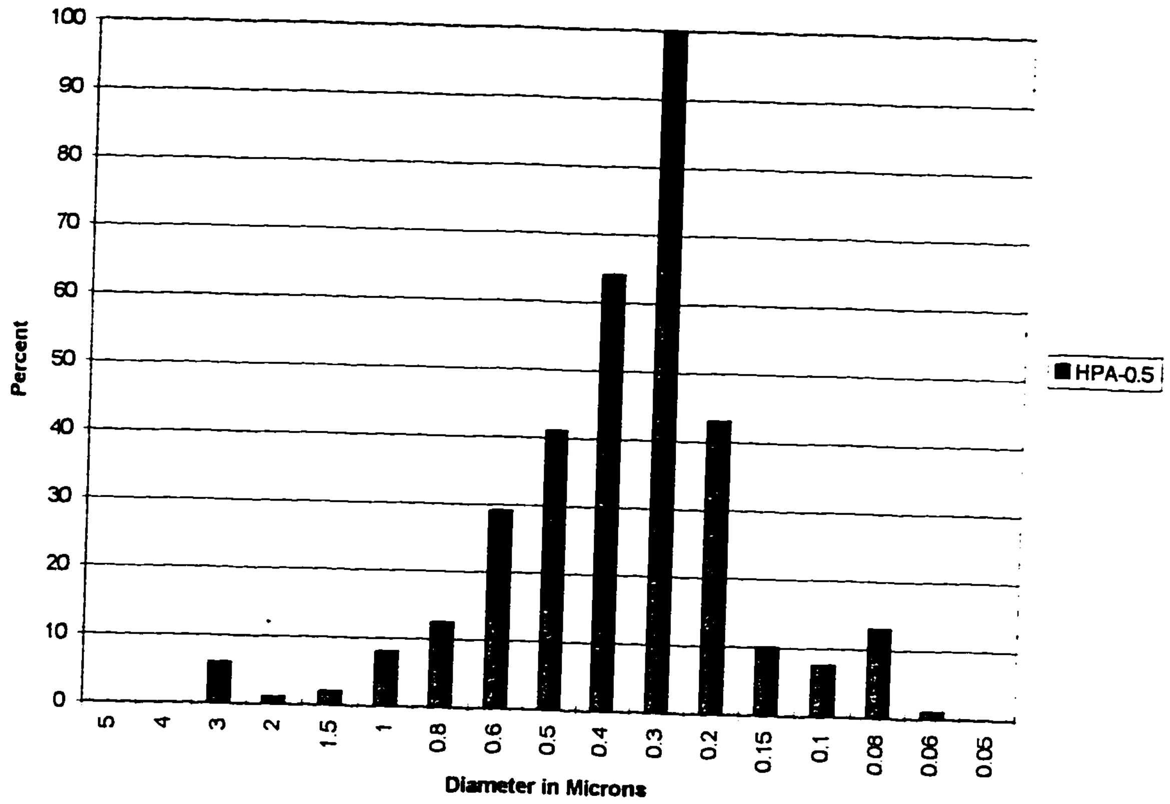

Figure 22. Particle Size Analysis for Medium Component

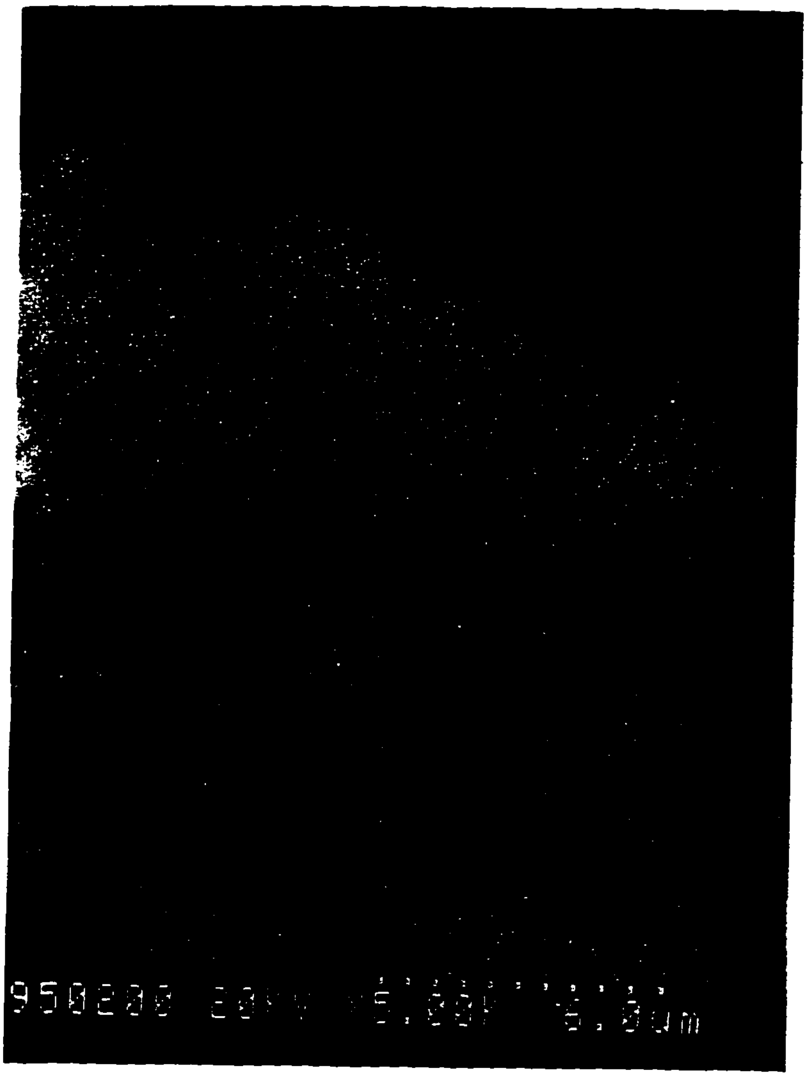

Figure 23. SEM micrograph of Medium Component

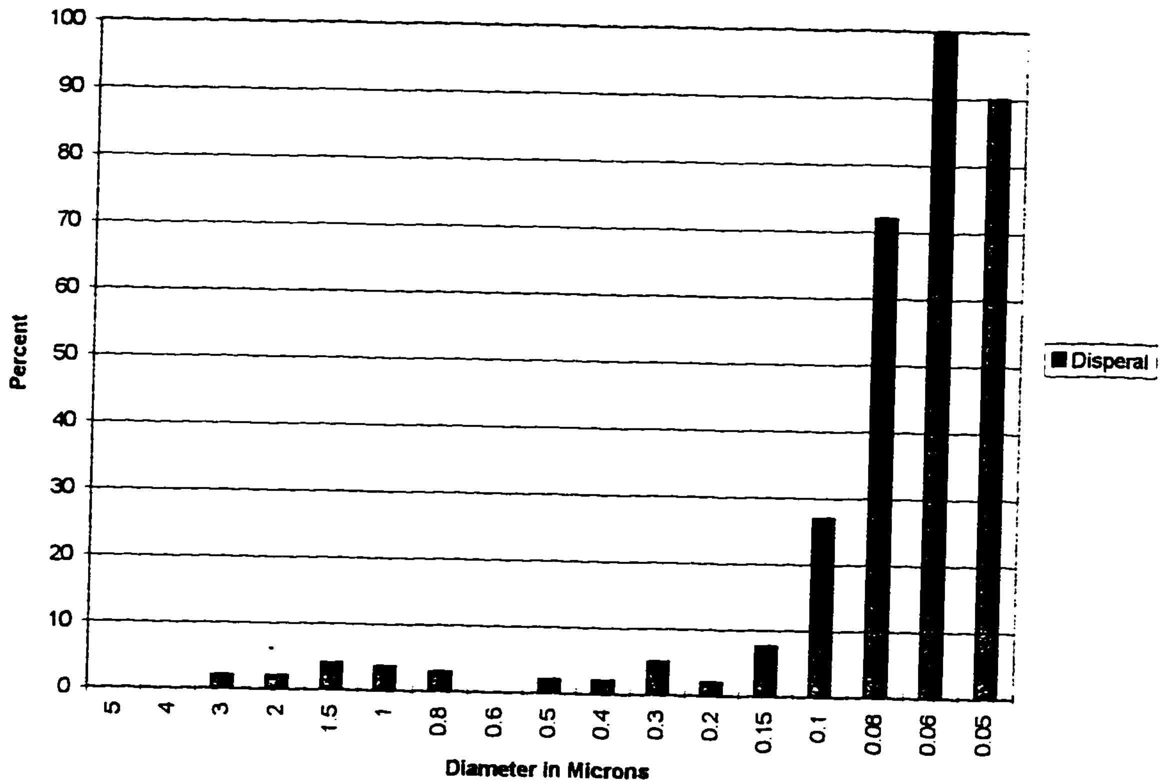

Figure 24. Particle Size Analysis for Fine Component

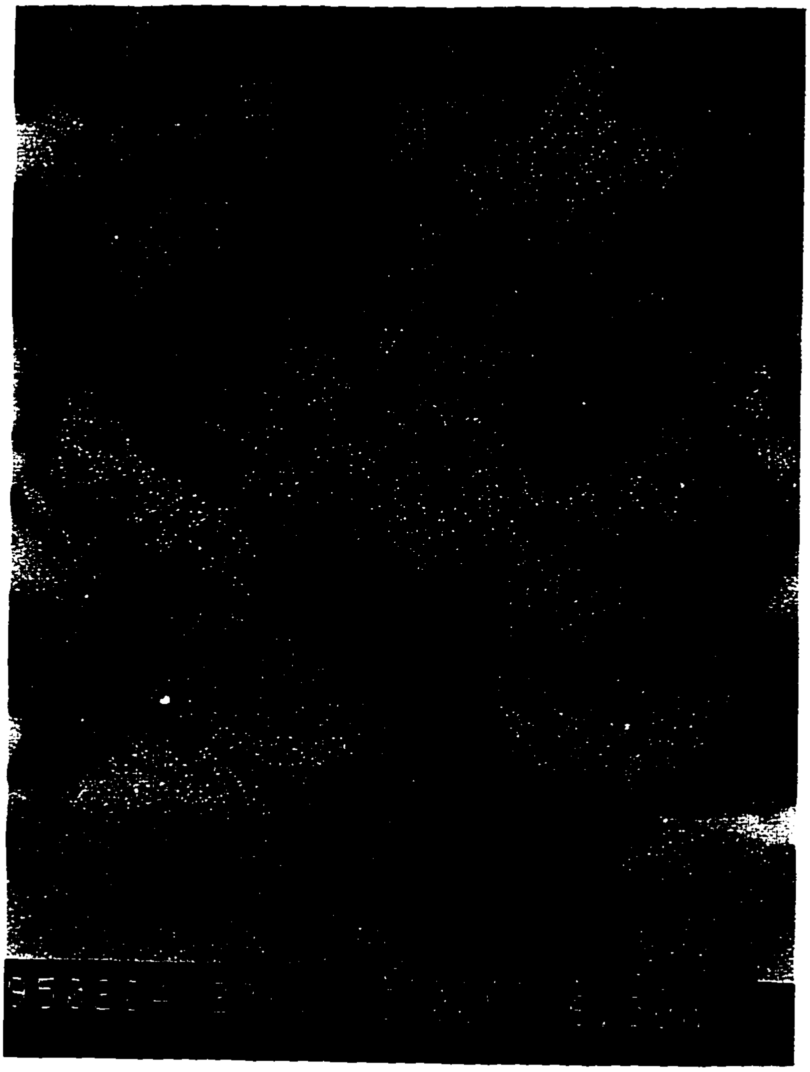

Figure 25. SEM micrograph of Fine Component

7.1 APPARENT DENSITY, TAP DENSITY and the HAUSNER RATIO

Apparent density measurements for the sixteen mixtures produced for this study are shown in Table V. Although the differences in apparent density were not great, slightly higher density was obtained with a bimodal or trimodal particle size distribution. The specimen containing a ratio of 70:20:10, coarse:medium:fine had the highest apparent density of 1.06 g/cc, followed closely by the mixture containing a ratio of 80:0:20 with an apparent density of 1.05 g/cc.

Tap density measurements for the sixteen mixtures produced for this study are shown in Table VI. The tap density measurements for the 80:0:20 bimodal mixture and all seven trimodal mixtures were higher than all of the other specimens. This would indicate that the trimodal mixtures form random dense packing configurations more easily and are more dense than bimodal mixtures that contain 40% fine material or contain only coarse and medium materials.

The Hausner Ratio[3] was first proposed by Hausner [20] as a measure of the "friction condition" in metal powders. It gives an indication of the variations in interparticle forces. The Hausner Ratio was also calculated for each powder and is shown in Table VII. The Hausner ratio of a specimen of 100%

[3] The Hausner Ratio is the ratio of the tap density to the apparent density.

Table V. Apparent Density (g/cc) of Particle Mixtures

% Fines	% Coarse				
	60%	70%	80%	90%	100%
40%	0.89 (0.01)				
30%	0.99 (0.02)	0.95 (0.01)			
20%	1.01 (0.03)	1.00 (0.03)	1.05 (0.02)		
10%	1.00 (0.03)	1.06 (0.03)	1.04 (0.01)		
5%				0.96 (0.02)	
0%	0.93 (0.01)	1.01 (0.03)	0.95 (0.02)		0.95 (0.01)

100% Fines 0.66 (0.01) 100% Medium 0.98 (0.02)

The data in parentheses are standard deviations.

Table VI. Tap Density (g/cc) of Particle Mixtures

% Fines	% Coarse				
	60%	70%	80%	90%	100%
40%	1.35 (0.00)				
30%	1.47 (0.01)	1.44 (0.01)			
20%	1.51 (0.02)	1.53 (0.01)	1.57 (0.02)		
10%	1.48 (0.02)	1.52 (0.02)	1.53 (0.01)		
5%				1.44 (0.03)	
0%	1.33 (0.00)	1.40 (0.02)	1.37 (0.01)		1.31 (0.01)

100% Fines 0.99 (0.00) 100% Medium 1.29 (0.01)

The data in parentheses are standard deviations.

Table VII. Hausner Ratio of Particle Mixtures

% Fines	% Coarse				
	60%	70%	80%	90%	100%
40%	1.51 (0.02)				
30%	1.49 (0.02)	1.52 (0.01)			
20%	1.49 (0.03)	1.53 (0.03)	1.49 (0.02)		
10%	1.48 (0.04)	1.43 (0.03)	1.47 (0.01)		
5%				1.50 (0.06)	
0%	1.43 (0.01)	1.39 (0.02)	1.44 (0.02)		1.38 (0.01)

100% Fines 1.49 (0.02) 100% Medium 1.32 (0.01)

The data in parentheses are standard deviations.

coarse material was measured to be 1.38. The Hausner ratio of a mixture containing 60% coarse and 40% medium was 1.43 and the Hausner ratio of a mixture containing 60% coarse and 40% fine was 1.51. In all three of these materials the apparent density is relatively low, i.e., <0.95 g/cc.

This indicates a high degree of void space and or particle agglomeration. A high Hausner ratio would indicate that a large amount of this void space or agglomeration was eliminated during the tapping operation. This could be a measure of the hardness or softness of particle agglomeration within a sample and may be useful in determining fairly large differences in powder characteristics.

7.2 GREEN DENSITY VARIATIONS with COMPOSITION

In this investigation the green density[4] was measured using a balance and a pair of calipers. The green density of pellets pressed from the various powder mixtures and standard deviation are shown in Table VIII.

From previous discussions it is expected that higher green densities should result from bimodal and trimodal mixtures. To determine this effect, the green density was plotted as a function of % fines and % medium in Figures 26 and 27. As can be seen from these figures the maximum green

---

[4] The green density is the density of the pressed pellet in g/cc.

Table VIII. Green Density (g/cc) of Powder Compacts

% Fines	% Coarse				
	60%	70%	80%	90%	100%
40%	2.30 (0.006)				
30%	2.34 (0.011)	2.35 (0.012)			
20%	2.42 (0.006)	2.44 (0.012)	2.42 (0.016)		
10%	2.54 (0.012)	2.55 (0.012)	2.51 (0.015)		
5%				2.50 (0.009)	
0%	2.52 (0.009)	2.50 (0.011)	2.46 (0.009)		2.44 (0.020)

100% Fines 1.62 (0.101) 100% Medium 2.46 (0.011)

The data in parentheses are standard deviations.

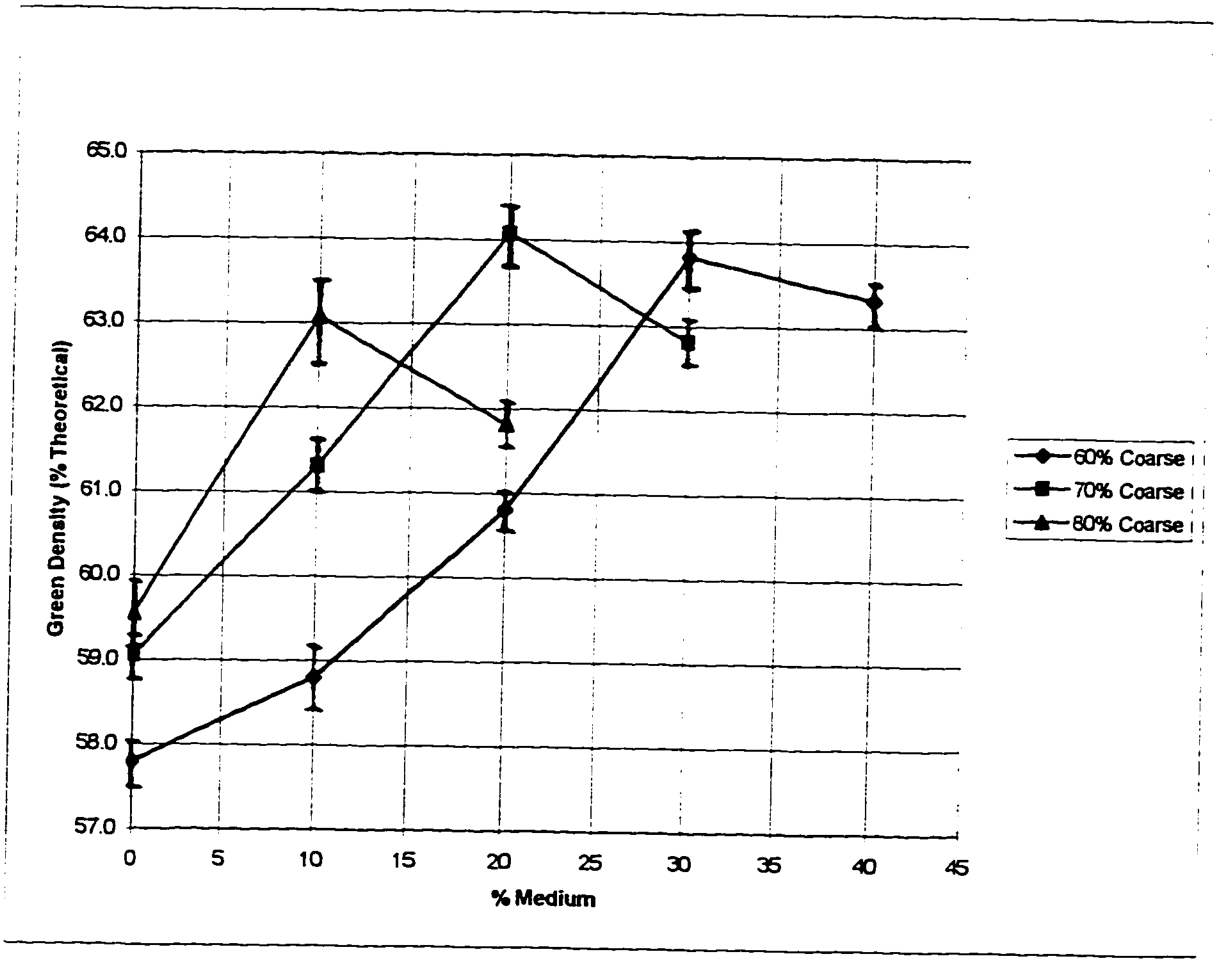

Figure 26. Green Density as a Function of % Medium Component

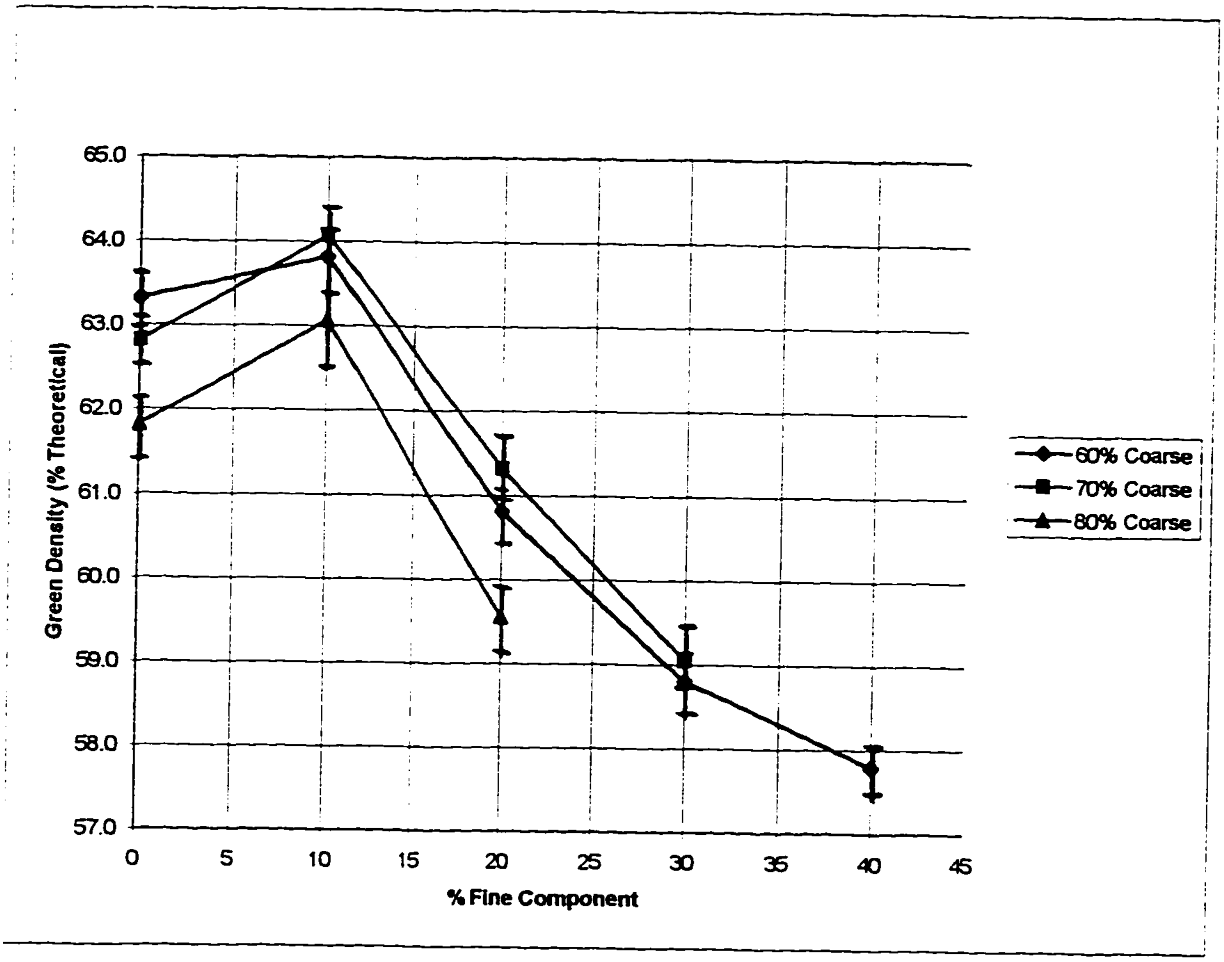

Figure 27. Green Density as a Function of % Fine Component

density was obtained when the composition contained 10% of the fine component. Figures 26 and 27 essentially show the same data from a slightly different viewpoint. In a three component mixture, if the composition of one component remains constant, then for the other two, as one increases the other must decrease. In Figure 26, as the composition of the coarse component increases, the composition of the medium component decreases since the composition of the fine component at the locally highest density remains at 10%.

7.3 SINTERED DENSITY

Five pellets were sintered from each powder mixture. The sintered density and standard deviation of each pellet are shown in Table IX. Individual sintered density measurements can be found in Appendix F. The sintered density as a function of % fines for a mixture composed of 80% coarse material, is shown in Figure 28. The sintered density as a function of % fines for a mixture composed of 70% coarse material is shown in Figure 29 and similarly the sintered density as a function of % fines for a mixture composed of 60% coarse material is shown in Figure 30. The sintered density increases with an increase in the % fines used in the mixture.

Table IX. Sintered Density (g/cc) of Powder Compacts

% Fines	% Coarse				
	60%	70%	80%	90%	100%
40%	3.934 (0.023)				
30%	3.926 (0.020)	3.929 (0.016)			
20%	3.914 (0.020)	3.913 (0.011)	3.929 (0.012)		
10%	3.892 (0.023)	3.936 (0.015)	3.895 (0.009)		
5%				3.937 (0.007)	
0%	3.858 (0.009)	3.904 (0.017)	3.883 (0.015)		3.951 (0.013)

100% Fines 4.058 (0.050) 100% Medium 3.917 (0.016)

The data in parentheses are standard deviations.

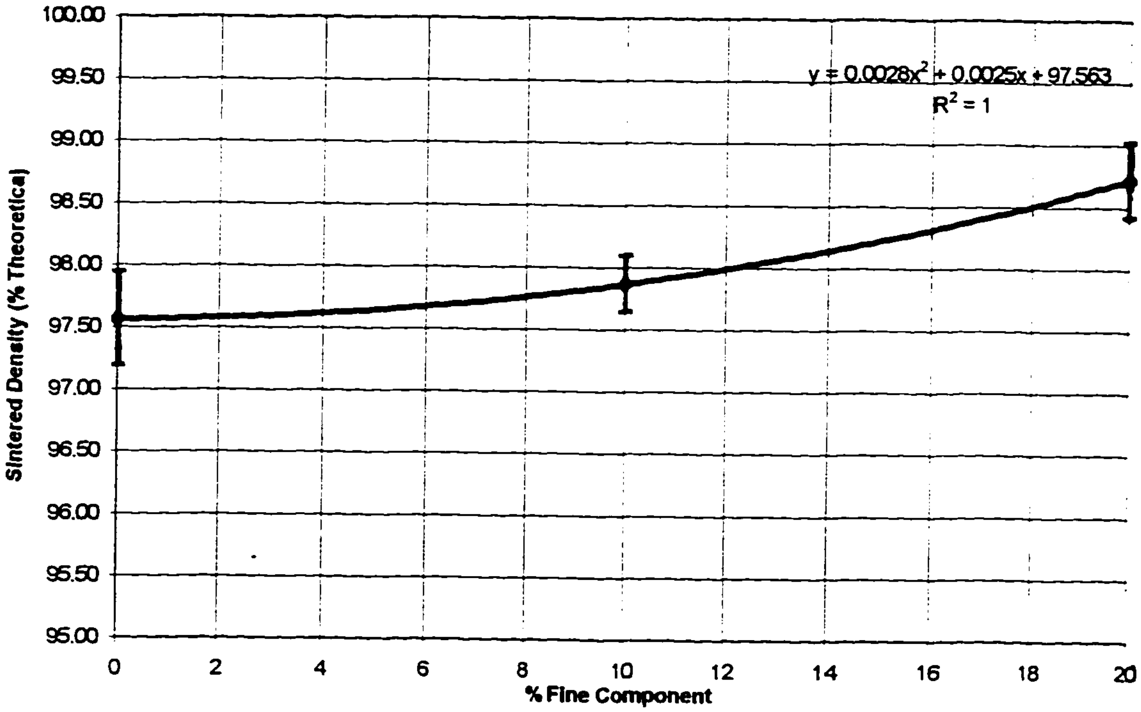

Figure 28. Sintered Density as a Function of % Fine Component for a Mixture Composed of 80% Coarse Material

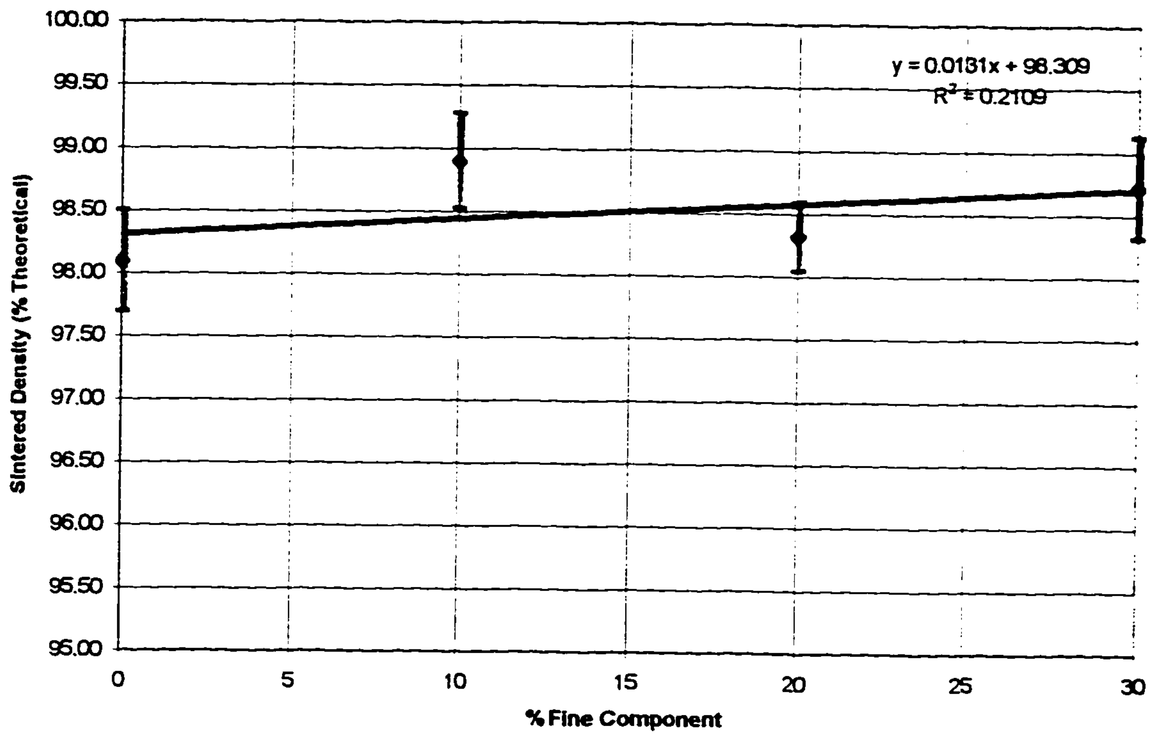

Figure 29. Sintered Density as a Function of % Fine Component for a Mixture Composed of 70% Coarse Material

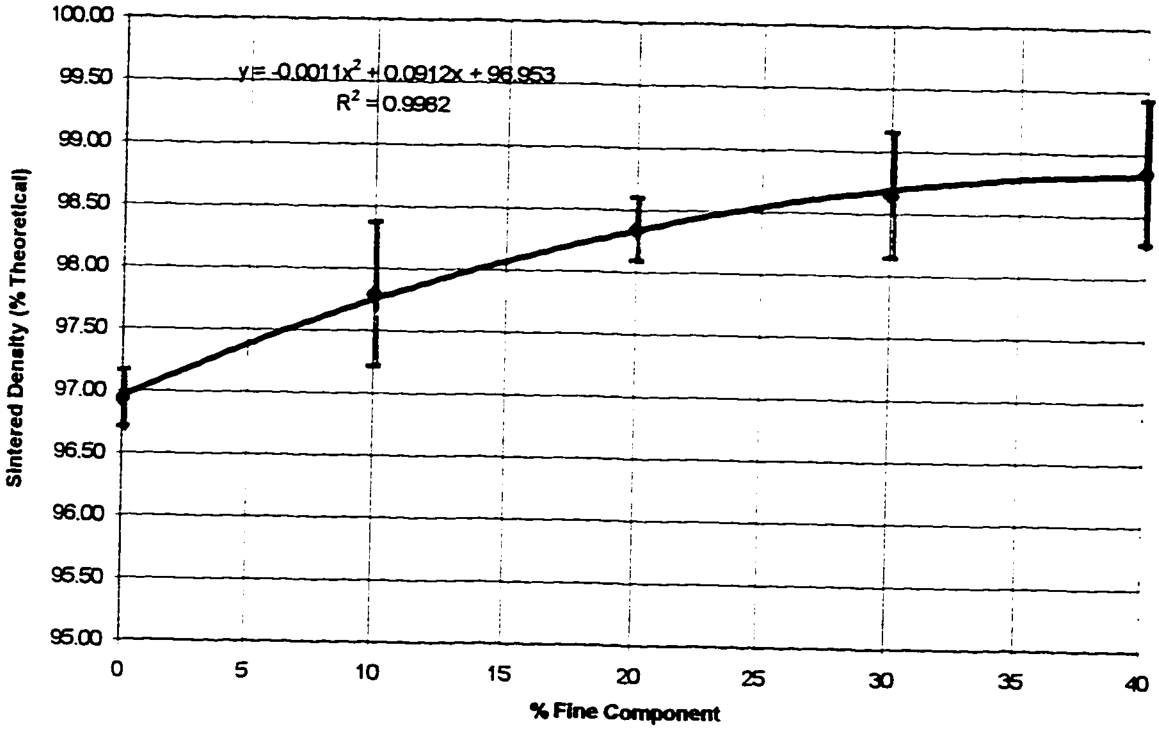

Figure 30. Sintered Density as a Function of % Fine Component for a Mixture Composed of 60% Coarse Material

CHAPTER 8

DISCUSSION OF RESULTS

There are many variables that could be evaluated in a study such as this one. The main areas of discussion here are restricted to, raw material selection, maximizing green density and minimizing shrinkage. Each of these aspects of this evaluation have played important roles in the results of this research project.

8.1 RAW MATERIAL SELECTION

In preliminary powder processing test runs, identical particle compositions gave results varying by up to approximately 2%. Variations in materials produced under identical conditions gave differences of less than 1%, as estimated from the data in Appendix G. This shows the importance of processing conditions on the resulting product characteristics.

Two of the three materials used in this investigation were high purity alumina whereas the third component, i.e., the fine component, was a monohydrate of alumina. Decomposition of the hydrate no doubt is one of the reasons why there is an increase in open porosity as a function of the concentration of fines in the composition, as shown in Figure 31. However, the extent of aggregation and homogeneity of the

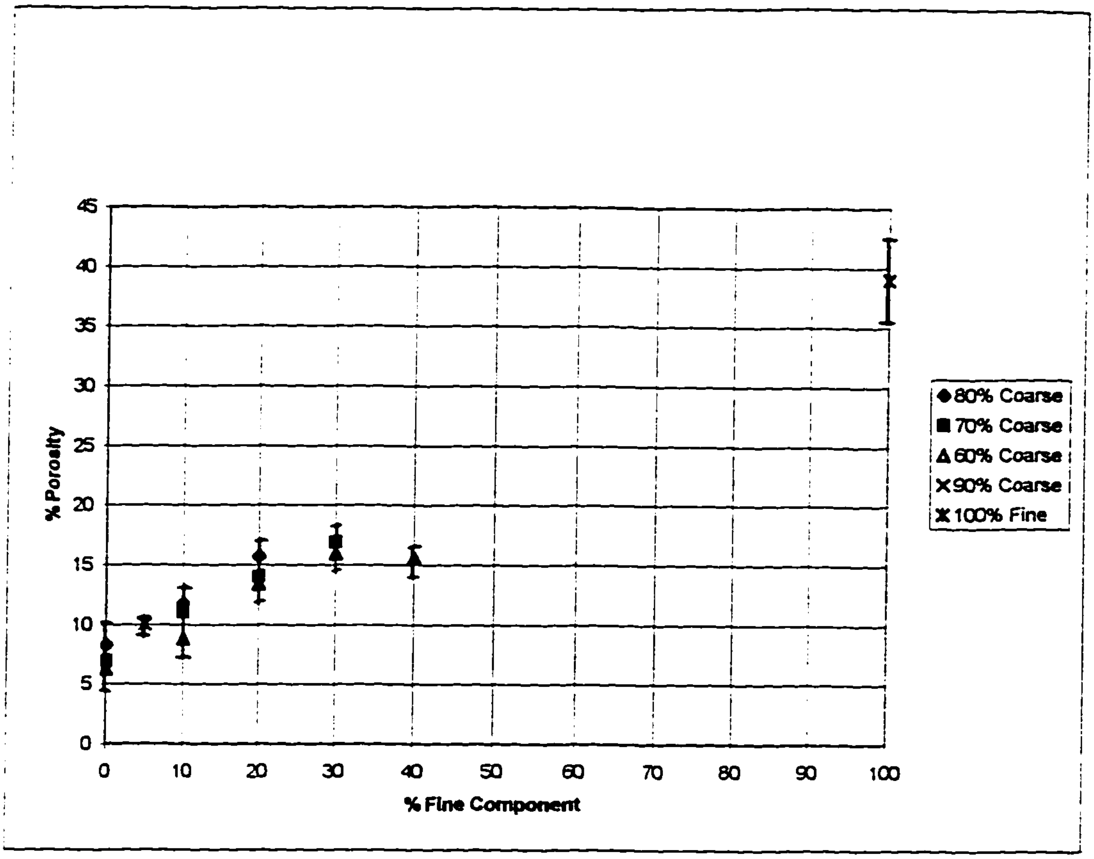

Figure 31. Open Porosity as a Function of % Fine Component

mixed powders would also contribute to the porosity of the final product.

As mentioned in the preceding section, the sintered density also appears to increase with an increase in fines concentration. This was shown most dramatically in Figure 30. The asymptotic nature of the curve fitting the data in Figure 30 is reasonable because under any set of conditions the sintered density has an upper limit. The sintered density approaches the upper limit as the concentration of the fine component is increased. It would also follow that shrinkage would also increase with an increase in the percent fines, as shown in Figure 32. Shrinkage of compositions containing greater than 30% fines may also approach an upper limit asymptotically.

8.2 MAXIMIZING DENSITY and MINIMIZING SHRINKAGE

Shrinkage observed for specimens containing 0%, 10% and 20% fines are very similar. It is not until the fine content exceeds about 30% that shrinkage increases significantly. This indicates, as described by Smith and Messing [17] and in Section 3.5, that shrinkage is controlled by the coarse component, or in this case the coarse and possibly medium components, until the composition approaches 30% fines. It should also be noted that the point where the shrinkage is a minimum corresponds to the point where the green density

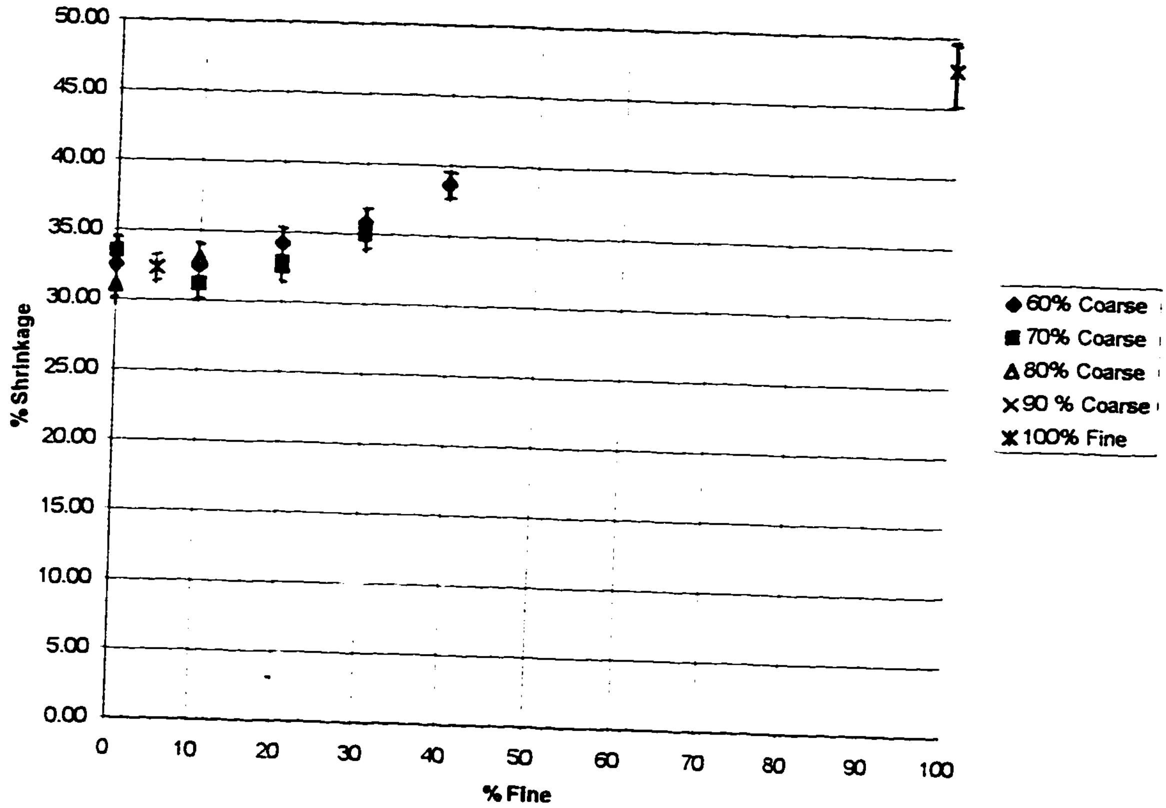

Figure 32. Shrinkage as a Function of % Fine Component

reaches a maximum. This is shown for compositions containing 80% coarse, 70% coarse and 60% coarse material in Figures 33, 34 and 35, respectively. This confirms the idea that by increasing green density shrinkage can be minimized. Also in general, the percent shrinkage decreases as the green density increases. Figure 36 shows this trend.

8.3 Conformance with Previous Studies

The fractional packing density of an FCC structure is 0.74. From calculations, presented in Appendices C and D, the fractional volume occupied by tetrahedral and octahedral sites in an FCC structure makes up only about 7% of the total volume of the structure. The residual porosity remaining after filling tetrahedral and octahedral sites is still about 19%. If this residual porosity could be filled with spherical particles, their radii would have to be on the order of one tenth, or less than, the size of the particles making up the FCC structure. This is consistent with a particle size ratio of approximately 1:5:25 which consists of 21.6% fine, 9.2% medium and 69.2% coarse, as shown in Table II, from German [8]. However, as the particle size ratio gets larger, e.g., 1:7:77, the optimal packing gets closer to that found in this study. That is, green density is maximized in mixtures containing approximately 10% fines. The highest green density observed in this study was produced with the specimen that

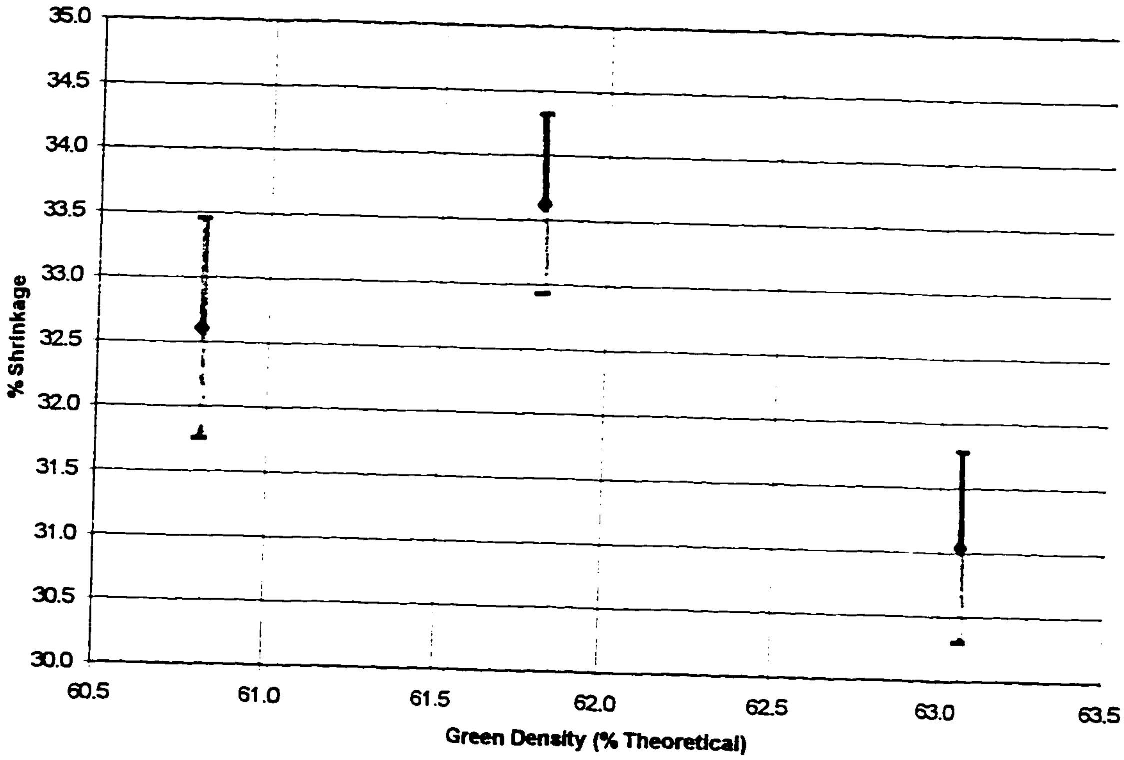

Figure 33. Shrinkage as a Function of Green Density for a Mixture Composed of 80% Coarse Material

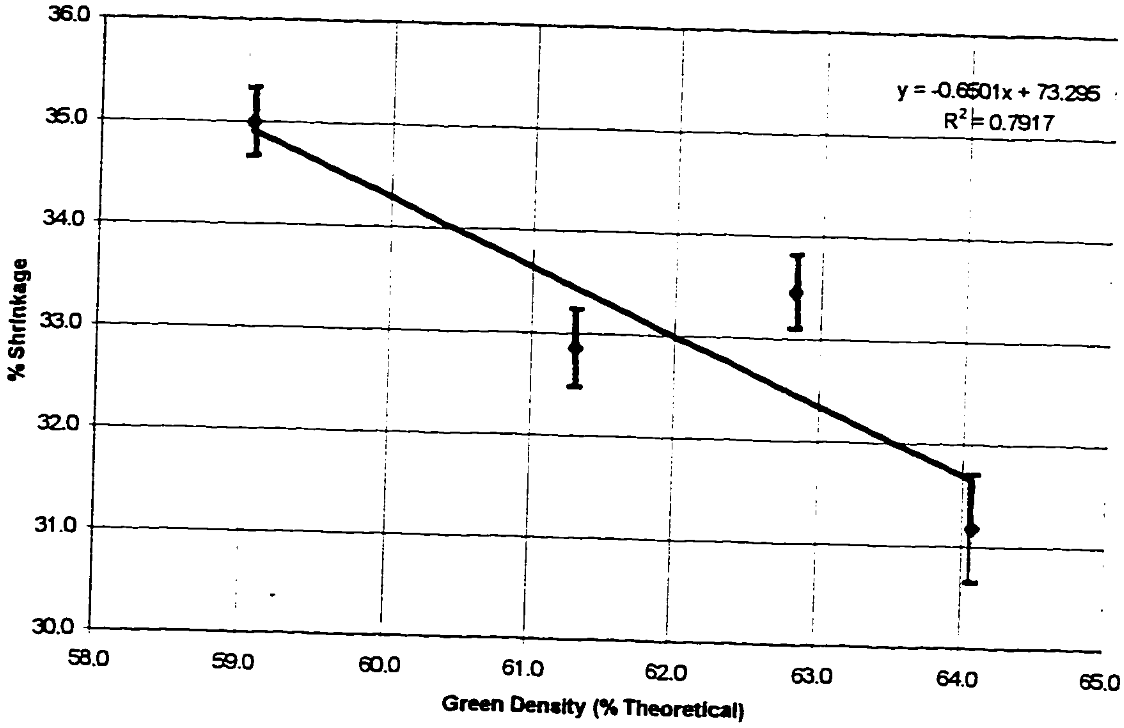

Figure 34. Shrinkage as a Function of Green Density for a Mixture Composed of 70% Coarse Material

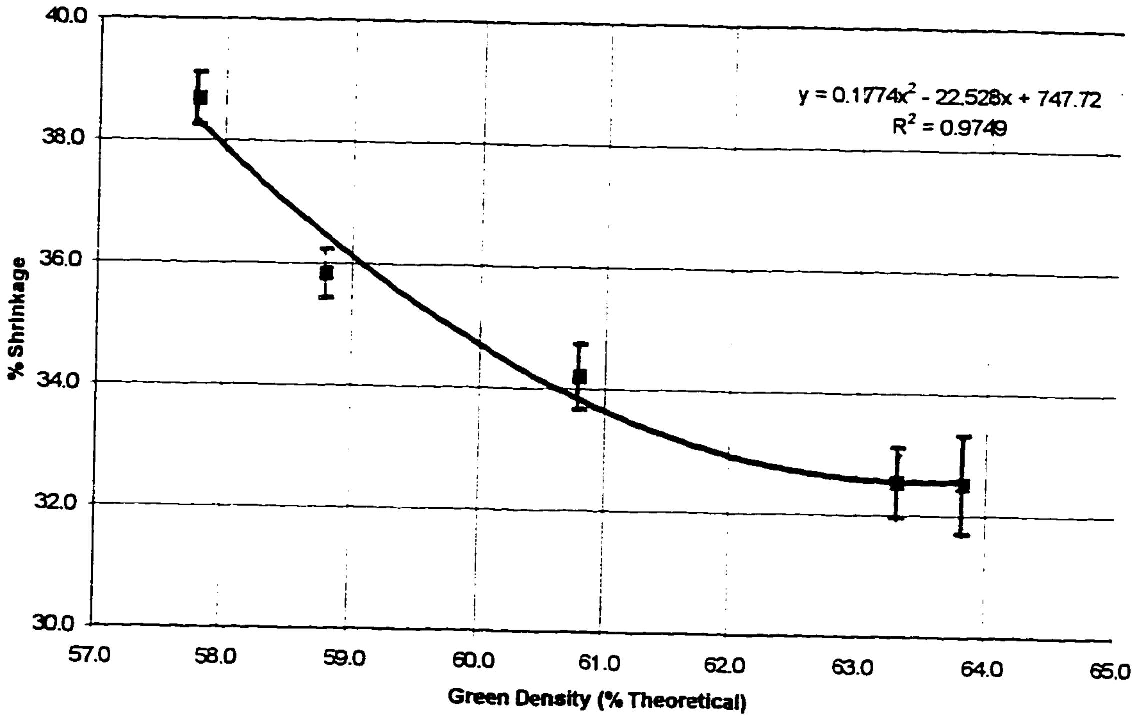

Figure 35. Shrinkage as a Function of Green Density for a Mixture Composed of 60% Coarse Material

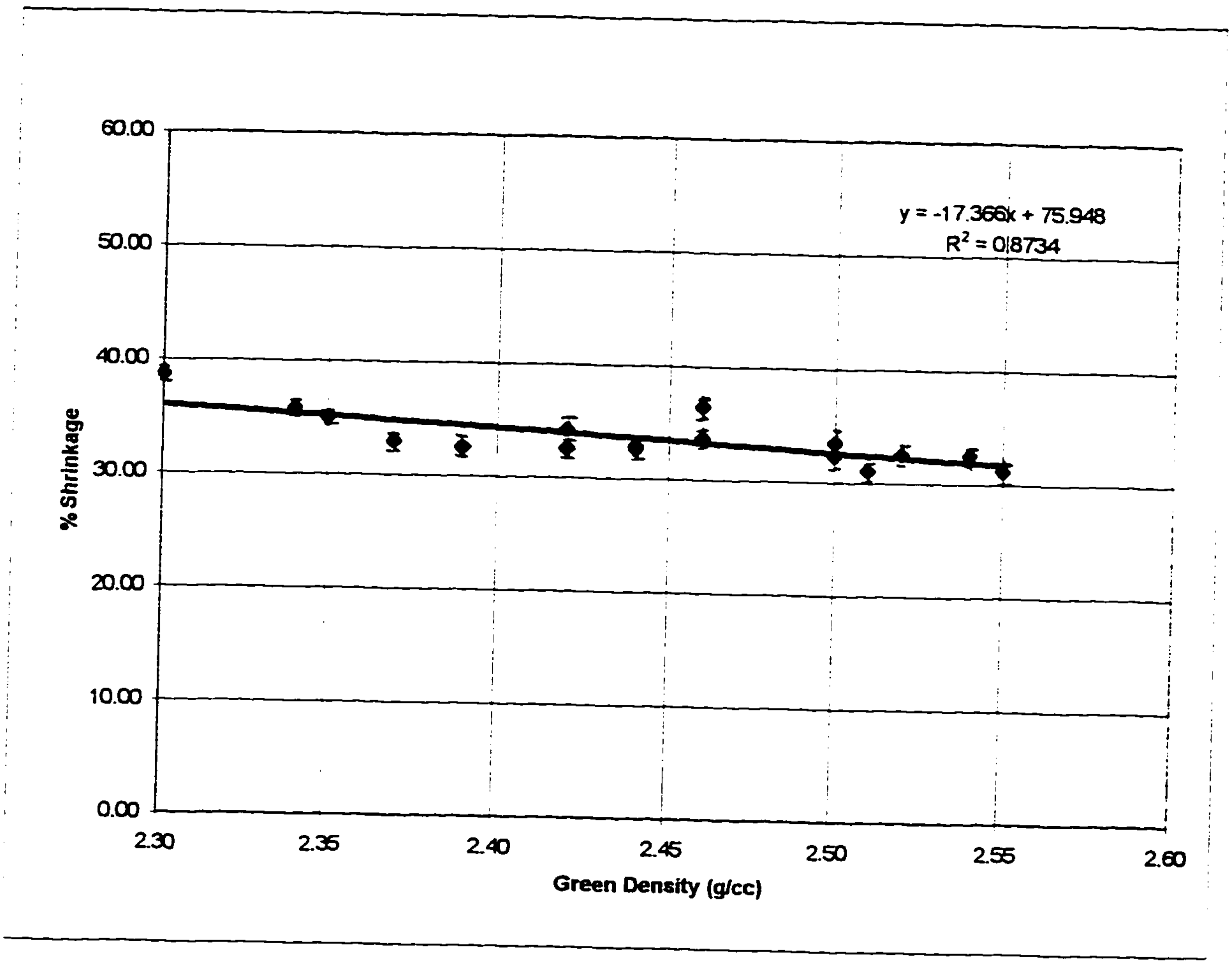

Figure 36. Shrinkage as a Function of Green Density

contained 10% fines, 20% medium and 70% coarse material. From the particle size analysis of the raw materials used in this study, a ratio of approximately 1:5:12 was obtained. However, if the fine component had a mean radius that was significantly smaller than 0.05 microns, which is highly probable as evident from Figure 18, the ratio may be greatly different.

Six specimens in this study were binary mixtures, three consisting of coarse and fine materials and three consisting of coarse and medium materials. The green density obtained from the coarse/medium binary mixtures varied by only a little more than 2%, whereas the green density obtained from the binary mixtures made from the coarse and fine materials varied by as much as 5%. From preliminary processing data, as described in Section 8.1, a 2% difference in green density could be the result of a slight difference in processing conditions. The 5% difference observed in the coarse/fine binary system however is significant and in fact the highest green density found in this study, i.e. 70% coarse, 20% medium and 10% fines, falls on the line perpendicular to the coarse/fine side of the ternary diagram at the point of the maximum density observed for the binary system, as shown in Figure 4.

CHAPTER 9

CONCLUSIONS

Sintered density increases with an increase in the percent fines in the mixture. The specimen comprised of 100% fines also gave the highest sintered density. Although density may increase with an increase in the % fines, in general so does the shrinkage. Shrinkage is minimized when the green density is maximized. In this study the green density was maximized when the mixture contained 10% fines; this condition also showed the least shrinkage. This is important because the production of dense ceramic components made with a minimum of shrinkage is a primary objective of the ceramic industry.

As mentioned in Section 2.1, if the maximum packing density of spheres of a single particle size is estimated to be 60-65% of theoretical, and the maximum packing density for a trimodal mixture is 90-95% of theoretical, then the weight fraction or volume fraction[5] made up of the medium and fine particles must be approximately 30%. The specimen with the highest green density in this study had a composition of 70% coarse, 20% medium and 10% fine material. This composition is consistent with optimum trimodal packings obtained from

[5] The weight fraction and the volume fraction are equivalent when all particles are of the same density.

various sources, as described by German and presented in Table II in Section 2.2.

In bimodal mixtures of the coarse and medium materials, the standard deviation of the green density increases with an increase in the coarse component. However in these same specimens, the standard deviation of the sintered density decreases with an increase in the coarse component. No similar trend was observed in trimodal mixtures which indicates that trimodal mixtures may not give greater product reproducibility but do result in less shrinkage, at least under the conditions of this study.

REFERENCES

[1] W. Gitzen, Alumina as a Ceramic Material, Am. Ceram. Soc., 1970., Chapter 16.

[2] W. D. Kingery, H. K. Bowen and D. R. Uhlmann, Introduction to Ceramics, 2nd Ed., John Wiley and Sons, 1976.

[3] R. L. Coble, "Effects of Particle Size Distribution in Initial-Stage Sintering", J. Am. Ceram. Soc., **56[9]**, 461-66 (1973).

[4] A. E. R. Westman and H. R. Hugill, The Packing of Particles, J. Am. Ceram. Soc., **13**, 767-779, (1930).

[5] M. Komatsu, T. Miyano, A. Ando, M. Nakanishi and Y. Fujimoto, Method of Manufacturing Sintered Ceramic Body, US Patent Number 4,671,912, (1987).

[6] J. Denevi, Effect of Particle Size Distribution on Densification Behavior of Alumina Powders., unpublished work, 1989.

[7] A. E. R. Westman and H. R. Hugill, The Packing of Particles, J. Am. Ceram. Soc., **13**, 767-779, (1930).

[8] R. M. German, Particle Packing Characteristics, Metal Powder Ind. Fed.,Princeton N.J., (1989).

[9] C.C. Furnas, Grading Aggregates I - Mathematical Relations for Beds of Broken Solids of Maximum Density, Ind. and Eng. Chem., **23**, 1052-58, (1931).

[10] F. W. Dynys and J. W. Halloran, Influence of Aggregates on Sintering, J. Am. Ceram. Soc., **67[9]**, 596-601, (1984).

[11] A. Roosen, S. Sumita and K. Bowen, Powders, Interfaces and Processing: Alumina as a Case Study, Ceramic Microstructures '86 Role of Interfaces, Materials Science Research vol. 21, J. A. Pask and A. G. Evans ed., Plenum Press, NY 1987.

[12] F.F. Lange, Sinterability of Agglomerated Powders, J. Am. Ceram. Soc., **67[2]**, 83-89, (1984).

REFERENCES - continued

[13] W. D. Kingery and B. Francois, Sintering of Crystalline Oxides, I. Interactions Between Grain Boundaries and Pores., pp.471-98 in Sintering and Related Phenomena. Ed.G. C. Kuczynske, N. A. Hooton and G. F. Gibbon. Gordon Breach, NY 1967.

[14] B. J. Kellett and F. F. Lange, Thermodynamics of Densification: I, Sintering of Simple Particle Arrays, Equilibrium Configurations, Pore Stability, and Shrinkage, J. Am. Ceram. Soc., **72[5]**, 725-34, (1989)

[15] J. Zheng and J. S. Reed, Effects of Particle Packing Characteristics on Solid-State Sintering, J. Am. Ceram. Soc., **72[5]**, 810-17, (1989).

[16] J. Zheng and J. S. Reed, The Different Roles of Forming and Sintering on Densification of Powder Compacts, Am. Ceram. Soc. Bull., **71[9]**, 1410-16, (1992).

[17] J. P. Smith and G. L. Messing, Sintering of Bimodally Distributed Alumina Powders, J. Am. Ceram. Soc., **67[4]**, 238-42, (1984).

[18] S. Taruta, K. Okada and N. Otsuka, Micropore Distribution Change of Heated Powder Compacts Using Binary Alumina Powder Mixtures, J. Ceram. Soc. Jpn. Inter. Ed., **98[30-36]**, 32-8, (1990)

[19] W. J. Walker, Jr., J. S. Reed and S. K. Verma, Polyethylene Glycol Binders for Advanced Ceramics, Ceram. Eng. Sci. Proc. 14[11-12] pp 58-79 (1993).

[20] H. H. Hausner, Int. J. Powder Met. 3(1967) 7.

Appendix A. Technical Data Sheets

CERALOX

A Division of Vista Chemical Company

San Jose University
Dept. of Material Engineering
129 S. 10th Street
San Jose, CA. 95192-0086

Date: June 6, 1995
Product Type: HPA-1.0
Al_2O_3 Purity: 99.99%
Number: 52549
Shipment Weight: 1.5 kgs

Attn: Guna Selvaduney

LOT ANALYSIS

CHEMICAL ANALYSIS

Trace Impurities (ppm)

Na	Si	Fe	Ca	Mg	Ga	Cr	Ni	Ti	Mn	Cu	Mo	Li	Zn	Zr
28	21	6	5	4	<4	<1	<1	3	<1	<1	<4	<1	<1	2

PHYSICAL PROPERTIES

Particle Size Distribution

Microns	Wt%
+10	<1
+5	2
+3	5
+2	10
+1	30
+0.7	49
+0.5	67
+0.4	78
+0.3	88
+0.2	97
+0.1	100
D-50, microns	0.70

Density, g/cm^3

Green	Fired
2.24	3.83

Surface Area, m^2/gm

4.3

Linear Shrinkage, %

16.2

METHODOLOGY

Chemical Analysis: Inductively Coupled Argon Plasma/Atomic Absorption.
Particle Size Distribution: By Laser Diffraction
Surface Area: B.E.T. Monosorb
Green & Fired Density, Linear Shrinkage: Alumina Ceramic Manufacturing Assn. (ACMC) Test 6, ASTM C-373-2
Green density values are determined on a 10 gram pellet, pressed at 5000 psi (34.47 Mpa) in a 1" floating die. Fired density values are determined from a pellet sintered at 1510°C for 2 hours.

[illegible]

CERALOX

A Division of Vista Chemical Company

San Jose University
Dept. of Material Engineering
129 S. 10th Street
San Jose, CA. 95192-0086

Date: June 6, 1995
Product Type: HPA-0.5
Al_2O_3 Purity: 99.99%
Number: 31163
Shipment Weight: 1.0 kgs

Attn: Guna Selvaduney

LOT ANALYSIS

CHEMICAL ANALYSIS

Trace Impurities (ppm)

Na	Si	Fe	Ca	Mg	Ga	Cr	Ni	Ti	Mn	Cu	Mo	Li	Zn	Zr
18	31	12	7	1	<4	<1	<1	2	<1	<1	<4	<1	<1	4

PHYSICAL PROPERTIES

Particle Size Distribution

Microns	Wt%
+10	0
+5	<1
+3	1
+2	3
+1	13
+0.7	28
+0.5	48
+0.4	62
+0.3	77
+0.2	93
+0.1	100
D-50, microns	0.48

Density, g/cm^3

Green	Fired
2.19	3.92

Surface Area, m^2/gm

10.0

Linear Shrinkage, %

17.3

METHODOLOGY

Chemical Analysis: Inductively Coupled Argon Plasma/Atomic Absorption.
Particle Size Distribution: By Laser Diffraction
Surface Area: B.E.T. Monosorb
Green & Fired Density, Linear Shrinkage: Alumina Ceramic Manufacturing Assn (ACMC) Test 6, ASTM C-373-2
Green density values are determined on a 10 gram pellet, pressed at 5000 psi (34.47 Mpa) in a 1" floating die. Fired density values are determined from a pellet sintered at 1510°C for 2 hours.

7800 South Kolb Road • Tucson, Arizona 85706 • (602) 294-5201 • FAX (602) 294-5408

CONDEA Chemie GmbH
Postfach 60 04 49
22204 Hamburg

CONDEA

08-07-95P03:54 RCVD

SAN JOSE UNIVERSITY
Attn.: Mrs. Luna Selvadunay
Dept. of Material Eng.
129 S. 10th Street

San Jose, CA 95192-0086
U.S.A.

21-Jul-95 , TL/ot

PROFORMA-RECHNUNG-NO.:23.042/95
(PROFORMA-INVOICE)

Auf Ihre Anfrage senden wir Ihnen per DHL am: 28.7.1995
(UPON YOUR REQUEST WE HAVE SENT BY) (on)

Ein Muster ohne Handelswert
(A SAMPLE WITHOUT ANY COMMERCIAL VALUE)

Menge (Quantity) kg	Ware (PRODUCT)	Lot-No.	Gebinde (Packing)	Gewichte brutto (gross) kg	(Weights) netto (net) kg	Betrag (Amount) DM
1 kg	DISPERAL	57771	Karton	1,1	1,0	5.–
	Alumina sample for test use only.			No charge,	value for customs clearance only	

Bemerkungen
(Remarks) Sample shipment as agreed upon with Dr. Thomas Lüdemann on July 20, 1995.

Tosca-Certificate attached.

Material Safety Data Sheet and Certificate of Analysis will follow by separate mail.

Ursprungserklärung
(certificate of origin)

CONDEA CHEMIE GmbH

cc: ATA, Labor, V+G

CONDEA Chemie GmbH
Überseering 40
22297 Hamburg

CONDEA

SAN JOSE UNIVERSITY

MRS LUNA SELVADUNAY

Sample request no.: 23042/95

Product: DISPERAL

Lot-no.: 57771

* Analytical Data *

Date: 26.07.95

Test	Unit	Result
Surface area	m2/g	173
Al2O3 - content	%	77.7
Loose bulk density	g/ml	0.52
Particle size: < 25 micron	%	83.1
Particle size: < 45 micron	%	92.4
Particle size: < 90 micron	%	100.0
Dispersibility	%	98.5

Best regards

CONDEA Chemie GmbH
Works' Inspector

Manufacturer:

RWE-DEA AG
P.O.Box 1160
D-25534 BRUNSBÜTTEL

Phone: 04852/ 392-0
Fax: 04852/ 3285

T E C H N I C A L   I N F O R M A T I O N

CARBOWAX® Polyethylene Glycols Compound 20M

CAS # 42617-82-3
CHEMICAL FAMILY – Oxyalkylene Polymer
CTFA NOMENCLATURE – PEG-350

TYPICAL PHYSICAL PROPERTIES	Average Molecular Weight Range	15,000 to 20,000
	Density (g/cm³ @ 60°C)	1.0540
	Melting or Freezing Range	61 to 64°C (142 to 147°F)
	Solubility in Water (Wt% @ 20°C)	≈ 65
	Viscosity (cSt @ 99°C)	18,650
	Avg. Liquid Specific Heat (cal/g/°C)	0.59
	Heat of Fusion (cal/g)	41
	pH at 25°C (5% Aqueous Solution)	6.5 to 8.0

SHIPPING INFORMATION	Physical Form	Flake
	Bulk Density	30 lbs/ft³
	Flash Point	
	Pensky-Martens closed cup (ASTM D93)	>180°C (350°F)
	Cleveland open cup (ASTM D92)	>180°C (350°F)

UC-864

Union Carbide Corporation has compiled the information contained herein from what it believes are authoritative sources and believes that it is accurate and factual as of the date printed. It is offered solely as a convenience to its customers and is intended only as a guide concerning the products mentioned. Since the user's product formulation, specific use application, and conditions of use are beyond Union Carbide's control, Union Carbide makes no warranty or representation regarding the results that may be obtained by the user. It shall be the responsibility of the user to determine the suitability of any products mentioned for the user's specific application. This information is not to be taken as a warranty or representation for which Union Carbide assumes legal responsibility nor as permission to practice any patented invention without a license.

UNION CARBIDE CORPORATION
Industrial Performance Chemicals
39 Old Ridgebury Road
Danbury, CT 06817-0001

TYPICAL KNOWN APPLICATIONS FOR POLYETHYLENE GLYCOL	**ADHESIVES - AGRICULTURE - CERAMICS - CHEMICAL INTERMEDIATES - COSMETICS - TOILETRIES - ELECTROPLATING/ELECTROPOLISHING - FOOD PROCESSING - HOUSEHOLD PRODUCTS - LUBRICANTS - METAL/METAL FABRICATION - PAINTS & COATINGS - PAPER INDUSTRY-PHARMACEUTICALS - PRINTING - RUBBER & ELASTOMERS - TEXTILES - WOOD PROCESSING**

FDA STATUS

CARBOWAX® compound 20M is cleared under the following Food Additive Regulation for indirect use:

§177.1680 Stabilizer in polyurethane resins forming the food contact surface of articles intended for use in contact with bulk quantities of dry food.

HANDLING AND STORAGE

CARBOWAX Compound 20M is usually sold as a solid in bags or in fiber drums. The containers should be kept sealed and should not be stored next to steam lines or other heat sources that could cause the product to soften or melt. Recommended storage temperature is below 40°C (105°F).

PRODUCT SAFETY

When considering the use of any Union Carbide products in a particular application, you should review our latest Material Safety Data Sheets and ensure that the use you intend can be accomplished safely. For Material Safety Data Sheets and other product safety information, contact the Union Carbide Sales Office nearest you. Before handling any other products mentioned in the text, you should obtain available product safety information and take necessary steps to ensure safety of use.

No chemical should be used as or in a food, drug, medical device, or cosmetic, or in a product or process in which it may contact a food, drug, medical device, or cosmetic, until the user has determined the safety and legality of the use. Since government regulations and use conditions are subject to change, it is the user's responsibility to determine that the information contained herein is appropriate and suitable under current, applicable laws and regulations.

Union Carbide requests that the customer read, understand and comply with the information contained in this product information booklet and the current Material Safety Data Sheet. The customer should furnish the information in this product information booklet to its employees, contractors, and customers or other downstream users of the product and request that they do the same.

For technical information call: **1-800-UCC-PEGS**

For samples and small containers call: **1-800-969-2707**

For drums, bulk orders & customer service call: **1-800-568-4000**

Appendix B. Particle Size Measurements

■ Example of Data Printout

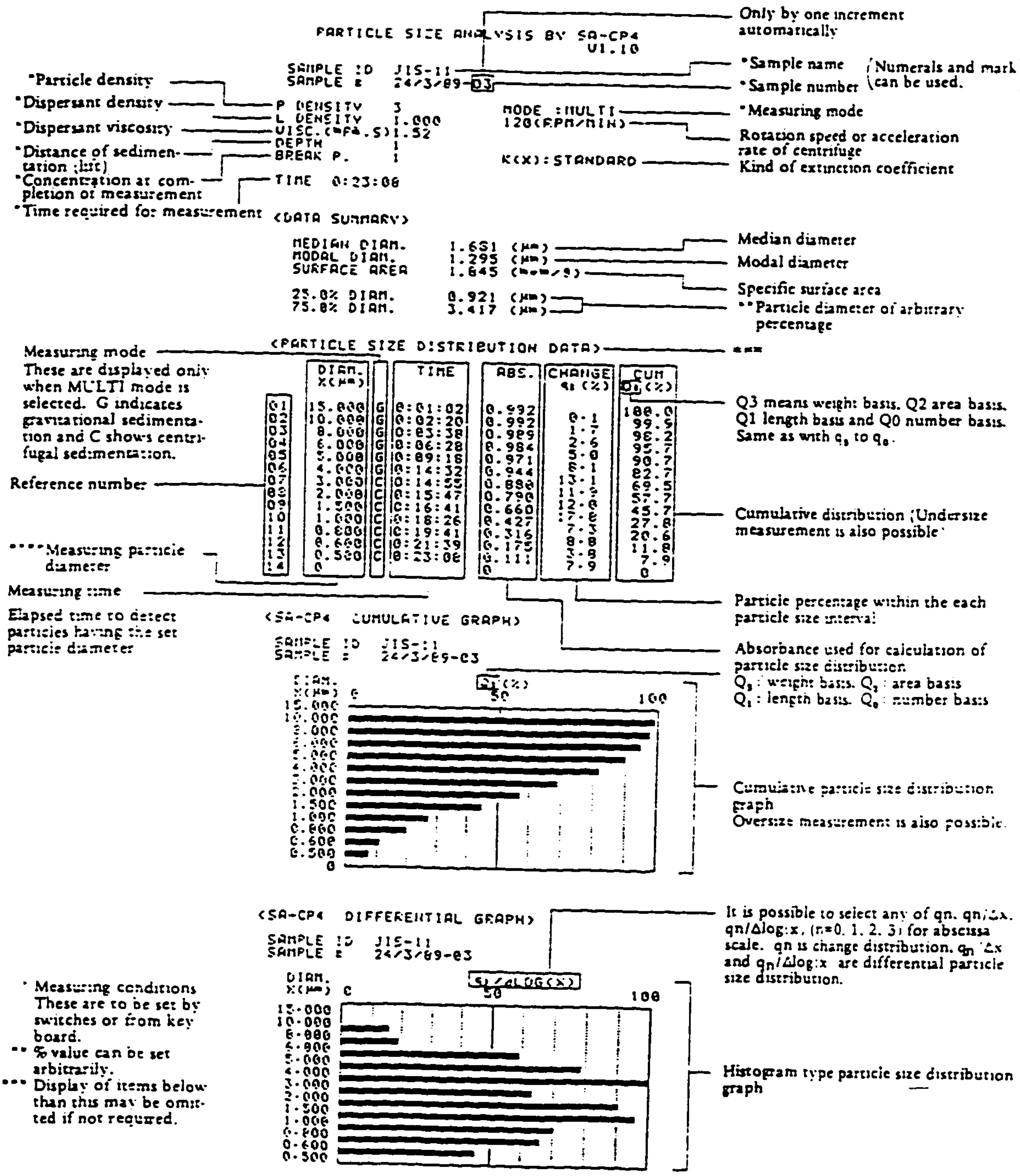

PARTICLE SIZE ANALYSIS BY SA-CP4 V1.00

SAMPLE ID - HPA-1
SAMPLE # 2/13/96 RUN01

P DENSITY	3.95	MODE :CENT
L DENSITY	0.9978	480(RPM/MIN)
VISC.(mPa.S)	0.96	
DEPTH	2	
BREAK P.	0	K(X):STANDARD

TIME 0:21:38

DATA SUMMARY>

MEDIAN DIAM.	0.634	(μm)
MODAL DIAM.	0.678	(μm)
SURFACE AREA	3.406	(m*m/g)
95.0% DIAM.	1.341	(μm)
5.0% DIAM.	0.281	(μm)

	DIAM. X(μm)	CUM Q_3(%)
1	1.200	92.8
2	1.000	89.7
3	0.800	77.0
4	0.500	25.1
5	0.100	2.1

SA-CP4 CUMULATIVE GRAPH>

SAMPLE ID 100
SAMPLE # 2/13/96 RUN01

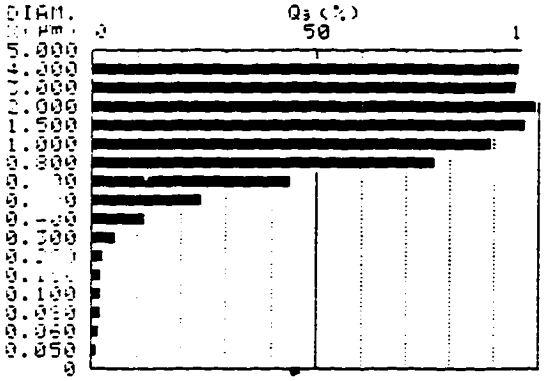

SA-CP4 DIFFERENTIAL GRAPH>

SAMPLE ID 100
SAMPLE # 2/13/96 RUN01

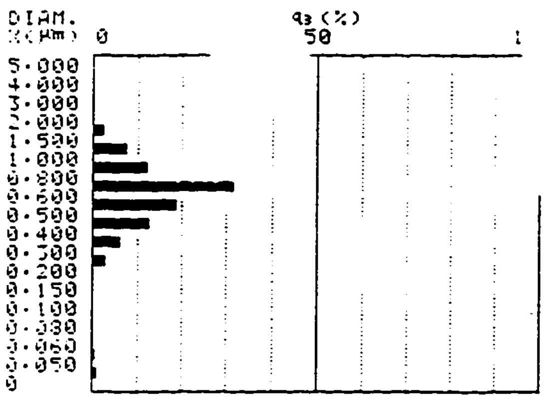

PARTICLE SIZE ANALYSIS BY SA-CP4 V1.00

SAMPLE ID HPA-1
SAMPLE # 2/13/96 RUN01

DENSITY 3.95 MODE :CENT
DENSITY 0.9978 480(RPM/MIN)
(mPa.S) 0.96
DEPTH 2
BREAK P. 0 K(X):STANDARD

TIME 0:21:38

DATA SUMMARY>

MEDIAN DIAM. 0.634 (μm)
MODAL DIAM. 0.678 (μm)
SURFACE AREA 3.406 (m*m/g)

95.0% DIAM. 1.341 (μm)
5.0% DIAM. 0.281 (μm)

DIAM. X(μm) CUM Q3(%)
1.200 92.8
1.000 89.7
0.800 77.0
0.500 25.1
0.100 2.1

SA-CP4 CUMULATIVE GRAPH>

SAMPLE ID 100
SAMPLE # 2/13/96 RUN01

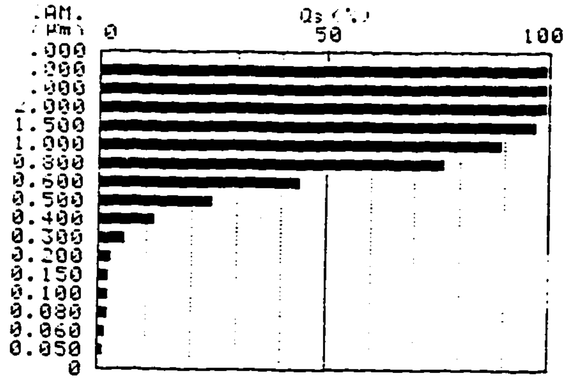

SA-CP4 DIFFERENTIAL GRAPH>

SAMPLE ID 100
SAMPLE # 2/13/96 RUN01

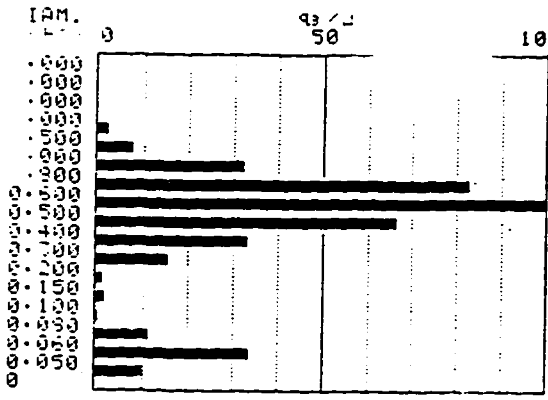

PARTICLE SIZE ANALYSIS BY SA-CP4
V1.00

SAMPLE ID → HPA-0.5
SAMPLE # 2/13/96 RUN02

F DENSITY 3.95 MODE :CENT
L DENSITY 0.9978 480(RPM/MIN)
VISC.(mPa.S)0.96
DEPTH 2
BREAK P. 0 K(X):STANDARD

TIME 0:17:09

<DATA SUMMARY>

MEDIAN DIAM. 0.331 (µm)
MODAL DIAM. 0.266 (µm)
SURFACE AREA 4.908 (m*m/g)

95.0% DIAM. 0.985 (µm)
5.0% DIAM. 0.169 (µm)

	DIAM. X(µm)	CUM Q3(%)
1	1.200	97.2
2	1.000	95.3
3	0.800	91.6
4	0.500	77.9
5	0.100	0.7

<SA-CP4 CUMULATIVE GRAPH>

SAMPLE ID 010
SAMPLE # 2/13/96 RUN02

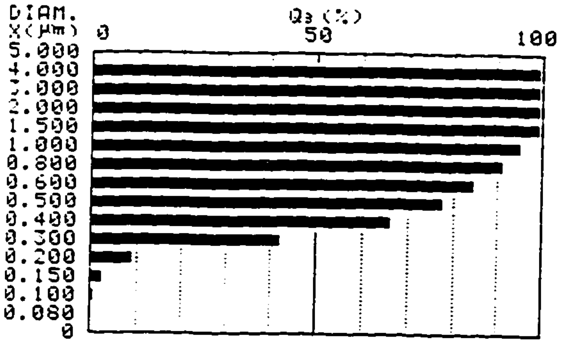

<SA-CP4 DIFFERENTIAL GRAPH>

SAMPLE ID 010
SAMPLE # 2/13/96 RUN02

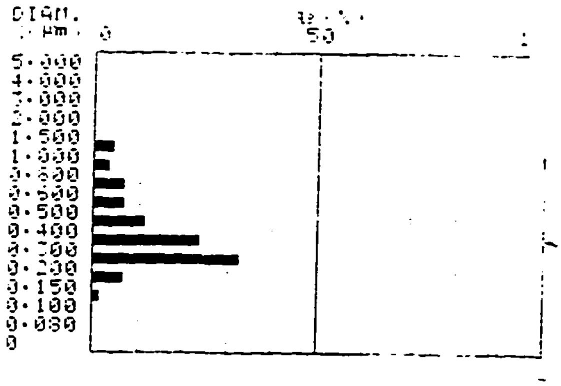

PARTICLE SIZE ANALYSIS BY SA-CP4
V1.00

PLE ID HPA-0.5
PLE # 2/13/96 RUN02

NSITY 3.95 MODE :CENT
NSITY 0.9978 480(RPM/MIN)
.(mPa.S)0.96
TH 2
AK P. 0 K(X):STANDARD

IE 0:17:09

DATA SUMMARY>

MEDIAN DIAM. 0.331 (µm)
MODAL DIAM. 0.266 (µm)
SURFACE AREA 4.908 (m*m/g)

95.0% DIAM. 0.985 (µm)
5.0% DIAM. 0.169 (µm)

DIAM. X(µm) CUM Q3(%)
1.200 97.2
1.000 95.3
0.800 91.6
0.500 77.9
0.100 0.7

A-CP4 CUMULATIVE GRAPH>

AMPLE ID 010
AMPLE # 2/13/96 RUN02

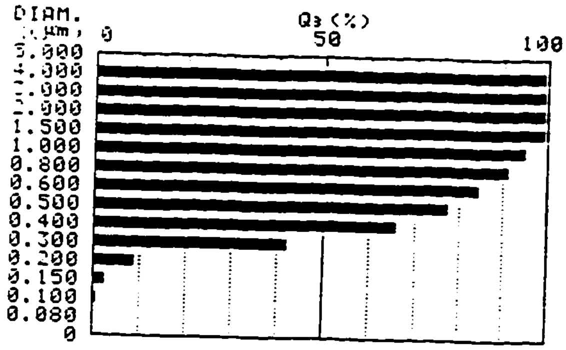

CP4 DIFFERENTIAL GRAPH>

LE ID 010
LE # 2/13/96 RUN02

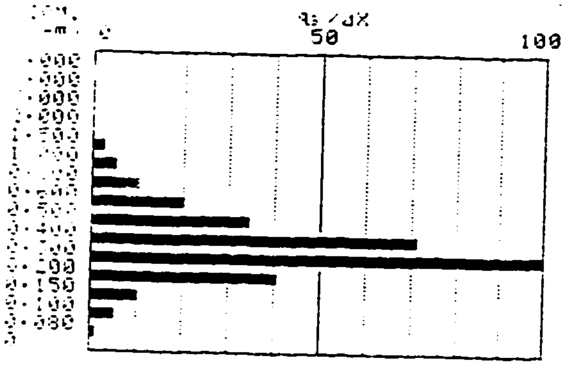

PARTICLE SIZE ANALYSIS BY SA-CP4
V1.00

SAMPLE ID   DISP
SAMPLE #   2/13/96 RUN03

P DENSITY   3.95
L DENSITY   0.9978
VISC.(mPa.S) 0.96
DEPTH   2
BREAK P.   0

MODE :CENT
480(RPM/MIN)

K(X):STANDARD

TIME   0:21:38

DATA SUMMARY>

MEDIAN DIAM.	1.145	(μm)
MODAL DIAM.	1.770	(μm)
SURFACE AREA	5.083	(m*m/g)
95.0% DIAM.	3.769	(μm)
5.0% DIAM.	0.058	(μm)

	DIAM. X(μm)	CUM Q3(%)
1	1.200	51.7
2	1.000	45.6
3	0.800	38.8
4	0.500	24.0
5	0.100	8.2

SA-CP4 CUMULATIVE GRAPH>

SAMPLE ID   001
SAMPLE #   2/13/96 RUN03

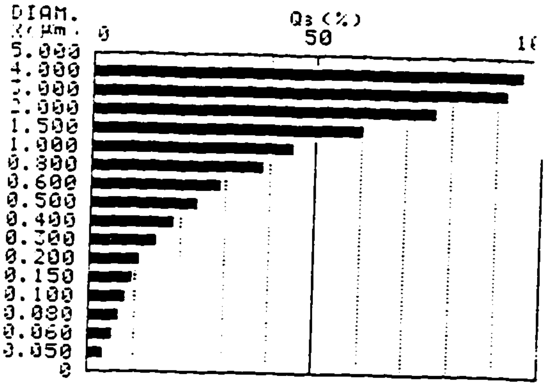

SA-CP4 DIFFERENTIAL GRAPH>

SAMPLE ID   001
SAMPLE #   2/13/96 RUN03

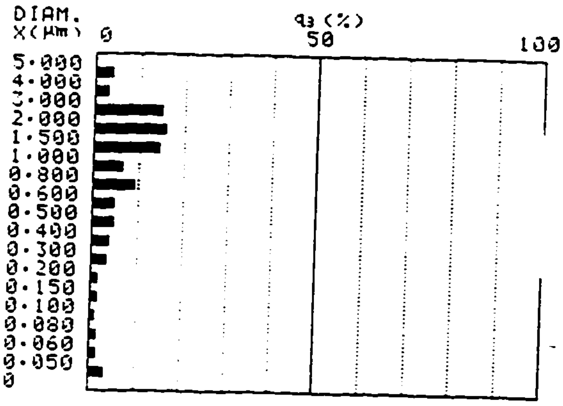

PARTICLE SIZE ANALYSIS BY SA-CP4
V1.00

LE ID   DISP
LE #   2/13/96 RUN03

SITY   3.95
SITY   0.9978
mPa.S 0.96
2
P.   0

MODE :CENT
480(RPM/MIN)

K(X):STANDARD

0:21:38

DATA SUMMARY>

MEDIAN DIAM.   1.145 (μm)
MODAL DIAM.   1.770 (μm)
SURFACE AREA   5.083 (m*m/g)
95.0% DIAM.   3.769 (μm)
5.0% DIAM.   0.058 (μm)

DIAM. X(μm)   CUM Q3(%)
1.200   51.7
1.000   45.6
0.800   38.8
0.500   24.0
0.100   8.2

F4 CUMULATIVE GRAPH>

LE ID   001
LE #   2/13/96 RUN03

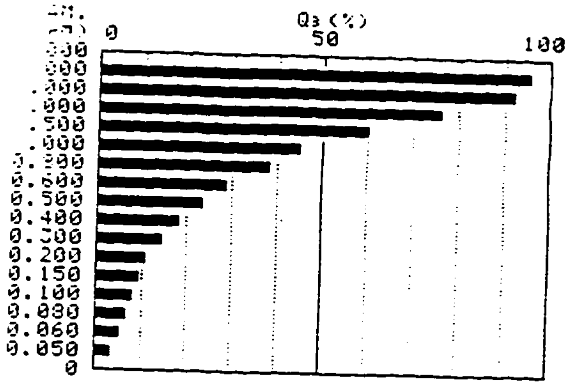

SA-CP4 DIFFERENTIAL GRAPH>

SAMPLE ID   001
SAMPLE #   2/13/96 RUN03

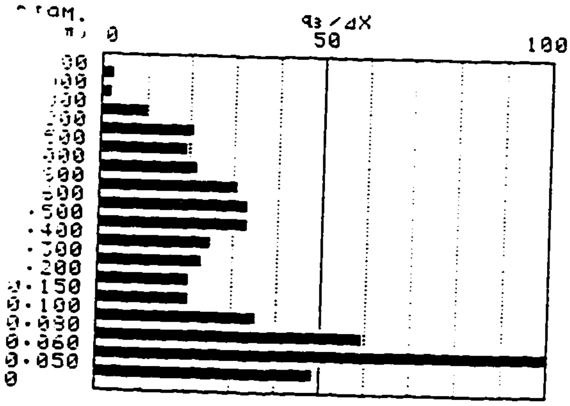

PARTICLE SIZE ANALYSIS BY SA-CP4
V1.00

SAMPLE ID 100
SAMPLE # 2/14/96 RUN01

P DENSITY	3.95	MODE :CENT
L DENSITY	0.9978	480(RPM/MIN)
VISC.(mPa.S)	0.96	
DEPTH	2	
BREAK P.	0	K(X):STANDARD

TIME 0:21:38

DATA SUMMARY>

MEDIAN DIAM.	0.588	(µm)
MODAL DIAM.	0.607	(µm)
SURFACE AREA	3.526	(m*m/g)
95.0% DIAM.	1.163	(µm)
5.0% DIAM.	0.281	(µm)

	DIAM. X(µm)	CUM Q3(%)
1	1.200	95.5
2	1.000	92.8
3	0.800	76.5
4	0.500	28.6
5	0.100	2.1

SA-CP4 CUMULATIVE GRAPH>

SAMPLE ID 100
SAMPLE # 2/14/96 RUN01

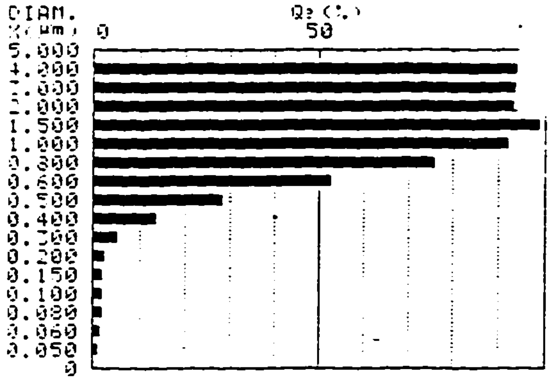

SA-CP4 DIFFERENTIAL GRAPH>

SAMPLE ID 100
SAMPLE # 2/14/96 RUN01

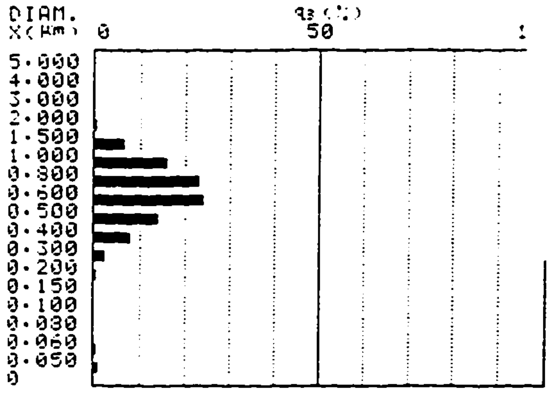

PARTICLE SIZE ANALYSIS BY SA-CP4
V1.00

LE ID 100
LE # 2/14/96 RUN01

NSITY	3.95	MODE :CENT
NSITY	0.9978	480(RPM/MIN)
.(mPa.S)	0.96	
H	2	
K P.	0	K(X):STANDARD

0:21:38

TA SUMMARY>

MEDIAN DIAM.	0.588	(µm)
MODAL DIAM.	0.607	(µm)
SURFACE AREA	3.526	(m*m/g)
95.0% DIAM.	1.163	(µm)
5.0% DIAM.	0.281	(µm)

	DIAM. X(µm)	CUM Q3(%)
	1.200	95.5
	1.000	92.8
	0.800	76.5
4	0.500	28.6
5	0.100	2.1

CP4 CUMULATIVE GRAPH>

PLE ID 100
PLE # 2/14/96 RUN01

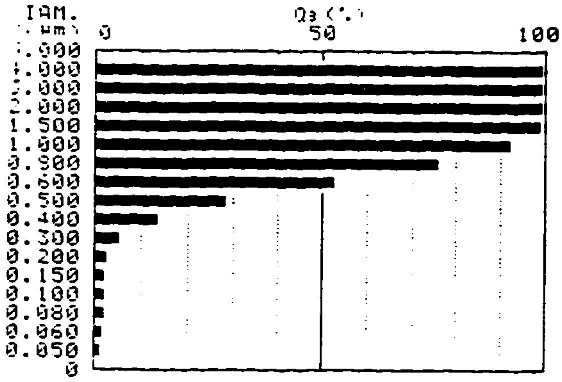

SA-CP4 DIFFERENTIAL GRAPH

SAMPLE ID 100
SAMPLE # 2/14/96 RUN01

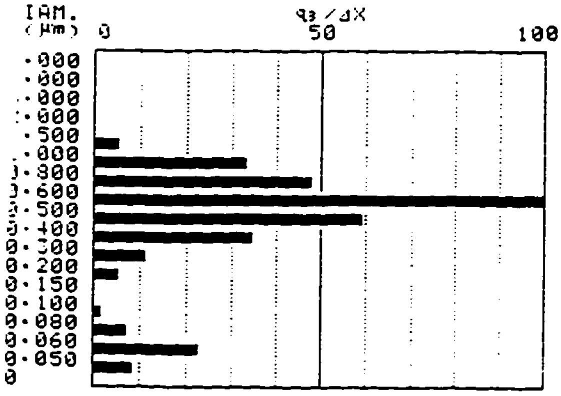

PARTICLE SIZE ANALYSIS BY SA-CP4
V1.00

SAMPLE ID 010
SAMPLE # 2/14/96 RUN02

P DENSITY	3.95	MODE :CENT
L DENSITY	0.9978	480(RPM/MIN)
VISC.(mPa.S)	0.96	
DEPTH	2	
BREAK P.	0	K(X):STANDARD

TIME 0:19:32

DATA SUMMARY>

MEDIAN DIAM.	0.408	(μm)
MODAL DIAM.	0.261	(μm)
SURFACE AREA	4.078	(m*m/g)
95.0% DIAM.	2.731	(μm)
5.0% DIAM.	0.172	(μm)

	DIAM. X(μm)	CUM Q_3(%)
1	1.200	79.4
2	1.000	78.7
3	0.800	74.2
4	0.500	59.7
5	0.100	1.3

SA-CP4 CUMULATIVE GRAPH>

SAMPLE ID 010
SAMPLE # 2/14/96 RUN02

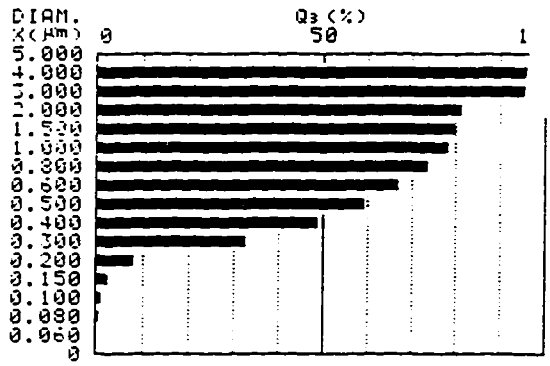

SA-CP4 DIFFERENTIAL GRAPH>

SAMPLE ID 010
SAMPLE # 2/14/96 RUN02

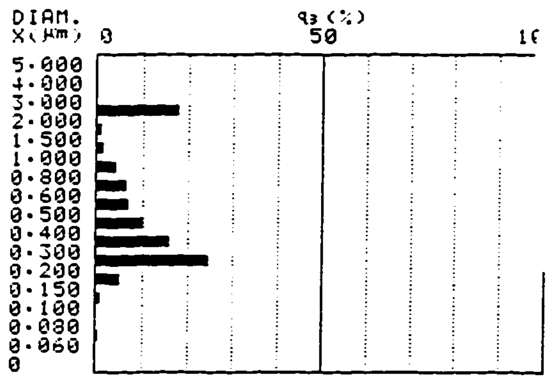

PARTICLE SIZE ANALYSIS BY SA-CP4
V1.00

SAMPLE ID 010
SAMPLE # 2/14/96 RUN02

MODE :CENT
480(RPM/MIN)
K(X):STANDARD

0:19:32

SUMMARY>

MEDIAN DIAM. 0.408 (μm)
MODAL DIAM. 0.261 (μm)
SURFACE AREA 4.078 (m*m/g)
95.0% DIAM. 2.731 (μm)
5.0% DIAM. 0.172 (μm)

DIAM. CUM
1.200 79.4
1.000 78.7
0.800 74.2
0.500 59.7
0.100 1.3

CUMULATIVE GRAPH>
2/14/96 RUN02

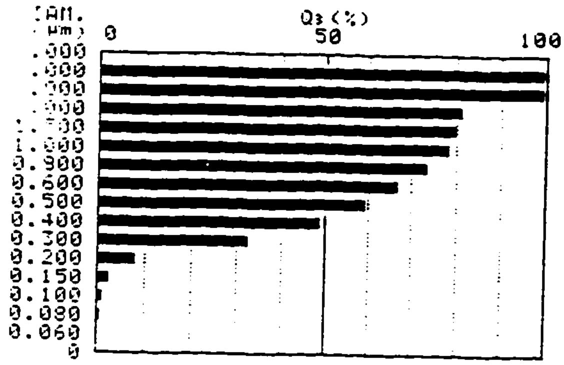

SA-CP4 DIFFERENTIAL GRAPH>
SAMPLE ID 010
SAMPLE # 2/14/96 RUN02

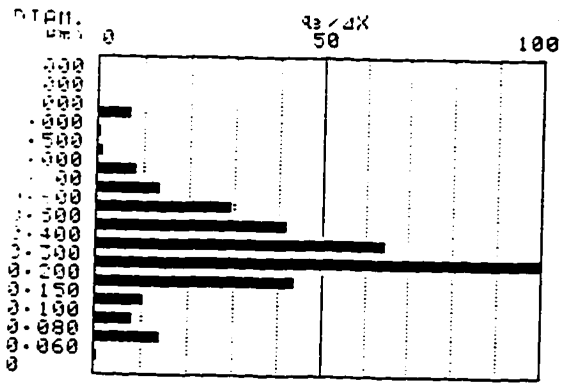

PARTICLE SIZE ANALYSIS BY SA-CP4
V1.00

SAMPLE ID 001
SAMPLE # 2/14/96 RUN03

F DENSITY 3.95 MODE :CENT
L DENSITY 0.9978 480(RPM/MIN)
VISC.(mPa.S) 0.96
DEPTH 2
BREAK P. 0 K(X):STANDARD

TIME 0:21:38

DATA SUMMARY>

MEDIAN DIAM.	1.453	(μm)
MODAL DIAM.	2.332	(μm)
SURFACE AREA	2.525	(m²/g)
95.0% DIAM.	4.676	(μm)
5.0% DIAM.	0.186	(μm)

	DIAM. X(μm)	CUM Q3(%)
1	1.200	41.3
2	1.000	34.5
3	0.800	26.5
4	0.500	15.9
5	0.100	2.8

SA-CP4 CUMULATIVE GRAPH>

SAMPLE ID 001
SAMPLE # 2/14/96 RUN03

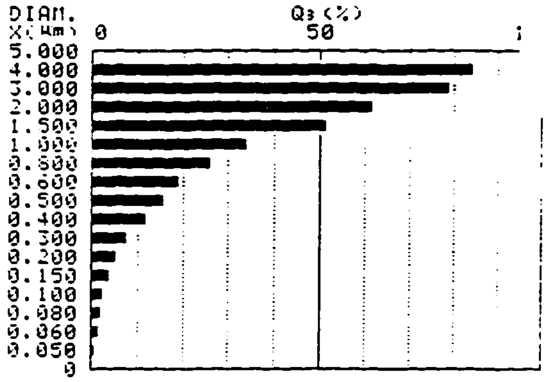

SA-CP4 DIFFERENTIAL GRAPH>

SAMPLE ID 001
SAMPLE # 2/14/96 RUN03

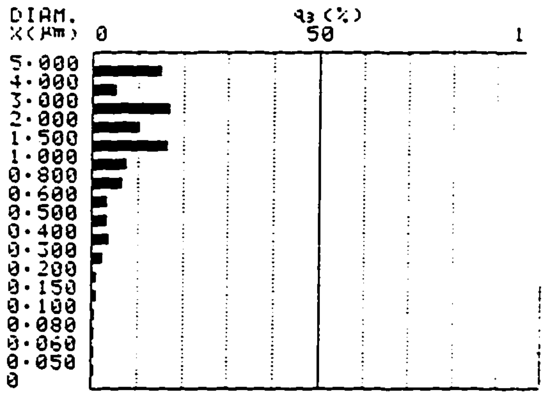

PARTICLE SIZE ANALYSIS BY SA-CP4
V1.00

E ID 001
E # 2/14/96 RUN03

SITY 3.95 MODE :CENT
SITY 0.9978 480(RPM/MIN)
(mPa.S) 0.96
2
K P. 0 K(X):STANDARD

0:21:38

TA SUMMARY>

MEDIAN DIAM. 1.453 (μm)
MODAL DIAM. 2.332 (μm)
SURFACE AREA 2.525 (m²/g)
95.0% DIAM. 4.676 (μm)
5.0% DIAM. 0.186 (μm)

DIAM. X(μm) CUM Q3(%)
1.200 41.3
1.000 34.5
0.800 26.5
0.500 15.9
0.100 2.8

CP4 CUMULATIVE GRAPH>

PLE ID 001
PLE # 2/14/96 RUN03

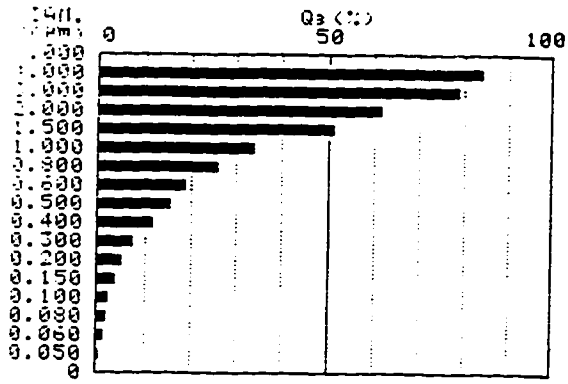

SA-CP4 DIFFERENTIAL GRAPH>

SAMPLE ID 001
SAMPLE # 2/14/96 RUN03

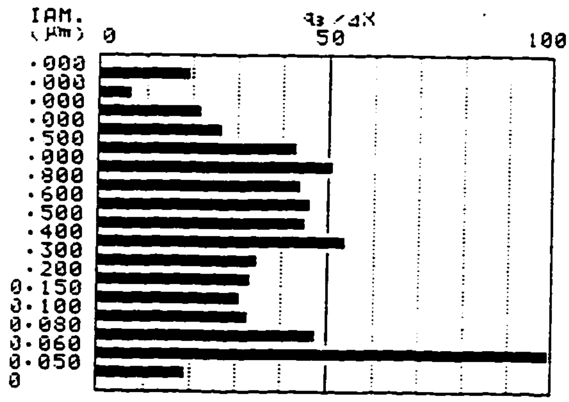

PARTICLE SIZE ANALYSIS BY SA-CP4
V1.00

SAMPLE ID 001
SAMPLE # 2/15/96 RUN01

F DENSITY 3.95
L DENSITY 0.9978
VISC.(mpa.S) 0.96
DEPTH 2
BREAK P. 0

MODE :CENT
480(RPM/MIN)

K(X):STANDARD

TIME 0:21:38

DATA SUMMARY>

MEDIAN DIAM.	0.938	(μm)
MODAL DIAM.	1.303	(μm)
SURFACE AREA	7.253	(m*m/g)
95.0% DIAM.	2.666	(μm)
5.0% DIAM.	0.039	(μm)

	DIAM. X(μm)	CUM Q_3(%)
1	1.200	60.0
2	1.000	51.9
3	0.800	45.7
4	0.500	31.9
5	0.100	12.6

SA-CP4 CUMULATIVE GRAPH>

SAMPLE ID 001
SAMPLE # 2/15/96 RUN01

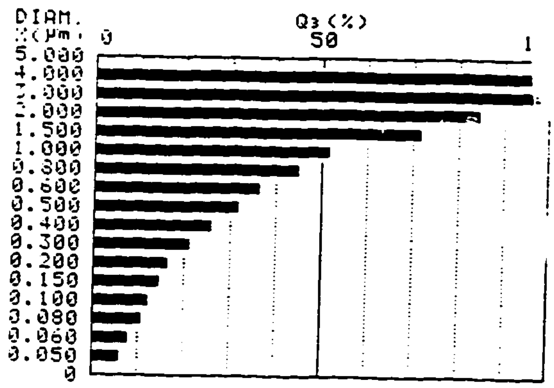

SA-CP4 DIFFERENTIAL GRAPH>

SAMPLE ID 001
SAMPLE # 2/15/96 RUN01

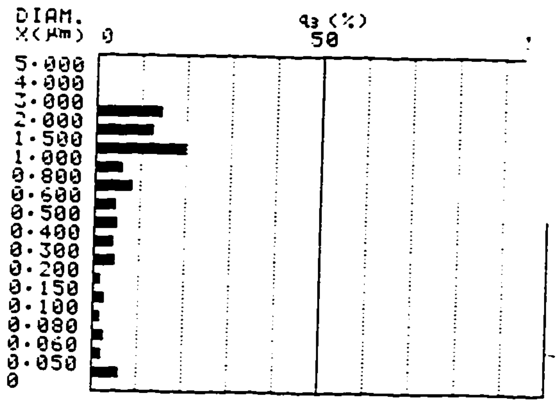

PARTICLE SIZE ANALYSIS BY SA-CP4
V1.00

PLE ID 001
PLE # 2/15/96 RUN01

NSITY 3.95
NSITY 0.9978
.(mpa.S) 0.96
H 2
P. 0

MODE :CENT
480(RPM/MIN)

K(X):STANDARD

IME 0:21:38

DATA SUMMARY>

MEDIAN DIAM. 0.938 (μm)
MODAL DIAM. 1.303 (μm)
SURFACE AREA 7.253 (m*m/g)

95.0% DIAM. 2.666 (μm)
5.0% DIAM. 0.039 (μm)

DIAM. X(μm) CUM Q3(%)
1.200 60.0
1.000 51.9
0.800 45.7
0.500 31.9
0.100 12.6

CUMULATIVE GRAPH>

PLE ID 001
PLE # 2/15/96 RUN01

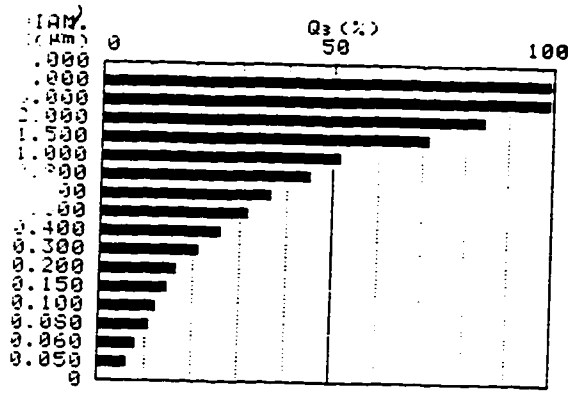

SA-CP4 DIFFERENTIAL GRAPH>

PLE ID 001
PLE # 2/15/96 RUN01

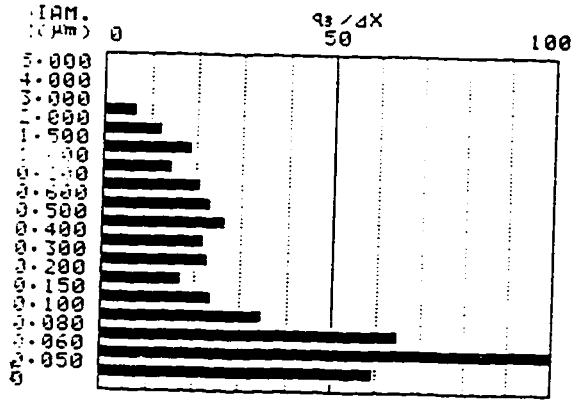

PARTICLE SIZE ANALYSIS BY SA-CP4
V1.00

SAMPLE ID 100
SAMPLE # 2/15/96 RUN02

P DENSITY	3.95	MODE :CENT
L DENSITY	0.9978	480(RPM/MIN)
VISC.(mPa.S)	0.96	
DEPTH	2	
BREAK P.	0	K(X):STANDARD

TIME 0:21:38

DATA SUMMARY>

MEDIAN DIAM.	0.628	(μm)
MODAL DIAM.	0.661	(μm)
SURFACE AREA	3.349	(m*m/g)
95.0% DIAM.	1.458	(μm)
5.0% DIAM.	0.279	(μm)

	DIAM. X(μm)	CUM Q_3(%)
1	1.200	88.9
2	1.000	84.2
3	0.800	74.2
4	0.500	25.4
5	0.100	1.8

SA-CP4 CUMULATIVE GRAPH>

SAMPLE ID 100
SAMPLE # 2/15/96 RUN02

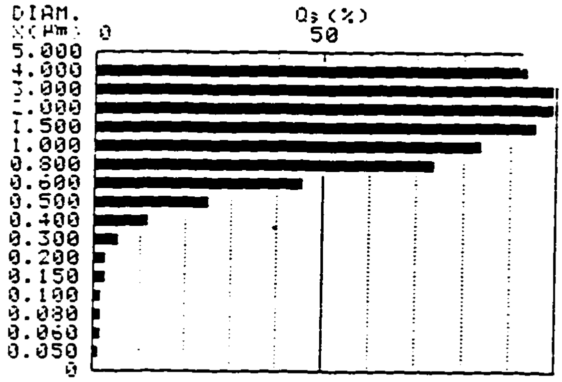

SA-CP4 DIFFERENTIAL GRAPH>

SAMPLE ID 100
SAMPLE # 2/15/96 RUN02

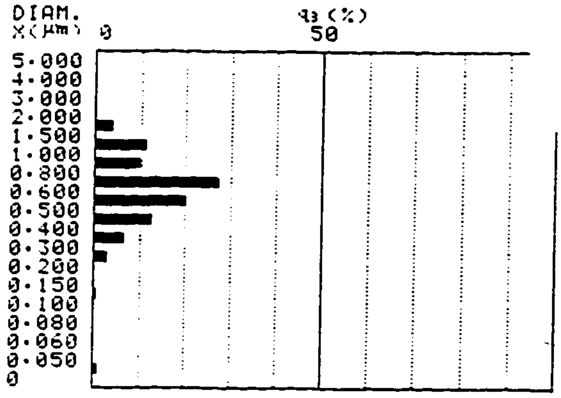

PARTICLE SIZE ANALYSIS BY SA-CP4
V1.00

PLE ID 100
PLE # 2/15/96 RUN02

NSITY	3.95	MODE :CENT
NSITY	0.9978	480(RPM/MIN)
.(mPa.S)	0.96	
H	2	
K P.	0	K(X):STANDARD

0:21:38

ATA SUMMARY>

MEDIAN DIAM.	0.628	(μm)
MODAL DIAM.	0.661	(μm)
SURFACE AREA	3.349	(m*m/g)
95.0% DIAM.	1.458	(μm)
5.0% DIAM.	0.279	(μm)

DIAM. X(μm)	CUM Q_3(%)
1.200	88.9
1.000	84.2
0.800	74.2
0.500	25.4
0.100	1.8

CP4 CUMULATIVE GRAPH>

IPLE ID 100
IPLE # 2/15/96 RUN02

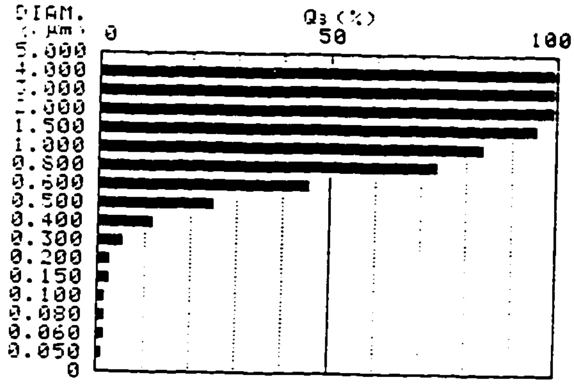

CP4 DIFFERENTIAL GRAPH>

PLE ID 100
PLE # 2/15/96 RUN02

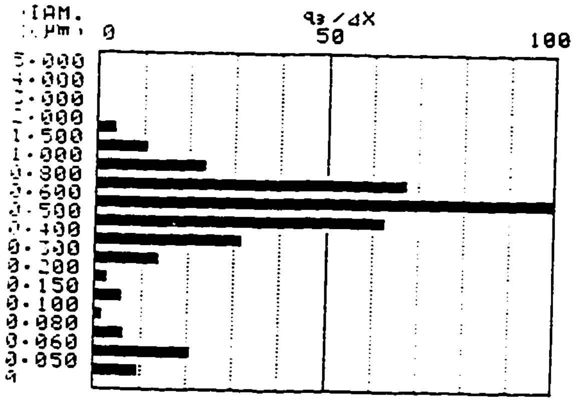

PARTICLE SIZE ANALYSIS BY SA-CP4
V1.00

SAMPLE ID 010
SAMPLE # 2/15/96 RUN03

P DENSITY	3.95	MODE :CENT
L DENSITY	0.9978	480(RPM/MIN)
VISC.(mPa.S)	0.96	
DEPTH	2	
EPEAK P.	0	K(X):STANDARD

TIME 0:21:38

DATA SUMMARY>

MEDIAN DIAM.	0.313	(µm)
MODAL DIAM.	0.262	(µm)
SURFACE AREA	5.323	(m*m/g)
95.0% DIAM.	0.802	(µm)
5.0% DIAM.	0.157	(µm)

	DIAM. X(µm)	CUM Q_3(%)
1	1.200	99.3
2	1.000	98.8
3	0.800	95.0
4	0.500	81.8
5	0.100	1.6

SA-CP4 CUMULATIVE GRAPH>

SAMPLE ID 010
SAMPLE # 2/15/96 RUN03

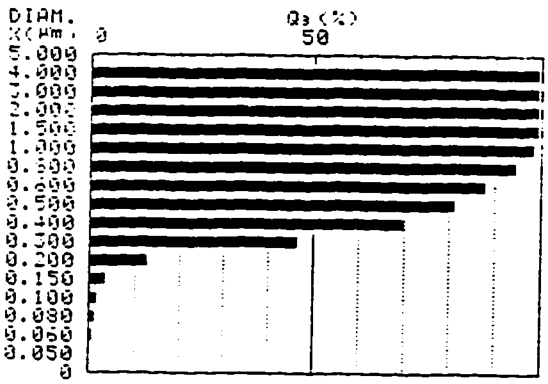

SA-CP4 DIFFERENTIAL GRAPH>

SAMPLE ID 010
SAMPLE # 2/15/96 RUN03

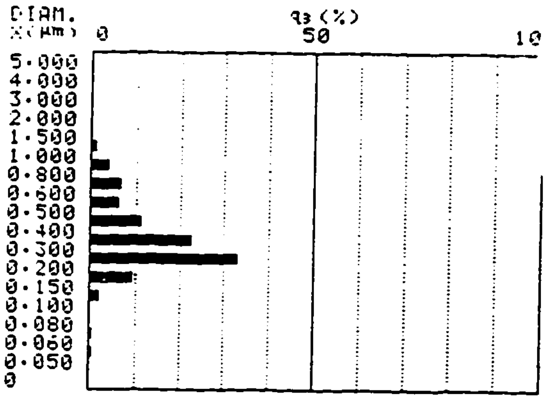

PARTICLE SIZE ANALYSIS BY SA-CP4
V1.00

LE ID 010
LE # 2/15/96 RUN03

ISITY 3.95 MODE :CENT
ISITY 0.9978 480(RPM/MIN)
.(mPa.S)0.96
H 2
K P. 0 K(X):STANDARD

0:21:38

TA SUMMARY>

MEDIAN DIAM. 0.313 (µm)
MODAL DIAM. 0.262 (µm)
SURFACE AREA 5.323 (m*m/g)

95.0% DIAM. 0.802 (µm)
5.0% DIAM. 0.157 (µm)

DIAM. X(µm) CUM Q3(%)
1.200 99.3
1.000 98.8
0.800 95.0
0.500 81.8
0.100 1.6

CP4 CUMULATIVE GRAPH>

PLE ID 010
PLE # 2/15/96 RUN03

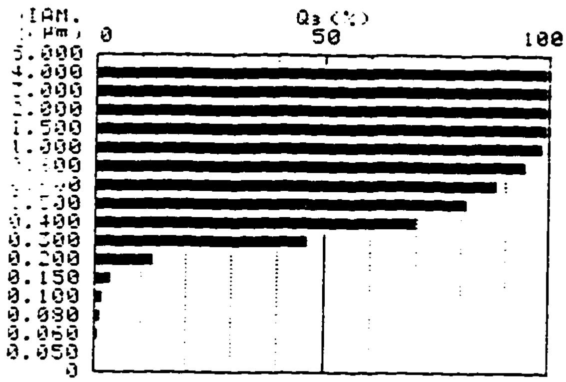

4 DIFFERENTIAL GRAPH

LE ID 010
LE # 2/15/96 RUN03

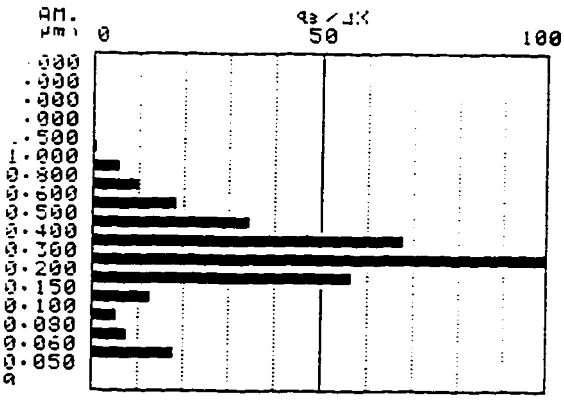

PARTICLE SIZE ANALYSIS BY SA-CP4
V1.00

SAMPLE ID 955
SAMPLE # 2/16/96 RUN01

P DENSITY 3.95 MODE :CENT
L DENSITY 0.9978 480(RPM/MIN)
VISC.(mPa.S) 0.96
DEPTH 2
BREAK P. 0 K(X):STANDARD

TIME 0:21:38

DATA SUMMARY>

MEDIAN DIAM. 0.599 (µm)
MODAL DIAM. 0.655 (µm)
SURFACE AREA 3.561 (m*m/g)

95.0% DIAM. 1.397 (µm)
5.0% DIAM. 0.249 (µm)

	DIAM. X(µm)	CUM Q3(%)
1	1.200	91.0
2	1.000	86.9
3	0.800	76.1
4	0.500	29.7
5	0.100	2.2

SA-CP4 CUMULATIVE GRAPH>

SAMPLE ID 955
SAMPLE # 2/16/96 RUN01

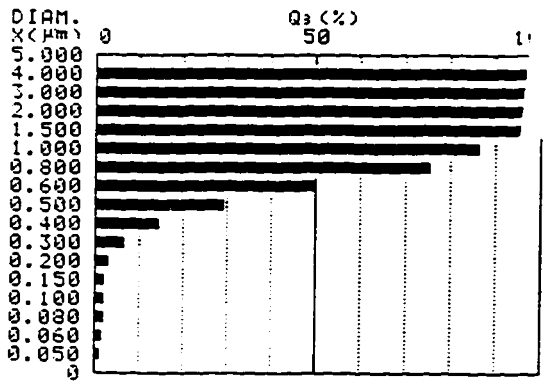

SA-CP4 DIFFERENTIAL GRAPH>

SAMPLE ID 955
SAMPLE # 2/16/96 RUN01

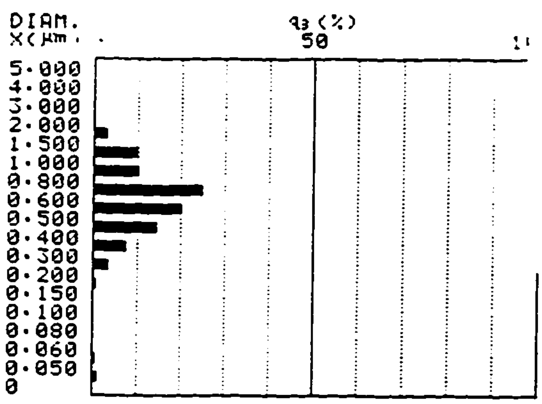

PARTICLE SIZE ANALYSIS BY SA-CP4
V1.00

PLE ID 955
PLE # 2/16/96 RUN01

NSITY 3.95 MODE :CENT
NSITY 0.9978 480(RPM/MIN)
.(mPa.S) 0.96
H 2
K P. 0 K(X):STANDARD

0:21:38

A SUMMARY>

MEDIAN DIAM. 0.599 (µm)
MODAL DIAM. 0.655 (µm)
SURFACE AREA 3.561 (m*m/g)

95.0% DIAM. 1.397 (µm)
5.0% DIAM. 0.249 (µm)

DIAM. X(µm) CUM Q3(%)
1 1.200 91.0
2 1.000 86.9
3 0.800 76.1
4 0.500 29.7
5 0.100 2.2

P4 CUMULATIVE GRAPH>

LE ID 955
LE # 2/16/96 RUN01

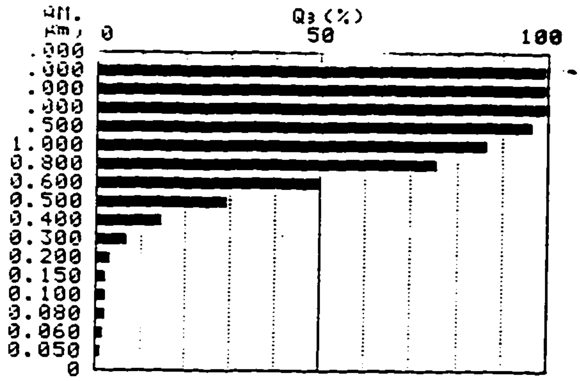

SA-CP4 DIFFERENTIAL GRAPH>

SAMPLE ID 955
SAMPLE # 2/16/96 RUN01

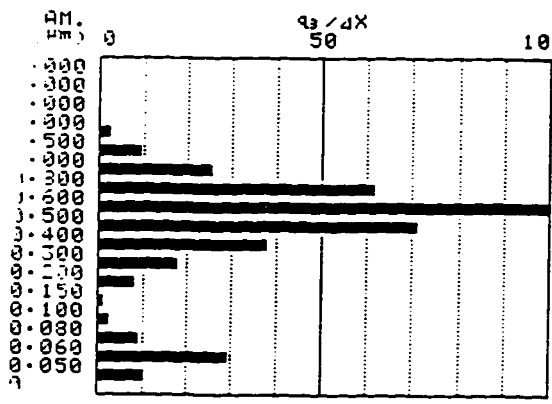

PARTICLE SIZE ANALYSIS BY SA-CP4
V1.00

SAMPLE ID 811
SAMPLE # 2/16/96 RUN02

P DENSITY	3.95	MODE :CENT
L DENSITY	0.9978	480(RPM/MIN)
VISC.(mPa.S)	0.96	
DEPTH	2	
BREAK P.	0	K(X):STANDARD

TIME 0:19:44

<DATA SUMMARY>

MEDIAN DIAM.	0.590	(μm)
MODAL DIAM.	0.669	(μm)
SURFACE AREA	3.065	(m*m/g)
95.0% DIAM.	1.155	(μm)
5.0% DIAM.	0.259	(μm)

	DIAM. X(μm)	CUM Q_3(%)
1	1.200	95.6
2	1.000	92.7
3	0.800	81.2
4	0.500	31.7
5	0.100	0.8

<SA-CP4 CUMULATIVE GRAPH>

SAMPLE ID 811
SAMPLE # 2/16/96 RUN02

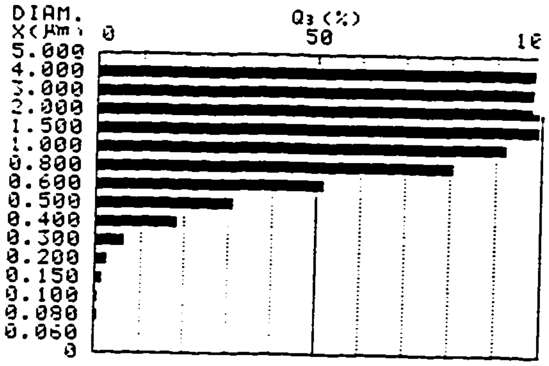

<SA-CP4 DIFFERENTIAL GRAPH>

SAMPLE ID 811
SAMPLE # 2/16/96 RUN02

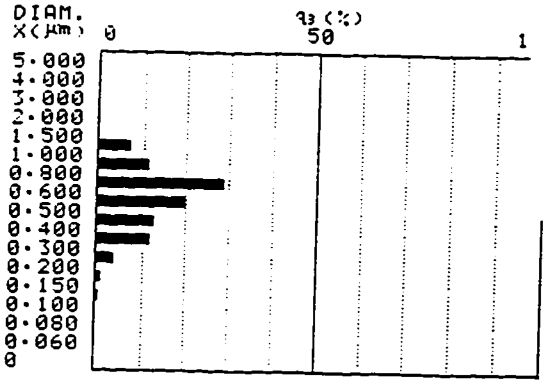

ARTICLE SIZE ANALYSIS BY SA-CP4
V1.00

PLE ID 811
PLE # 2/16/96 RUN02

NSITY 3.95 MODE :CENT
NSITY 0.9978 480(RPM/MIN)
(mPa.S)0.96
TH 2
AK P. 0 K(X):STANDARD

ME 0:19:44

<DATA SUMMARY>

MEDIAN DIAM. 0.590 (μm)
MODAL DIAM. 0.669 (μm)
SURFACE AREA 3.065 (m*m/g)

95.0% DIAM. 1.155 (μm)
5.0% DIAM. 0.259 (μm)

DIAM. X(μm) CUM Q3(%)
1.200 95.6
1.000 92.7
0.800 81.2
0.500 31.7
0.100 0.8

P4 CUMULATIVE GRAPH>

LE ID 811
LE # 2/16/96 RUN02

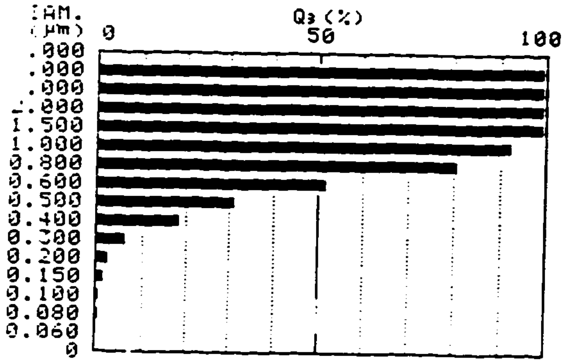

SA-CP4 DIFFERENTIAL GRAPH>

SAMPLE ID 811
IPLE # 2/16/96 RUN02

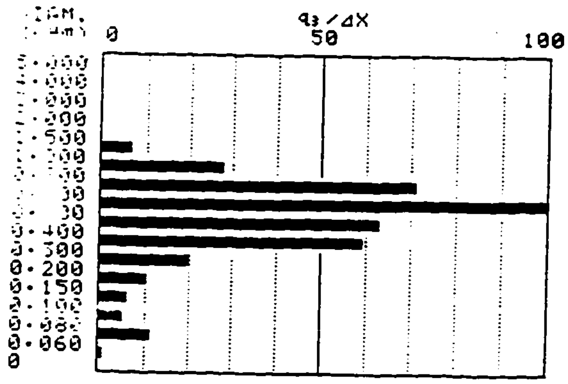

PARTICLE SIZE ANALYSIS BY SA-CP4
V1.00

SAMPLE ID F100
SAMPLE # 2/16/96 RUN03

P DENSITY 3.95 MODE :CENT
L DENSITY 0.9978 480(RPM/MIN)
VISC.(mPa.S) 0.96
DEPTH 2
BREAK P. 0 K(X):STANDARD

TIME 0:25:47

DATA SUMMARY>

MEDIAN DIAM.	1.056	(µm)
MODAL DIAM.	1.386	(µm)
SURFACE AREA	4.265	(m*m/g)
95.0% DIAM.	2.406	(µm)
5.0% DIAM.	0.091	(µm)

	DIAM. X(µm)	CUM Q3(%)
1	1.200	56.7
2	1.000	47.4
3	0.800	37.0
4	0.500	22.1
5	0.100	5.4

SA-CP4 CUMULATIVE GRAPH>

SAMPLE ID F100
SAMPLE # 2/16/96 RUN03

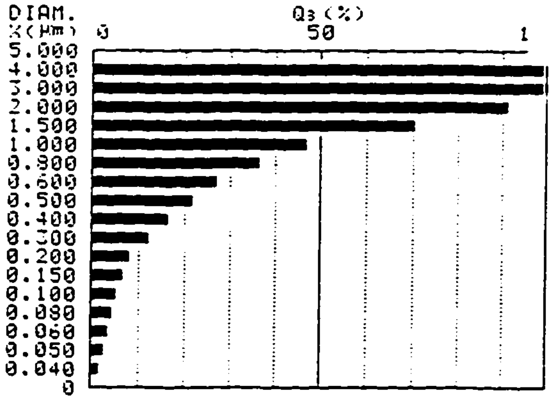

SA-CP4 DIFFERENTIAL GRAPH>

SAMPLE ID F100
SAMPLE # 2/16/96 RUN03

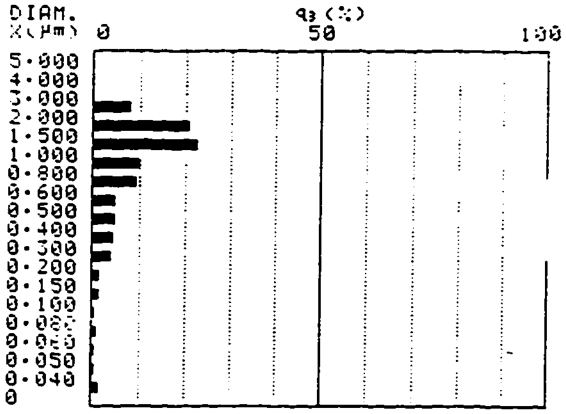

PARTICLE SIZE ANALYSIS BY SA-CP4
V1.00

ID F100
2/16/96 RUN03

ITY 3.95 MODE :CENT
ITY 0.9978 480(RPM/MIN)
mPa.S) 0.96
2
P. 0 K(X):STANDARD

0:25:47

A SUMMARY>

MEDIAN DIAM. 1.056 (µm)
MODAL DIAM. 1.386 (µm)
SURFACE AREA 4.265 (m*m/g)
95.0% DIAM. 2.406 (µm)
5.0% DIAM. 0.091 (µm)

DIAM. X(µm) CUM Q3(%)
1 1.200 56.7
1.000 47.4
0.800 37.0
0.500 22.1
0.100 5.4

P4 CUMULATIVE GRAPH>

LE ID F100
LE # 2/16/96 RUN03

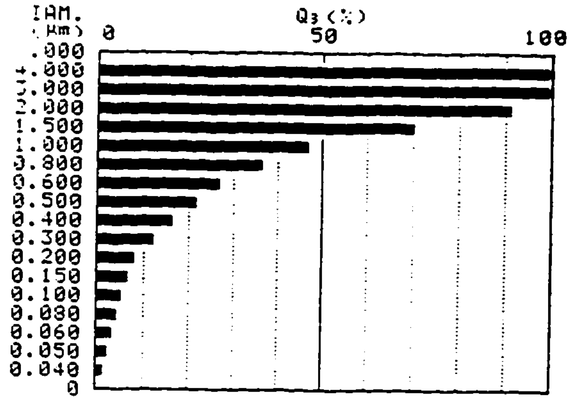

SA-CP4 DIFFERENTIAL GRAPH>

SAMPLE ID F100
SAMPLE # 2/16/96 RUN03

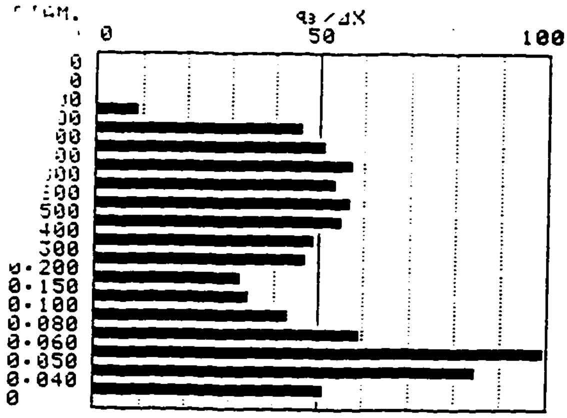

PARTICLE SIZE ANALYSIS BY SA-CP4
V1.00

SAMPLE ID 721
SAMPLE # 2/17/96 RUN01

P DENSITY 3.95 MODE :CENT
L DENSITY 0.9978 480(RPM/MIN)
VISC.(mPa.S)0.96
DEPTH 2
BREAK P. 0 K(X):STANDARD

TIME 0:20:58

<DATA SUMMARY>

MEDIAN DIAM.	0.591	(μm)
MODAL DIAM.	0.681	(μm)
SURFACE AREA	3.346	(m*m/g)
95.0% DIAM.	1.259	(μm)
5.0% DIAM.	0.223	(μm)

	DIAM. X(μm)	CUM Q_3(%)
1	1.200	93.8
2	1.000	89.6
3	0.800	77.6
4	0.500	35.3
5	0.100	1.3

<SA-CP4 CUMULATIVE GRAPH>

SAMPLE ID 721
SAMPLE # 2/17/96 RUN01

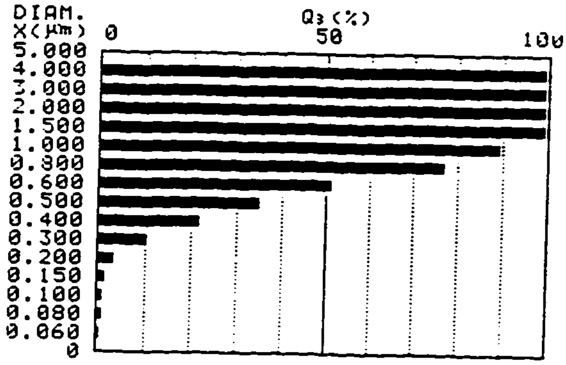

<SA-CP4 DIFFERENTIAL GRAPH>

SAMPLE ID 721
SAMPLE # 2/17/96 RUN01

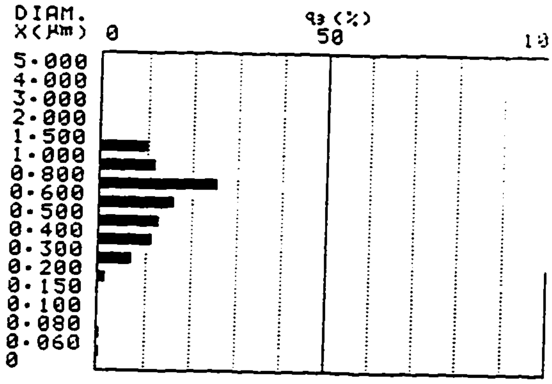

PARTICLE SIZE ANALYSIS BY SA-CP4
V1.00

PLE ID - 721
PLE # 2/17/96 RUN01

NSITY 3.95 MODE :CENT
NSITY 0.9978 480(RPM/MIN)
.(mPa.S)0.96
H 2
K P. 0 K(X):STANDARD

E 0:20:58

DATA SUMMARY>

MEDIAN DIAM. 0.591 (μm)
MODAL DIAM. 0.661 (μm)
SURFACE AREA 3.346 (m*m/g)

95.0% DIAM. 1.259 (μm)
5.0% DIAM. 0.223 (μm)

DIAM. X(μm) CUM Q3(%)
1 1.200 93.8
1.000 89.6
0.800 77.6
0.500 35.3
0.100 1.3

CP4 CUMULATIVE GRAPH>

PLE ID 721
PLE # 2/17/96 RUN01

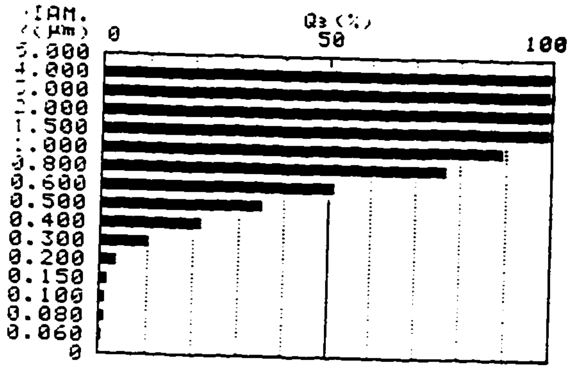

SA-CP4 DIFFERENTIAL GRAPH>

SAMPLE ID 721
SAMPLE # 2/17/96 RUN01

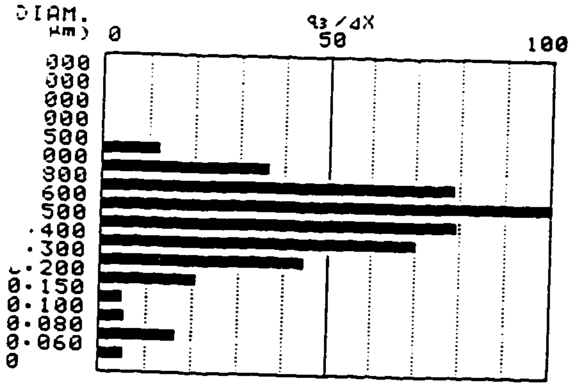

PARTICLE SIZE ANALYSIS BY SA-CP4 V1.00

SAMPLE ID 712
SAMPLE # 2/17/96 RUN02

P DENSITY	3.95	MODE :CENT
L DENSITY	0.9978	480(RPM/MIN)
VISC.(mPa.S)	0.96	
DEPTH	2	
BREAK P.	0	K(X):STANDARD

TIME 0:19:02

<DATA SUMMARY>

MEDIAN DIAM.	0.671	(μm)
MODAL DIAM.	0.727	(μm)
SURFACE AREA	2.829	(m*m/g)
95.0% DIAM.	1.398	(μm)
5.0% DIAM.	0.288	(μm)

	DIAM. X(μm)	CUM Q_3(%)
1	1.200	91.2
2	1.000	87.3
3	0.800	66.7
4	0.500	26.4
5	0.100	0.8

<SA-CP4 CUMULATIVE GRAPH>

SAMPLE ID 712
SAMPLE # 2/17/96 RUN02

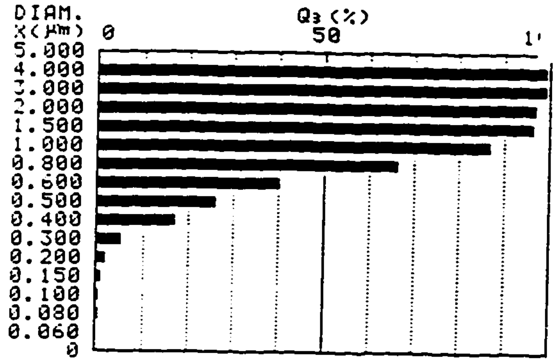

<SA-CP4 DIFFERENTIAL GRAPH>

SAMPLE ID 712
SAMPLE # 2/17/96 RUN02

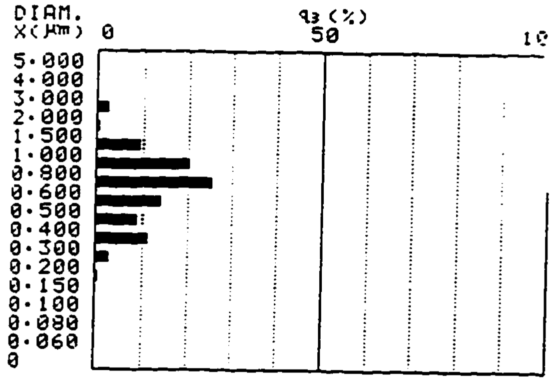

PARTICLE SIZE ANALYSIS BY SA-CP4 V1.00

MPLE ID 712
MPLE # 2/17/96 RUN02

ENSITY 3.95 MODE :CENT
ENSITY 0.9978 480(RPM/MIN)
C.(mPa.S)0.96
TH 2
AK P. 0 K(X):STANDARD

TIME 0:19:02

DATA SUMMARY>

MEDIAN DIAM. 0.671 (μm)
MODAL DIAM. 0.727 (μm)
SURFACE AREA 2.829 (m*m/g)

95.0% DIAM. 1.398 (μm)
5.0% DIAM. 0.288 (μm)

DIAM. X(μm) CUM Q3(%)
1 1.200 91.2
1.000 87.3
0.800 66.7
0.500 26.4
0.100 0.8

P4 CUMULATIVE GRAPH>

LE ID 712
LE # 2/17/96 RUN02

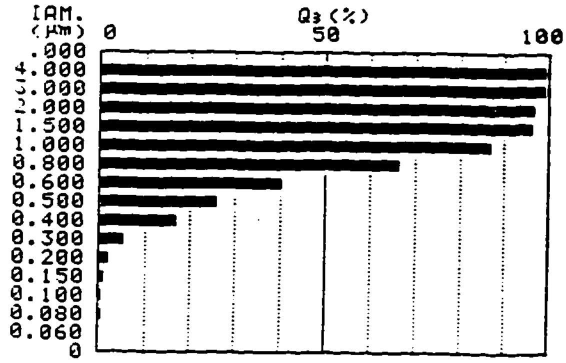

SA-CP4 DIFFERENTIAL GRAPH>

LE ID 712
LE # 2/17/96 RUN02

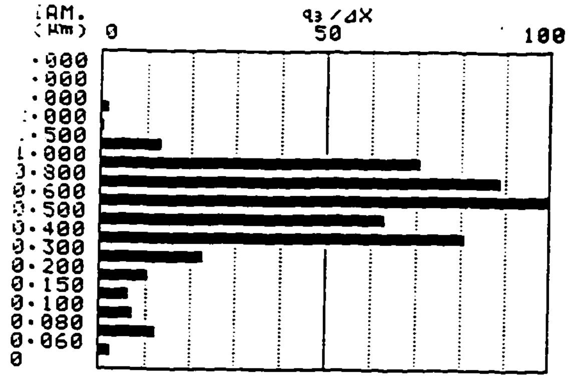

PARTICLE SIZE ANALYSIS BY SA-CP4
V1.00

SAMPLE ID 622
SAMPLE # 2/17/96 RUN03

P DENSITY 3.95
L DENSITY 0.9978
VISC.(mPa.S) 0.96
DEPTH 2
BREAK P. 0

MODE :CENT
480(RPM/MIN)
K(X):STANDARD

TIME 0:20:08

DATA SUMMARY>

MEDIAN DIAM. 0.639 (μm)
MODAL DIAM. 0.700 (μm)
SURFACE AREA 3.022 (m*m/g)

95.0% DIAM. 1.422 (μm)
5.0% DIAM. 0.235 (μm)

	DIAM. X(μm)	CUM Q3(%)
1	1.200	90.2
2	1.000	85.9
3	0.800	71.1
4	0.500	31.2
5	0.100	0.9

SA-CP4 CUMULATIVE GRAPH>

SAMPLE ID 622
SAMPLE # 2/17/96 RUN03

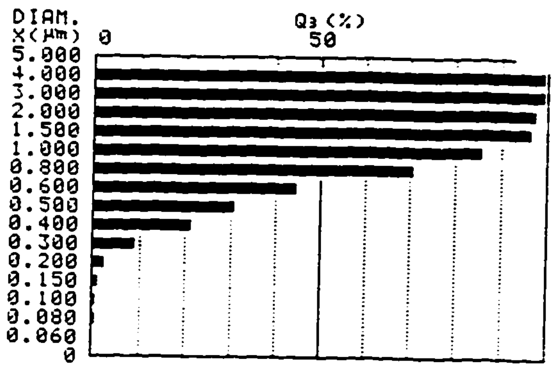

SA-CP4 DIFFERENTIAL GRAPH>

SAMPLE ID 622
SAMPLE # 2/17/96 RUN03

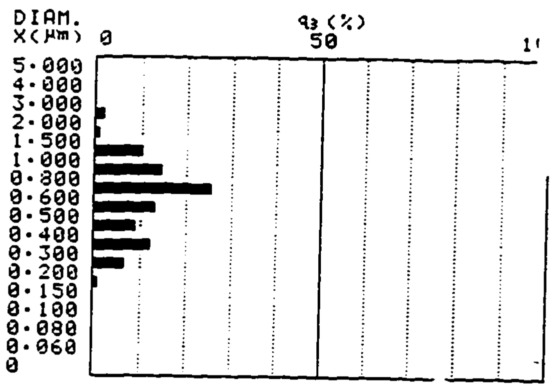

PARTICLE SIZE ANALYSIS BY SA-CP4
V1.00

PLE ID 622
PLE # 2/17/96 RUN03

NSITY 3.95
NSITY 0.9978
.(mPa.S) 0.96
H 2
K P. 0

MODE :CENT
480(RPM/MIN)
K(X):STANDARD

0:20:08

DATA SUMMARY>

MEDIAN DIAM. 0.639 (μm)
MODAL DIAM. 0.700 (μm)
SURFACE AREA 3.022 (m*m/g)

95.0% DIAM. 1.422 (μm)
5.0% DIAM. 0.235 (μm)

DIAM. X(μm) CUM Q3(%)
1.200 90.2
1.000 85.9
0.800 71.1
0.500 31.2
0.100 0.9

P4 CUMULATIVE GRAPH>

PLE ID 622
PLE # 2/17/96 RUN03

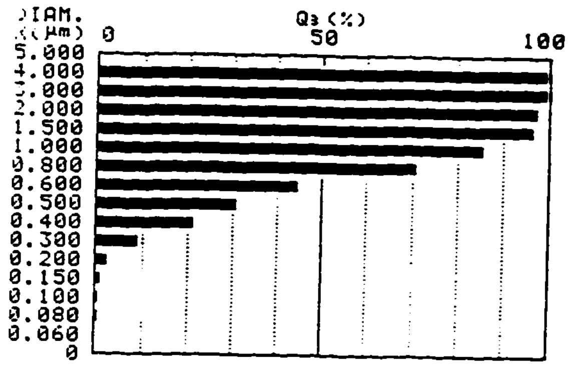

P4 DIFFERENTIAL GRAPH>

LE ID 622
LE # 2/17/96 RUN03

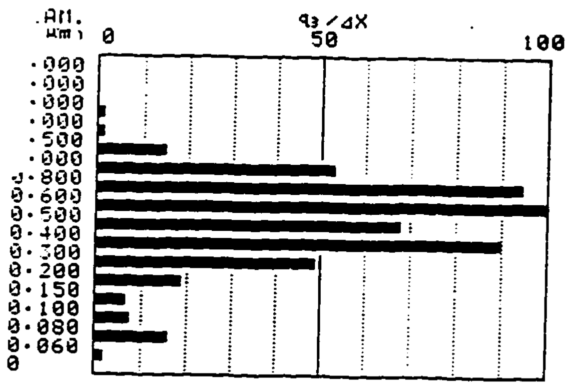

PARTICLE SIZE ANALYSIS BY SA-CP4
V1.00

SAMPLE ID 613
SAMPLE # 2/17/96 RUN04

P DENSITY	3.95	MODE :CENT
L DENSITY	0.9978	480(RPM/MIN)
VISC.(mPa.S)	0.96	
DEPTH	2	
BREAK P.	0	K(X):STANDARD

TIME 0:21:12

DATA SUMMARY>

MEDIAN DIAM.	0.645 (μm)
MODAL DIAM.	0.694 (μm)
SURFACE AREA	2.979 (m*m/g)
95.0% DIAM.	1.472 (μm)
5.0% DIAM.	0.262 (μm)

	DIAM. X(μm)	CUM Q_3(%)
1	1.200	89.3
2	1.000	85.1
3	0.800	72.9
4	0.500	29.9
5	0.100	1.1

SA-CP4 CUMULATIVE GRAPH>

SAMPLE ID 613
SAMPLE # 2/17/96 RUN04

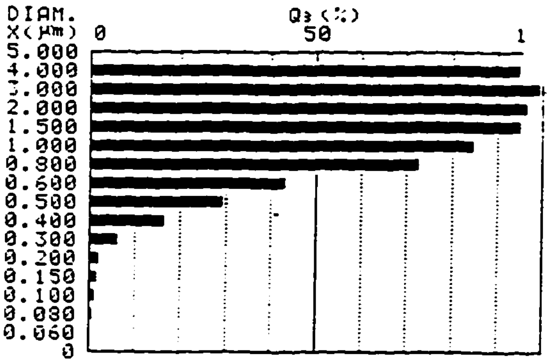

SA-CP4 DIFFERENTIAL GRAPH>

SAMPLE ID 613
SAMPLE # 2/17/96 RUN04

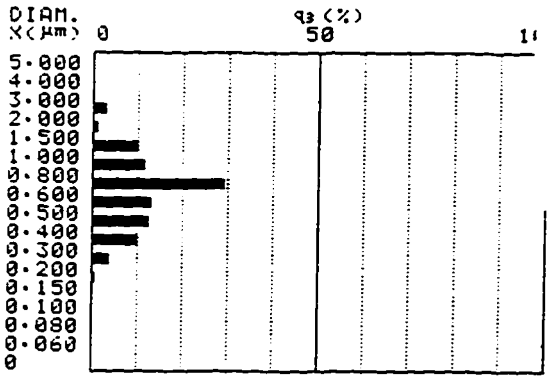

PARTICLE SIZE ANALYSIS BY SA-CP4
V1.00

PLE ID 613
PLE # 2/17/96 RUN04

NSITY 3.95 MODE :CENT
NSITY 0.9978 480(RPM/MIN)
.(mPa.S)0.96
H 2
AK P. 0 K(X):STANDARD

TIME 0:21:12

DATA SUMMARY>

MEDIAN DIAM. 0.645 (μm)
MODAL DIAM. 0.694 (μm)
SURFACE AREA 2.979 (m*m/g)

95.0% DIAM. 1.472 (μm)
5.0% DIAM. 0.262 (μm)

DIAM. X(μm) CUM Q3(%)
1 1.200 89.3
2 1.000 85.1
3 0.800 72.9
0.500 29.9
0.100 1.1

F4 CUMULATIVE GRAPH>

LE ID 613
LE # 2/17/96 RUN04

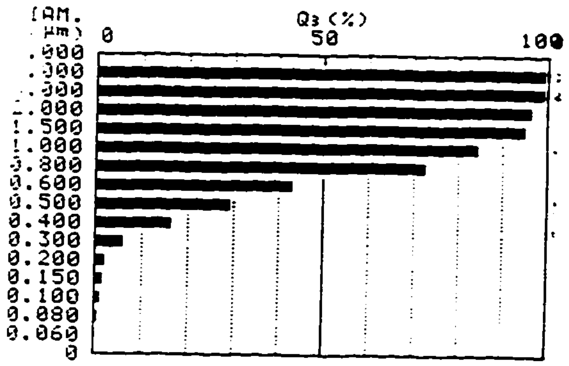

SA-CP4 DIFFERENTIAL GRAPH>

E ID 613
E # 2/17/96 RUN04

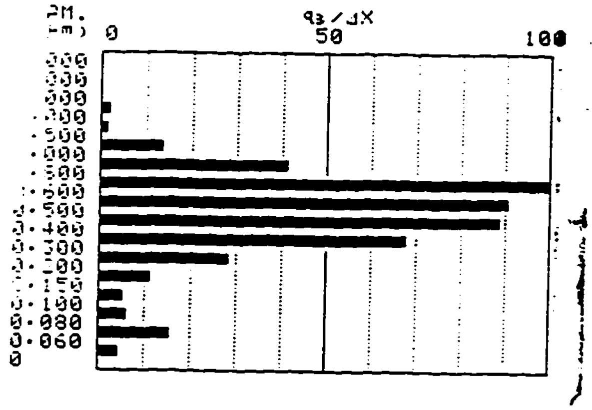

PARTICLE SIZE ANALYSIS BY SA-CP4
V1.00

SAMPLE ID 703
SAMPLE # 2/21/96 RUN01

P DENSITY	3.95	MODE :CENT
L DENSITY	0.9978	480(RPM/MIN)
VISC.(mPa.S)	0.96	
DEPTH	2	
BREAK P.	0	K(X):STANDARD

TIME 0:21:38

<DATA SUMMARY>

MEDIAN DIAM.	0.602	(μm)
MODAL DIAM.	0.676	(μm)
SURFACE AREA	3.061	(m*m/g)
95.0% DIAM.	1.242	(μm)
5.0% DIAM.	0.293	(μm)

	DIAM. X(μm)	CUM Q3(%)
1	1.200	94.3
2	1.000	90.9
3	0.800	79.0
4	0.500	30.9
5	0.100	1.5

<SA-CP4 CUMULATIVE GRAPH>

SAMPLE ID 703
SAMPLE # 2/21/96 RUN01

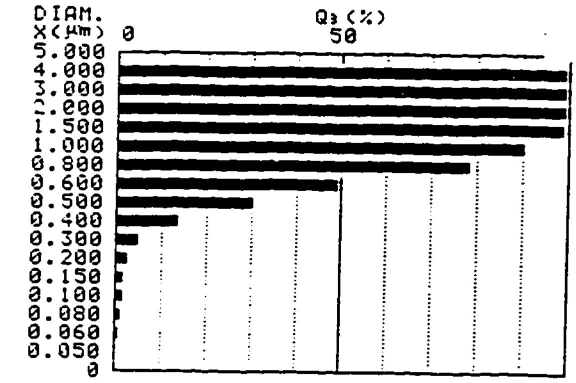

<SA-CP4 DIFFERENTIAL GRAPH>

SAMPLE ID 703
SAMPLE # 2/21/96 RUN01

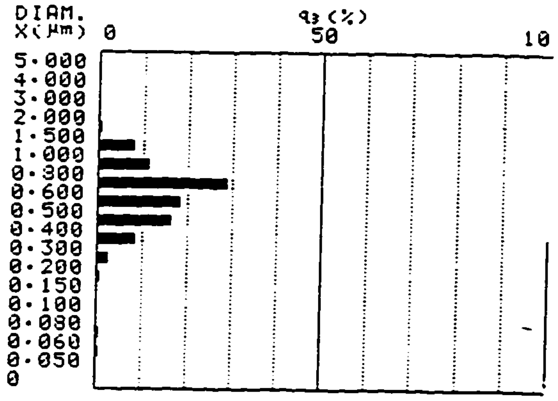

PARTICLE SIZE ANALYSIS BY SA-CP4
V1.00

PLE ID 703
PLE # 2/21/96 RUN01

NSITY 3.95 MODE :CENT
NSITY 0.9978 480(RPM/MIN)
.(mPa.S)0.96
H 2
K P. 0 K(X):STANDARD

0:21:38

A SUMMARY>

MEDIAN DIAM. 0.602 (μm)
MODAL DIAM. 0.676 (μm)
SURFACE AREA 3.061 (m*m/g)

95.0% DIAM. 1.242 (μm)
5.0% DIAM. 0.293 (μm)

DIAM. X(μm) CUM Q3(%)
1.200 94.3
1.000 90.9
0.800 79.0
0.500 30.9
0.100 1.5

CP4 CUMULATIVE GRAPH>

PLE ID 703
PLE # 2/21/96 RUN01

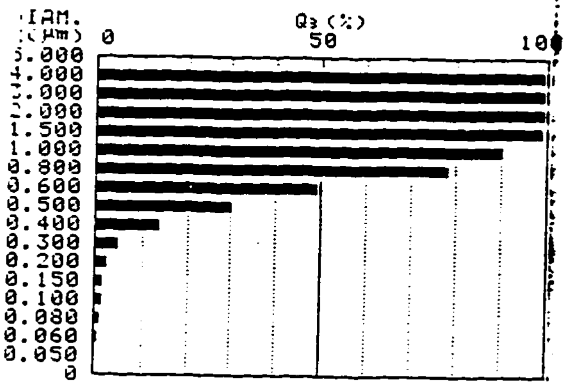

CP4 DIFFERENTIAL GRAPH>

E ID 703
E # 2/21/96 RUN01

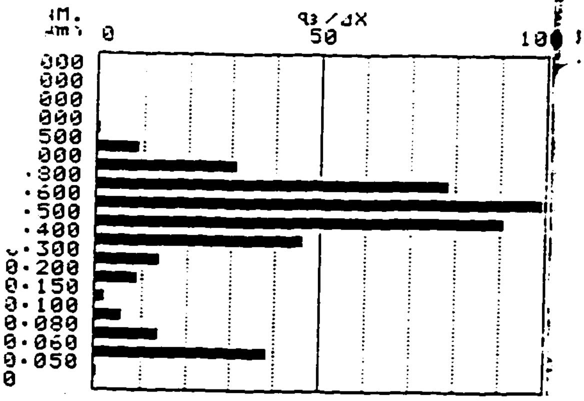

PARTICLE SIZE ANALYSIS BY SA-CP4
V1.00

SAMPLE ID ~~703~~ 604
SAMPLE # 2/21/96 RUN02

P DENSITY	3.95	MODE :CENT
L DENSITY	0.9978	480(RPM/MIN)
VISC.(mPa.S)	0.96	
DEPTH	2	
BREAK P.	0	K(X):STANDARD

TIME 0:20:01

<DATA SUMMARY>

MEDIAN DIAM.	0.595	(μm)
MODAL DIAM.	0.661	(μm)
SURFACE AREA	2.957	(m*m/g)
95.0% DIAM.	1.352	(μm)
5.0% DIAM.	0.294	(μm)

	DIAM. X(μm)	CUM Q3(%)
1	1.200	92.2
2	1.000	88.5
3	0.800	75.6
4	0.500	31.5
5	0.100	1.0

<SA-CP4 CUMULATIVE GRAPH>

SAMPLE ID 703
SAMPLE # 2/21/96 RUN02

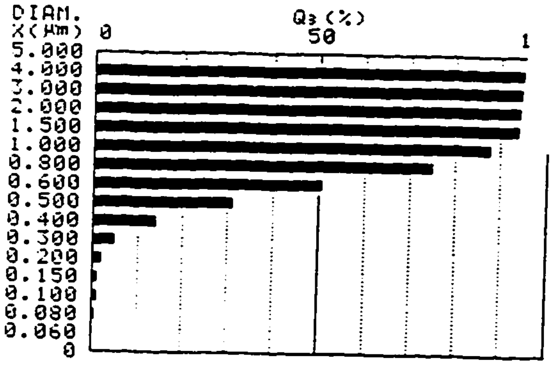

<SA-CP4 DIFFERENTIAL GRAPH>

SAMPLE ID 703
SAMPLE # 2/21/96 RUN02

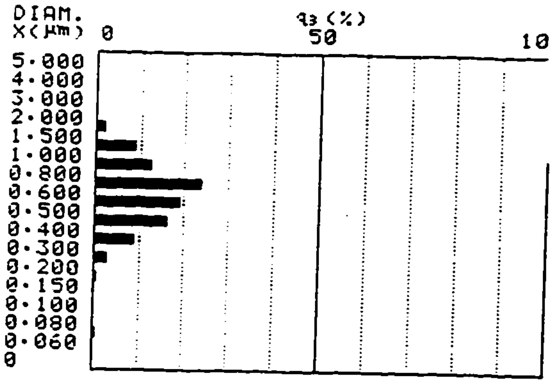

PARTICLE SIZE ANALYSIS BY SA-CP4
V1.00

IPLE ID ~~703~~ 604
IPLE # 2/21/96 RUN02

:NSITY	3.95	MODE :CENT
:NSITY	0.9978	480(RPM/MIN)
:.(mPa.S)	0.96	
H	2	
?K P.	0	K(X):STANDARD

E 0:20:01

DATA SUMMARY>

MEDIAN DIAM.	0.595	(μm)
MODAL DIAM.	0.661	(μm)
SURFACE AREA	2.957	(m*m/g)
95.0% DIAM.	1.352	(μm)
5.0% DIAM.	0.294	(μm)

	DIAM. X(μm)	CUM Q3(%)
1	1.200	92.2
2	1.000	88.5
3	0.800	75.6
4	0.500	31.5
5	0.100	1.0

CP4 CUMULATIVE GRAPH>

PLE ID 703
PLE # 2/21/96 RUN02

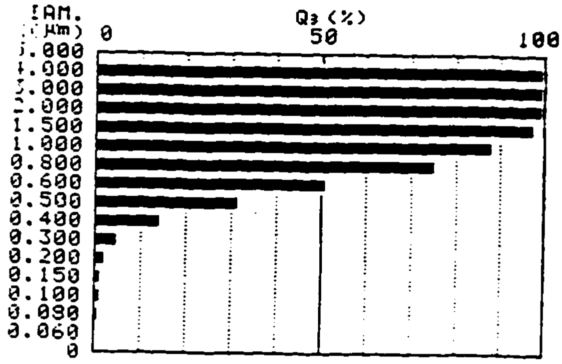

P4 DIFFERENTIAL GRAPH>

LE ID ~~703~~ 604
LE # 2/21/96 RUN02

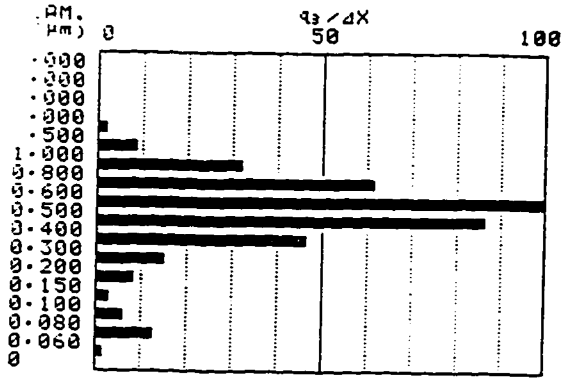

PARTICLE SIZE ANALYSIS BY SA-CP4
V1.00

SAMPLE ID N2802
SAMPLE # 2/21/96 RUN03

P DENSITY 3.95 MODE :CENT
L DENSITY 0.9978 480(RPM/MIN)
VISC.(mPa.S)0.96
DEPTH 2
BREAK P. 0 K(X):STANDARD

TIME 0:19:26

DATA SUMMARY>

MEDIAN DIAM.	0.597	(μm)
MODAL DIAM.	0.670	(μm)
SURFACE AREA	2.913	(m*m/g)
95.0% DIAM.	1.215	(μm)
5.0% DIAM.	0.300	(μm)

	DIAM. X(μm)	CUM Q_3(%)
1	1.200	94.8
2	1.000	91.7
3	0.800	78.5
4	0.500	30.7
5	0.100	0.9

SA-CP4 CUMULATIVE GRAPH>

SAMPLE ID N2802
SAMPLE # 2/21/96 RUN03

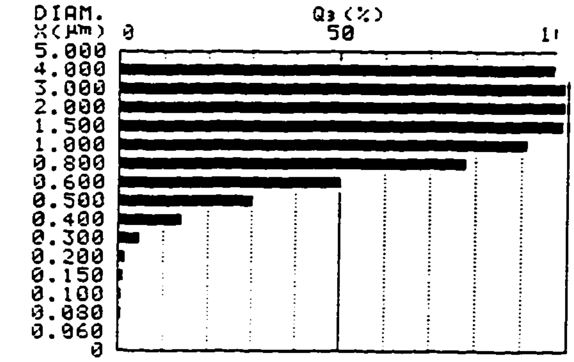

<SA-CP4 DIFFERENTIAL GRAPH>

SAMPLE ID N2802
SAMPLE # 2/21/96 RUN03

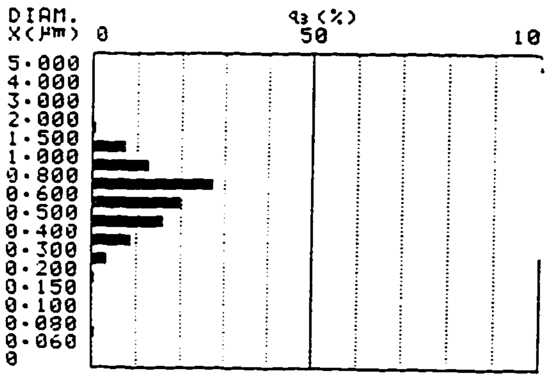

ARTICLE SIZE ANALYSIS BY SA-CP4
V1.00

LE ID N2802
LE # 2/21/96 RUN03

NSITY 3.95 MODE :CENT
NSITY 0.9978 480(RPM/MIN)
.(mPa.S)0.96
H 2
K P. 0 K(X):STANDARD

0:19:26

DATA SUMMARY>

MEDIAN DIAM.	0.597	(μm)
MODAL DIAM.	0.670	(μm)
SURFACE AREA	2.913	(m*m/g)
95.0% DIAM.	1.215	(μm)
5.0% DIAM.	0.300	(μm)

	DIAM. X(μm)	CUM Q_3(%)
1	1.200	94.8
2	1.000	91.7
3	0.800	78.5
4	0.500	30.7
	0.100	0.9

P4 CUMULATIVE GRAPH>

LE ID N2802
LE # 2/21/96 RUN03

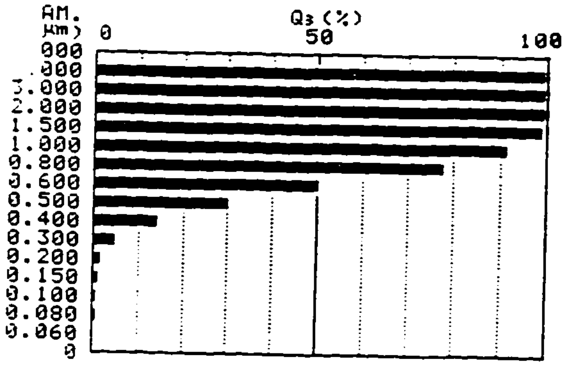

SA-CP4 DIFFERENTIAL GRAPH>

SAMPLE ID N2802
E # 2/21/96 RUN03

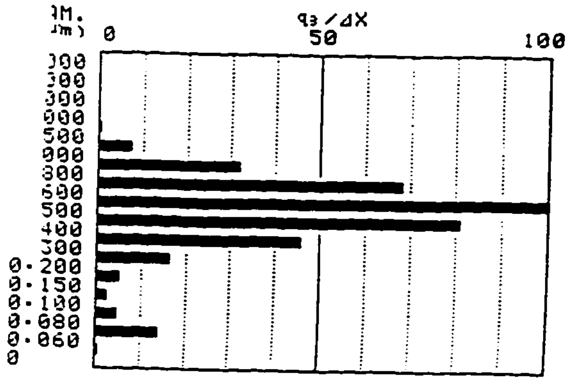

PARTICLE SIZE ANALYSIS BY SA-CP4
V1.00

SAMPLE ID ~~640~~ 820
SAMPLE # 2/23/96 RUN1

F DENSITY 3.95 MODE :CENT
L DENSITY 0.9978 480(RPM/MIN)
VISC.(mPa.S)0.96
DEPTH 2
BREAK P. 0 K(X):STANDARD

TIME 0:21:38

DATA SUMMARY>

MEDIAN DIAM. 0.547 (µm)
MODAL DIAM. 0.671 (µm)
SURFACE AREA 4.535 (m*m/g)

95.0% DIAM. 0.995 (µm)
5.0% DIAM. 0.194 (µm)

	DIAM. X(µm)	CUM Q_3(%)
1	1.200	97.2
2	1.000	95.3
3	0.800	84.0
4	0.500	41.8
5	0.100	3.0

SA-CP4 CUMULATIVE GRAPH>

SAMPLE ID ~~640~~ 820
SAMPLE # 2/23/96 RUN1

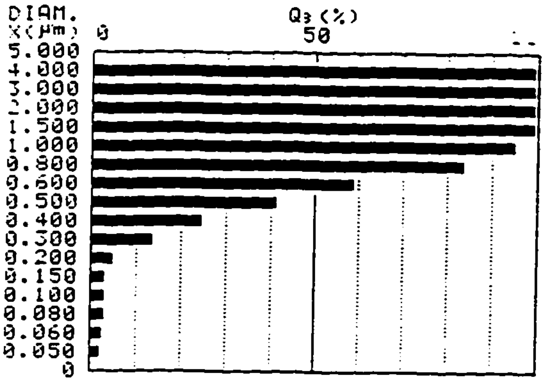

SA-CP4 DIFFERENTIAL GRAPH>

SAMPLE ID ~~640~~ 820
SAMPLE # 2/23/96 RUN1

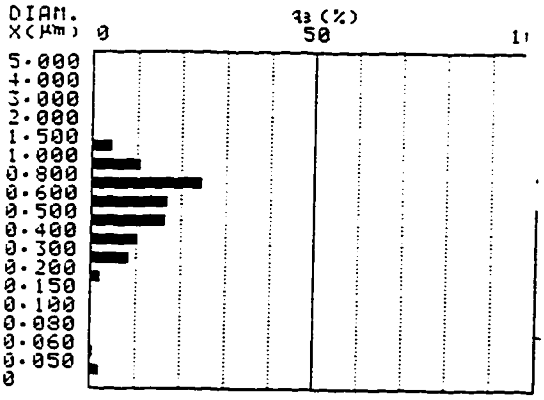

PARTICLE SIZE ANALYSIS BY SA-CP4
V1.00

LE ID ~~640~~ 820
LE # 2/23/96 RUN1

NSITY 3.95 MODE :CENT
NSITY 0.9978 480(RPM/MIN)
.(mPa.S)0.96
H 2
K P. 0 K(X):STANDARD

0:21:38

A SUMMARY>

MEDIAN DIAM. 0.547 (µm)
MODAL DIAM. 0.671 (µm)
SURFACE AREA 4.535 (m*m/g)

95.0% DIAM. 0.995 (µm)
5.0% DIAM. 0.194 (µm)

DIAM. X(µm) CUM Q3(%)
1.200 97.2
1.000 95.3
0.800 84.0
0.500 41.8
0.100 3.0

P4 CUMULATIVE GRAPH>

PLE ID ~~640~~ 820
PLE # 2/23/96 RUN1

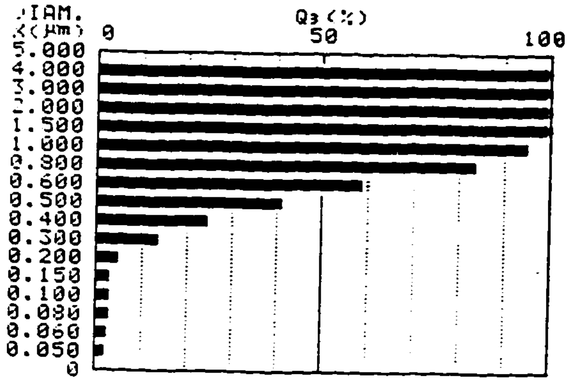

SA-CP4 DIFFERENTIAL GRAPH>

PLE ID ~~640~~ 820
PLE # 2/23/96 RUN1

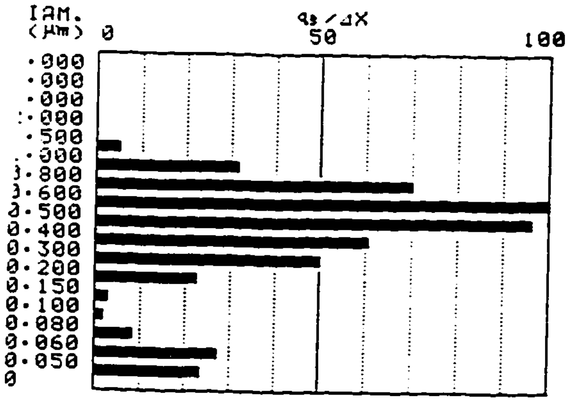

PARTICLE SIZE ANALYSIS BY SA-CP4
V1.00

SAMPLE ID 730
SAMPLE # 2/23/96 RUN2

P DENSITY	3.95	MODE :CENT
L DENSITY	0.9978	480(RPM/MIN)
VISC.(mPa.S)	0.96	
DEPTH	2	
BREAK P.	0	K(X):STANDARD

TIME 0:21:38

DATA SUMMARY>

MEDIAN DIAM.	0.566 (μm)
MODAL DIAM.	0.696 (μm)
SURFACE AREA	3.791 (m*m/g)
95.0% DIAM.	1.418 (μm)
5.0% DIAM.	0.198 (μm)

	DIAM. X(μm)	CUM Q3(%)
1	1.200	91.8
2	1.000	88.9
3	0.800	76.0
4	0.500	41.5
5	0.100	1.9

SA-CP4 CUMULATIVE GRAPH>

SAMPLE ID 730
SAMPLE # 2/23/96 RUN2

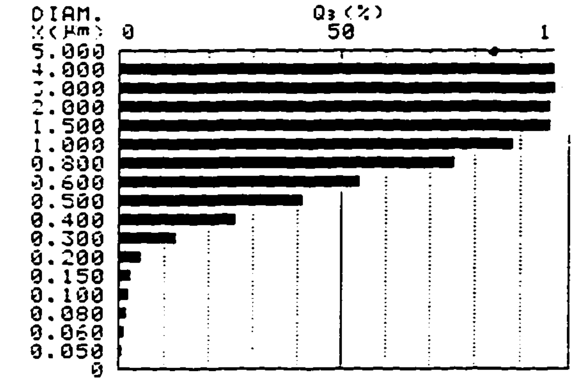

SA-CP4 DIFFERENTIAL GRAPH>

SAMPLE ID 730
SAMPLE # 2/23/96 RUN2

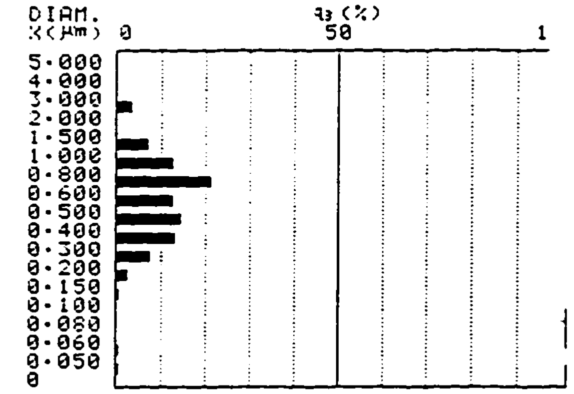

PARTICLE SIZE ANALYSIS BY SA-CP4
V1.00

SAMPLE ID 730
2/23/96 RUN2

ITY 3.95 MODE :CENT
ITY 0.9978 480(RPM/MIN)
mPa.S)0.96
2
P. 0 K(X):STANDARD

0:21:38

SUMMARY>

IAN DIAM. 0.566 (μm)
AL DIAM. 0.696 (μm)
FACE AREA 3.791 (m*m/g)

95.0% DIAM. 1.418 (μm)
5.0% DIAM. 0.198 (μm)

	DIAM. X(μm)	CUM Q3(%)
1	1.200	91.8
2	1.000	88.9
3	0.800	76.0
4	0.500	41.5
	0.100	1.9

CP4 CUMULATIVE GRAPH>

PLE ID 730
PLE # 2/23/96 RUN2

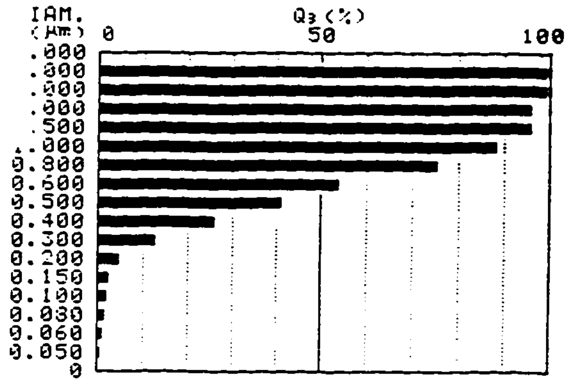

SA-CP4 DIFFERENTIAL GRAPH>

SAMPLE ID 730
SAMPLE # 2/23/96 RUN2

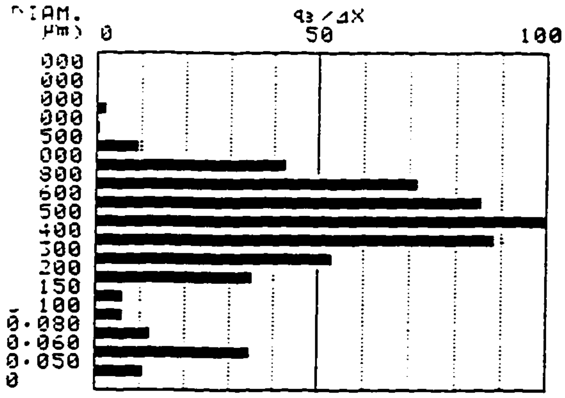

PARTICLE SIZE ANALYSIS BY SA-CP4 V1.00

SAMPLE ID 640
SAMPLE # 2/23/96 RUN3

P DENSITY	3.95	MODE :CENT	
L DENSITY	0.9978	480(RPM/MIN)	
VISC.(mPa.S)	0.96		
DEPTH	2		
BREAK P.	0	K(X):STANDARD	

TIME 0:21:38

DATA SUMMARY>

MEDIAN DIAM.	0.520	(μm)
MODAL DIAM.	0.675	(μm)
SURFACE AREA	4.288	(m*m/g)
95.0% DIAM.	1.292	(μm)
5.0% DIAM.	0.179	(μm)

	DIAM. X(μm)	CUM Q3(%)
1	1.200	92.8
2	1.000	88.0
3	0.800	80.9
4	0.500	47.5
5	0.100	2.4

<SA-CP4 CUMULATIVE GRAPH>

SAMPLE ID 640
SAMPLE # 2/23/96 RUN3

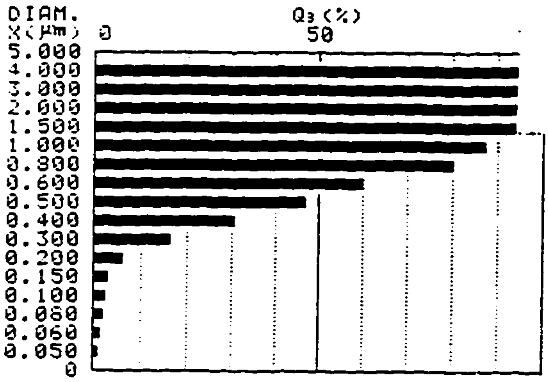

<SA-CP4 DIFFERENTIAL GRAPH>

SAMPLE ID 640
SAMPLE # 2/23/96 RUN3

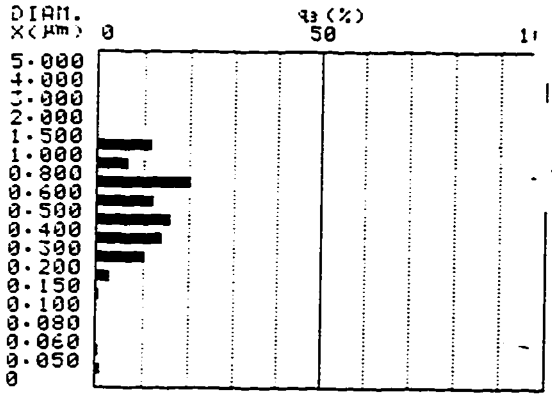

PARTICLE SIZE ANALYSIS BY SA-CP4 V1.00

SAMPLE ID 640
SAMPLE # 2/23/96 RUN3

NSITY	3.95	MODE :CENT	
NSITY	0.9978	480(RPM/MIN)	
.(mPa.S)	0.96		
...H	2		
BREAK P.	0	K(X):STANDARD	

0:21:38

A SUMMARY>

DIAN DIAM.	0.520	(μm)
MODAL DIAM.	0.675	(μm)
SURFACE AREA	4.288	(m*m/g)
95.0% DIAM.	1.292	(μm)
5.0% DIAM.	0.179	(μm)

	DIAM. X(μm)	CUM Q3(%)
1	1.200	92.8
2	1.000	88.0
3	0.800	80.9
	0.500	47.5
	0.100	2.4

CP4 CUMULATIVE GRAPH>

PLE ID 640
PLE # 2/23/96 RUN3

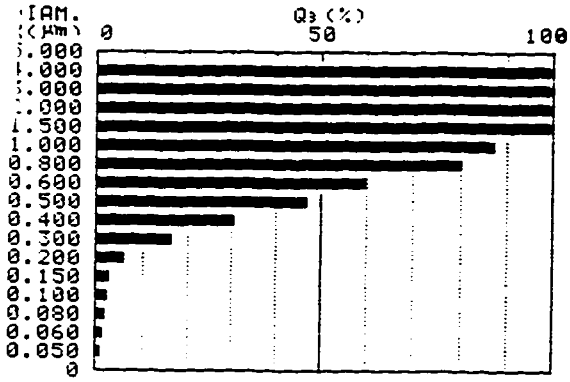

<SA-CP4 DIFFERENTIAL GRAPH>

SAMPLE ID 640
SAMPLE # 2/23/96 RUN3

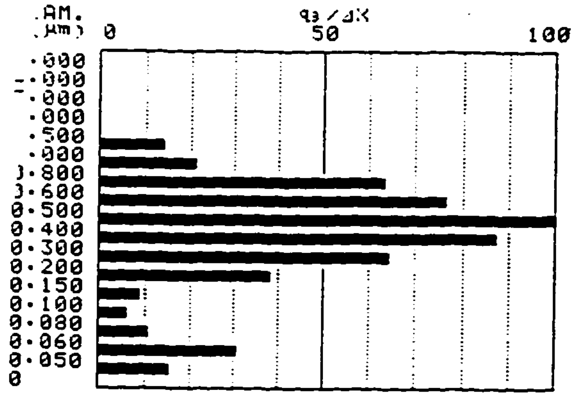

PARTICLE SIZE ANALYSIS BY SA-CP4
V1.00

SAMPLE ID 631
SAMPLE # 2/24/96 RUN01

P DENSITY 3.95 MODE :CENT
L DENSITY 0.9978 480(RPM/MIN)
VISC.(mPa.S) 0.96
DEPTH 2
BREAK P. 0 K(X):STANDARD

TIME 0:21:38

<DATA SUMMARY>

MEDIAN DIAM.	0.560	(μm)
MODAL DIAM.	0.676	(μm)
SURFACE AREA	4.173	(m*m/g)
95.0% DIAM.	1.348	(μm)
5.0% DIAM.	0.192	(μm)

	DIAM. X(μm)	CUM Q3(%)
1	1.200	92.6
2	1.000	89.4
3	0.800	78.8
4	0.500	40.8
5	0.100	2.5

<SA-CP4 CUMULATIVE GRAPH>

SAMPLE ID 631
SAMPLE # 2/24/96 RUN01

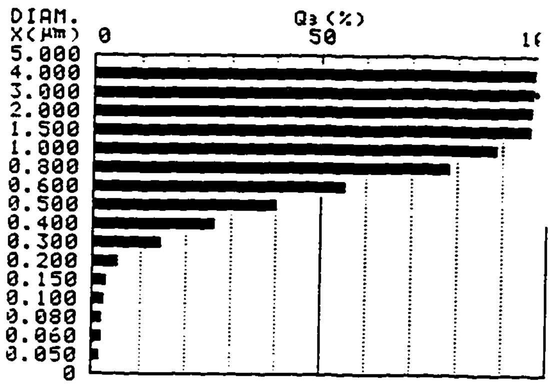

<SA-CP4 DIFFERENTIAL GRAPH>

SAMPLE ID 631
SAMPLE # 2/24/96 RUN01

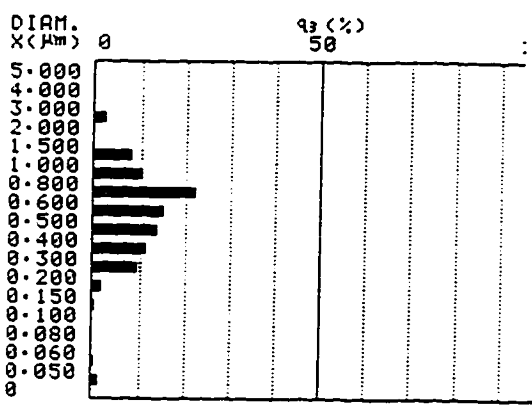

'ARTICLE SIZE ANALYSIS BY SA-CP4
V1.00

PLE ID 631
PLE # 2/24/96 RUN01

NSITY 3.95 MODE :CENT
NSITY 0.9978 480(RPM/MIN)
.(mPa.S) 0.96
TH 2
AK P. 0 K(X):STANDARD

E 0:21:38

DATA SUMMARY>

MEDIAN DIAM.	0.560	(μm)
MODAL DIAM.	0.676	(μm)
SURFACE AREA	4.173	(m*m/g)
95.0% DIAM.	1.348	(μm)
5.0% DIAM.	0.192	(μm)

	DIAM. X(μm)	CUM Q3(%)
1	1.200	92.6
2	1.000	89.4
3	0.800	78.8
4	0.500	40.8
5	0.100	2.5

:P4 CUMULATIVE GRAPH>

PLE ID 631
PLE # 2/24/96 RUN01

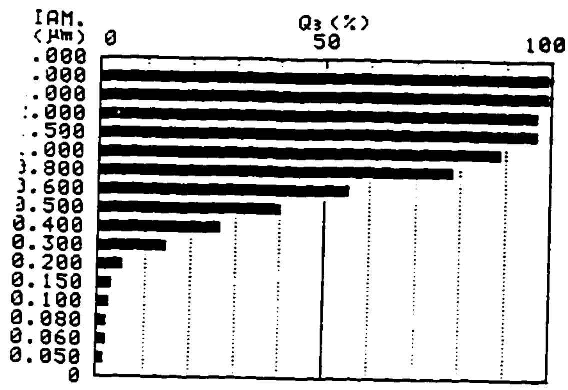

<SA-CP4 DIFFERENTIAL GRAPH>

MPLE ID 631
MPLE # 2/24/96 RUN01

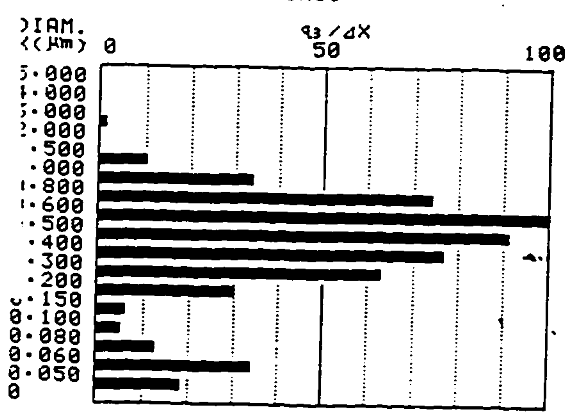

PARTICLE SIZE ANALYSIS BY SA-CP4
V1.00

SAMPLE ID DISPERAL
SAMPLE # 2/24/96 RUN02

P DENSITY	3.95	MODE :CENT
L DENSITY	0.9978	480(RPM/MIN)
VISC.(mPa.S)	0.96	
DEPTH	2	
BREAK P.	0	K(X):STANDARD

TIME 0:21:38

DATA SUMMARY>

MEDIAN DIAM.	1.186	(μm)
MODAL DIAM.	2.196	(μm)
SURFACE AREA	3.328	(m*m/g)
95.0% DIAM.	4.356	(μm)
5.0% DIAM.	0.087	(μm)

	DIAM. X(μm)	CUM Q_3(%)
1	1.200	50.3
2	1.000	45.8
3	0.800	37.2
4	0.500	23.0
5	0.100	5.6

<SA-CP4 CUMULATIVE GRAPH>

SAMPLE ID DISPERAL
SAMPLE # 2/24/96 RUN02

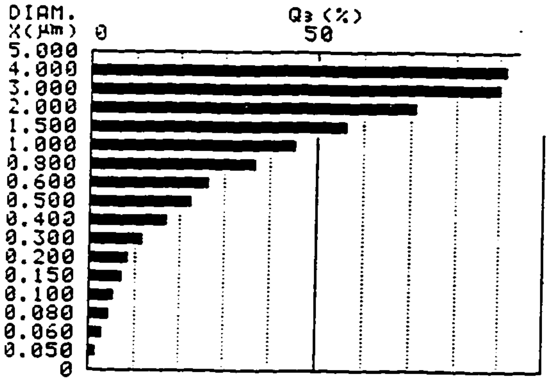

<SA-CP4 DIFFERENTIAL GRAPH>

SAMPLE ID DISPERAL
SAMPLE # 2/24/96 RUN02

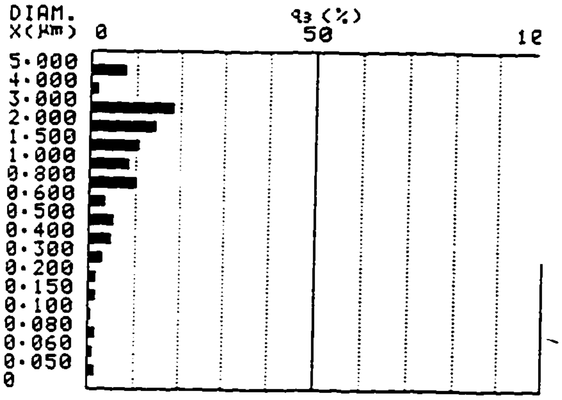

PARTICLE SIZE ANALYSIS BY SA-CP4
V1.00

PLE ID DISPERAL
PLE # 2/24/96 RUN02

ENSITY 3.95 MODE :CENT
ENSITY 0.9978 480(RPM/MIN)
C.(mPa.S)0.96
TH 2
AK P. 0 K(X):STANDARD

TIME 0:21:38

DATA SUMMARY>

MEDIAN DIAM. 1.186 (μm)
MODAL DIAM. 2.196 (μm)
SURFACE AREA 3.328 (m*m/g)

95.0% DIAM. 4.356 (μm)
5.0% DIAM. 0.087 (μm)

DIAM. X(μm) CUM Q3(%)
1.200 50.3
1.000 45.8
0.800 37.2
0.500 23.0
0.100 5.6

-CP4 CUMULATIVE GRAPH>

MPLE I- DISPERAL
MPLE # 2/24/96 RUN02

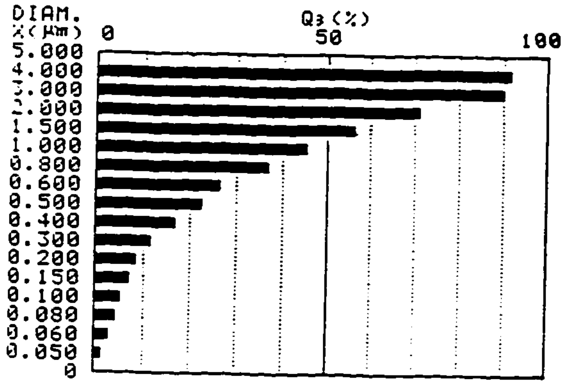

<SA-CP4 DIFFERENTIAL GRAPH>

LE ID DISPERAL
LE # 2/24/96 RUN02

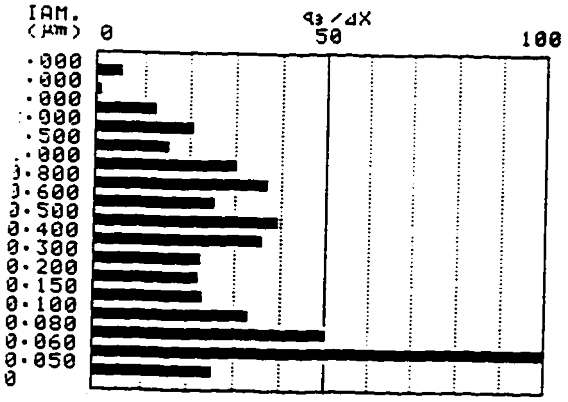

PARTICLE SIZE ANALYSIS BY SA-CP4
V1.00

SAMPLE ID F100
SAMPLE # 2/24/96 RUN03

P DENSITY 3.95 MODE :CENT
L DENSITY 0.9978 480(RPM/MIN)
VISC.(mPa.S) 0.96
DEPTH 2
BREAK P. 0 K(X):STANDARD

TIME 0:21:38

<DATA SUMMARY>

MEDIAN DIAM. 0.030 (μm)
MODAL DIAM. 0 (μm)
SURFACE AREA 3.378 (m*m/g)

95.0% DIAM. 0.072 (μm)
5.0% DIAM. 0.003 (μm)

	DIAM. X(μm)	CUM Qo(%)
1	1.200	00
2	1.000	00
3	0.800	00
4	0.500	99.9
5	0.100	98.3

<SA-CP4 CUMULATIVE GRAPH>

SAMPLE ID F100
SAMPLE # 2/24/96 RUN03

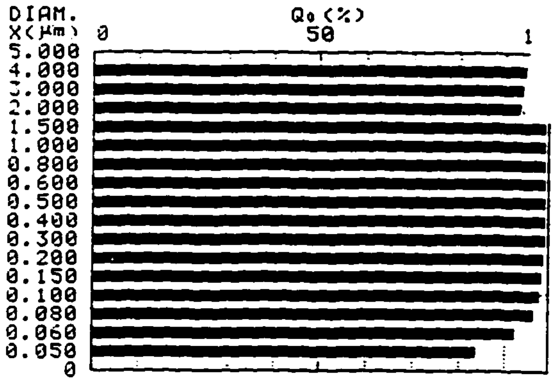

<SA-CP4 DIFFERENTIAL GRAPH>

SAMPLE ID F100
SAMPLE # 2/24/96 RUN03

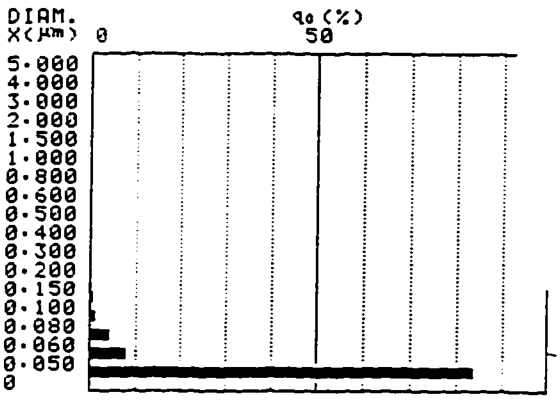

ARTICLE SIZE ANALYSIS BY SA-CP4
V1.00

PLE ID F100
PLE # 2/24/96 RUN03

ENSITY 3.95 MODE :CENT
ENSITY 0.9978 480(RPM/MIN)
C.(mPa.S) 0.96
TH 2
AK P. 0 K(X):STANDARD

TIME 0:21:38

DATA SUMMARY>

MEDIAN DIAM. 0.030 (μm)
MODAL DIAM. 0 (μm)
SURFACE AREA 3.378 (m*m/g)

95.0% DIAM. 0.072 (μm)
5.0% DIAM. 0.003 (μm)

DIAM. X(μm) CUM Qo(%)
1 1.200 00
1.000 00
0.800 00
0.500 99.9
0.100 98.3

CP4 CUMULATIVE GRAPH>

IPLE ID F100
IPLE # 2/24/96 RUN03

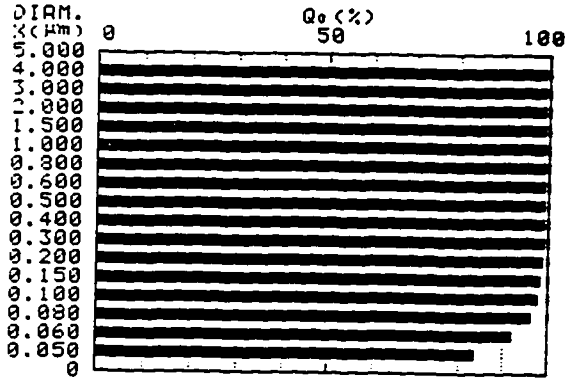

A-CP4 DIFFERENTIAL GRAPH>

AMPLE ID F100
AMPLE # 2/24/96 RUN03

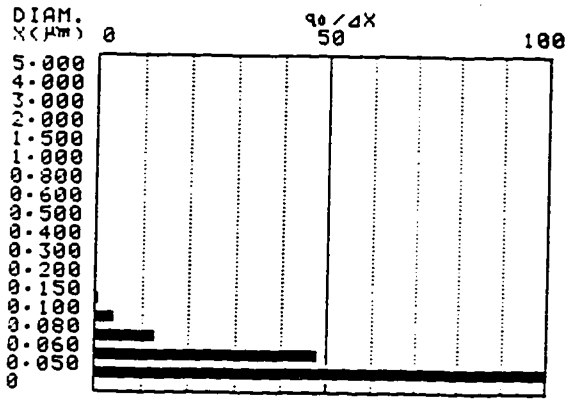

PARTICLE SIZE ANALYSIS BY SA-CP4
V1.00

SAMPLE ID F100
SAMPLE # 2/24/96 RUN03

P DENSITY	3.95	MODE :CENT
L DENSITY	0.9978	480(RPM/MIN)
VISC.(mPa.S)	0.96	
DEPTH	2	
BREAK P.	0	K(X):STANDARD

TIME 0:21:38

<DATA SUMMARY>

MEDIAN DIAM.	1.022	(μm)
MODAL DIAM.	1.245	(μm)
SURFACE AREA	3.378	(m*m/g)
95.0% DIAM.	4.388	(μm)
5.0% DIAM.	0.126	(μm)

	DIAM. X(μm)	CUM Q_3(%)
1	1.200	58.0
2	1.000	49.0
3	0.800	39.3
4	0.500	23.1
5	0.100	4.4

<SA-CP4 CUMULATIVE GRAPH>

SAMPLE ID F100
SAMPLE # 2/24/96 RUN03

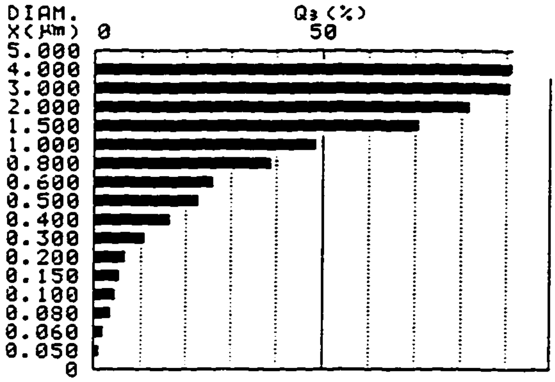

<SA-CP4 DIFFERENTIAL GRAPH>

SAMPLE ID F100
SAMPLE # 2/24/96 RUN03

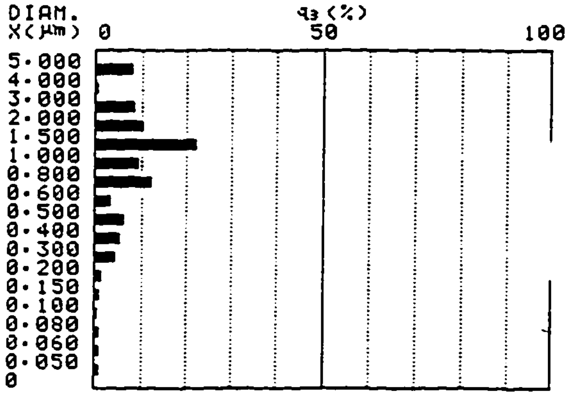

PARTICLE SIZE ANALYSIS BY SA-CP4
V1.00

MPLE ID F100
MPLE # 2/24/96 RUN03

ENSITY 3.95 MODE :CENT
ENSITY 0.9978 480(RPM/MIN)
C.(mPa.S)0.96
TH 2
AK P. 0 K(X):STANDARD

E 0:21:38

DATA SUMMARY>

MEDIAN DIAM. 1.022 (μm)
MODAL DIAM. 1.245 (μm)
SURFACE AREA 3.378 (m*m/g)

95.0% DIAM. 4.388 (μm)
5.0% DIAM. 0.126 (μm)

DIAM. X(μm) CUM Q3(%)
1.200 58.0
1.000 49.0
0.800 39.3
0.500 23.1
0.100 4.4

I-CP4 CUMULATIVE GRAPH>

AMPLE ID F100
AMPLE # 2/24/96 RUN03

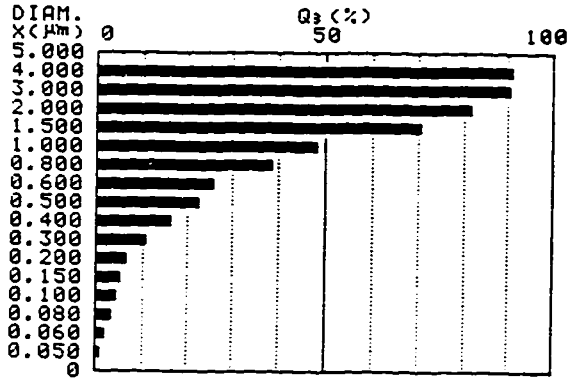

<SA-CP4 DIFFERENTIAL GRAPH>

SAMPLE ID F100
SAMPLE # 2/24/96 RUN03

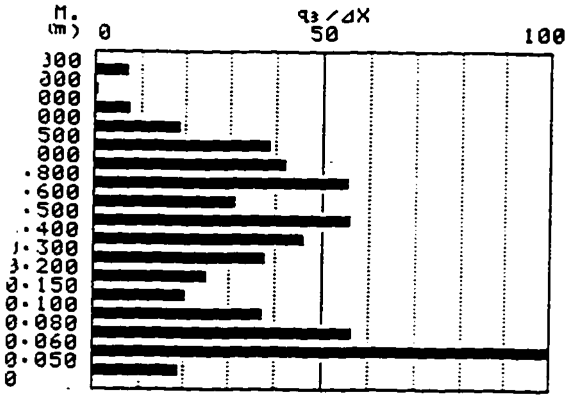

PARTICLE SIZE ANALYSIS BY SA-CP4
V1.00

SAMPLE ID F100
SAMPLE # 2/24/96 RUN03

P DENSITY 3.95
L DENSITY 0.9978
VISC.(mPa.S) 0.96
DEPTH 2
BREAK P. 0

MODE :CENT
480(RPM/MIN)

K(X):STANDARD

TIME 0:21:38

<DATA SUMMARY>

MEDIAN DIAM.	0.030	(μm)
MODAL DIAM.	0	(μm)
SURFACE AREA	3.378	(m*m/g)
95.0% DIAM.	0.072	(μm)
5.0% DIAM.	0.003	(μm)

	DIAM. X(μm)	CUM Q_0(%)
1	1.200	00
2	1.000	00
3	0.800	00
4	0.500	99.9
5	0.100	98.3

<SA-CP4 CUMULATIVE GRAPH>

SAMPLE ID F100
SAMPLE # 2/24/96 RUN03

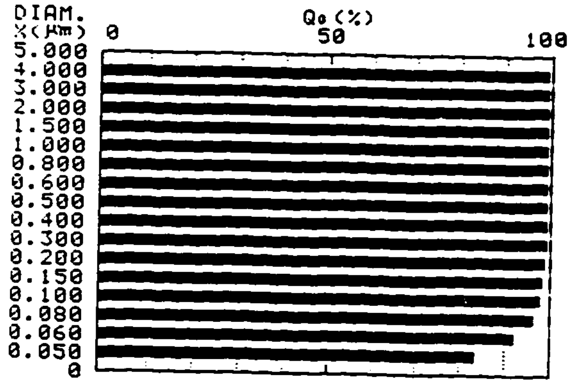

<SA-CP4 DIFFERENTIAL GRAPH>

SAMPLE ID F100
SAMPLE # 2/24/96 RUN03

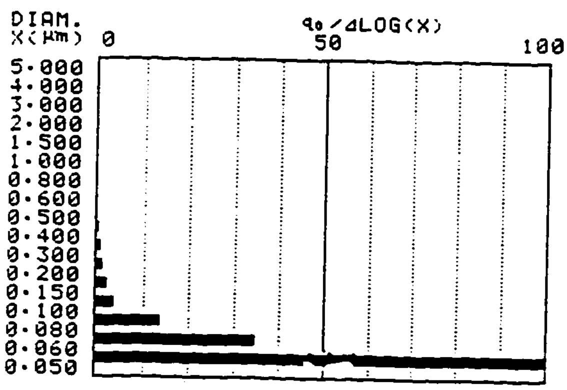

PARTICLE SIZE ANALYSIS BY SA-CP4
V1.00

SAMPLE ID 001
SAMPLE # 2/24/96 RUN04

P DENSITY 3.95 MODE :CENT
L DENSITY 0.9978 480(RPM/MIN)
VISC.(mPa.S)0.96
DEPTH 2
BREAK P. 0 K(X):STANDARD

TIME 0:21:38

<DATA SUMMARY>

MEDIAN DIAM.	0.897	(μm)
MODAL DIAM.	1.204	(μm)
SURFACE AREA	4.748	(m*m/g)
95.0% DIAM.	2.578	(μm)
5.0% DIAM.	0.071	(μm)

	DIAM. X(μm)	CUM Q3(%)
1	1.200	65.3
2	1.000	56.7
3	0.800	43.7
4	0.500	27.2
5	0.100	6.4

<SA-CP4 CUMULATIVE GRAPH>

SAMPLE ID 001
SAMPLE # 2/24/96 RUN04

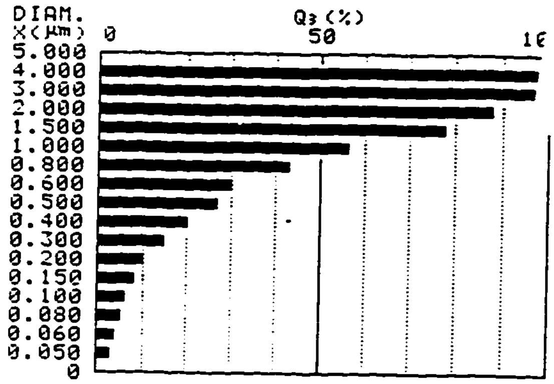

<SA-CP4 DIFFERENTIAL GRAPH>

SAMPLE ID 001
SAMPLE # 2/24/96 RUN04

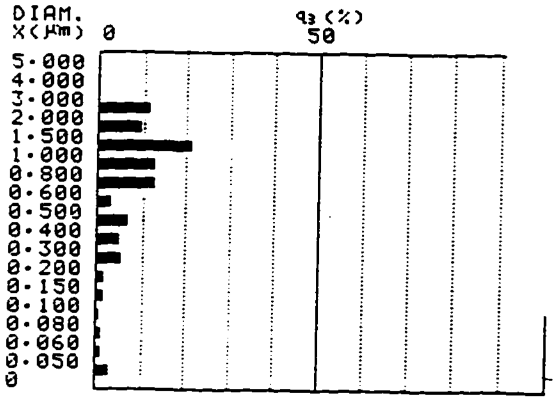

PARTICLE SIZE ANALYSIS BY SA-CP4
V1.00

MPLE ID 001
MPLE # 2/24/96 RUN04

ENSITY 3.95 MODE :CENT
ENSITY 0.9978 480(RPM/MIN)
C.(mPa.S)0.96
TH 2
AK P. 0 K(X):STANDARD

E 0:21:38

A SUMMARY>

DIAN DIAM. 0.897 (μm)
MODAL DIAM. 1.204 (μm)
SURFACE AREA 4.748 (m*m/g)

95.0% DIAM. 2.578 (μm)
5.0% DIAM. 0.071 (μm)

DIAM. X(μm) CUM Q3(%)
1 1.200 65.3
2 1.000 56.7
0.800 43.7
0.500 27.2
0.100 6.4

P4 CUMULATIVE GRAPH>

LE ID 001
LE # 2/24/96 RUN04

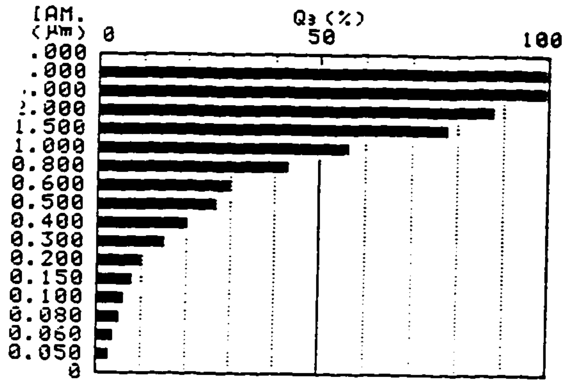

SA-CP4 DIFFERENTIAL GRAPH>

SAMPLE ID 001
SAMPLE # 2/24/96 RUN04

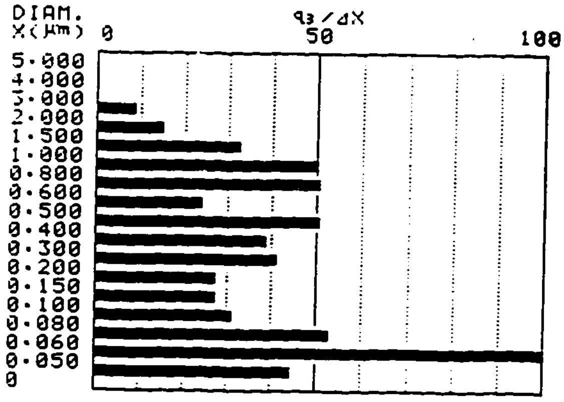

PARTICLE SIZE ANALYSIS BY SA-CP4
V1.00

SAMPLE ID 001
SAMPLE # 2/24/96 RUN04

P DENSITY 3.95 MODE :CENT
L DENSITY 0.9978 480(RPM/MIN)
VISC.(mPa.S) 0.96
DEPTH 2
BREAK P. 0 K(X):STANDARD

TIME 0:21:38

DATA SUMMARY>

MEDIAN DIAM. 0.026 (μm)
MODAL DIAM. 0 (μm)
SURFACE AREA 4.748 (m*m/g)

95.0% DIAM. 0.057 (μm)
5.0% DIAM. 0.003 (μm)

	DIAM. X(μm)	CUM Qo(%)
1	1.200	00
2	1.000	00
3	0.800	00
4	0.500	00
5	0.100	99.1

SA-CP4 CUMULATIVE GRAPH>

SAMPLE ID 001
SAMPLE # 2/24/96 RUN04

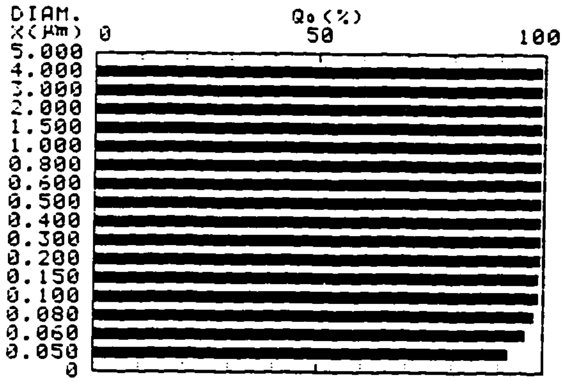

<SA-CP4 DIFFERENTIAL GRAPH>

SAMPLE ID 001
SAMPLE # 2/24/96 RUN04

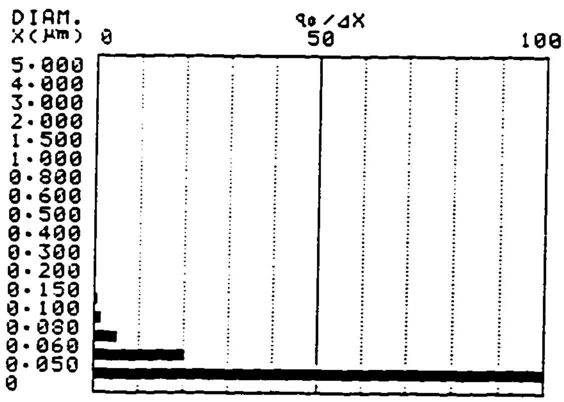

PARTICLE SIZE ANALYSIS BY SA-CP4
V1.00

SAMPLE ID 622
SAMPLE # 2/24/96 RUN05

P DENSITY 3.95 MODE :CENT
L DENSITY 0.9978 480(RPM/MIN)
VISC.(mPa.S) 0.96
DEPTH 2
BREAK P. 0 K(X):STANDARD

TIME 0:20:19

<DATA SUMMARY>

MEDIAN DIAM. 0.042 (μm)
MODAL DIAM. 0 (μm)
SURFACE AREA 3.332 (m*m/g)

95.0% DIAM. 0.275 (μm)
5.0% DIAM. 0.005 (μm)

	DIAM. X(μm)	CUM Qo(%)
1	1.200	00
2	1.000	00
3	0.800	99.9
4	0.500	98.4
5	0.100	87.2

SA-CP4 CUMULATIVE GRAPH>

SAMPLE ID 622
SAMPLE # 2/24/96 RUN05

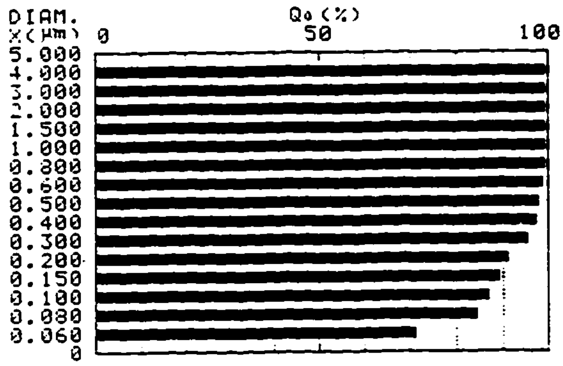

SA-CP4 DIFFERENTIAL GRAPH>

SAMPLE ID 622
SAMPLE # 2/24/96 RUN05

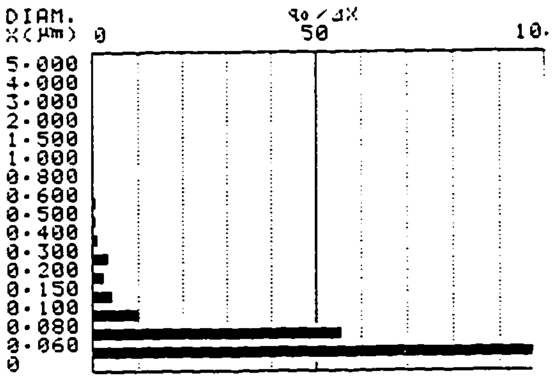

PARTICLE SIZE ANALYSIS BY SA-CP4
V1.00

SAMPLE ID 622
SAMPLE # 2/24/96 RUN05

P DENSITY 3.95 MODE :CENT
L DENSITY 0.9978 480(RPM/MIN)
VISC.(mPa.S) 0.96
DEPTH 2
BREAK P. 0 K(X):STANDARD

TIME 0:20:19

<DATA SUMMARY>

MEDIAN DIAM.	0.580	(µm)
MODAL DIAM.	0.637	(µm)
SURFACE AREA	3.332	(m*m/g)
95.0% DIAM.	1.243	(µm)
5.0% DIAM.	0.218	(µm)

	DIAM. X(µm)	CUM Q_3(%)
1	1.200	94.1
2	1.000	90.2
3	0.800	80.2
4	0.500	31.2
5	0.100	1.2

<SA-CP4 CUMULATIVE GRAPH>

SAMPLE ID 622
SAMPLE # 2/24/96 RUN05

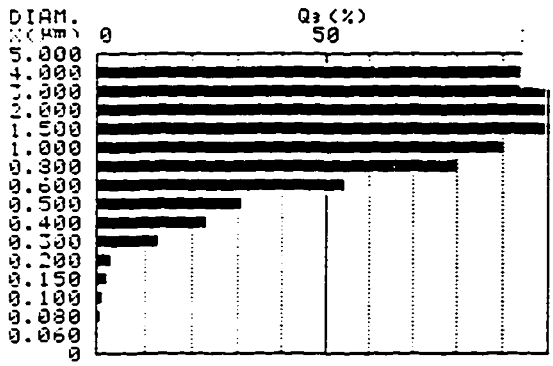

<SA-CP4 DIFFERENTIAL GRAPH>

SAMPLE ID 622
SAMPLE # 2/24/96 RUN05

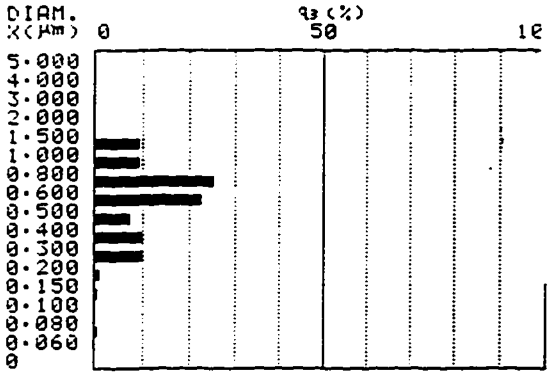

ARTICLE SIZE ANALYSIS BY SA-CP4
V1.00

PLE ID 622
PLE # 2/24/96 RUN05

NSITY 3.95 MODE :CENT
NSITY 0.9978 480(RPM/MIN)
.(mPa.S) 0.96
TH 2
AK P. 0 K(X):STANDARD

E 0:20:19

<DATA SUMMARY>

MEDIAN DIAM. 0.580 (µm)
MODAL DIAM. 0.637 (µm)
SURFACE AREA 3.332 (m*m/g)

95.0% DIAM. 1.243 (µm)
5.0% DIAM. 0.218 (µm)

DIAM. X(µm) CUM Q3(%)
1.200 94.1
1.000 90.2
0.800 80.2
0.500 31.2
0.100 1.2

-CP4 CUMULATIVE GRAPH>

MPLE ID 622
MPLE # 2/24/96 RUN05

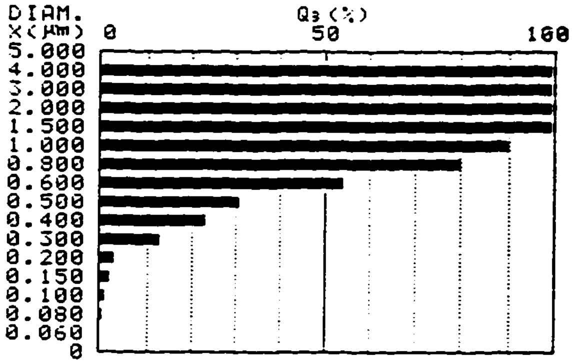

P4 DIFFERENTIAL GRAPH>

PLE ID 622
PLE # 2/24/96 RUN05

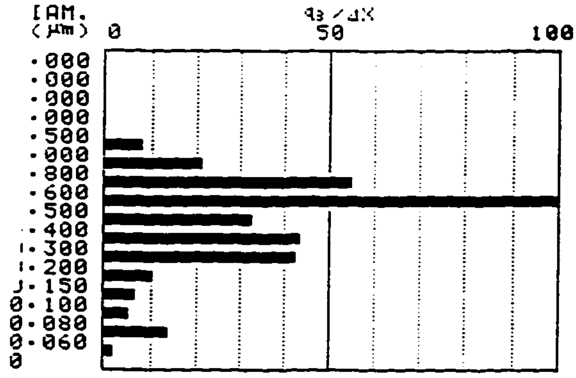

PARTICLE SIZE ANALYSIS BY SA-CP4
V1.00

SAMPLE ID DISPERAL 2
SAMPLE # 3/02/96 RUN01

P DENSITY	3.95	MODE :CENT
L DENSITY	0.9978	480(RPM/MIN)
VISC.(mPa.S)	0.96	
DEPTH	2	
BREAK P.	0	K(X):STANDARD

TIME 0:21:38

<DATA SUMMARY>

MEDIAN DIAM.	0.828	(μm)
MODAL DIAM.	1.241	(μm)
SURFACE AREA	11.53	(m*m/g)
95.0% DIAM.	2.702	(μm)
5.0% DIAM.	0.021	(μm)

	DIAM. X(μm)	CUM Q_3(%)
1	1.200	64.0
2	1.000	57.0
3	0.800	48.8
4	0.500	38.8
5	0.100	22.4

<SA-CP4 CUMULATIVE GRAPH>

SAMPLE ID DISPERAL 2
SAMPLE # 3/02/96 RUN01

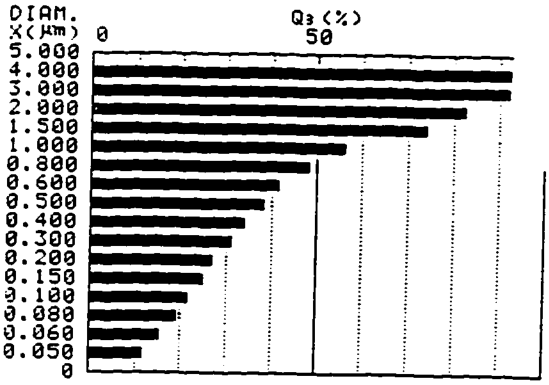

<SA-CP4 DIFFERENTIAL GRAPH>

SAMPLE ID DISPERAL 2
SAMPLE # 3/02/96 RUN01

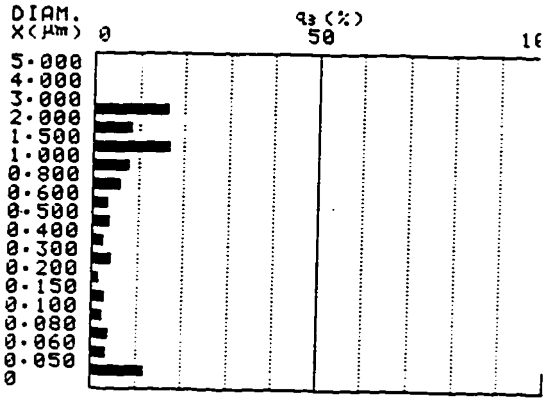

ARTICLE SIZE ANALYSIS BY SA-CP4
V1.00

LE ID DISPERAL 2
LE # 3/02/96 RUN01

NSITY 3.95 MODE :CENT
NSITY 0.9978 480(RPM/MIN)
.(mPa.S)0.96
TH 2
AK P. 0 K(X):STANDARD

E 0:21:38

TA SUMMARY>

MEDIAN DIAM. 0.828 (μm)
MODAL DIAM. 1.241 (μm)
SURFACE AREA 11.53 (m*m/g)

95.0% DIAM. 2.702 (μm)
5.0% DIAM. 0.021 (μm)

DIAM. X(μm) CUM Q3(%)
1.200 64.0
1.000 57.0
0.800 48.8
0.500 38.8
0.100 22.4

-CP4 CUMULATIVE GRAPH>

AMPLE ID DISPERAL 2
AMPLE # 3/02/96 RUN01

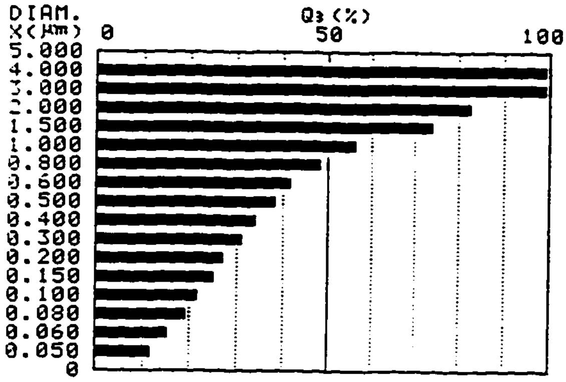

<SA-CP4 DIFFERENTIAL GRAPH>

SAMPLE ID DISPERAL 2
SAMPLE # 3/02/96 RUN01

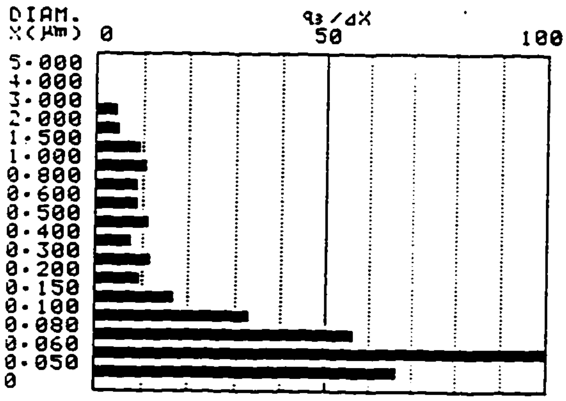

PARTICLE SIZE ANALYSIS BY SA-CP4
V1.00

SAMPLE ID 001 - 2
SAMPLE # 3/02/96 RUN02

P DENSITY	3.95	MODE :CENT
L DENSITY	0.9978	480(RPM/MIN)
VISC.(mPa.S)	0.96	
DEPTH	2	
BREAK P.	0	K(X):STANDARD

TIME 0:21:38

<DATA SUMMARY>

MEDIAN DIAM.	0.760	(μm)
MODAL DIAM.	1.308	(μm)
SURFACE AREA	10.47	(m*m/g)
95.0% DIAM.	2.628	(μm)
5.0% DIAM.	0.023	(μm)

	DIAM. X(μm)	CUM Q_3(%)
1	1.200	65.5
2	1.000	59.1
3	0.800	52.0
4	0.500	37.3
5	0.100	19.9

<SA-CP4 CUMULATIVE GRAPH>

SAMPLE ID 001 - 2
SAMPLE # 3/02/96 RUN02

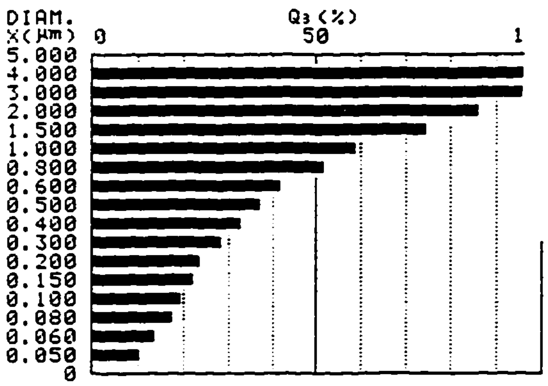

<SA-CP4 DIFFERENTIAL GRAPH>

SAMPLE ID 001 - 2
SAMPLE # 3/02/96 RUN02

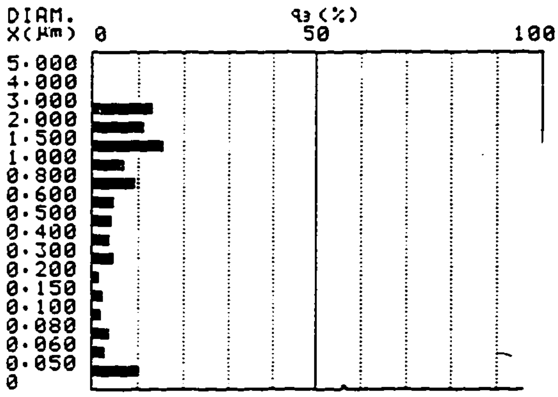

PARTICLE SIZE ANALYSIS BY SA-CP4
V1.00

PLE ID 001 - 2
PLE # 3/02/96 RUN02

NSITY 3.95 MODE :CENT
NSITY 0.9978 480(RPM/MIN)
.(mPa.S)0.96
H 2
K P. 0 K(X):STANDARD

0:21:38

TA SUMMARY>

EDIAN DIAM. 0.760 (μm)
ODAL DIAM. 1.308 (μm)
URFACE AREA 10.47 (m*m/g)

95.0% DIAM. 2.628 (μm)
5.0% DIAM. 0.023 (μm)

DIAM. X(μm) CUM Q3(%)
1 1.200 65.5
2 1.000 59.1
3 0.800 52.0
4 0.500 37.3
5 0.100 19.9

P4 CUMULATIVE GRAPH>

PLE ID 001 - 2
PLE # 3/02/96 RUN02

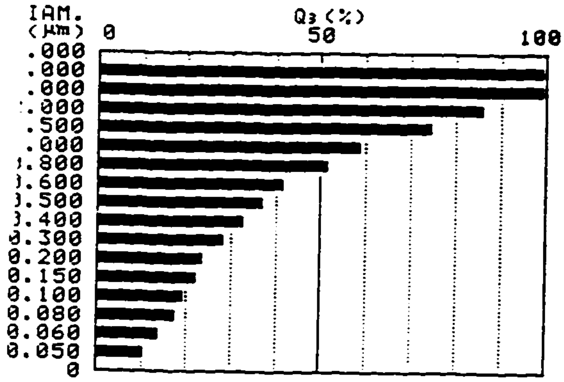

<SA-CP4 DIFFERENTIAL GRAPH>

SAMPLE ID 001 - 2
SAMPLE # 3/02/96 RUN02

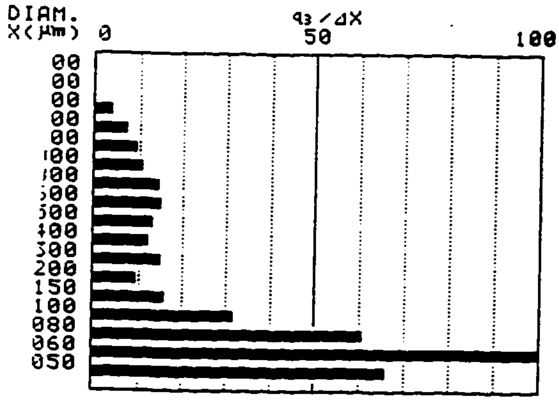

PARTICLE SIZE ANALYSIS BY SA-CP4
V1.00

SAMPLE ID F100 - 2
SAMPLE # 3/02/96 RUN03

P DENSITY 3.95 MODE :CENT
L DENSITY 0.9978 480(RPM/MIN)
VISC.(mPa.S) 0.96
DEPTH 2
BREAK P. 0 K(X):STANDARD

TIME 0:21:38

DATA SUMMARY>

MEDIAN DIAM. 0.027 (μm)
MODAL DIAM. 0 (μm)
SURFACE AREA 8.738 (m*m/g)

95.0% DIAM. 0.050 (μm)
5.0% DIAM. 0.003 (μm)

	DIAM. X(μm)	CUM Q0(%)
1	1.200	00
2	1.000	00
3	0.800	00
4	0.500	00
5	0.100	99.6

SA-CP4 CUMULATIVE GRAPH>

SAMPLE ID F100 - 2
SAMPLE # 3/02/96 RUN03

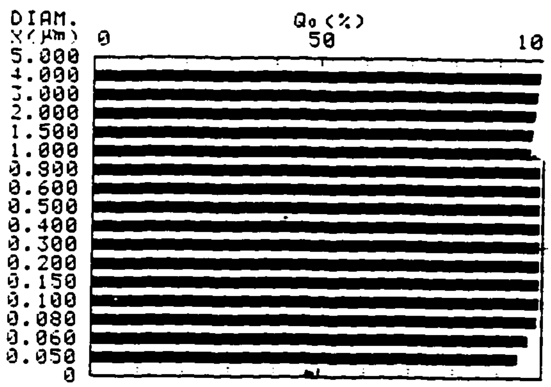

SA-CP4 DIFFERENTIAL GRAPH>

SAMPLE ID F100 - 2
SAMPLE # 3/02/96 RUN03

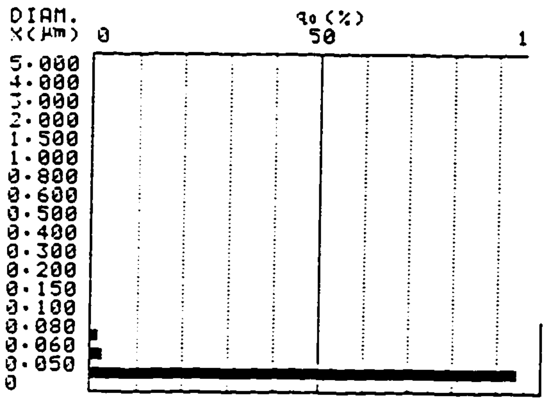

PARTICLE SIZE ANALYSIS BY SA-CP4
V1.00

IMPLE ID F100 - 2
IMPLE # 3/02/96 RUN03

DENSITY 3.95 MODE :CENT
DENSITY 0.9978 480(RPM/MIN)
SC.(mPa.S) 0.96
PTH 2
EAK P. 0 K(X):STANDARD

ME 0:21:38

DATA SUMMARY>

MEDIAN DIAM. 0.027 (μm)
MODAL DIAM. 0 (μm)
SURFACE AREA 8.738 (m*m/g)

95.0% DIAM. 0.050 (μm)
5.0% DIAM. 0.003 (μm)

	DIAM. X(μm)	CUM Q0(%)
1	1.200	00
2	1.000	00
3	0.800	00
	0.500	00
	0.100	99.6

CP4 CUMULATIVE GRAPH>

IPLE ID F100 - 2
IPLE # 3/02/96 RUN03

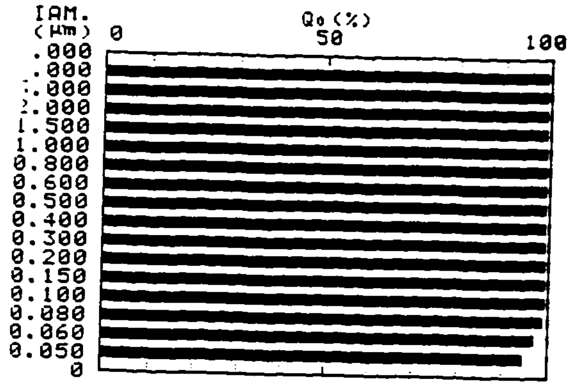

<SA-CP4 DIFFERENTIAL GRAPH>

SAMPLE ID F100 - 2
IPLE # 3/02/96 RUN03

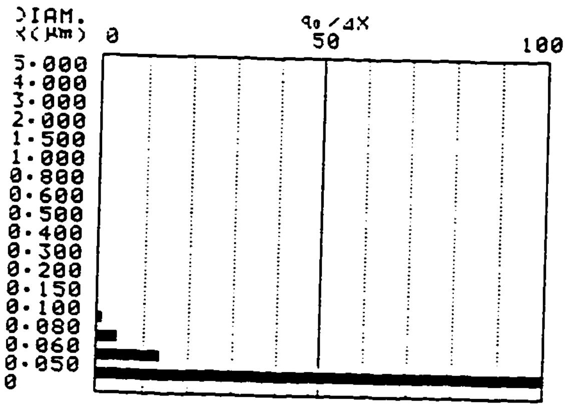

PARTICLE SIZE ANALYSIS BY SA-CP4
V1.00

SAMPLE ID F100 - 2
SAMPLE # 3/02/96 RUN03

P DENSITY	3.95	MODE :CENT
L DENSITY	0.9978	480(RPM/MIN)
VISC.(mPa.S)	0.96	
DEPTH	2	
BREAK P.	0	K(X):STANDARD

TIME 0:21:38

<DATA SUMMARY>

MEDIAN DIAM.	0.874	(μm)
MODAL DIAM.	1.218	(μm)
SURFACE AREA	8.738	(m*m/g)
95.0% DIAM.	2.689	(μm)
5.0% DIAM.	0.030	(μm)

	DIAM. X(μm)	CUM Q_3(%)
1	1.200	64.0
2	1.000	56.4
3	0.800	46.2
4	0.500	34.0
5	0.100	16.0

<SA-CP4 CUMULATIVE GRAPH>

SAMPLE ID F100 - 2
SAMPLE # 3/02/96 RUN03

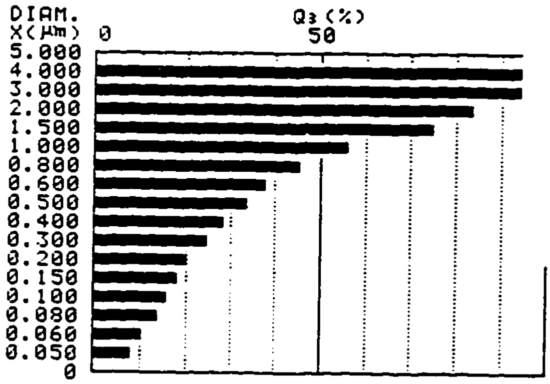

<SA-CP4 DIFFERENTIAL GRAPH>

SAMPLE ID F100 - 2
SAMPLE # 3/02/96 RUN03

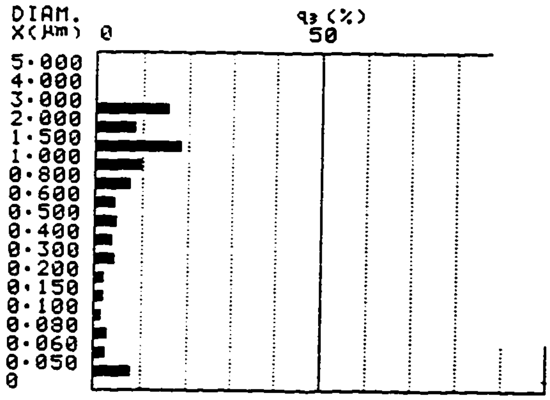

ARTICLE SIZE ANALYSIS BY SA-CP4
V1.00

PLE ID F100 - 2
PLE # 3/02/96 RUN03

NSITY 3.95 MODE :CENT
NSITY 0.9978 480(RPM/MIN)
.(mPa.S)0.96
H 2
K P. 0 K(X):STANDARD

: 0:21:38

TA SUMMARY>

EDIAN DIAM. 0.874 (μm)
MODAL DIAM. 1.218 (μm)
SURFACE AREA 8.738 (m*m/g)

95.0% DIAM. 2.689 (μm)
5.0% DIAM. 0.030 (μm)

DIAM. X(μm) CUM Q3(%)

1 1.200 64.0
2 1.000 56.4
3 0.800 46.2
4 0.500 34.0
5 0.100 16.0

-CP4 CUMULATIVE GRAPH>

MPLE ID F100 - 2
MPLE # 3/02/96 RUN03

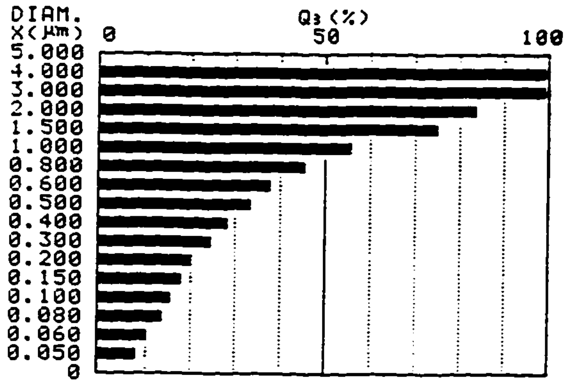

SA-CP4 DIFFERENTIAL GRAPH>

SAMPLE ID F100 - 2
SAMPLE # 3/02/96 RUN03

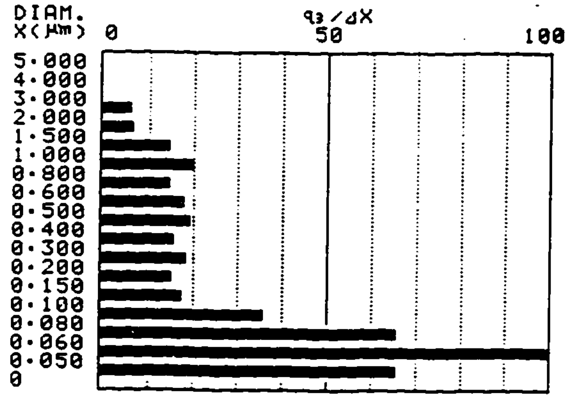

PARTICLE SIZE ANALYSIS BY SA-CP4 V1.00

SAMPLE ID 622 - 2
SAMPLE # 3/02/96 RUN04

P DENSITY	3.95	MODE :CENT
L DENSITY	0.9978	480(RPM/MIN)
VISC.(mPa.S)	0.96	
DEPTH	2	
BREAK P.	0	K(X):STANDARD

TIME 0:20:29

<DATA SUMMARY>

MEDIAN DIAM.	0.613	(μm)
MODAL DIAM.	0.690	(μm)
SURFACE AREA	3.088	(m*m/g)
95.0% DIAM.	1.663	(μm)
5.0% DIAM.	0.226	(μm)

	DIAM. X(μm)	CUM Q3(%)
1	1.200	87.8
2	1.000	83.4
3	0.800	70.4
4	0.500	34.5
5	0.100	1.0

<SA-CP4 CUMULATIVE GRAPH>

SAMPLE ID 622 - 2
SAMPLE # 3/02/96 RUN04

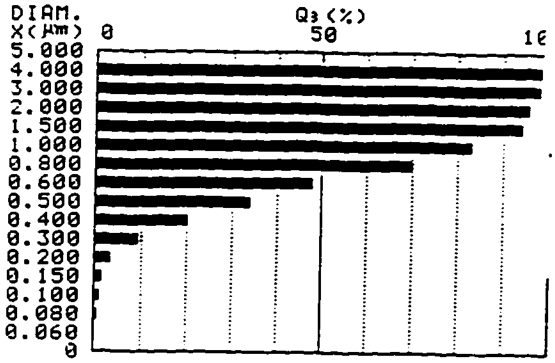

<SA-CP4 DIFFERENTIAL GRAPH>

SAMPLE ID 622 - 2
SAMPLE # 3/02/96 RUN04

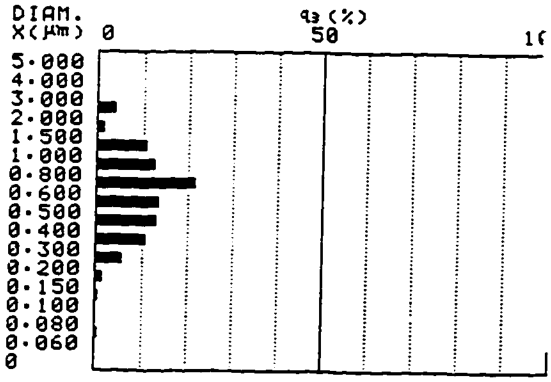

PARTICLE SIZE ANALYSIS BY SA-CP4 V1.00

SAMPLE ID 622 - 2
SAMPLE # 3/02/96 RUN04

ENSITY 3.95 MODE :CENT
ENSITY 0.9978 480(RPM/MIN)
C.(mPa.S)0.96
TH 2
AK P. 0 K(X):STANDARD

E 0:20:29

TA SUMMARY>

EDIAN DIAM. 0.613 (μm)
ODAL DIAM. 0.690 (μm)
SURFACE AREA 3.088 (m*m/g)
5.0% DIAM. 1.663 (μm)
5.0% DIAM. 0.226 (μm)

DIAM. X(μm) CUM Q3(%)
1 1.200 87.8
2 1.000 83.4
3 0.800 70.4
4 0.500 34.5
5 0.100 1.0

<SA-CP4 CUMULATIVE GRAPH>

PLE ID 622 - 2
PLE # 3/02/96 RUN04

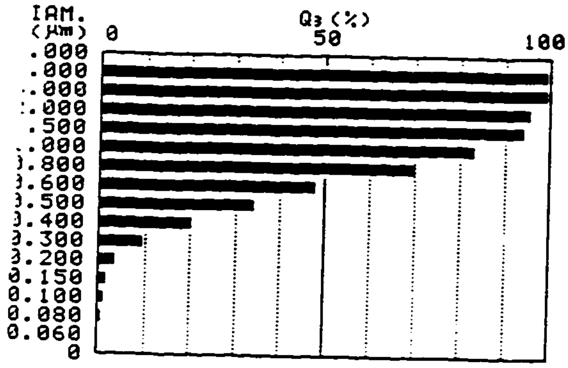

<SA-CP4 DIFFERENTIAL GRAPH>

SAMPLE ID 622 - 2
SAMPLE # 3/02/96 RUN04

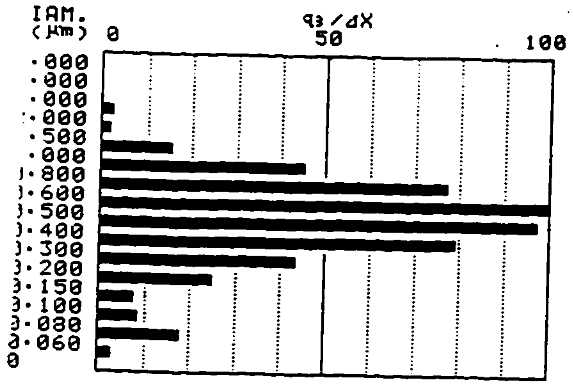

PARTICLE SIZE ANALYSIS BY SA-CP4
V1.00

SAMPLE ID 622 - 2
SAMPLE # 3/02/96 RUN04

P DENSITY	3.95	MODE :CENT
L DENSITY	0.9978	480(RPM/MIN)
VISC.(mPa.S)	0.96	
DEPTH	2	
BREAK P.	0	K(X):STANDARD

TIME 0:20:29

DATA SUMMARY>

MEDIAN DIAM.	0.041	(μm)
MODAL DIAM.	0	(μm)
SURFACE AREA	3.088	(m*m/g)
95.0% DIAM.	0.279	(μm)
5.0% DIAM.	0.004	(μm)

	DIAM. X(μm)	CUM Qo(%)
1	1.200	00
2	1.000	00
3	0.800	99.8
4	0.500	98.7
5	0.100	88.0

SA-CP4 CUMULATIVE GRAPH>

SAMPLE ID 622 - 2
SAMPLE # 3/02/96 RUN04

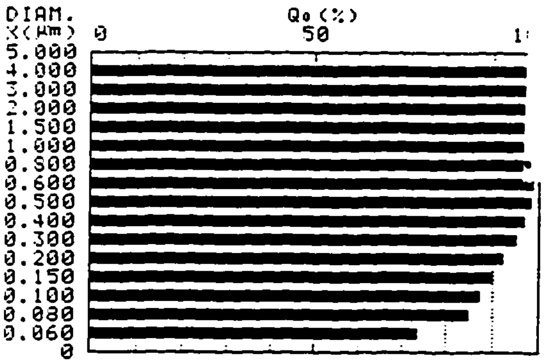

SA-CP4 DIFFERENTIAL GRAPH>

SAMPLE ID 622 - 2
SAMPLE # 3/02/96 RUN04

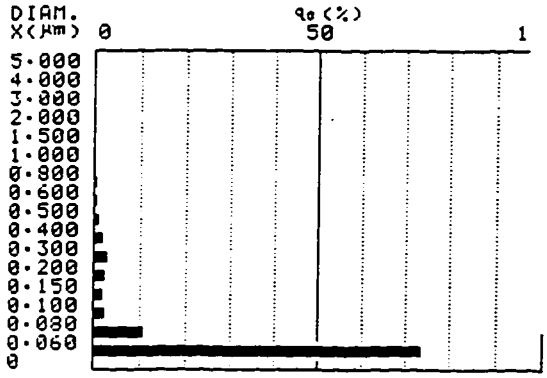

PARTICLE SIZE ANALYSIS BY SA-CP4
V1.00

AMPLE ID 622 - 2
AMPLE # 3/02/96 RUN04

ENSITY 3.95 MODE :CENT
ENSITY 0.9978 480(RPM/MIN)
C.(mPa.S)0.96
TH 2
AK P. 0 K(X):STANDARD

E 0:20:29

A SUMMARY>

DIAN DIAM. 0.041 (μm)
ODAL DIAM. 0 (μm)
SURFACE AREA 3.088 (m*m/g)

95.0% DIAM. 0.279 (μm)
5.0% DIAM. 0.004 (μm)

DIAM. X(μm) CUM Qo(%)
1 1.200 00
2 1.000 00
3 0.800 99.8
4 0.500 98.7
5 0.100 88.0

CP4 CUMULATIVE GRAPH>

PLE ID 622 - 2
PLE # 3/02/96 RUN04

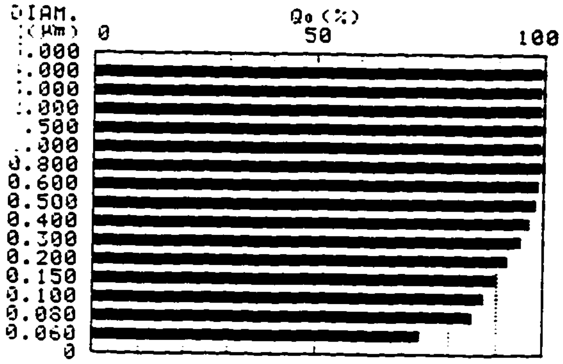

SA-CP4 DIFFERENTIAL GRAPH>

SAMPLE ID 622 - 2
PLE # 3/02/96 RUN04

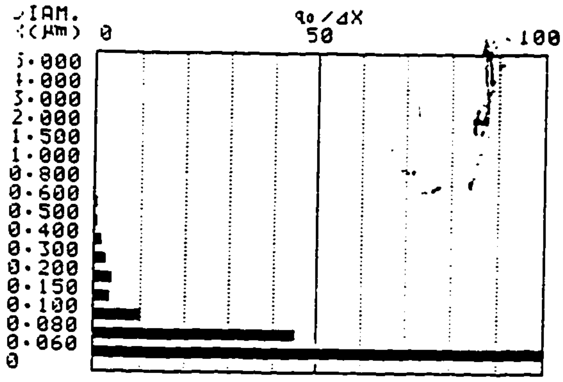

PARTICLE SIZE ANALYSIS BY SA-CP4
V1.00

SAMPLE ID DISPERAL
SAMPLE # 6/29/96 RUN1

P DENSITY 3.95 MODE :CENT
L DENSITY 0.9978 480(RPM/MIN)
VISC.(mPa.S) 0.96
DEPTH 2
BREAK P. 0 K(X):STANDARD

TIME 0:21:45

<DATA SUMMARY>

MEDIAN DIAM. 0.239 (µm)
MODAL DIAM. 0 (µm)
SURFACE AREA 22.56 (m*m/g)

95.0% DIAM. 2.613 (µm)
5.0% DIAM. 0.009 (µm)

	DIAM. X(µm)	CUM Q_3(%)
1	5.000	00
2	1.200	71.3
3	0.800	63.6
4	0.200	48.3
5	0.050	28.3

<SA-CP4 CUMULATIVE GRAPH>

SAMPLE ID DISPERAL
SAMPLE # 6/29/96 RUN1

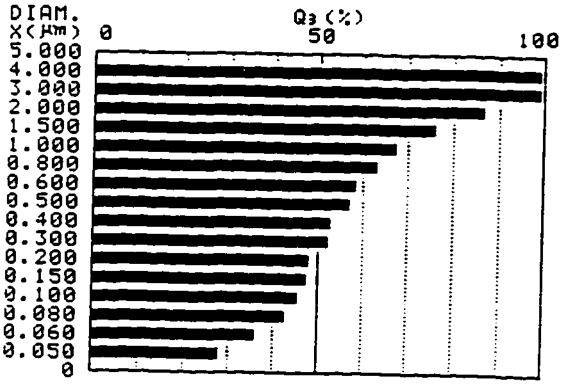

<SA-CP4 DIFFERENTIAL GRAPH>

SAMPLE ID DISPERAL
SAMPLE # 6/29/96 RUN1

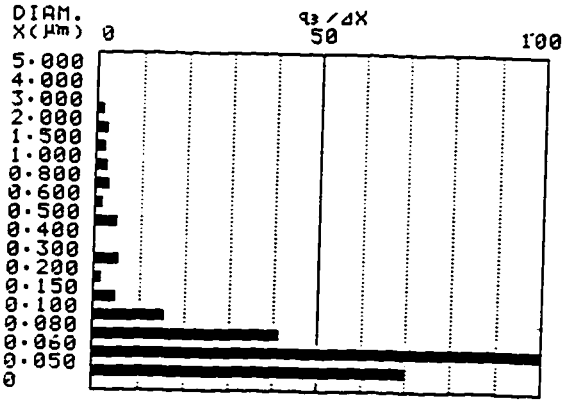

PARTICLE SIZE ANALYSIS BY SA-CP4
V1.00

SAMPLE ID DISPERAL
SAMPLE # 6/29/96 RUN1

P DENSITY 3.95 MODE :CENT
L DENSITY 0.9978 480(RPM/MIN)
VISC.(mPa.S) 0.96
DEPTH 2
BREAK P. 0 K(X):STANDARD

TIME 0:21:45

<DATA SUMMARY>

MEDIAN DIAM. 0.239 (µm)
MODAL DIAM. 0 (µm)
SURFACE AREA 22.56 (m*m/g)

95.0% DIAM. 2.613 (µm)
5.0% DIAM. 0.009 (µm)

	DIAM. X(µm)	CUM Q_3(%)
1	5.000	00
2	1.200	71.3
3	0.800	63.6
4	0.200	48.3
5	0.050	28.3

<SA-CP4 CUMULATIVE GRAPH>

SAMPLE ID DISPERAL
SAMPLE # 6/29/96 RUN1

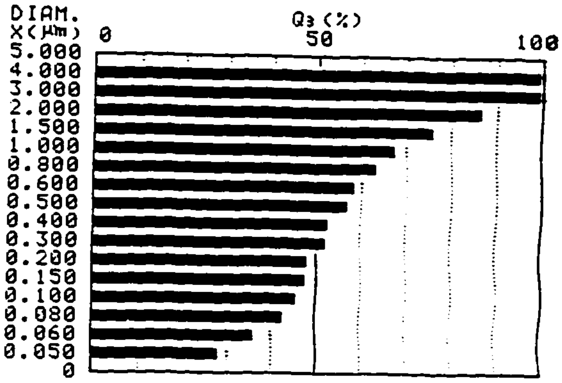

<SA-CP4 DIFFERENTIAL GRAPH>

SAMPLE ID DISPERAL
SAMPLE # 6/29/96 RUN1

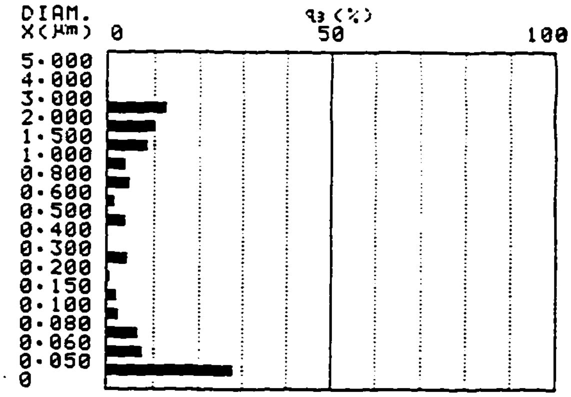

PARTICLE SIZE ANALYSIS BY SA-CP4
V1.00

SAMPLE ID DISPERAL
SAMPLE # 6/29/96 RUN1

P DENSITY 3.95 MODE :CENT
L DENSITY 0.9978 480(RPM/MIN)
VISC.(mPa.S) 0.96
DEPTH 2
BREAK P. 0 K(X):STANDARD

TIME 0:21:45

<DATA SUMMARY>

MEDIAN DIAM. 0.026 (μm)
MODAL DIAM. 0 (μm)
SURFACE AREA 22.56 (m*m/g)

95.0% DIAM. 0.050 (μm)
5.0% DIAM. 0.002 (μm)

	DIAM. X(μm)	CUM Q_0(%)
1	5.000	00
2	1.200	00
3	0.800	00
4	0.200	00
5	0.050	96.1

<SA-CP4 CUMULATIVE GRAPH>

SAMPLE ID DISPERAL
SAMPLE # 6/29/96 RUN1

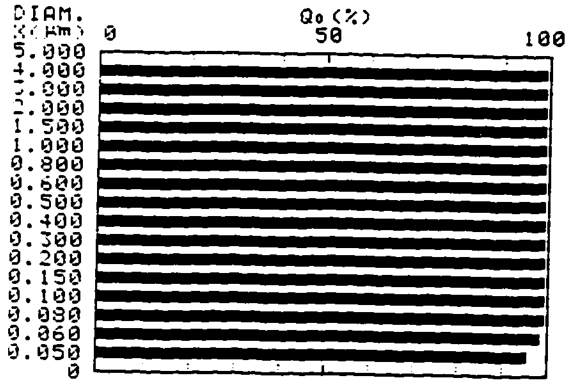

<SA-CP4 DIFFERENTIAL GRAPH>

SAMPLE ID DISPERAL
SAMPLE # 6/29/96 RUN1

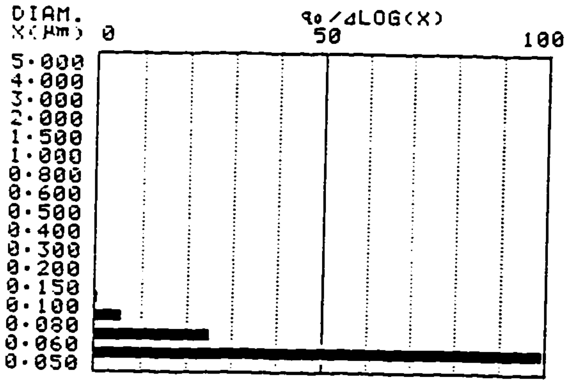

PARTICLE SIZE ANALYSIS BY SA-CP4
V1.00

SAMPLE ID DISPERAL
SAMPLE # 6/29/96 RUN1

P DENSITY 3.95 MODE :CENT
L DENSITY 0.9978 480(RPM/MIN)
VISC.(mPa.S) 0.96
DEPTH 2
BREAK P. 0 K(X):STANDARD

TIME 0:21:45

<DATA SUMMARY>

MEDIAN DIAM. 0.229 (μm)
MODAL DIAM. 0 (μm)
SURFACE AREA 22.56 (m*m/g)

95.0% DIAM. 2.613 (μm)
5.0% DIAM. 0.009 (μm)

	DIAM. X(μm)	CUM Q_3(%)
1	5.000	00
2	1.200	71.3
3	0.800	63.6
4	0.200	48.3
5	0.050	28.3

<SA-CP4 CUMULATIVE GRAPH>

SAMPLE ID DISPERAL
SAMPLE # 6/29/96 RUN1

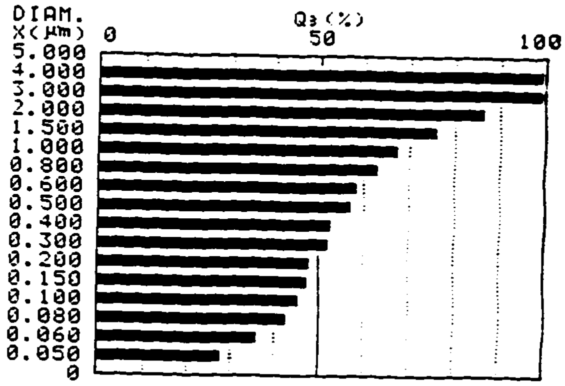

<SA-CP4 DIFFERENTIAL GRAPH>

SAMPLE ID DISPEPAL
SAMPLE # 6/29/96 RUN1

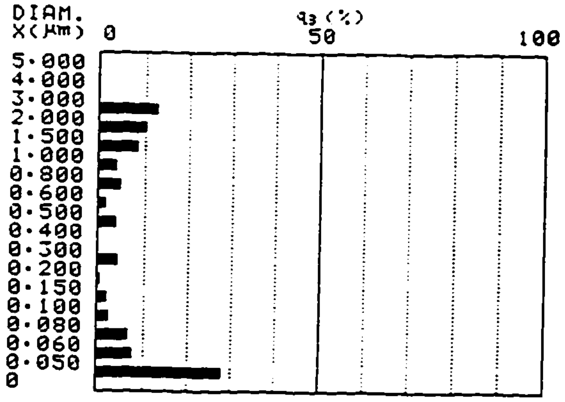

PARTICLE SIZE ANALYSIS BY SA-CP4
V1.00

SAMPLE ID DISPERAL
SAMPLE # 6/29/96 RUN1

P DENSITY 3.95 MODE :CENT
L DENSITY 0.9978 480(RPM/MIN)
VISC.(mPa.S) 0.96
DEPTH 2
BREAK P. 0 K(X):STANDARD

TIME 0:21:45

<DATA SUMMARY>

MEDIAN DIAM. 0.239 (μm)
MODAL DIAM. 0 (μm)
SURFACE AREA 22.56 (m*m/g)

95.0% DIAM. 2.613 (μm)
5.0% DIAM. 0.009 (μm)

	DIAM. X(μm)	CUM Q3(%)
1	5.000	00
2	1.200	71.3
3	0.800	63.6
4	0.200	48.3
5	0.050	28.3

<SA-CP4 CUMULATIVE GRAPH>

SAMPLE ID DISPERAL
SAMPLE # 6/29/96 RUN1

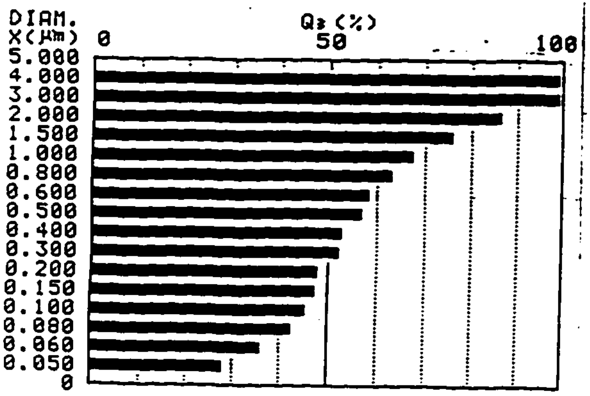

<SA-CP4 DIFFERENTIAL GRAPH>

SAMPLE ID DISPERAL
SAMPLE # 6/29/96 RUN1

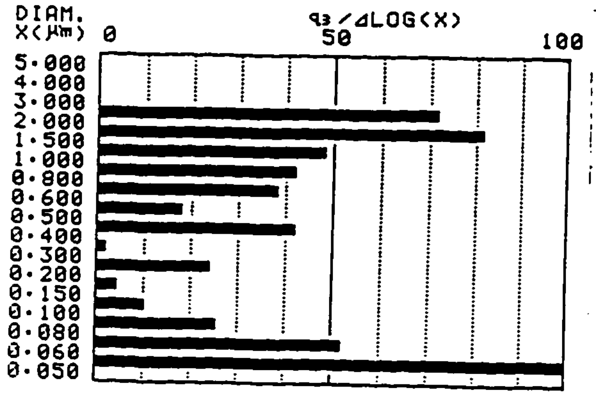

PARTICLE SIZE ANALYSIS BY SA-CP4
V1.00

SAMPLE ID DISPERAL
SAMPLE # 6/29/96 RUN1

P DENSITY 3.95 MODE :CENT
L DENSITY 0.9978 480(RPM/MIN)
VISC.(mPa.S) 0.96
DEPTH 2
BREAK P. 0 K(X):STANDARD

TIME 0:21:45

<DATA SUMMARY>

MEDIAN DIAM. 0.026 (μm)
MODAL DIAM. 0 (μm)
SURFACE AREA 22.56 (m*m/g)

95.0% DIAM. 0.050 (μm)
5.0% DIAM. 0.002 (μm)

	DIAM. X(μm)	CUM Q0(%)
1	5.000	00
2	1.200	00
3	0.800	00
4	0.200	00
5	0.050	96.1

<SA-CP4 CUMULATIVE GRAPH>

SAMPLE ID DISPERAL
SAMPLE # 6/29/96 RUN1

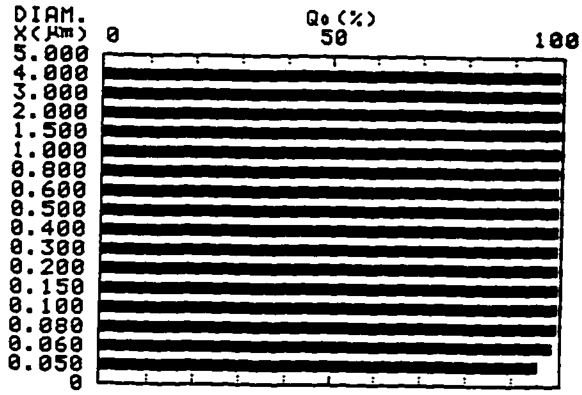

<SA-CP4 DIFFERENTIAL GRAPH>

SAMPLE ID DISPERAL
SAMPLE # 6/29/96 RUN1

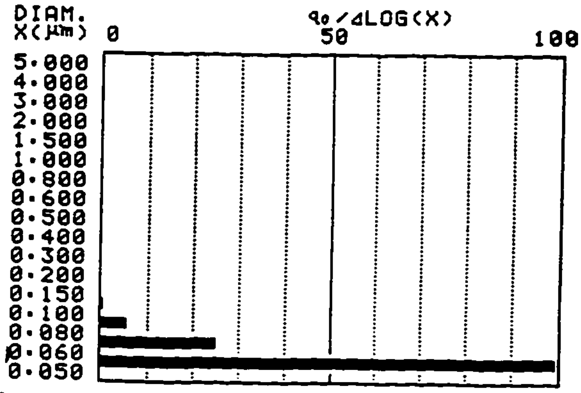

PARTICLE SIZE ANALYSIS BY SA-CP4
V1.00

SAMPLE ID 001
SAMPLE # 6/29/96 RUN2

P DENSITY 3.95 MODE :CENT
L DENSITY 0.9978 480(RPM/MIN)
VISC.(mpa.S)0.96
DEPTH 2
BREAK P. 0 K(X):STANDARD

TIME 0:21:38

<DATA SUMMARY>

MEDIAN DIAM.	0.419	(μm)
MODAL DIAM.	0	(μm)
SURFACE AREA	18.80	(m*m/g)
95.0% DIAM.	2.695	(μm)
5.0% DIAM.	0.011	(μm)

	DIAM. X(μm)	CUM Q3(%)
1	5.000	00
2	1.200	72.1
3	0.800	61.4
4	0.200	43.3
5	0.050	22.0

<SA-CP4 CUMULATIVE GRAPH>

SAMPLE ID 001
SAMPLE # 6/29/96 RUN2

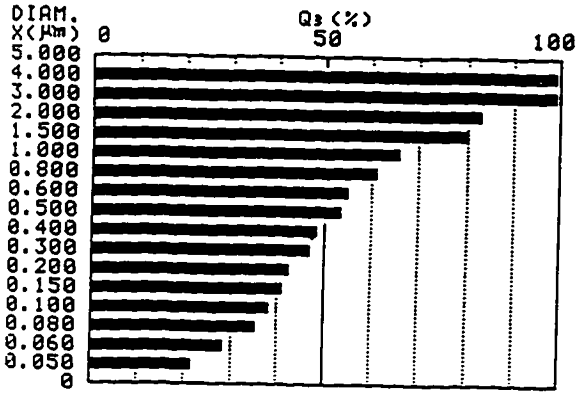

<SA-CP4 DIFFERENTIAL GRAPH>

SAMPLE ID 001
SAMPLE # 6/29/96 RUN2

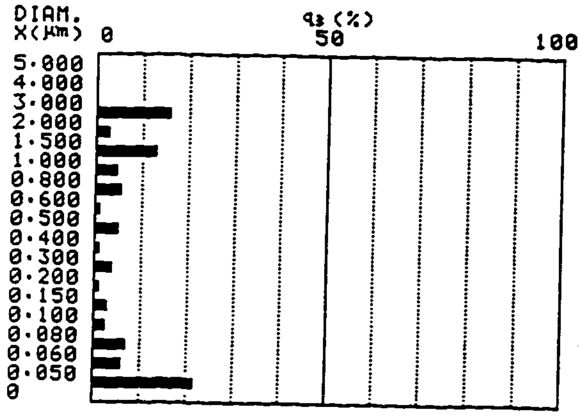

PARTICLE SIZE ANALYSIS BY SA-CP4
V1.00

SAMPLE ID 001
SAMPLE # 6/29/96 RUN2

P DENSITY 3.95 MODE :CENT
L DENSITY 0.9978 480(RPM/MIN)
VISC.(mpa.S)0.96
DEPTH 2
BREAK P. 0 K(X):STANDARD

TIME 0:21:38

<DATA SUMMARY>

MEDIAN DIAM. 0.419 (μm)
MODAL DIAM. 0 (μm)
SURFACE AREA 18.80 (m*m/g)
95.0% DIAM. 2.695 (μm)
5.0% DIAM. 0.011 (μm)

DIAM. X(μm) CUM Q3(%)
1 5.000 00
2 1.200 72.1
3 0.800 61.4
4 0.200 43.3
5 0.050 22.0

<SA-CP4 CUMULATIVE GRAPH>

SAMPLE ID 001
SAMPLE # 6/29/96 RUN2

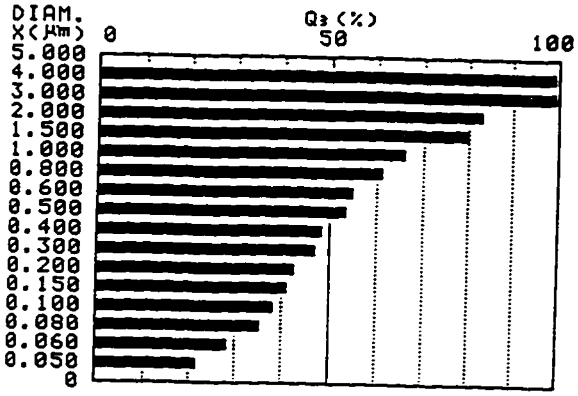

<SA-CP4 DIFFERENTIAL GRAPH>

SAMPLE ID 001
SAMPLE # 6/29/96 RUN2

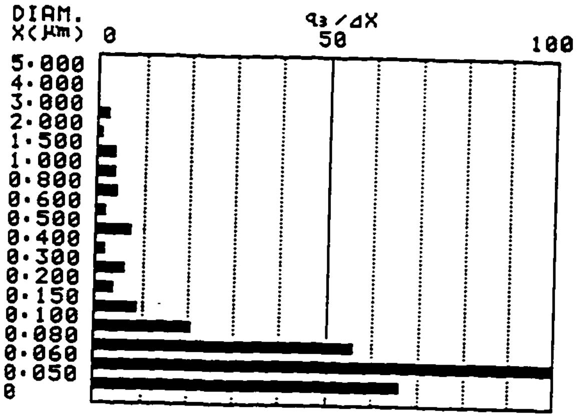

PARTICLE SIZE ANALYSIS BY SA-CP4
V1.00

SAMPLE ID F100
SAMPLE # 6/29/96 RUN3

P DENSITY 3.95 MODE :CENT
L DENSITY 0.9978 480(RPM/MIN)
VISC.(mPa.S) 0.96
DEPTH 2
BREAK P. 0 K(X):STANDARD

TIME 0:21:38

DATA SUMMARY>

MEDIAN DIAM. 0.395 (μm)
MODAL DIAM. 0 (μm)
SURFACE AREA 18.05 (m*m/g)

95.0% DIAM. 1.969 (μm)
5.0% DIAM. 0.013 (μm)

	DIAM. X(μm)	CUM Q_3(%)
1	5.000	00
2	1.200	76.5
3	0.800	63.9
4	0.200	41.9
5	0.050	20.5

SA-CP4 CUMULATIVE GRAPH>

SAMPLE ID F100
SAMPLE # 6/29/96 RUN3

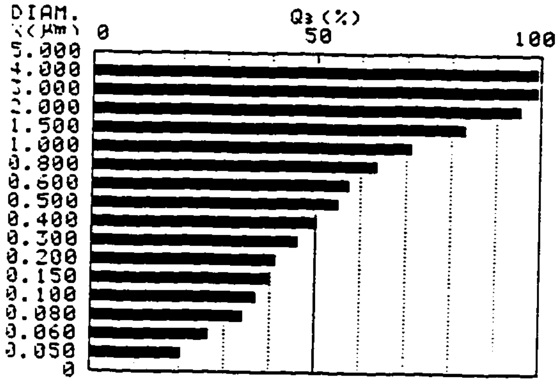

SA-CP4 DIFFERENTIAL GRAPH>

SAMPLE ID F100
SAMPLE # 6/29/96 RUN3

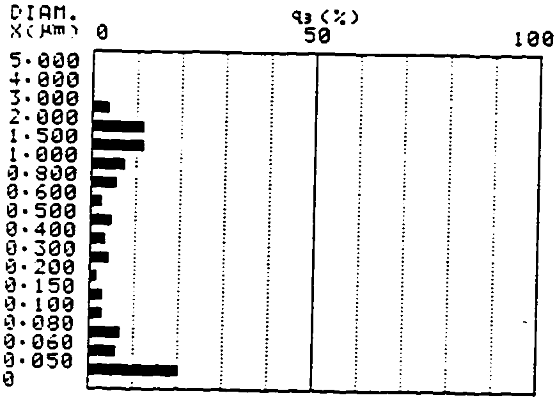

PARTICLE SIZE ANALYSIS BY SA-CP4
V1.00

SAMPLE ID F100
SAMPLE # 6/29/96 RUN3

P DENSITY 3.95 MODE :CENT
L DENSITY 0.9978 480(RPM/MIN)
VISC.(mPa.S) 0.96
DEPTH 2
BREAK P. 0 K(X):STANDARD

TIME 0:21:38

DATA SUMMARY>

MEDIAN DIAM. 0.395 (μm)
MODAL DIAM. 0 (μm)
SURFACE AREA 18.05 (m*m/g)

95.0% DIAM. 1.969 (μm)
5.0% DIAM. 0.013 (μm)

DIAM. X(μm) CUM Q3(%)
1 5.000 00
2 1.200 76.5
3 0.800 63.9
4 0.200 41.9
5 0.050 20.5

SA-CP4 CUMULATIVE GRAPH>

SAMPLE ID F100
SAMPLE # 6/29/96 RUN3

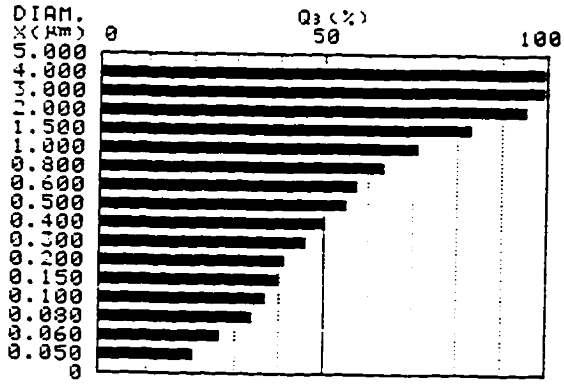

<SA-CP4 DIFFERENTIAL GRAPH>

SAMPLE ID F100
SAMPLE # 6/29/96 RUN3

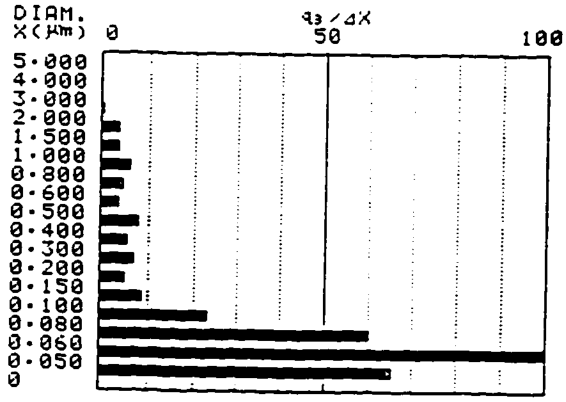

PARTICLE SIZE ANALYSIS BY SA-CP4
V1.00

SAMPLE ID 622
SAMPLE # 6/29/96 RUN4

P DENSITY 3.95
L DENSITY 0.9978
VISC.(mPa.S) 0.96
DEPTH 2
BREAK P. 0

MODE :CENT
480(RPM/MIN)

K(X):STANDARD

TIME 0:09:29

<DATA SUMMARY>

MEDIAN DIAM.	0.601	(μm)
MODAL DIAM.	0.676	(μm)
SURFACE AREA	2.999	(m*m/g)
95.0% DIAM.	1.399	(μm)
5.0% DIAM.	0.242	(μm)

	DIAM. X(μm)	CUM Q_3(%)
1	5.000	00
2	1.200	90.8
3	0.800	78.9
4	0.200	1.6
5	0.050	0.4

<SA-CP4 CUMULATIVE GRAPH>

SAMPLE ID 622
SAMPLE # 6/29/96 RUN4

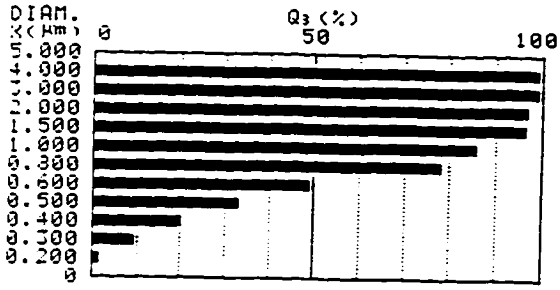

<SA-CP4 DIFFERENTIAL GRAPH>

SAMPLE ID 622
SAMPLE # 6/29/96 RUN4

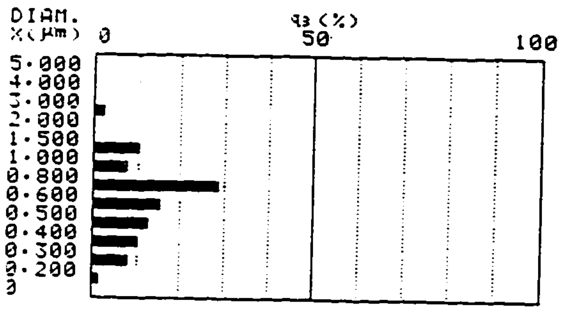

PARTICLE SIZE ANALYSIS BY SA-CP4
V1.00

SAMPLE ID 622
SAMPLE # 6/29/96 RUN4

P DENSITY 3.95
L DENSITY 0.9978
VISC.(mPa.S) 0.96
DEPTH 2
BREAK P. 0

MODE :CENT
480(RPM/MIN)

K(X):STANDARD

TIME 0:09:29

<DATA SUMMARY>

MEDIAN DIAM. 0.601 (μm)
MODAL DIAM. 0.676 (μm)
SURFACE AREA 2.999 (m*m/g)
95.0% DIAM. 1.399 (μm)
5.0% DIAM. 0.242 (μm)

DIAM. X(μm) CUM Q3(%)
1 5.000 00
2 1.200 90.8
3 0.800 78.9
4 0.200 1.6
5 0.050 0.4

<SA-CP4 CUMULATIVE GRAPH>

SAMPLE ID 622
SAMPLE # 6/29/96 RUN4

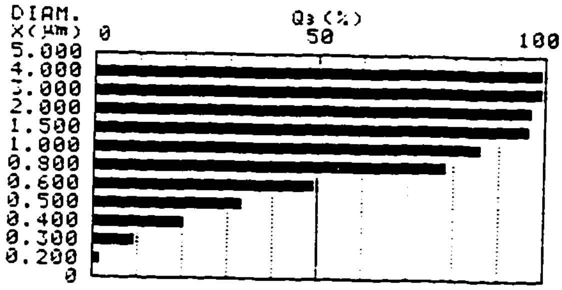

<SA-CP4 DIFFERENTIAL GRAPH>

SAMPLE ID 622
SAMPLE # 6/29/96 RUN4

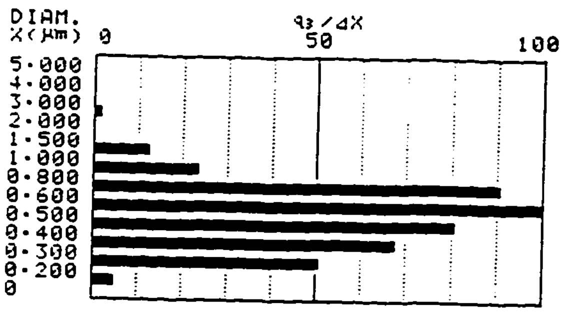

PARTICLE SIZE ANALYSIS BY SA-CP4
V1.00

SAMPLE ID 622
SAMPLE # 6/29/96 RUN4

P DENSITY 3.95
L DENSITY 0.9978
VISC.(mPa.S) 0.96
DEPTH 2
BREAK P. 0

MODE :CENT
480(RPM/MIN)

K(X):STANDARD

TIME 0:09:29

<DATA SUMMARY>

MEDIAN DIAM.	0.171	(μm)
MODAL DIAM. 0		(μm)
SURFACE AREA	2.999	(m*m/g)
95.0% DIAM.	0.566	(μm)
5.0% DIAM.	0.018	(μm)

	DIAM. X(μm)	CUM Qo(%)
1	5.000	00
2	1.200	99.9
3	0.800	99.4
4	0.200	58.3
5	0.050	14.6

<SA-CP4 CUMULATIVE GRAPH>

SAMPLE ID 622
SAMPLE # 6/29/96 RUN4

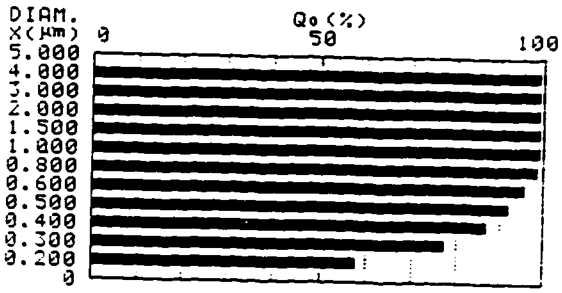

SA-CP4 DIFFERENTIAL GRAPH>

SAMPLE ID 622
SAMPLE # 6/29/96 RUN4

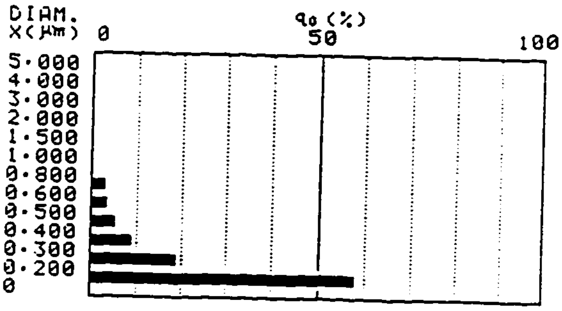

Appendix C. Analysis of Optimal Particle Size Distribution for Trimodal Packing of Spheres

Appendix C

Determination of size of sphere fitting in tetrahedral site

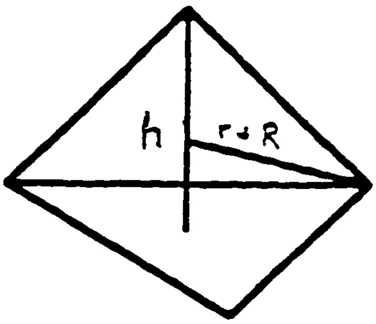

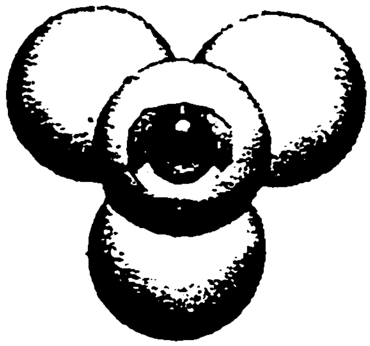

(from Kingery p.57)

R = Radius of large spheres

r = Radius of sphere in tetrahedral site

h = Height of tetrahedron with edges of 2R

$= (2)^{1/2}/(3)^{1/2}*2R$

$R+r = 3/4*h = (3)^{1/2}/(2)^{1/2}*R$

$r = (3^{1/2}-2^{1/2})/2^{1/2}*R = 0.225\ R$

Appendix C

Determination of size of spheres fitting in voids of packing of larger spheres

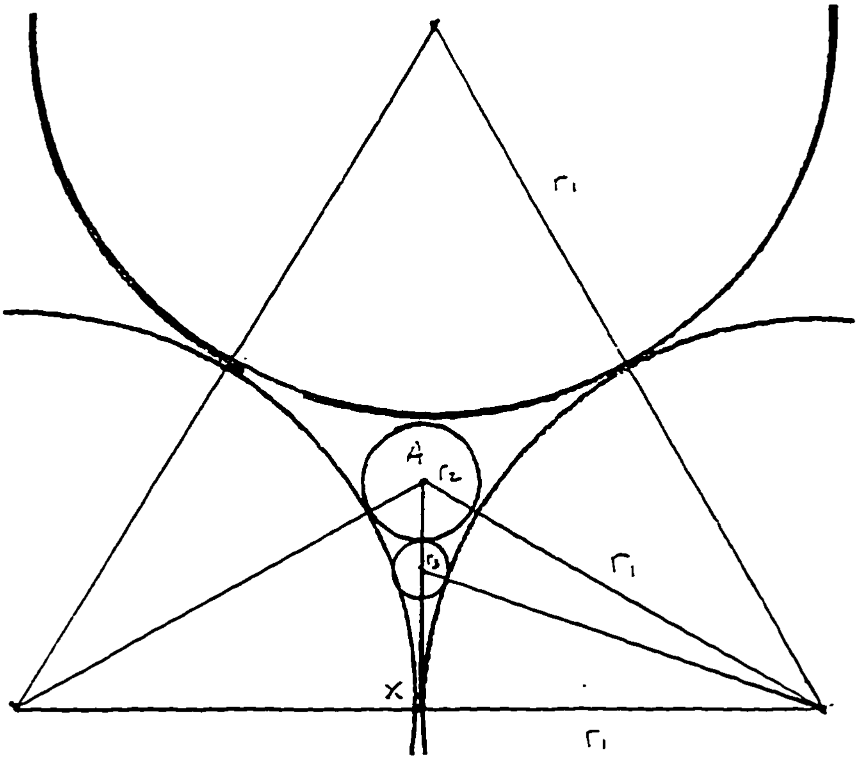

r_1 = Radius of large spheres = 1.0

r_2 = Radius of medium sphere = 0.155 r_1

r_3 = Radius of smallest sphere = 0.063 r_1

AX = Radius of inscribed circle in equilateral triangle with side =2r_1

$$AX=1/6(2r_1)3^{1/2}$$

(from Standard Mathematical Tables, 16th Ed., p8.)

$$AX^2+r_1^2=(r_2+r_1)^2$$

$$3r_2^2+6r_1r_2-r_1^2=0$$

$$\mathbf{r_2=0.155r_1}$$

$$(AX-r_2-r_3)^2+r_1^2=(r_3+r_1)^2$$

$$r_3=(AX-r_2)^2/(2r_1+2(AX-r_2))=\mathbf{0.063r_1}$$

Appendix C

Determination of size of sphere fitting in octahedral site

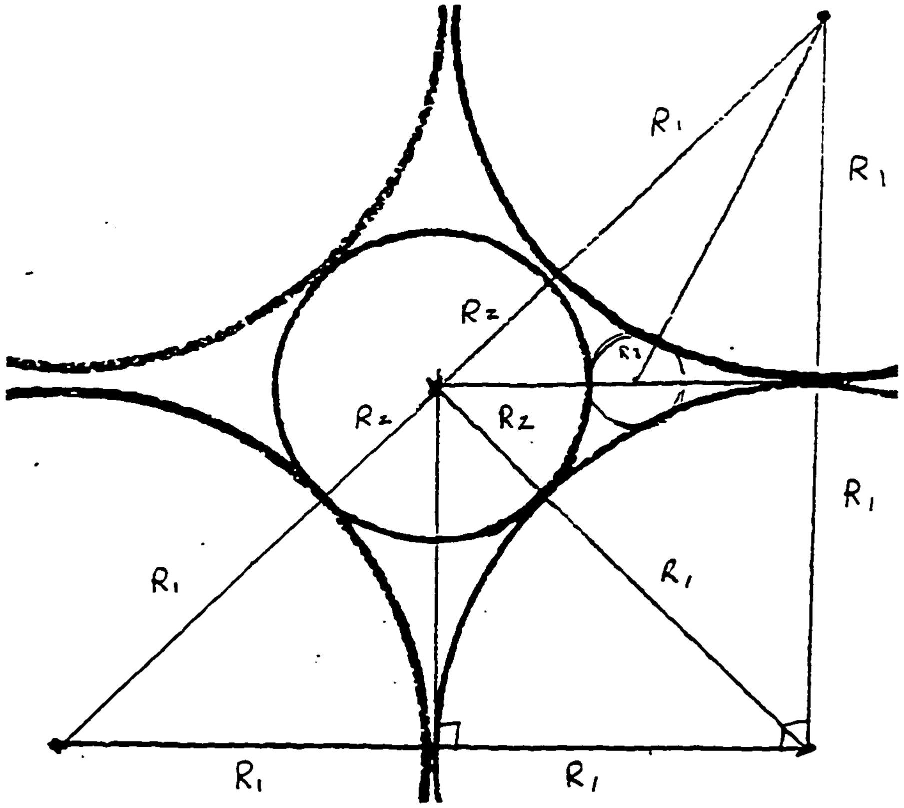

R_1 = Radius of large spheres = 1.0

R_2 = Radius of sphere in tetrahedral site = 0.414 R_1

R_3 = Radius of smallest sphere = 0.108 R_1

$$(2R_1)^2+(2R_1)^2=(2R_1+2R_2)^2$$

$$R_2^2+2R_1R_2-R_1^2=0$$

$$\mathbf{R_2=(R_1^2+1)^{1/2}-R_1=0.414R_1}$$

$$(R_1+R_3)^2=(R_1-(R_2+R_3))^2+R_1^2$$

$$\mathbf{R_3=(R_1-R_2)^2/(4R_1-2R_2)=0.108R_1}$$

Appendix D. Calculation of Particle Weight Distribution for Optimal Packing

Appendix D

Calculation of optimal particle size weight distribution

There are two tetrahedral sites and one octahedral site per large sphere in a FCC packing. FCC fractional packing density is 0.7405. The fractional packing density occupied by spheres located in tetrahedral sites is the volume of the tetrahedral sphere multiplied by the number of tetrahedral spheres per large sphere multiplied by the fractional packing density of the large spheres. The fractional packing density of the octahedral spheres is determined in a similar manner.

Material	Fractional Packing Density
Large spheres	0.7405
Tetrahedral spheres	0.0169
Octahedral spheres	0.0525
Residual porosity	0.1901
Total	1.0000

For a 100g sample, assuming all materials have the same density

Material	grams	Percent by Weight
Large spheres	91.4	91.4
Tetrahedral spheres	2.1	2.1
Octahedral spheres	6.5	6.5
Total		100.0

If the density of each component is not the same, then the fractional packing density for each component must be multiplied by the density of the component. Each result is then divided by the total weight to determine the weight percent of each component.

Appendix E. TAP Density Measurements

Designation: B 527 – 85 (Reapproved 1991)$^{\epsilon 1}$

Standard Test Method for Tap Density of Powders of Refractory Metals and Compounds by Tap-Pak Volumeter[1]

This standard is issued under the fixed designation B 527; the number immediately following the designation indicates the year of original adoption or, in the case of revision, the year of last revision. A number in parentheses indicates the year of last reapproval. A superscript epsilon (ε) indicates an editorial change since the last revision or reapproval.

ε¹ Note—The Keywords section was added editorially, and other editorial changes made, in August 1991.

1. Scope

1.1 This test method covers determination of the tap density (packed density) of refractory metal powders and compounds by means of the Tap-Pak Volumeter.[2]

1.2 *This standard does not purport to address the safety problems, if any, associated with its use. It is the responsibility of the user of this standard to establish appropriate safety and health practices and determine the applicability of regulatory limitations prior to use.*

2. Significance and Use

2.1 This test method covers the evaluation of the tapped density physical characteristic of powders. The degree of correlation between the results of this test and the quality of powders in use will vary with each particular application and has not been fully determined.

3. Apparatus

3.1 *Graduated Cylinder*,[3] calibrated to contain 25 mL at 20°C, internal diameter 15 mm, height 180 mm and weight approximately 60 g.

3.2 *Holder*—A cylinder holder weighing 1 lb (454 g).

3.3 *Tapping Device*, consisting of a baseplate with single-phase a-c condenser motor, with worm drive, reduction ratio 15 to 1, cam shaft speed 250 r/min, tapping stroke travel 3.2 mm.

3.4 *Counter*—A four-digit adjustable counter, which can be preset to deliver numbers of taps between 1 and 9999.

3.5 *Balance*, having a capacity of at least 100 g and a sensitivity of 0.1 g.

4. Test Specimen

4.1 The test specimen shall be 50 g except as noted in 4.2.

4.2 For refractory metal and compound powders too voluminous to fit into the 25-mL graduated cylinder, reduce sample size to 20 g or 10 g, as necessary, and follow the standard procedure.

5. Procedure

5.1 Weigh 50 g of the test specimen to an accuracy of ±0.1 g.

5.2 Pour the test specimen carefully into the graduated cylinder, using a funnel. To ensure proper level, rotate the funnel while pouring the test specimen.

5.3 Preset the counter for 3000 taps.

5.4 Start tapping device.

5.5 Read the tapped volume, V, in millilitres, by calculating the mean value between the highest and the lowest point at the tapped volume.

6. Calculation and Report

6.1 Calculate tap density in grams per cubic centimetre, to the nearest tenth by dividing 50 g (10 or 20 g for samples as noted in 4.2) by the tapped volume, V, read in millilitres, as follows:

$$\text{Tap density, g/cm}^3 = 50\ \text{g}/V$$

7. Precision and Bias

7.1 Precision has been determined from round-robin testing performed prior to the approval of this test method. Those results which have been re-verified show a precision of from ± 1 to 2 % of the value determined as the 2 σ limits. The variation depends upon the tap density of the powder being determined which can vary between 2.0 and 8.0 g/cm³.

7.2 Bias cannot be stated since there is no universally accepted standard instrument, nor are instruments sold as certified standards.

8. Keywords

8.1 molybdenum; packed density; powder(s); refractory metals; rhenium; tantalum; tap density; Tap-Pak Volumeter; tungsten; tungsten carbide

---

[1] This test method is under the jurisdiction of ASTM Committee B-9 on Metal Powders and Metal Powder Products and is the direct responsibility of Subcommittee B09.03 on Refractory Metal Powders.

Current edition approved Aug. 30, 1985. Published December 1985. Originally published as B 527 – 70. Last previous edition B 527 – 81.

[2] Tap-Pak Volumeter Model No. JEL ST2 manufactured by J. Engelsmann A.G. of Ludwigshafen a. Rh. West Germany. Available through Shandon Southern Instruments Inc., 171 Industry Drive, Pittsburgh, PA 15275.

[3] Corning, No. 3046, Pyrex Brand, has been found satisfactory for this purpose.

Sample ID	initial wt(g)	initial vol (cc)	final vol. (cc)	Apparent density	Ave	+/-std dev	Tap density	Ave	+/- std dev	Hausner Ratio	Ave	+/- std dev
F100	7.209	10.00	6.74	0.72	0.72		1.07	1.06		1.48	1.47	
	7.171	9.90	6.78	0.72		0.00	1.06		0.01	1.46		0.01
	7.105	9.90	6.74	0.72			1.05			1.47		
OO1	6.494	9.70	6.58	0.67	0.66		0.99	0.99		1.47	1.49	
	6.342	9.55	6.40	0.66		0.01	0.99		0.00	1.49		0.02
	6.442	9.85	6.52	0.65			0.99			1.51		
N2802	10.660	10.00	6.70	1.07	1.05		1.59	1.57		1.49	1.49	
	10.565	10.00	6.80	1.06		0.02	1.55		0.02	1.47		0.02
	10.514	10.30	6.78	1.02			1.55			1.52		
N802	9.987	10.10	6.65	0.99	0.97		1.50	1.50		1.52	1.54	
	9.896	10.30	6.60	0.96		0.01	1.50		0.00	1.56		0.02
	9.855	10.15	6.55	0.97			1.50			1.55		
802	10.456	10.00	6.90	1.05	1.01		1.52	1.51		1.45	1.50	
	10.147	10.30	6.72	0.99		0.03	1.51		0.00	1.53		0.05
	10.283	10.40	6.80	0.99			1.51			1.53		
100	9.506	10.10	7.28	0.94	0.95		1.31	1.31		1.39	1.38	
	9.358	9.80	7.11	0.95		0.01	1.32		0.01	1.38		0.01
	9.361	9.75	7.10	0.96			1.32			1.37		
O10	10.250	10.25	7.85	1.00	0.98		1.31	1.29		1.31	1.32	
	9.994	10.20	7.70	0.98		0.02	1.30		0.01	1.32		0.01
	10.093	10.50	7.90	0.96			1.28			1.33		
820	9.525	9.80	6.90	0.97	0.95		1.38	1.37		1.42	1.44	
	9.170	9.80	6.70	0.94		0.02	1.37		0.01	1.46		0.02
	9.187	9.80	6.75	0.94			1.36			1.45		
730	10.821	10.40	7.60	1.04	1.01		1.42	1.40		1.37	1.39	
	9.616	9.65	6.90	1.00		0.03	1.39		0.02	1.40		0.02
	10.348	10.40	7.46	1.00			1.39			1.39		
640	9.347	9.95	7.00	0.94	0.93		1.34	1.33		1.42	1.43	
	9.255	9.90	6.95	0.93		0.01	1.33		0.00	1.42		0.01
	9.246	9.95	6.95	0.93			1.33			1.43		
604	9.035	9.95	6.68	0.91	0.89		1.35	1.35		1.49	1.51	
	8.980	10.10	6.65	0.89		0.01	1.35		0.00	1.52		0.02
	8.813	10.00	6.55	0.88			1.35			1.53		
703	9.576	10.05	6.60	0.95	0.95		1.45	1.44		1.52	1.52	
	9.474	9.95	6.60	0.95		0.01	1.44		0.01	1.51		0.01
	9.426	10.00	6.55	0.94			1.44			1.53		
955	9.815	10.00	6.97	0.98	0.96		1.41	1.44		1.43	1.50	
	9.753	10.20	6.60	0.96		0.02	1.48		0.03	1.55		0.06
	9.426	10.00	6.55	0.94			1.44			1.53		
811	10.660	10.10	6.95	1.06	1.04		1.53	1.53		1.45	1.47	
	10.487	10.10	6.85	1.04		0.01	1.53		0.01	1.47		0.01
	10.485	10.20	6.90	1.03			1.52			1.48		
721	11.271	10.30	7.35	1.09	1.06		1.53	1.52		1.40	1.43	
	10.808	10.40	7.15	1.04		0.03	1.51		0.02	1.45		0.03
	10.948	10.45	7.28	1.05			1.50			1.44		
712	10.266	10.00	6.65	1.03	1.00		1.54	1.53		1.50	1.53	
	10.194	10.25	6.70	0.99		0.03	1.52		0.01	1.53		0.03
	10.169	10.50	6.70	0.97			1.52			1.57		
613	10.123	10.00	6.85	1.01	0.99		1.48	1.47		1.46	1.49	
	9.974	10.20	6.80	0.98		0.02	1.47		0.01	1.50		0.02
	9.742	10.05	6.68	0.97			1.46			1.50		
631	10.454	10.10	7.00	1.04	1.00		1.49	1.48		1.44	1.48	
	9.823	10.00	6.62	0.98		0.03	1.48		0.02	1.51		0.04
	9.712	9.95	6.65	0.98			1.46			1.50		
622	10.502	10.00	6.85	1.05	1.01		1.53	1.51		1.46	1.49	
	9.836	9.90	6.53	0.99		0.03	1.51		0.02	1.52		0.03
	9.986	10.00	6.65	1.00			1.50			1.50		

Appendix F. Sintered Density Measurements

Date 8/796 — V=7.552-6.288/(B3/C3-1)

Sample ID	P1	P2	V(sample)	Weight(g)	Density	Average density	Ave. Volume	% Theor.	Ave sample Den
100-1	19.614	10.412	0.437	1.730	3.957	3.96	0.437	99.4	3.951
	19.430	10.314	0.438	1.730	3.953	0.005			0.013
	19.666	10.440	0.437	1.730	3.962				
100-2	19.476	10.337	0.440	1.741	3.959	3.96	0.440	99.4	
	19.507	10.352	0.442	1.741	3.940	0.014			
	19.701	10.457	0.439	1.741	3.967				
100-3	19.506	10.355	0.437	1.718	3.934	3.95	0.435	99.2	
	19.609	10.411	0.435	1.718	3.952	0.012			
	19.578	10.395	0.434	1.718	3.958				
100-4	19.607	10.409	0.436	1.716	3.935	3.93	0.437	98.7	
	19.591	10.400	0.437	1.716	3.928	0.004			
	19.627	10.419	0.437	1.716	3.927				
100-5	19.587	10.400	0.434	1.712	3.947	3.96	0.432	99.6	
	19.774	10.501	0.431	1.712	3.969	0.015			
	19.489	10.350	0.431	1.712	3.974				

Date 8/796 — V=7.580-6.309/(B3/C3-1)

Sample ID	P1	P2	V(sample)	Weight(g)	Density	Average density	Ave. Volume	% Theor.	Ave sample Den
955-1	19.534	10.375	0.433	1.705	3.934	3.93	0.434	98.8	3.937
	19.539	10.377	0.434	1.705	3.925	0.006			0.007
	19.675	10.450	0.433	1.705	3.935				
955-2	19.511	10.360	0.437	1.721	3.935	3.95	0.436	99.2	
	19.536	10.374	0.436	1.721	3.944	0.015			
	19.616	10.418	0.434	1.721	3.965				
955-3	19.578	10.397	0.435	1.712	3.933	3.94	0.435	98.9	
	19.612	10.415	0.435	1.712	3.932	0.007			
	19.471	10.341	0.434	1.712	3.944				
955-4	19.635	10.425	0.439	1.728	3.938	3.94	0.439	98.9	
	19.595	10.403	0.440	1.728	3.928	0.007			
	19.548	10.379	0.438	1.728	3.940				
955-5	19.670	10.446	0.435	1.711	3.932	3.93	0.435	98.8	
	19.542	10.378	0.435	1.711	3.932	0.002			
	19.549	10.382	0.435	1.711	3.935				

Date 8/796 — V=7.580-6.309/(B3/C3-1)

Sample ID	P1	P2	V(sample)	Weight(g)	Density	Average density	Ave. Volume	% Theor.	Ave sample Den
001-1&2	19.425	10.463	0.214	0.874	4.076	4.12	0.212	103.5	4.058
	19.622	10.571	0.211	0.874	4.131	0.037			0.050
	19.569	10.543	0.211	0.874	4.147				
001-3	19.581	10.603	0.129	0.525	4.063	4.09	0.128	102.9	
	19.550	10.587	0.128	0.525	4.102	0.027			
	19.603	10.616	0.127	0.525	4.116				
001-4	19.544	10.579	0.135	0.544	4.021	4.06	0.134	102.1	
	19.523	10.568	0.135	0.544	4.038	0.060			
	19.571	10.596	0.132	0.544	4.133				

001-5b	19.523	10.486	0.259	1.033	3.983	4.00	0.258	100.6	
	19.567	10.511	0.257	1.033	4.015	0.018			
	19.459	10.453	0.257	1.033	4.015				
piece	19.537	10.585	0.120	0.474	3.946	4.01	0.118	100.8	
	19.602	10.622	0.117	0.474	4.038	0.057			
	19.537	10.587	0.117	0.474	4.049				
Date 8/8/96						V=7.559-6.290/(B3/C3-1)			
Sample ID	P1	P2	V(sample)	Weight(g)	Density	Average density	Ave. Volume	% Theor.	Ave sample Den
604-1	19.601	10.435	0.398	1.560	3.918	3.93	0.397	98.9	3.934
	19.636	10.455	0.396	1.560	3.938	0.015			0.023
	19.524	10.396	0.395	1.560	3.947				
604-2	19.575	10.419	0.401	1.568	3.907	3.91	0.401	98.2	
	19.712	10.492	0.401	1.568	3.908	0.005			
	19.587	10.426	0.400	1.568	3.915				
604-3	19.561	10.418	0.392	1.552	3.960	3.97	0.391	99.7	
	19.571	10.424	0.391	1.552	3.970	0.009			
	19.463	10.367	0.390	1.552	3.978				
604-4	19.587	10.425	0.402	1.574	3.916	3.92	0.401	98.5	
	19.580	10.421	0.402	1.574	3.912	0.011			
	19.611	10.439	0.400	1.574	3.933				
604-5	19.592	10.430	0.398	1.565	3.926	3.94	0.398	98.9	
	19.671	10.473	0.397	1.565	3.940	0.008			
	19.500	10.382	0.397	1.565	3.940				
Date 8/10/96						V=7.55-6.290/(B3/C3-1)			
Sample ID	P1	P2	V(sample)	Weight(g)	Density	Average density	Ave. Volume	% Theor.	Ave sample Den
613-1	19.591	10.417	0.408	1.610	3.948	3.95	0.408	99.3	3.926
	19.609	10.427	0.407	1.610	3.955	0.004			0.020
	19.576	10.409	0.408	1.610	3.948				
613-2	19.540	10.383	0.418	1.631	3.904	3.90	0.418	97.9	
	19.513	10.368	0.419	1.631	3.895	0.005			
	19.447	10.333	0.419	1.631	3.896				
613-3	19.608	10.423	0.412	1.612	3.911	3.92	0.411	98.6	
	19.632	10.437	0.410	1.612	3.928	0.010			
	19.583	10.411	0.410	1.612	3.929				
613-4	19.530	10.386	0.406	1.597	3.936	3.94	0.405	99.0	
	19.568	10.406	0.406	1.597	3.933	0.009			
	19.611	10.430	0.404	1.597	3.950				
613-5	19.548	10.391	0.412	1.608	3.900	3.92	0.410	98.5	
	19.513	10.373	0.411	1.608	3.9[illegible]	0.027			
	19.639	10.443	0.407	1.608	3.951				

Date 8/10/96						V=7.55-6.290/(B3/C3-1)			
Sample ID	P1	P2	V(sample)	Weight(g)	Density	Average density	Ave. Volume	% Theor.	Ave sample Den
622-1	19.507	10.364	0.420	1.646	3.918	3.92	0.420	98.5	3.914
	19.508	10.365	0.419	1.646	3.924	0.003			0.010
	19.550	10.387	0.420	1.646	3.920				
622-2	19.477	10.345	0.425	1.659	3.907	3.91	0.424	98.3	
	19.452	10.332	0.424	1.659	3.911	0.004			
	19.572	10.396	0.424	1.659	3.915				
622-3	19.546	10.383	0.423	1.643	3.889	3.90	0.422	97.9	
	19.469	10.343	0.421	1.643	3.901	0.008			
	19.525	10.373	0.421	1.643	3.904				
622-4	19.613	10.418	0.423	1.657	3.913	3.92	0.422	98.6	
	19.510	10.364	0.422	1.657	3.922	0.011			
	19.576	10.400	0.421	1.657	3.935				
622-5	19.514	10.366	0.423	1.650	3.906	3.92	0.421	98.5	
	19.554	10.388	0.421	1.650	3.916	0.014			
	19.529	10.376	0.420	1.650	3.934				

Date 8/10/96						V=7.558-6.297/(B3/C3-1)			
Sample ID	P1	P2	V(sample)	Weight(g)	Density	Average density	Ave. Volume	% Theor.	Ave sample Den
622-1	19.507	10.364	0.420	1.646	3.917	3.92	0.420	98.5	3.914
	19.508	10.365	0.419	1.646	3.924	0.003			0.010
	19.550	10.387	0.420	1.646	3.919				
622-2	19.477	10.345	0.425	1.659	3.907	3.91	0.424	98.3	
	19.452	10.332	0.424	1.659	3.911	0.004			
	19.572	10.396	0.424	1.659	3.914				
622-3	19.546	10.383	0.423	1.643	3.888	3.90	0.422	97.9	
	19.469	10.343	0.421	1.643	3.900	0.008			
	19.525	10.373	0.421	1.643	3.904				
622-4	19.613	10.418	0.423	1.657	3.912	3.92	0.422	98.6	
	19.510	10.364	0.422	1.657	3.922	0.011			
	19.576	10.400	0.421	1.657	3.935				
622-5	19.514	10.366	0.423	1.650	3.905	3.92	0.421	98.4	
	19.554	10.388	0.421	1.650	3.915	0.014			
	19.529	10.376	0.420	1.650	3.933				

Date 8/10/96						V=7.558-6.297/(B3/C3-1)			
Sample ID	P1	P2	V(sample)	Weight(g)	Density	Average density	Ave. Volume	% Theor.	Ave sample Den
631-1	19.503	10.354	0.432	1.690	3.915	3.92	0.431	98.6	3.892
	19.624	10.420	0.429	1.690	3.939	0.014			0.023
	19.539	10.373	0.432	1.690	3.914				
631-2	19.487	10.337	0.444	1.712	3.854	3.87	0.442	97.2	
	19.553	10.374	0.441	1.712	3.880	0.014			
	19.510	10.351	0.441	1.712	3.877				

631-3	19.510	10.356	0.434	1.684	3.879	3.89	0.433	97.7	
	19.587	10.397	0.434	1.684	3.881	0.013			
	19.452	10.327	0.432	1.684	3.902				
631-4	19.556	10.377	0.439	1.693	3.855	3.87	0.437	97.2	
	19.526	10.362	0.438	1.693	3.867	0.017			
	19.487	10.343	0.435	1.693	3.889				
631-5	19.485	10.346	0.429	1.673	3.897	3.91	0.428	98.2	
	19.536	10.374	0.428	1.673	3.909	0.012			
	19.508	10.360	0.427	1.673	3.921				
Date 8/10/96						V=7.558-6.297/(B3/C3-1)			
Sample ID	P1	P2	V(sample)	Weight(g)	Density	Average density	Ave. Volume	% Theor.	Ave sample Den
640-1	19.590	10.391	0.445	1.712	3.847	3.85	0.445	96.7	3.858
	19.479	10.332	0.445	1.712	3.846	0.006			0.009
	19.515	10.352	0.444	1.712	3.857				
640-2	19.586	10.388	0.446	1.723	3.861	3.86	0.447	96.9	
	19.590	10.390	0.446	1.723	3.860	0.003			
	19.553	10.370	0.447	1.723	3.855				
640-3	19.466	10.321	0.451	1.732	3.837	3.85	0.450	96.7	
	19.524	10.353	0.449	1.732	3.853	0.010			
	19.531	10.357	0.449	1.732	3.856				
640-4	19.457	10.316	0.452	1.741	3.855	3.86	0.451	97.0	
	19.473	10.325	0.451	1.741	3.862	0.006			
	19.525	10.353	0.450	1.741	3.867				
640-5	19.517	10.353	0.444	1.714	3.860	3.87	0.443	97.3	
	19.445	10.315	0.444	1.714	3.862	0.019			
	19.725	10.466	0.440	1.714	3.894				
Date 8/10/96						V=7.513-6.261/(B3/C3-1)			
Sample ID	P1	P2	V(sample)	Weight(g)	Density	Average density	Ave. Volume	% Theor.	Ave sample Den
640-1	19.590	10.391	0.441	1.712	3.885	3.89	0.440	97.7	3.896
	19.479	10.332	0.441	1.712	3.883	0.006			0.010
	19.515	10.352	0.440	1.712	3.895				
640-2	19.586	10.388	0.442	1.723	3.899	3.90	0.442	97.9	
	19.590	10.390	0.442	1.723	3.898	0.003			
	19.553	10.370	0.443	1.723	3.893				
640-3	19.466	10.321	0.447	1.732	3.875	3.89	0.446	97.7	
	19.524	10.353	0.445	1.732	3.891	0.010			
	19.531	10.357	0.445	1.732	3.894				
640-4	19.457	10.316	0.447	1.741	3.893	3.90	0.446	98.0	
	19.473	10.325	0.446	1.741	3.899	0.006			
	19.525	10.353	0.446	1.741	3.905				
640-5	19.517	10.353	0.440	1.714	3.898	3.91	0.438	98.2	
	19.445	10.315	0.439	1.714	3.900	0.019			
	19.725	10.466	0.436	1.714	3.932				

Date 8/10/96						V=7.513-6.261/(B3/C3-1)			
Sample ID	P1	P2	V(sample)	Weight(g)	Density	Average density	Ave. Volume	% Theor.	Ave sample Den
703-1	19.580	10.407	0.410	1.621	3.957	3.95	0.410	99.3	3.929
	19.600	10.417	0.411	1.621	3.948	0.005			0.016
	19.601	10.418	0.410	1.621	3.955				
703-2	19.561	10.395	0.413	1.607	3.897	3.92	0.410	98.4	
	19.503	10.366	0.410	1.607	3.922	0.017			
	19.549	10.391	0.409	1.607	3.930				
703-3	19.497	10.357	0.418	1.633	3.904	3.92	0.416	98.6	
	19.548	10.386	0.416	1.633	3.930	0.018			
	19.686	10.460	0.415	1.633	3.939				
703-4	19.643	10.437	0.415	1.623	3.913	3.92	0.414	98.4	
	19.561	10.394	0.414	1.623	3.920	0.004			
	19.511	10.367	0.415	1.623	3.914				
703-5	19.476	10.350	0.412	1.615	3.917	3.93	0.411	98.8	
	19.555	10.393	0.411	1.615	3.931	0.017			
	19.588	10.412	0.409	1.615	3.952				

Date 8/14/96						V=7.567-6.299/(B3/C3-1)			
Sample ID	P1	P2	V(sample)	Weight(g)	Density	Average density	Ave. Volume	% Theor.	Ave sample Den
730-1	19.607	10.407	0.442	1.714	3.881	3.88	0.442	97.5	3.904
	19.653	10.431	0.442	1.714	3.875	0.004			0.017
	19.601	10.404	0.441	1.714	3.883				
730-2	19.601	10.404	0.441	1.731	3.923	3.92	0.441	98.6	
	19.627	10.418	0.441	1.731	3.926	0.003			
	19.530	10.366	0.442	1.731	3.919				
730-3	19.510	10.354	0.444	1.730	3.898	3.91	0.443	98.2	
	19.636	10.422	0.442	1.730	3.913	0.008			
	19.467	10.332	0.443	1.730	3.909				
730-4	19.655	10.432	0.442	1.723	3.894	3.89	0.442	97.8	
	19.522	10.361	0.443	1.723	3.889	0.004			
	19.602	10.404	0.442	1.723	3.896				
730-5	19.539	10.370	0.443	1.734	3.914	3.92	0.443	98.4	
	19.597	10.401	0.443	1.734	3.917	0.003			
	19.476	10.337	0.442	1.734	3.920				

Date 8/15/96						V=7.552-6.291/(B3/C3-1)			
Sample ID	P1	P2	V(sample)	Weight(g)	Density	Average density	Ave. Volume	% Theor.	Ave sample Den
721-1	19.596	10.406	0.429	1.689	3.940	3.94	0.429	99.0	3.936
	19.590	10.402	0.430	1.689	3.929	0.010			0.015
	19.508	10.360	0.428	1.689	3.950				
721-3	19.532	10.371	0.430	1.692	3.934	3.94	0.429	99.1	
	19.554	10.383	0.430	1.692	3.938	0.015			
	19.564	10.390	0.427	1.692	3.961				
721-2	19.476	10.343	0.428	1.678	3.925	3.93	0.427	98.7	
	19.480	10.345	0.428	1.678	3.923	0.009			
	19.538	10.377	0.426	1.678	3.940				

721-4	19.494	10.353	0.427	1.679	3.934	3.95	0.425	99.3	
	19.608	10.415	0.425	1.679	3.954	0.017			
	19.431	10.322	0.423	1.679	3.968				
721-5	19.556	10.383	0.431	1.690	3.919	3.91	0.432	98.3	
	19.459	10.331	0.432	1.690	3.912	0.006			
	19.599	10.405	0.432	1.690	3.908				
Date 8/15/96						V=7.581-6.31/(B3/C3-1)			
Sample ID	P1	P2	V(sample)	Weight(g)	Density	Average density	Ave. Volume	% Theor.	Ave sample Den
712-1	19.549	10.390	0.423	1.651	3.905	3.92	0.421	98.5	3.913
	19.543	10.388	0.421	1.651	3.921	0.016			0.011
	19.601	10.420	0.419	1.651	3.937				
712-2	19.561	10.395	0.425	1.660	3.907	3.92	0.424	98.4	
	19.552	10.391	0.424	1.660	3.917	0.009			
	19.583	10.408	0.423	1.660	3.924				
712-3	19.624	10.435	0.415	1.619	3.898	3.89	0.416	97.8	
	19.478	10.357	0.416	1.619	3.893	0.003			
	19.529	10.384	0.416	1.619	3.891				
712-4	19.570	10.402	0.422	1.654	3.922	3.92	0.422	98.5	
	19.581	10.407	0.423	1.654	3.911	0.010			
	19.565	10.400	0.421	1.654	3.931				
712-5	19.575	10.404	0.423	1.649	3.902	3.91	0.422	98.3	
	19.457	10.342	0.422	1.649	3.912	0.010			
	19.546	10.390	0.421	1.649	3.921				
Date 8/16/96						V=7.525-6.258/(B3/C3-1)			
Sample ID	P1	P2	V(sample)	Weight(g)	Density	Average density	Ave. Volume	% Theor.	Ave sample Den
N802-1	19.568	10.402	0.423	1.642	3.881	3.89	0.422	97.9	3.879
	19.547	10.392	0.421	1.642	3.897	0.012			0.015
	19.433	10.332	0.421	1.642	3.905				
N802-2	19.564	10.398	0.426	1.645	3.864	3.88	0.424	97.5	
	19.573	10.404	0.424	1.645	3.880	0.014			
	19.543	10.389	0.423	1.645	3.893				
N802-3	19.533	10.384	0.422	1.628	3.855	3.86	0.421	97.1	
	19.560	10.399	0.421	1.628	3.864	0.010			
	19.487	10.361	0.420	1.628	3.875				
Date 8/16/96						V=7.525-6.258/(B3/C3-1)			
Sample ID	P1	P2	V(sample)	Weight(g)	Density	Average density	Ave. Volume	% Theor.	Ave sample Den
802-2	19.540	10.389	0.420	1.639	3.899	3.91	0.419	98.3	3.902
	19.551	10.396	0.419	1.639	3.915	0.011			0.015
	19.520	10.380	0.418	1.639	3.922				
802-4	19.485	10.356	0.426	1.652	3.879	3.89	0.424	97.8	
	19.462	10.344	0.426	1.652	3.882	0.019			
	19.529	10.382	0.422	1.652	3.914				
Date 8/17/96						V=7.530-6.269/(B3/C3-1)			
Sample ID	P1	P2	V(sample)	Weight(g)	Density	Average density	Ave. Volume	% Theor.	Ave sample Den
o10-1	19.506	10.356	0.435	1.705	3.923	3.93	0.434	98.7	3.917
	19.460	10.332	0.434	1.705	3.929	0.003			0.016
	19.494	10.350	0.434	1.705	3.928				

o10-2	19.541	10.370	0.441	1.729	3.917	3.92	0.441	98.5	
	19.467	10.331	0.441	1.729	3.920	0.006			
	19.447	10.321	0.440	1.729	3.928				
o10-3	19.461	10.331	0.436	1.708	3.914	3.92	0.435	98.6	
	19.537	10.372	0.435	1.708	3.922	0.010			
	19.524	10.366	0.434	1.708	3.934				
o10-4	19.489	10.345	0.438	1.715	3.919	3.93	0.437	98.6	
	19.540	10.373	0.436	1.715	3.932	0.006			
	19.494	10.348	0.437	1.715	3.924				
o10-5	19.484	10.339	0.442	1.716	3.878	3.89	0.441	97.7	
	19.469	10.332	0.441	1.716	3.891	0.008			
	19.525	10.362	0.441	1.716	3.894				

Date 8/17/96 — **V=7.530-6.269/(B3/C3-1)**

Sample ID	P1	P2	V(sample)	Weight(g)	Density	Average density	Ave. Volume	% Theor.	Ave sample Den
F100.	19.490	10.412	0.340	1.355	3.988	4.01	0.338	100.9	
	19.516	10.428	0.337	1.355	4.025	0.024			
	19.461	10.399	0.336	1.355	4.032				

Appendix G. Preliminary Powder Processing Data

PRELIMINARY POWDER PROCESSING TEST RUNS

During the initial determination of the mixing procedure to be used in this evaluation three different changes were made. A sample mixture containing 80% coarse and 20% fine material was used to evaluate various ways to minimize segregation during the drying process. Initially a sample was dried to a constant weight in a shallow pan at 45°C. This is below the melting point of the binder. This dried material, sample #802, appeared to show signs of segregation. It looked like a bed of white powder with a shiny off-white flaky material on top. In an attempt to minimize segregation, the next sample, #N802, was made using a higher solids content in the slurry. A final sample was produced using the increased solids procedure and also increasing the drying temperature to 95°C, to speed up the drying process. This sample was #N2802. This last process was used for all subsequent mixtures made in this study. Variations in measured characteristics between these three materials are shown in Table VIII.

From a comparison of the green densities obtained from the three samples shown in Table VIII, it appears as though each successive change may have contributed to an improvement in "mixedness" of the materials. This shows how important processing is in the resulting character of the product.

Table G-1 Effect of Process on Measured Characteristics

Sample ID	Tap Density	Green Density	Sintered Density	Shrinkage %
802	1.51 (0.00)	2.37 (0.005)	3.902 (0.015)	33.0 (0.42)
N802	1.50 (0.00)	2.39 (0.009)	3.879 (0.015)	32.5 (0.70)
N2802	1.57 (0.02)	2.42 (0.016)	3.929 (0.012)	32.6 (0.85)

The data in parentheses are standard deviations.

Appendix H. Pycnometer Calibration Records

7/20/96										
V_{calib5}										
Calibration Sample: Ball Bearing										
p1	p2	c	p1*	p2*	d-e	c*e	f-g	Vcell (cc)	Vexp (cc)
19.7	10.756	0.831536	19.651	10.125	9.526	8.419301	1.106699	7.556593	6.283579
19.654	10.732	0.831346	19.685	10.142	9.543	8.431506	1.111494	7.537423	6.266203
19.709	10.761	0.831521	19.606	10.102	9.504	8.400028	1.103972	7.557762	6.28444
19.743	10.78	0.831447	19.751	10.176	9.575	8.460806	1.114194	7.54437	6.272745
19.788	10.806	0.831205	19.449	10.020	9.429	8.328673	1.100327	7.522963	6.253123
							Average:	**7.544**	**6.272**
							Std. Dev.:	**0.014**	**0.013**
								0.001914	0.002078
7/20/96									
V_{calib5}									
Calibration Sample: Ball Bearing									
p1	p2	c	p1*	p2*	d-e	c*e	f-g	Vcell (cc)	Vexp (cc)
19.715	10.755	0.833101	19.618	10.102	9.516	8.415985	1.100015	7.59453	6.32701
19.504	10.64	0.833083	19.536	10.060	9.476	8.380812	1.095188	7.595938	6.328045
19.633	10.711	0.832975	19.671	10.128	9.543	8.436375	1.106625	7.570588	6.306114
19.592	10.689	0.832912	19.448	10.013	9.435	8.339951	1.095049	7.564035	6.300178
19.457	10.614	0.833145	19.594	10.088	9.506	8.404766	1.101234	7.578149	6.313697
							Average:	**7.581**	**6.315**
							Std. Dev.:	**0.014**	**0.012**
								0.001877	0.001963
7/30/96									
V_{calib5}									
Calibration Sample: Ball Bearing									
p1	p2	c	p1*	p2*	d-e	c*e	f-g	Vcell (cc)	Vexp (cc)
19.527	10.659	0.831973	19.691	10.142	9.549	8.437870	1.111130	7.544632	6.27693
19.627	10.714	0.831902	19.689	10.141	9.548	8.436320	1.111680	7.54011	6.272634
19.622	10.711	0.831948	19.521	10.053	9.468	8.363578	1.104422	7.526069	6.261302
19.623	10.712	0.831871	19.592	10.090	9.502	8.393576	1.108424	7.525828	6.260517
19.739	10.776	0.831756	19.697	10.145	9.552	8.438162	1.113838	7.528655	6.262002
							Average:	**7.533**	**6.267**
							Std. Dev.:	**0.009**	**0.008**
								0.001158	0.001208
7/31/96									
V_{calib5}									
Calibration Sample: Ball Bearing									
p1	p2	c	p1*	p2*	d-e	c*e	f-g	Vcell (cc)	Vexp (cc)
19.542	10.657	0.833724	19.628	10.099	9.529	8.419782	1.109218	7.541807	6.287788
19.665	10.723	0.833908	19.485	10.024	9.461	8.359098	1.101902	7.537705	6.285756
19.706	10.747	0.833628	19.709	10.140	9.569	8.452988	1.116012	7.52736	6.275018
19.324	10.537	0.833919	19.661	10.115	9.546	8.435086	1.110914	7.543731	6.290857
19.622	10.701	0.83366	19.711	10.142	9.569	8.454984	1.114016	7.540847	6.286505
							Average:	**7.538**	**6.285**
							Std. Dev.:	**0.006**	**0.006**
								0.000861	0.000956

8/1/96									
V_{calib5}									
Calibration Sample: Ball Bearing									
p1	p2	c	p1*	p2*	d-e	c*e	f-g	Vcell (cc)	Vexp (cc)
19.7	10.748	0.832899	19.439	10.007	9.432	8.334822	1.097178	7.546953	6.285851
19.531	10.655	0.833036	19.547	10.062	9.485	8.382010	1.102990	7.549369	6.288897
19.386	10.575	0.833191	19.402	9.987	9.415	8.321083	1.093917	7.555812	6.295439
19.592	10.689	0.832912	19.436	10.005	9.431	8.333288	1.097712	7.542483	6.282228
19.643	10.717	0.832882	19.638	10.110	9.528	8.420440	1.107560	7.552308	6.290184
							Average:	**7.549**	**6.289**
							Std. Dev.:	**0.005**	**0.005**
								0.000673	0.000785
8/3/96									
V_{calib5}									
Calibration Sample: Ball Bearing									
p1	p2	c	p1*	p2*	d-e	c*e	f-g	Vcell (cc)	Vexp (cc)
19.611	10.699	0.832975	19.487	10.028	9.459	8.353074	1.105926	7.508689	6.25455
19.632	10.71	0.833053	19.550	10.061	9.489	8.381348	1.107652	7.520771	6.265202
19.668	10.731	0.832821	19.548	10.061	9.487	8.379010	1.107990	7.516889	6.260221
19.389	10.577	0.833128	19.660	10.120	9.540	8.431260	1.108740	7.553771	6.293262
19.671	10.731	0.8331	19.652	10.115	9.537	8.426810	1.110190	7.541532	6.282853
							Average:	**7.528**	**6.271**
							Std. Dev.:	**0.019**	**0.016**
								0.002481	0.002591
8/3/96									
V_{calib5}									
Calibration Sample: Ball Bearing									
p1	p2	c	p1*	p2*	d-e	c*e	f-g	Vcell (cc)	Vexp (cc)
19.557	10.666	0.833583	19.476	10.024	9.452	8.355839	1.096161	7.569978	6.310208
19.539	10.657	0.833443	19.414	9.991	9.423	8.326927	1.096073	7.547355	6.290289
19.549	10.662	0.833521	19.527	10.050	9.477	8.376885	1.100115	7.562718	6.303684
19.629	10.706	0.833458	19.483	10.028	9.455	8.357916	1.097084	7.566003	6.305945
19.594	10.688	0.833271	19.432	10.000	9.432	8.332710	1.099290	7.532452	6.276574
							Average:	**7.556**	**6.297**
							Std. Dev.:	**0.016**	**0.014**
								0.00206	0.00219
8/7/96									
V_{calib5}									
Calibration Sample: Ball Bearing									
p1	p2	c	p1*	p2*	d-e	c*e	f-g	Vcell (cc)	Vexp (cc)
19.655	10.724	0.832805	19.602	10.093	9.509	8.405500	1.103500	7.564977	6.30015
19.728	10.764	0.832776	19.532	10.056	9.476	8.374395	1.101605	7.551688	6.288864
19.613	10.703	0.832477	19.487	10.033	9.454	8.352240	1.101760	7.533102	6.271133
19.741	10.773	0.832451	19.597	10.091	9.506	8.400268	1.105732	7.547324	6.282781
19.522	10.653	0.832535	19.605	10.096	9.509	8.405278	1.103722	7.563453	6.296843
							Average:	**7.552**	**6.288**
							Std. Dev.:	**0.013**	**0.012**
								0.001725	0.001845

8/7/96									
V_{calib5}									
Calibration Sample: Ball Bearing									
p1	p2	c	p1*	p2*	d-e	c*e	f-g	Vcell (cc)	Vexp (cc)
19.707	10.754	0.832527	19.504	10.046	9.458	8.363571	1.094429	7.586764	6.31619
19.476	10.628	0.832518	19.657	10.125	9.532	8.429244	1.102756	7.588387	6.317468
19.631	10.714	0.832276	19.571	10.080	9.491	8.389337	1.101663	7.563249	6.294707
19.604	10.699	0.832321	19.533	10.061	9.472	8.373979	1.098021	7.573144	6.303285
19.482	10.632	0.832393	19.452	10.020	9.432	8.340576	1.091424	7.58674	6.315147
							Average:	**7.580**	**6.309**
							Std. Dev.:	**0.011**	**0.010**
								0.001458	0.00158
8/8/96									
V_{calib5}									
Calibration Sample: Ball Bearing									
p1	p2	c	p1*	p2*	d-e	c*e	f-g	Vcell (cc)	Vexp (cc)
19.575	10.683	0.83235	19.598	10.094	9.504	8.401746	1.102254	7.569542	6.300512
19.734	10.771	0.832142	19.456	10.021	9.435	8.338894	1.096106	7.556736	6.288276
19.724	10.766	0.832064	19.546	10.067	9.479	8.376387	1.102613	7.547178	6.279734
19.595	10.695	0.832165	19.589	10.090	9.499	8.396540	1.102460	7.564152	6.29462
19.45	10.616	0.83214	19.621	10.106	9.515	8.409609	1.105391	7.556796	6.288314
							Average:	**7.559**	**6.290**
							Std. Dev.:	**0.008**	**0.008**
								0.001121	0.001238
8/10/96									
V_{calib5}									
Calibration Sample: Ball Bearing									
p1	p2	c	p1*	p2*	d-e	c*e	f-g	Vcell (cc)	Vexp (cc)
19.759	10.78	0.832931	19.569	10.073	9.496	8.390118	1.105882	7.538358	6.278935
19.564	10.672	0.833208	19.594	10.086	9.508	8.403740	1.104260	7.558974	6.2982
19.525	10.651	0.833161	19.513	10.044	9.469	8.368271	1.100729	7.552119	6.292132
							Average:	**7.550**	**6.290**
							Std. Dev.:	**0.010**	**0.010**
								0.001391	0.001566
8/10/96									
V_{calib5}									
Calibration Sample: Ball Bearing									
p1	p2	c	p1*	p2*	d-e	c*e	f-g	Vcell (cc)	Vexp (cc)
19.588	10.684	0.833396	19.542	10.060	9.482	8.383961	1.098039	7.581013	6.317984
19.66	10.725	0.8331	19.421	9.996	9.425	8.327670	1.097330	7.540309	6.281833
19.403	10.585	0.833066	19.704	10.143	9.561	8.449785	1.111215	7.553535	6.292591
							Average:	**7.558**	**6.297**
							Std. Dev.:	**0.021**	**0.019**
								0.002747	0.002948

8/10/96 after power failure

V_{calib5}

Calibration Sample: Ball Bearing

p1	p2	c	p1*	p2*	d-e	c*e	f-g	Vcell (cc)	Vexp (cc)
19.604	10.692	0.83352	19.470	10.017	9.453	8.349374	1.103626	7.519564	6.26771
19.786	10.794	0.833055	19.553	10.060	9.493	8.380537	1.112463	7.491402	6.240753
19.424	10.594	0.833491	19.581	10.075	9.506	8.397418	1.108582	7.527923	6.274454
							Average:	**7.513**	**6.261**
							Std. Dev.:	**0.019**	**0.018**
								0.002547	0.002848

8/14/96

V_{calib5}

Calibration Sample: Ball Bearing

p1	p2	c	p1*	p2*	d-e	c*e	f-g	Vcell (cc)	Vexp (cc)
19.746	10.776	0.832405	19.518	10.052	9.466	8.367339	1.098661	7.563933	6.296258
19.62	10.707	0.832446	19.507	10.045	9.462	8.361921	1.100079	7.550992	6.285793
19.611	10.702	0.832461	19.624	10.108	9.516	8.414518	1.101482	7.584415	6.313731
19.611	10.703	0.83229	19.580	10.085	9.495	8.393645	1.101355	7.568549	6.299227
19.526	10.656	0.832395	19.554	10.071	9.483	8.383049	1.099951	7.568633	6.300092
							Average:	**7.567**	**6.299**
							Std. Dev.:	**0.012**	**0.010**
								0.001582	0.001588

8/15/96

V_{calib5}

Calibration Sample: Ball Bearing

p1	p2	c	p1*	p2*	d-e	c*e	f-g	Vcell (cc)	Vexp (cc)
19.678	10.735	0.833069	19.521	10.048	9.473	8.370681	1.102319	7.544412	6.285019
19.691	10.742	0.833085	19.493	10.034	9.459	8.359176	1.099824	7.550348	6.290083
19.404	10.585	0.83316	19.524	10.050	9.474	8.373259	1.100741	7.556026	6.295379
19.484	10.63	0.832926	19.611	10.096	9.515	8.409218	1.105782	7.554126	6.292025
19.542	10.661	0.833036	19.560	10.069	9.491	8.387843	1.103157	7.553	6.291923
							Average:	**7.552**	**6.291**
							Std. Dev.:	**0.005**	**0.004**
								0.000596	0.000603

8/15/96

V_{calib5}

Calibration Sample: Ball Bearing

p1	p2	c	p1*	p2*	d-e	c*e	f-g	Vcell (cc)	Vexp (cc)
19.61	10.7	0.83271	19.553	10.071	9.482	8.386225	1.095775	7.596678	6.325832
19.665	10.733	0.8322	19.412	10.001	9.411	8.322830	1.088170	7.592486	6.318465
19.551	10.67	0.832334	19.542	10.066	9.476	8.378270	1.097730	7.578352	6.307717
19.52	10.653	0.832348	19.489	10.038	9.451	8.355106	1.095894	7.571019	6.30172
19.521	10.654	0.83227	19.553	10.071	9.482	8.381787	1.100213	7.566032	6.296978
							Average:	**7.581**	**6.310**
							Std. Dev.:	**0.013**	**0.012**
								0.001755	0.001884

8/16/96

V_{calib5}

Calibration Sample: Ball Bearing

p1	p2	c	p1*	p2*	d-e	c*e	f-g	Vcell (cc)	Vexp (cc)
19.629	10.717	0.831576	19.553	10.071	9.482	8.374802	1.107198	7.5183	6.252038
19.515	10.654	0.831706	19.412	10.001	9.411	8.317896	1.093104	7.558215	6.286216
19.619	10.712	0.831497	19.542	10.066	9.476	8.369853	1.106147	7.52068	6.253426
19.531	10.663	0.831661	19.489	10.038	9.451	8.348212	1.102788	7.523688	6.257157
19.574	10.688	0.8314	19.553	10.071	9.482	8.373026	1.108974	7.506263	6.240705
							Average:	**7.525**	**6.258**
							Std. Dev.:	**0.019**	**0.017**
								0.002589	0.002712

8/17/96

V_{calib5}

Calibration Sample: Ball Bearing

p1	p2	c	p1*	p2*	d-e	c*e	f-g	Vcell (cc)	Vexp (cc)
19.493	10.636	0.832738	19.512	10.045	9.467	8.364852	1.102148	7.540801	6.279511
19.505	10.644	0.832488	19.589	10.085	9.504	8.395639	1.108361	7.52784	6.266835
19.462	10.62	0.83258	19.530	10.055	9.475	8.371592	1.103408	7.538557	6.276452
19.524	10.655	0.832379	19.462	10.020	9.442	8.340439	1.101561	7.524897	6.263568
19.596	10.695	0.832258	19.483	10.031	9.452	8.348381	1.103619	7.518816	6.257595
							Average:	**7.530**	**6.269**
							Std. Dev.:	**0.009**	**0.009**
								0.001234	0.001449

Appendix I. Shrinkage Data

Sample ID	diameter	height	weight	volume	density	ave. den.	Sample ID	diameter	height	weight	volume	density	ave. den.	% shrink	Temp(C)
820-1	1.272	0.572	1.802	0.727	2.479	2.47	820-1	1.128	0.519	1.739	0.519	3.353	3.53	28.6	
820-2	1.275	0.561	1.768	0.716	2.468	0.009	820-2	1.127	0.501	1.711	0.500	3.424	0.155	30.2	
820-3	1.274	0.568	1.781	0.724	2.460		820-3	1.114	0.505	1.721	0.492	3.500		32.1	
820-4	1.275	0.569	1.787	0.726	2.460		820-4	1.095	0.496	1.728	0.467	3.700		35.7	
820-5	1.274	0.569	1.783	0.725	2.458		820-5	1.100	0.492	1.722	0.468	3.683		35.5	1040
730-1	1.275	0.562	1.789	0.718	2.493	2.48	730-1	1.120	0.497	1.725	0.489	3.525	3.50	31.8	1022
730-2	1.275	0.560	1.771	0.715	2.477	0.011	730-2	1.124	0.492	1.703	0.488	3.488	0.025	31.7	914
730-3	1.275	0.565	1.791	0.721	2.483		730-3	1.118	0.506	1.726	0.496	3.477		31.2	978
730-4	1.275	0.570	1.797	0.728	2.469		730-4								
730-5	1.277	0.568	1.793	0.727	2.465		730-5								
640-1	1.275	0.565	1.793	0.721	2.486	2.49	640-1	1.113	0.500	1.729	0.486	3.554	3.53	32.6	996
640-2	1.277	0.560	1.789	0.717	2.494	0.007	640-2	1.119	0.501	1.730	0.493	3.511	0.022	31.3	1022
640-3	1.275	0.569	1.810	0.726	2.491		640-3	1.117	0.507	1.753	0.497	3.528		31.6	958
640-4	1.275	0.560	1.790	0.715	2.504		640-4								
640-5	1.275	0.558	1.774	0.712	2.490		640-5								
100-1	1.275	0.583	1.800	0.744	2.418	2.42	100-1	1.121	0.524	1.748	0.517	3.383	3.36	30.6	942
100-2	1.276	0.575	1.775	0.735	2.414	0.012	100-2	1.124	0.517	1.720	0.512	3.358	0.016	30.3	954
100-3	1.274	0.569	1.770	0.725	2.440		100-3	1.128	0.512	1.716	0.512	3.352		29.4	956
100-4	1.274	0.583	1.794	0.743	2.414		100-4								
100-5	1.275	0.573	1.780	0.732	2.433		100-5								
O10-1	1.275	0.574	1.800	0.733	2.456	2.46	O10-1	1.084	0.497	1.726	0.459	3.761	3.74	37.4	910
O10-2	1.275	0.563	1.780	0.719	2.476	0.010	O10-2	1.086	0.495	1.707	0.459	3.721	0.020	36.2	938
O10-3	1.275	0.568	1.782	0.725	2.457		O10-3	1.084	0.494	1.707	0.456	3.746		37.2	950
O10-4	1.275	0.559	1.756	0.714	2.460		O10-4								
O10-5	1.275	0.569	1.780	0.726	2.450		O10-5								
802-1	1.276	0.584	1.772	0.747	2.373	2.37	802-1	1.143	0.534	1.631	0.548	2.977	2.96	26.6	968
802-2	1.275	0.589	1.787	0.752	2.376	0.005	802-2*	1.107	0.521	1.639	0.501	3.269	0.179	33.3	
802-3	1.275	0.594	1.792	0.758	2.363		802-3	1.144	0.546	1.652	0.561	2.944		26.0	984
802-4	1.278	0.591	1.795	0.758	2.368		802-4*	1.107	0.530	1.653	0.510	3.241		32.7	
802-5	1.277	0.583	1.767	0.747	2.366		802-5								

Sample ID	diameter	height	weight	volume	density	ave. den.	Sample ID	diameter	height	weight	volume	density	ave. den.	% shrink	
820-1R	1.272	0.568	1.788	0.722	2.477	2.47	820-1R	1.118	0.509	1.730	0.500	3.462	3.37	30.8	874
820-2R	1.273	0.558	1.766	0.710	2.487	0.015	820-2R	1.129	0.509	1.704	0.510	3.344	0.077	28.3	922
820-3R	1.275	0.572	1.801	0.730	2.466		820-3R	1.136	0.517	1.739	0.524	3.319		28.2	874
820-4R	1.275	0.568	1.775	0.725	2.448		820-4R								
820-5R	1.277	0.564	1.779	0.722	2.463		820-5R								
N802-1	1.275	0.588	1.790	0.751	2.384	2.39	N802-1	1.108	0.520	1.643	0.501	3.277	3.24	33.2	
N802-2	1.276	0.589	1.794	0.753	2.382	0.009	N802-2	1.108	0.533	1.646	0.514	3.203	0.037	31.8	
N802-3	1.275	0.584	1.774	0.746	2.379		N802-3	1.109	0.521	1.628	0.503	3.235		32.5	
N802-4	1.275	0.587	1.785	0.749	2.382										
N802-5	1.276	0.584	1.794	0.747	2.402										
Sample ID	diameter	height	weight	volume	density	ave. den.	Sample ID	diameter	height	weight	volume	density	ave. den.	% shrink	ave%shrink
N2802-1	1.275	0.583	1.788	0.744	2.402	2.42	N2802-1	1.106	0.519	1.644	0.499	3.297	3.32	33.0	32.60
N2802-2	1.276	0.578	1.781	0.739	2.410	0.016	N2802-2	1.104	0.511	1.643	0.489	3.359	0.029	33.8	0.852
N2802-3	1.275	0.572	1.775	0.730	2.430		N2802-3	1.103	0.523	1.640	0.500	3.282		31.6	
N2802-4	1.275	0.571	1.777	0.729	2.437		N2802-4	1.105	0.515	1.639	0.494	3.319		32.3	
N2802-5	1.275	0.572	1.779	0.730	2.436		N2802-5	1.101	0.519	1.642	0.494	3.323		32.3	
811-1	1.275	0.559	1.782	0.714	2.497	2.51	811-1	1.115	0.498	1.683	0.486	3.461	3.44	31.9	31.04
811-2	1.276	0.548	1.775	0.701	2.533	0.015	811-2	1.116	0.499	1.673	0.488	3.428	0.031	30.3	0.737
811-3	1.275	0.557	1.782	0.711	2.506		811-3	1.117	0.506	1.681	0.496	3.390		30.3	
811-4	1.275	0.561	1.795	0.716	2.506		811-4	1.114	0.502	1.695	0.489	3.464		31.7	
811-5	1.275	0.557	1.796	0.711	2.525		811-5	1.112	0.505	1.694	0.490	3.454		31.0	
712-1	1.275	0.579	1.790	0.739	2.421	2.44	712-1	1.108	0.511	1.651	0.493	3.351	3.36	33.3	32.85
712-2	1.275	0.574	1.795	0.733	2.449	0.013	712-2	1.107	0.511	1.660	0.492	3.375	0.016	32.9	0.378
712-3	1.275	0.560	1.748	0.715	2.445		712-3	1.107	0.503	1.619	0.484	3.344		32.3	
712-4	1.275	0.570	1.787	0.728	2.455		712-4	1.106	0.509	1.654	0.489	3.382		32.8	
712-5	1.275	0.572	1.782	0.730	2.440		712-5	1.107	0.509	1.649	0.490	3.366		32.9	
721-1	1.275	0.550	1.789	0.702	2.548	2.55	721-1	1.114	0.491	1.689	0.479	3.529	3.50	31.8	31.17
721-2	1.275	0.545	1.778	0.696	2.555	0.012	721-2	1.114	0.492	1.678	0.480	3.499	0.018	31.1	0.532
721-3	1.275	0.548	1.791	0.700	2.560		721-3	1.116	0.497	1.692	0.486	3.480		30.5	
721-4	1.275	0.549	1.777	0.701	2.535		721-4	1.111	0.495	1.679	0.480	3.499		31.5	
721-5	1.273	0.548	1.790	0.697	2.566		721-5	1.116	0.493	1.690	0.482	3.504		30.9	

Sample ID	diameter	height	weight	volume	density	ave. den.	Sample ID	diameter	height	weight	volume	density	ave. den.	% shrink	ave%shrink
631-1	1.275	0.552	1.791	0.705	2.541	2.54	631-1	1.112	0.497	1.691	0.483	3.503	3.55	31.5	32.51
631-2	1.275	0.562	1.812	0.718	2.525	0.012	631-2	1.107	0.495	1.712	0.476	3.593	0.035	33.6	0.812
631-3	1.275	0.553	1.781	0.706	2.522		631-3	1.112	0.491	1.685	0.477	3.534		32.5	
631-4	1.275	0.553	1.791	0.706	2.537		631-4	1.108	0.491	1.692	0.473	3.574		32.9	
631-5	1.275	0.543	1.770	0.693	2.553		631-5	1.109	0.488	1.673	0.471	3.549		32.0	
622-1	1.275	0.579	1.781	0.739	2.409	2.42	622-1	1.098	0.510	1.645	0.483	3.406	3.39	34.7	34.19
622-2	1.276	0.578	1.792	0.739	2.424	0.006	622-2	1.100	0.515	1.658	0.489	3.388	0.020	33.8	0.543
622-3	1.278	0.576	1.781	0.739	2.410		622-3	1.098	0.509	1.646	0.482	3.415		34.8	
622-4	1.275	0.581	1.794	0.742	2.418		622-4	1.102	0.517	1.658	0.493	3.362		33.5	
622-5	1.275	0.579	1.786	0.739	2.416		622-5	1.100	0.512	1.651	0.487	3.393		34.2	
613-1	1.275	0.593	1.775	0.757	2.344	2.34	613-1	1.089	0.522	1.611	0.486	3.313	3.30	35.8	35.82
613-2	1.275	0.602	1.803	0.769	2.346	0.011	613-2	1.092	0.522	1.631	0.489	3.336	0.029	36.4	0.401
613-3	1.278	0.590	1.783	0.757	2.356		613-3	1.089	0.521	1.613	0.485	3.324		35.9	
613-4	1.276	0.594	1.767	0.760	2.326		613-4	1.091	0.522	1.597	0.488	3.273		35.8	
613-5	1.276	0.594	1.780	0.760	2.343		613-5	1.092	0.525	1.610	0.492	3.274		35.3	
955-1	1.275	0.558	1.782	0.712	2.501	2.50	955-1	1.111	0.498	1.705	0.483	3.532	3.54	32.2	32.34
955-2	1.275	0.561	1.793	0.716	2.503	0.009	955-2	1.107	0.501	1.721	0.482	3.569	0.021	32.7	0.433
955-3	1.275	0.560	1.785	0.715	2.497		955-3	1.111	0.503	1.713	0.488	3.513		31.8	
955-4	1.275	0.568	1.801	0.725	2.483		955-4	1.109	0.504	1.728	0.487	3.549		32.9	
955-5	1.275	0.557	1.783	0.711	2.507		955-5	1.111	0.498	1.711	0.483	3.544		32.1	
100-4	1.275	0.581	1.790	0.742	2.413	2.41	100-4	1.105	0.515	1.738	0.494	3.519	3.52	33.4	33.56
100-5	1.275	0.578	1.778	0.738	2.409	0.003	100-5	1.103	0.512	1.723	0.489	3.522	0.002	33.7	0.201
O10-4	1.275	0.563	1.751	0.719	2.436	2.44	O10-4	1.085	0.488	1.683	0.451	3.730	3.73	37.2	37.24
O10-5	1.275	0.569	1.775	0.726	2.443	0.005	O10-5	1.084	0.494	1.703	0.456	3.735	0.004	37.2	0.010
730r-1	1.275	0.558	1.772	0.712	2.487	2.50	730r-1	1.101	0.498	1.714	0.474	3.615	3.64	33.4	33.45
730r-2	1.275	0.561	1.790	0.716	2.499	0.011	730r-2	1.103	0.496	1.732	0.474	3.654	0.015	33.8	0.358
730r-3	1.275	0.559	1.791	0.714	2.509		730r-3	1.101	0.500	1.731	0.476	3.636		33.3	
730r-4	1.275	0.559	1.783	0.714	2.498		730r-4	1.102	0.496	1.723	0.473	3.642		33.7	
730r-5	1.275	0.558	1.793	0.712	2.517		730r-5	1.102	0.501	1.734	0.478	3.629		32.9	

Sample ID	diameter	height	weight	volume	density	ave. den.	Sample ID	diameter	height	weight	volume	density	ave. den.	% shrink	ave%shrink
703-1	1.275	0.598	1.793	0.764	2.348	2.35	703-1	1.094	0.531	1.622	0.499	3.250	3.27	34.6	34.99
703-2	1.278	0.589	1.778	0.756	2.353	0.012	703-2	1.093	0.523	1.607	0.491	3.275	0.013	35.1	0.331
703-3	1.276	0.603	1.807	0.771	2.343		703-3	1.091	0.533	1.634	0.498	3.279		35.4	
703-4	1.275	0.594	1.793	0.758	2.364		703-4	1.091	0.530	1.623	0.495	3.276		34.7	
703-5	1.277	0.598	1.786	0.766	2.332		703-5	1.095	0.527	1.616	0.496	3.256		35.2	
604-1	1.281	0.594	1.765	0.766	2.306	2.30	604-1	1.070	0.517	1.561	0.465	3.358	3.32	39.3	38.67
604-2	1.278	0.602	1.776	0.772	2.300	0.006	604-2	1.076	0.519	1.569	0.472	3.325	0.022	38.9	0.433
604-3	1.278	0.592	1.755	0.759	2.311		604-3	1.072	0.517	1.552	0.467	3.326		38.6	
604-4	1.275	0.603	1.779	0.770	2.311		604-4	1.077	0.523	1.574	0.476	3.304		38.1	
604-5	1.280	0.599	1.771	0.771	2.298		604-5	1.078	0.519	1.565	0.474	3.304		38.5	
640-1	1.275	0.549	1.770	0.701	2.525	2.52	640-1	1.104	0.494	1.713	0.473	3.622	3.62	32.5	32.53
640-2	1.274	0.553	1.778	0.705	2.522	0.009	640-2	1.108	0.500	1.724	0.482	3.576	0.028	31.6	0.574
640-3	1.275	0.553	1.786	0.706	2.530		640-3	1.100	0.500	1.732	0.475	3.645		32.7	
640-4	1.275	0.562	1.799	0.718	2.507		640-4	1.102	0.507	1.742	0.484	3.602		32.6	
640-5	1.272	0.555	1.772	0.705	2.513		640-5	1.102	0.494	1.715	0.471	3.640		33.2	
100-1	1.275	0.582	1.786	0.743	2.404	2.44	100-1	1.104	0.522	1.732	0.500	3.466	3.51	32.8	32.64
100-2	1.274	0.576	1.794	0.734	2.443	0.020	100-2	1.105	0.517	1.742	0.496	3.514	0.033	32.5	0.534
100-3	1.275	0.565	1.772	0.721	2.456		100-3	1.107	0.511	1.719	0.492	3.495		31.8	
100-4	1.273	0.568	1.770	0.723	2.448		100-4	1.102	0.506	1.717	0.483	3.558		33.2	
100-5	1.275	0.570	1.771	0.728	2.434		100-5	1.103	0.511	1.714	0.488	3.510		32.9	
o10-1	1.274	0.575	1.796	0.733	2.450	2.46	o10-1	1.082	0.503	1.726	0.463	3.732	3.72	36.9	36.47
o10-2	1.274	0.572	1.800	0.729	2.469	0.011	o10-2	1.083	0.504	1.729	0.464	3.724	0.025	36.3	0.393
o10-3	1.272	0.571	1.777	0.726	2.449		o10-3	1.080	0.502	1.709	0.460	3.716		36.6	
o10-4	1.272	0.568	1.786	0.722	2.474		o10-4	1.077	0.502	1.716	0.457	3.752		36.6	
o10-5	1.273	0.571	1.788	0.727	2.460		o10-5	1.084	0.505	1.717	0.466	3.684		35.9	
820CM-1	1.274	0.565	1.773	0.720	2.462	2.46	820CM-1	1.102	0.509	1.714	0.485	3.531	3.58	32.6	33.62
820CM-2	1.269	0.567	1.769	0.717	2.467	0.009	820CM-2	1.100	0.500	1.708	0.475	3.595	0.033	33.7	0.697
820CM-3	1.271	0.568	1.771	0.721	2.457		820CM-3	1.101	0.504	1.710	0.480	3.564		33.4	
820CM-4	1.274	0.569	1.774	0.725	2.446		820CM-4	1.102	0.503	1.715	0.480	3.575		33.9	
820CM-5	1.275	0.568	1.776	0.725	2.449		820CM-5	1.102	0.498	1.719	0.475	3.619		34.5	

Sample ID	diameter	height	weight	volume	density	ave. den.	Sample ID	diameter	height	weight	volume	density	ave. den.	% shrink	ave%shrink
F100-X	1.279	0.688	1.523	0.884	1.723	1.62	F100-X	1.031	0.557	1.162	0.465	2.499	2.34	47.4	47.69
OO1-2	1.278	0.341	0.674	0.437	1.541	0.101	OO1-2	1.031	0.269	0.510	0.225	2.271	0.132	48.7	1.652
OO1-3	1.280	0.356	0.693	0.458	1.513		OO1-3	1.030	0.276	0.526	0.230	2.287		49.8	
OO1-4	1.280	0.325	0.724	0.418	1.731		OO1-4	1.028	0.266	0.544	0.221	2.464		47.2	
OO1-5	1.280	0.309	0.637	0.398	1.602		OO1-5	1.033	0.259	0.476	0.217	2.193		45.4	

Appendix J. Surface-Free-Energy Calculations for Various Particle Size Mixtures

Appendix J

Surface-Free Energy Calculations

<u>Number of Particles</u>

FCC lattice constant = $2(2^{1/2})R = 2.83\times10^{-4}$ cm
Volume = 2.26×10^{-11} cm^3
Four particles per cell
Large (radius=1×10^{-4} cm) particles in 1 cm^3 = 1.77×10^{11} particles
tetrahedral particles in 1 cm^3 = 3.54×10^{11} particles
octahedral Particles in 1 cm^3 = 1.77×10^{11} particles

<u>Total Surface Area</u>

Large particles = $1.77\times10^{11}\times4\times3.14159\times(1\times10^{-4})^2 = 2.22\times10^4$ cm^2
tetrahedral particles= $3.54\times10^{11}\times4\times3.14159\times(2.25\times10^{-5})^2 = 2.25\times10^3$ cm^2
octahedral particles = $1.77\times10^{11}\times4\times3.14159\times(4.14\times10^{-5})^2 = 3.81\times10^3$ cm^2
Total surface area = 2.83×10^4 cm^2

	Volume X^3	X
Large particles	0.7405 cm^3	0.9047 cm
tetrahedral particles	0.0169	0.2566
octahedral particles	0.0525	0.3744

<u>Surface-Free Energy Calculation</u>

dG=(A(2))-A(1))xj where j=905 ergs/cm^2
dG = surface-free energy
A(2) = $6X^2$ from above
A(1) = surface area of particles
j = surface energy

Large particles: $dG_1=6(0.9047)^2-2.22\times10^4)\times905$ Joules
= -2.009 J

tetrahedral Particles: $dG_2=6(0.2566)^2-2.25\times10^3)\times905$ Joules
= -0.204 J

octahedral Particles: $dG_3=6(0.3746)^2-3.81\times10^3)\times905$ Joules
= -0.345 J

<u>Total Surface-Free Energy</u>

dG(total)= $dG_1+dG_2+dG_3$ = -(2.009+0.204+0.345) J
dG(total)= -2.559 J

Donald G. White, Executive Director

METAL POWDER
INDUSTRIES FEDERATION
105 COLLEGE ROAD EAST
PRINCETON, NEW JERSEY 08540-6692 USA
TEL: (609) 452-7700
FAX: (609) 987-8523

August 5, 1997

Dale L. Anderson
1471 Cordoba Ave.
Hayward, CA 94544

Dear Mr. Anderson:

We are happy to grant you permission to use the data in Table 8.1 on page 186 and Figure 2.7 on page 35, Figure 8.2 on page 184 and Figure 8.3 on page 185 from the book entitled "Particle Packing Characteristics" by Randall M. German. We grant permission for you to contain this information in all publications of your Master's Thesis.

We would appreciate receiving credit for the original figures as per the following statement:

CREDIT LINE

Reprinted with permission from Particle Packing Characteristics, 1989, Metal Powder Industries Federation, Princeton, New Jersey, USA, 1997.

Thank you for your interest in MPIF Publications.

Cindy Jablonowski

Cindy Jablonowski
Publications Manager